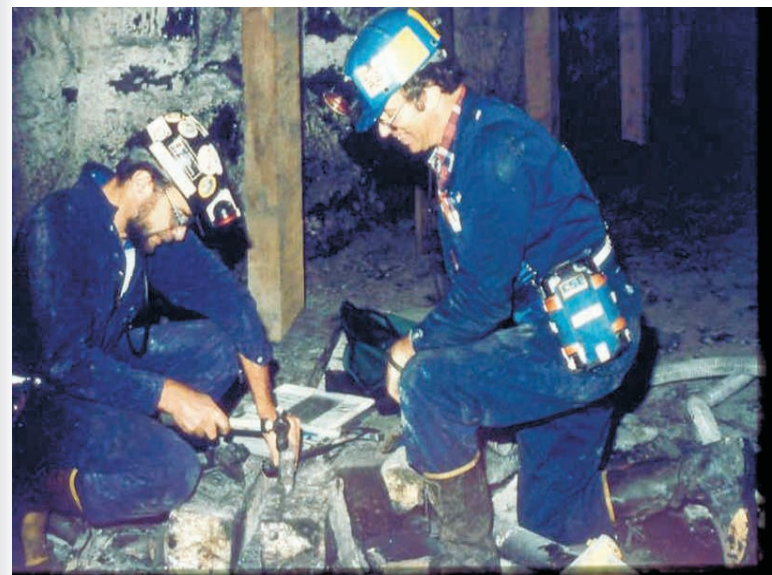
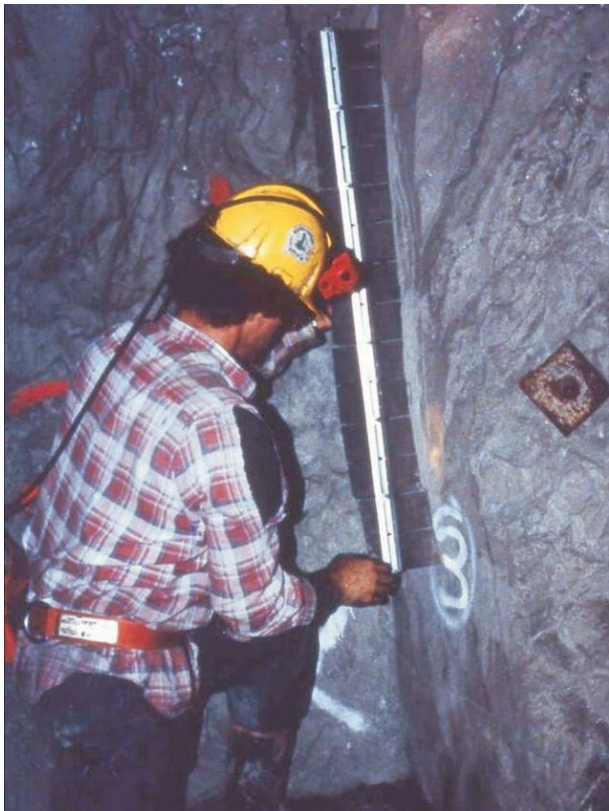


# Proceedings of the International Workshop on Rock Mass Classification in Underground Mining



Department of Health and Human Services  
Centers for Disease Control and Prevention  
National Institute for Occupational Safety and Health

**NIOSH**

**Information Circular 9498**

**Proceedings of the International Workshop on  
Rock Mass Classification in Underground Mining**

**Edited by Christopher Mark, Ph.D., P.E., Rimas Pakalnis, P.Eng., and Robert J. Tuchman**

DEPARTMENT OF HEALTH AND HUMAN SERVICES  
Centers for Disease Control and Prevention  
National Institute for Occupational Safety and Health  
Pittsburgh Research Laboratory  
Pittsburgh, PA

May 2007

**This document is in the public domain and may be freely copied or reprinted.**

## **DISCLAIMER**

Mention of any company or product does not constitute endorsement by the National Institute for Occupational Safety and Health (NIOSH). In addition, citations to Web sites external to NIOSH do not constitute NIOSH endorsement of the sponsoring organizations or their programs or products. Furthermore, NIOSH is not responsible for the content of these Web sites.

The views expressed by non-NIOSH authors in these proceedings are not necessarily those of NIOSH.

## **ORDERING INFORMATION**

To receive documents or other information about occupational safety and health topics, contact NIOSH at

NIOSH—Publications Dissemination  
4676 Columbia Parkway  
Cincinnati, OH 45226-1998

Telephone: **1-800-35-NIOSH** (1-800-356-4674)  
Fax: 513-533-8573  
e-mail: [pubstaft@cdc.gov](mailto:pubstaft@cdc.gov)

or visit the NIOSH Web site at **www.cdc.gov/niosh**

DHHS (NIOSH) Publication No. 2007-128

May 2007

**SAFER • HEALTHIER • PEOPLE™**

## CONTENTS

	<i>Page</i>
Abstract .....	1
Rock mass characterization for excavations in mining and civil engineering, by N. Barton.....	3
Mechanized excavability rating for hard-rock mining, by Z. T. Bieniawski and B. Celada.....	15
Rock mass characterization of primary copper ore for caving at the El Teniente mine, Chile, by A. Brzovic and E. Villaescusa .....	25
Stope design considerations using rock mass classification tools at the Xstrata Zinc George Fisher mine, by G. W. Capes, J. P. Doolan, and L. B. Neindorf .....	37
An integrated approach to support design in underground coal mines, by M. M. Gadde, J. A. Rusnak, and C. Mark.....	49
A rock mass rating scheme for clastic sediments based on geophysical logs, by P. J. Hatherly, T. P. Medhurst, and S. A. MacGregor.....	57
Practical experiences with application of the coal mine roof rating (CMRR) in Australian coal mines, by D. Hill .....	65
Use of the mining rock mass rating (MRMR) classification: industry experience, by J. Jakubec and G. S. Esterhuizen .....	73
Classification-based probabilistic design of ground support, by R. B. Langston, H. A. D. Kirsten, G. C. Howell, and J. A. Marjerison .....	79
The geological strength index (GSI): a characterization tool for assessing engineering properties for rock masses, by P. G. Marinos, V. Marinos, and E. Hoek.....	87
Development and application of the coal mine roof rating (CMRR), by C. Mark and G. M. Molinda.....	95
Problems with rock classification for empirical and numerical design, by D. Milne .....	111
Weak rock mass design for underground mining operations, by R. Pakalnis, T. M. Brady, P. Hughes, C. Caceres, A. M. Ouchi, and M. M. MacLaughlin.....	119
Application of the Q-system to Australian underground metal mines, by W. A. Peck and M. F. Lee .....	129
Rock mass classification in German hard-coal mining: standards and application, by H. Witthaus and N. Polysos .....	141
Numerical modeling procedures for practical coal mine design, by R. K. Zipf, Jr.....	153

## UNIT OF MEASURE ABBREVIATIONS USED IN THIS REPORT

cm	centimeter	$m^3$	cubic meter
ft	foot	m/day	meter per day
$g/cm^3$	gram per cubic centimeter	m/s	meter per second
g/t	gram per ton	min	minute
GPa	gigapascal	mm	millimeter
hr	hour	MN/m	meganewton per meter
in	inch	MPa	megapascal
kg	kilogram	mt	metric ton
$kJ/m^3$	kilojoule per cubic meter	mt/m	metric ton per meter
km	kilometer	Mt	million tons
$km^2$	square kilometer	N/m	newton per meter
km/s	kilometer per second	N/m/m	newton per meter per meter
kN	kilonewton	N/mm <sup>2</sup>	newton per square millimeter
kN/m	kilonewton per meter	psi	pound-force per square inch
$kN/m^2$	kilonewton per meter squared	rps	revolution per second
ksi	1,000 psi	t/m	ton per meter
L/min	liter per minute	$t/m^2$	ton per square meter
L/sec	liter per second	tnf	ton of force
lb	pound	$tnf/m^2$	ton of force per meter squared
m	meter	$\mu sec/m$	microsecond per meter
$m^2$	square meter		

# PROCEEDINGS OF THE INTERNATIONAL WORKSHOP ON ROCK MASS CLASSIFICATION IN UNDERGROUND MINING

Edited by Christopher Mark, Ph.D., P.E.,<sup>1</sup> Rimas Pakalnis, P.Eng.,<sup>2</sup> and Robert J. Tuchman<sup>3</sup>

---

## ABSTRACT

Rock mass classification is widely used throughout the underground mining industry—in both coal and hard-rock mines. It is used in all stages of the mining process, from site characterization to production operations. The goal of the International Workshop on Rock Mass Classification in Underground Mining was to provide a forum for leading practitioners of rock mass classification to come together and share their methods and experiences with the technique. The workshop was held in Vancouver, British Columbia, Canada, on May 31, 2007. It was co-chaired by Christopher Mark, Ph.D., P.E., National Institute for Occupational Safety and Health, Pittsburgh, PA, and Rimas Pakalnis, P.Eng., University of British Columbia, Vancouver, Canada.

The proceedings of the workshop contain 16 invited papers from 9 countries, reflecting the international depth and breadth of current practice. Applications in both hard-rock and coal mining are well represented. Some of the topics that were addressed at the workshop include:

- Major rock mass classification systems used in mining and their variants
- Collection of input data through observation, rock testing, and geophysics
- Design of mine layouts and rock support systems using classification
- Estimation of rock mass strength and other input parameters for numerical models from classification
- Applications in weak rock, raise boring, cavability assessment, and other special topics
- Risk assessment using rock mass classification

---

<sup>1</sup>Principal research mining engineer, Pittsburgh Research Laboratory, National Institute for Occupational Safety and Health, Pittsburgh, PA.

<sup>2</sup>Associate professor of mining engineering, University of British Columbia, Vancouver, British Columbia, Canada.

<sup>3</sup>Technical writer-editor, Writer-Editor Services Branch, Division of Creative Services, National Center for Health Marketing, Coordinating Center for Health Information and Service, Centers for Disease Control and Prevention, Pittsburgh, PA.



# ROCK MASS CHARACTERIZATION FOR EXCAVATIONS IN MINING AND CIVIL ENGINEERING

By Nick Barton, Ph.D.<sup>1</sup>

## ABSTRACT

When the Q-system was launched in 1974, the name referred to rock mass classification, with focus on tunnel and cavern support selection. Besides empirical design of support, the Q-value, or its normalized value  $Q_c$ , has been found to correlate with seismic P-wave velocity, with deformation modulus, and with deformation. The Q-system provides temporary or permanent support for road, rail, and mine roadway tunnels and for caverns for various uses. It also gives relative cost and time for tunnel construction for a complete range of rock qualities. There are also indications that Q has captured important elements of the cohesive and frictional strength of rock masses, with  $Q_c$  resembling the product of rock mass cohesion and rock mass friction coefficient.

## ROCK MASS VARIABILITY

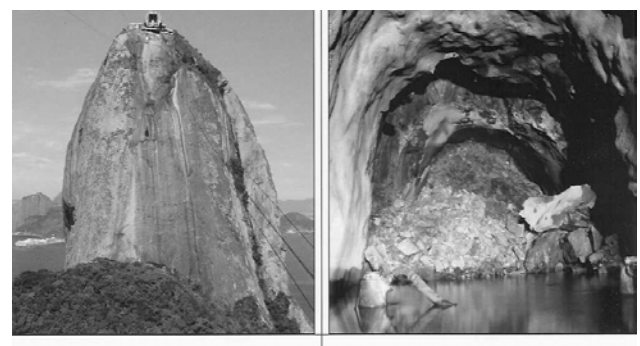
From the outset, the Q-system has focused on sound, simple empiricism that works because it reflects practice and that can be used because it is easily remembered. It is appropriate to start by illustrating the widely contrasting rock mass qualities that may challenge both the civil and mining professions, fortunately not on a daily basis, but therefore also unexpectedly.

Figure 1 shows a core box from a project that has not been completed during 10 years of trying. The massive core is from a project that may not be started for at least 10 years. The first should already have passing high-speed trains; the other may have high-level nuclear waste some time in the future. They are both from the same country, but may have six orders of magnitude contrast in Q-value. A second pair of examples shown in Figure 2 requires a cable car for access on the one hand, and successive boat trips to fault-blocked flooded sections of tunnel on the other.

The contrasting stiffness and strength of intact rock and wet clay is easy to visualize. One may be crushed by one and drowned in the other. There are sad and multiple examples of both in the tunneling and mining industries. They merit a widely different quality description, as for instance given by the wide range of the Q-value.



Figure 1.—The contrast shown by these two core boxes suggests orders of magnitude differences in quality. Quantitative descriptions of shear strength and deformation modulus would vary by orders of magnitude as well. Quality descriptors like RMR or GSI that suggest qualities differing from only 5 to 95, or 10 to 90, cannot then be as appropriate as the 0.001–1000 range of Q seen in these examples. Increasing the range of Q to  $Q_c$  adds further reality, since  $Q_c$  might range from 0.0005 to 2500 in these two cases.



Massive rock at the Sugar Loaf, Rio de Janeiro  
 $Q = 1000$  (or better)  
 $Q = 100/0.5 \times 4/0.75 \times 1/1$   
(low attenuation is implied by high Q-values)

Faulted rock causing tunnel collapse, Brazil  
 $Q = 0.001$  (or worse)  
 $Q = 10/20 \times 1/8 \times 0.5/20$   
(extreme attenuation is implied by low Q-values)

Figure 2.—Respective access by cable car and by boat, emphasizes the need for radically different magnitudes of rock quality and also radically different magnitudes of seismic quality, the inverse of attenuation [Barton 2006]. A single project beneath Hong Kong harbor demonstrated a length of core of 57 m without a joint and an even wider regional fault zone. With such extremes, RQD values of 100% and 0% are clearly inadequate, too, but can clearly be improved by using local Q-values of, for example, 1000 and 0.001.

<sup>1</sup>President, Nick Barton & Associates, Høvik, Norway.

The term Q is composed of fundamentally important parameters (Figure 3) that were each (besides Deere's Rock Quality Designation (RQD)) quantified by exhaustive case record analysis. The six orders of magnitude range of Q is a partial reflection of the potentially enormous variability of geology and structural geology. It is probably because of the relative sensitivity of a classification that can show wide numerical variation (i.e.,  $10^{-3}$  to  $10^3$ , or an even wider range using  $Q_c = Q \times \sigma_c/100$ ) that correlation with a very varied geologic and hydrogeologic reality is achieved, using rather simple correlations. Without this range of Q (approximately  $10^6$ ) or  $Q_c$  (approximately  $10^9$ ), correlation would be more complex, as it seems to be with the Geological Strength Index (GSI) in particular, since this is based on the limited numerical range of the Rock Mass Rating (RMR) system.

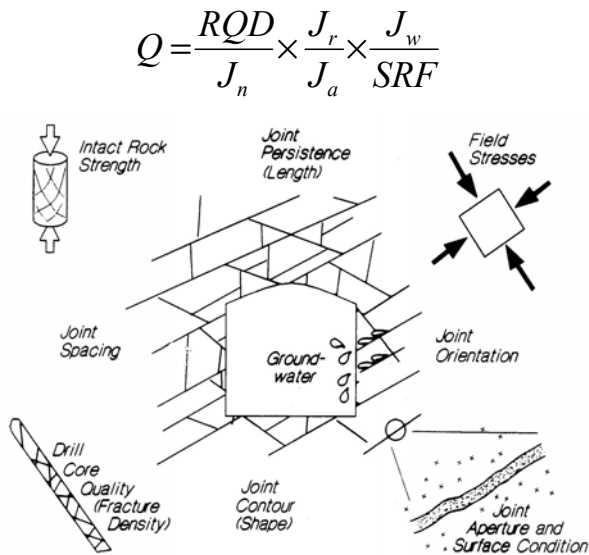


**Figure 3.**—A pictorial representation of the Q-parameters, from Hutchinson and Diederichs [1996]. The modern application of the Q-system [Barton 2002] includes both indirect and direct use of UCS. When the rock strength-to-stress ratio is unfavorable, in the case of massive (high RQD/J<sub>n</sub>) rock masses, the SRF value will need to be very high to represent excavation difficulties, i.e., deep-shaft excavation, due to potential stress slabbing or minor bursting. The high SRF and correspondingly low Q-value require heavy yielding support. In the case of jointed rock under high stress, SRF will not need to be so high.

#### COMMON ASPECTS OF OVERBREAK AND CAVABILITY IN MINING

Figure 4 shows the fundamental importance of the number of sets of joints and their roughness using the Q-system parameters J<sub>n</sub> (number of sets) and J<sub>r</sub> (roughness). This figure also shows overbreak (and therefore large-scale cavability, in principle) caused by three sets of joints, but with the important proviso that without a degree of joint

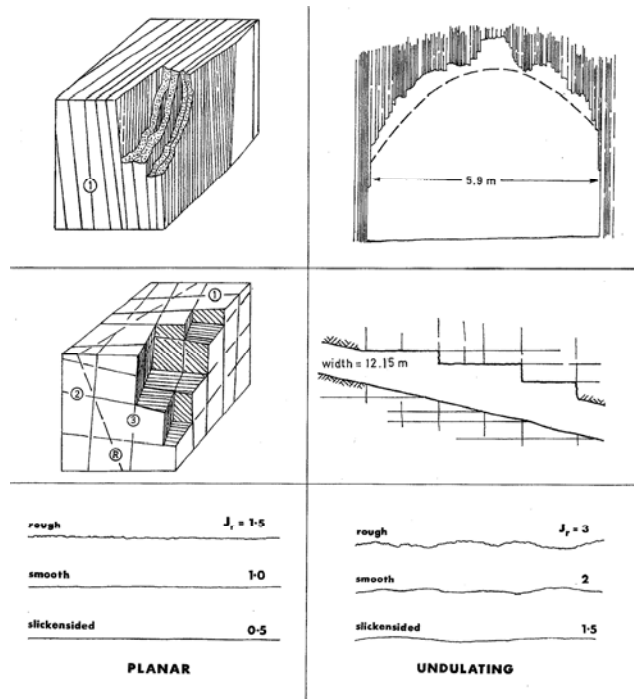


**Figure 4.**—Two of the most important components of Q and of rock mass stability are the number of joint sets (or degree of freedom for block definition and fallout) and the joint roughness (or interblock release-or-hold mechanism). The general level of overbreak and ease of carrying out characterization in tunnels are also fundamentally affected by these two parameters. In the case of block caving in mining, the ratio J<sub>n</sub>/J<sub>r</sub> is fundamental for initiating such mechanisms.

surface planarity, neither overbreak in a tunnel/roadway, nor block caving are likely to occur without significant assistance.

It is quite likely that, whatever the overall Q-value at a given (potential) block caving locality in an ore body, the actual combination J<sub>n</sub>/J<sub>r</sub> will need to be  $\geq 6$  for successful caving (e.g., 6/1, 9/1.5, 12/2), while such combinations as 9/3 might prove to be too dilatant. Even four joint sets (J<sub>n</sub> = 15) with too high J<sub>r</sub> (such as 3) would probably prejudice caving due to the strong dilation and need for a lot of long-hole drilling and blasting. Significantly, this last ratio (15/3 = 5) is also  $< 6$ .

The simple J<sub>r</sub> description shown in Figure 4, when combined with J<sub>a</sub>, also gives a realistic estimate of the interblock friction angle, as illustrated in Figure 5. These parameters form part of the first and second pairs of parameters describing the Q-value. (RQD/J<sub>n</sub> = relative block size, J<sub>r</sub>/J<sub>a</sub> = interblock friction coefficient). Obviously, a combination of J<sub>n</sub> = 6 to 9 (or more), and J<sub>r</sub> = 2, 1.5, or less, and J<sub>a</sub>  $\geq 1$  would be ideal attributes for block caving and equally *unfavorable* for overbreak and tunnel or cavern support needs, where permanent, or temporary, stability was required.

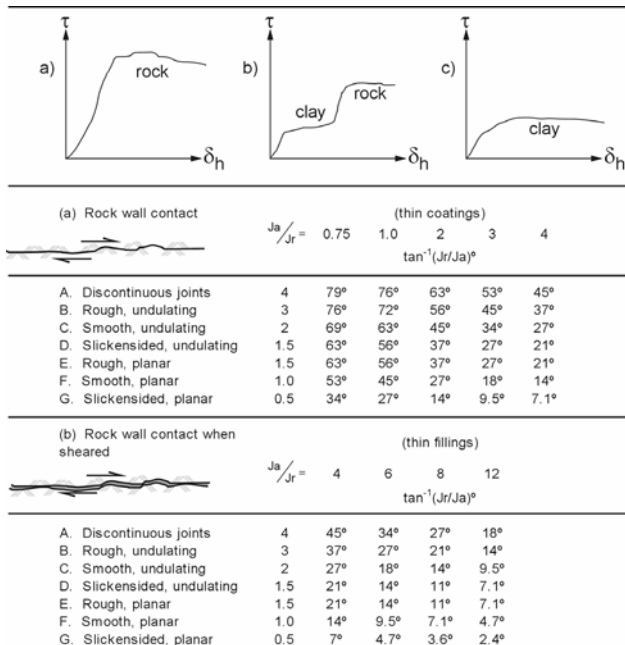


**Figure 5.—A graphic demonstration of the workings of  $J_r$  and  $J_a$  in the context of joint or clay-filled discontinuity friction angles. For minimal overbreak and tunnel support needs,  $J_r/J_a$  needs to be as large as possible. For block caving, a mostly “category a” (rock-to-rock joint wall contact) friction angle is expected. The  $J_r$  values (the vertical columns of ratings on the left side) will need to be 2 or less; otherwise, dilation during shear will stop block caving from occurring, unless block size is small enough for block rotation to occur, e.g., Barton [2004].**

## CONSEQUENCES OF OVERTAKE IN A CAVERNS AND IN A MINE

The 62-m span Gjøvik Olympic cavern in Norway typically had  $J_n/J_r$  of 9/2, and it was stable with the help of bolting and shotcrete and a favorable (horizontal) stress situation. Although it suffered significant overbreak,  $J_n/J_r$  of 9/2 prevented caving, i.e., locally excessive overbreak. With  $J_n/J_r$  of 9 (three sets) and  $J_r$  of 1 (planar), the project would have had another degree of complexity, i.e., it would have caved at the very wide face, without close-to-the-face rock support. Of course, the magnitude of RQD (where RQD/ $J_n$  represents relative block size) and the details of  $J_a$  (possible clay-filling or soft mineralization) will modify the above simplicity; hence the use of Q.

The typical Gjøvik cavern  $J_n/J_r$  ratio ( $9/2 = 4.5$ ), although not allowing caving (or uncontrolled overbreak) during blasting, did allow overbreak of 1 to 2 m, as seen through the 10 cm of S(fr) in the 62-m span arch seen about 20 m above the camera location in Figure 6. In such overbreak locations, there was invariably a local  $J_n = 12\text{--}15$  (up to four sets) character, with  $J_r$  of about 2, i.e., a ratio of  $J_n/J_r$  of  $\geq 6$ . This implies the likely need for support in civil engineering excavations and mine roadways, while in the



**Figure 6.—Example of a well-jointed rock mass with most typically  $J_n = 9$  (three sets of joints) and  $J_r = 2$ , seen in the Gjøvik Olympic cavern of 62-m span. Note the deep overbreak in the 25-m-high arch and the use of B + S(fr) permanent support [Barton et al. 1994].**

case of block caving, could signal relative ease of caving initiation, as shown in the following example.

In the steeply inclined Kiruna ore body in Sweden, the Q-system parameters were evaluated by systematic logging in  $>2$  km of upper-level long-hole drilling galleries and in corresponding ore-loading galleries at the base of the proposed LKAB Oscar (long-hole block caving) project [Barton 1988]. Roughness characterization of the jointing exposed by failed zones (extreme overbreak) in the drifts due to inadequate temporary support was used to evaluate the possibility of larger-scale block release and caving disruption, as illustrated schematically at the top of Figure 7 (see “J1” and “J2” areas).

As may be noted from the Q-histogram logging illustrated in Figure 7, the most frequent  $J_n/J_r$  ratings were 9/2. This proved insufficient for unassisted caving. Drift failures (few) tended to have occurred with  $J_n/J_r$  of, for example, 12/1.5, sometimes with the additional facilitation of  $J_a = 3$ , i.e., mineralized joints.

The above ratings for the various joint and rock mass parameters for the two example projects illustrate behavior with respect to overbreak and cavability—the former at stress levels of 3–5 MPa (Gjøvik Olympic cavern), the latter at 15–20 MPa (Kiruna’s LKAB Oscar project). Clearly, high initial and developing stress levels expected in a deep mine may give a necessary “boost” to block fracturing and interblock friction mechanisms, thereby demonstrating the need for block stress-fracturing and joint stress-propagation mechanisms, if initiation of caving should be modeled.

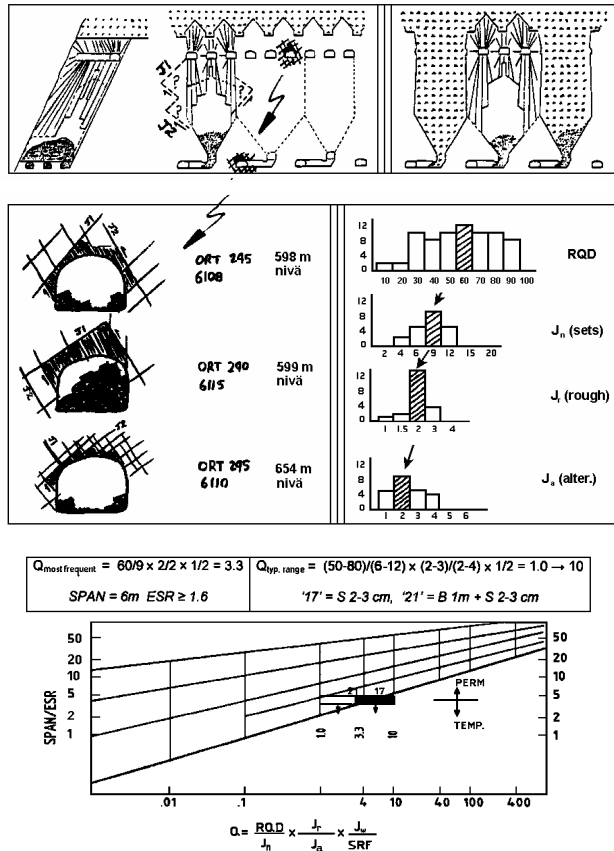


**Figure 7.—Kiruna's LKAB Oscar long-hole caving project.** Some details of rock mass Q-characterization, observations of drift collapse and overbreak, and a pre-1993 Q-system temporary support assessment (after Barton [1988]). Note the early use of Q-parameter histogram logging, a simple method of field logging used in the last 20 years.

These important aspects that are fundamental in caving initiation, can be studied by suitable combinations of block modeling (UDEC-BB) and block fracture modeling (FRACOD). There are also intimate cross-disciplinary links between this modelable “blockiness” and the resulting permeability, or “connectedness,” and the resultant effects on seismic attenuation and its inverse  $Q_{\text{seis}}$  [Barton 2006].

### EXTRAPOLATING Q USING SEISMIC REFRACTION PROFILES

Since there is a limit to how many boreholes can be drilled, how many cores can be logged, and how many permeability tests can be performed, it is useful to have alternative ways of estimating and extrapolating these point sources of information. This opinion applies, of course, to tunnels and to mining declines that can be reached, or almost reached, by boreholes or by deeply penetrating seismic refraction, with less constraints on

energy sources than will be the case with civil engineering tunnels near population centers.

One may start by looking at correlation between velocity and measures of quality. Sjøgren et al. [1979] used seismic profiles (totaling 113 km) and local core logging results (totaling 2.9 km of core) to derive these helpful mean trends for hard rocks (Figures 8–11).

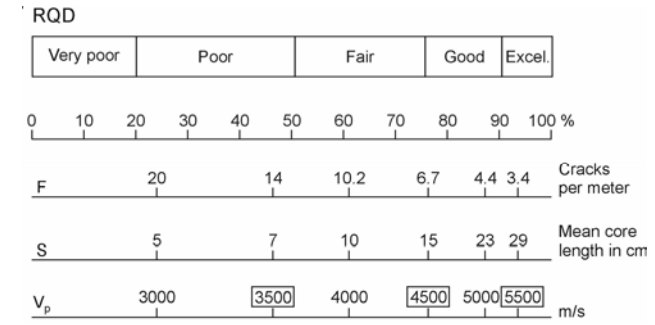


**Figure 8.—Hard-rock, shallow seismic refraction.** Sjøgren et al. [1979] combined 113 km of seismic profiles and 2.9 km of core logging to derive these mean trends for shallow tunnels.

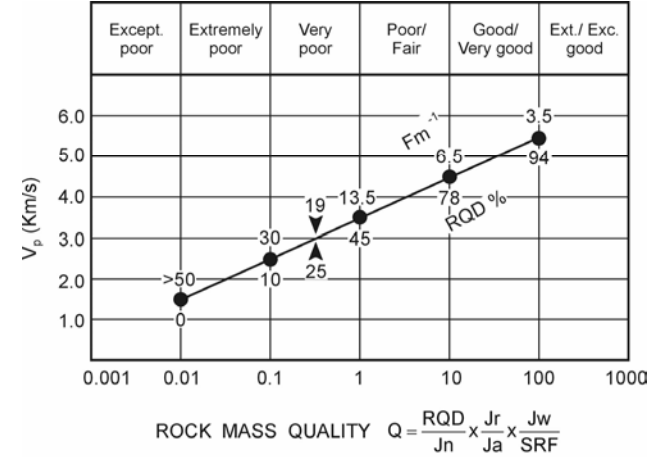
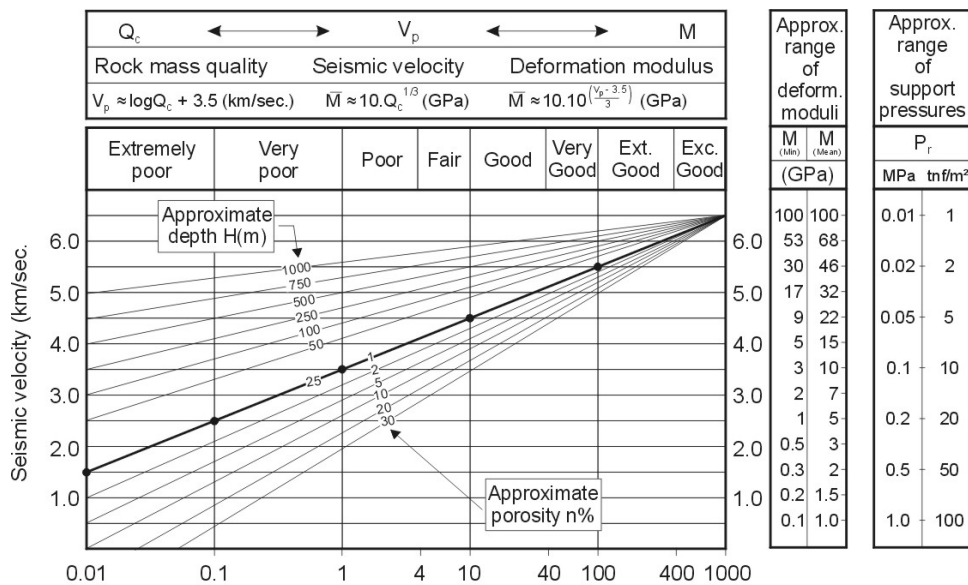


**Figure 9.—Hard-rock, shallow seismic refraction, mean trends from Sjøgren et al. [1979].** The Q-scale was added by Barton [1995] using the hard-rock correlation  $V_p \approx 3.5 + \log Q$ . By remembering  $Q = 1: V_p \approx 3.5 \text{ km/s}$ , and  $V_p = 3 \text{ km/s}: Q \approx 0.3$ , the Q- $V_p$  approximation to a wide range of near-surface qualities is at one's fingertips (e.g., for hard, massive rock:  $Q = 100: V_p \approx 5.5 \text{ km/s}$ , and when  $V_p = 5 \text{ km/s}: Q \approx 30$ ).



$$Q_c = \left[ \frac{RQD}{J_n} \times \frac{J_r}{J_a} \times \frac{J_w}{SRF} \right] \frac{\sigma_c}{100}$$

Figure 10.—An integrated empirical model for linking Q-value (via  $Q_c$ ) to P-wave velocity, depth, matrix porosity, deformation modulus, and approximate support pressure (based on a mean  $J_r = 2$ ). With this simplification, the independently derived Barton et al. [1974] support pressure formulation and the Barton [1995] deformation modulus formulation suggest inverse proportionality between support pressure and deformation modulus. This is logical, but the simplicity is nevertheless surprising [Barton 2002].

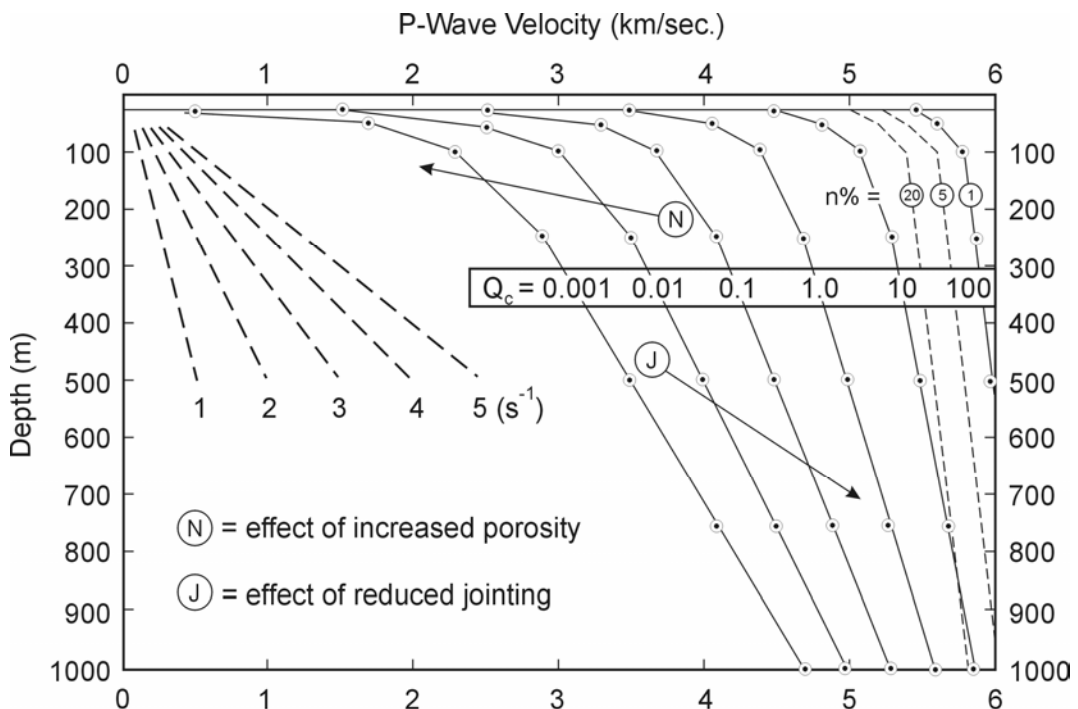


Figure 11.—The depth-velocity trends for different  $Q_c$  values. This graph explains why faulted rock ahead of a deep tunnel may sometimes be invisible or of such high velocity, like 4 km/s, that it is misinterpreted. It may subsequently cause tunnel collapse or trap a tunnel boring machine. In fact, such rock is still probably displaying an important contrast to the surrounding rock mass. In the case of soft rock, acoustic closure prevents such differentiation. In general, “Q-jumping” will be experienced when progressing downward to greater depth, i.e., rock qualities tend to improve, giving steeper  $V_p$ /depth ( $s^{-1}$ ) gradients [Barton 2006].

## TUNNEL AND DECLINE SUPPORT WHEN UNDER HIGH STRESS

The Q-system was developed from mostly civil engineering case records. Nevertheless, there are many tens of kilometers of semipermanent drifts and declines in most mines that have fundamentally similar needs to civil engineering tunnels, at least in their early years of life, before they become seriously affected by subsequent stress changes caused by the advancing mining front. In principle, one needs to design support (or select the correct support class) by classifying each round as the permanent mining drift or decline is driven. This is also a familiar task in civil engineering tunnels.

In mining situations, however, one may need to allow for future stress changes and deformations if a present location will soon become close to the mining front. The civil engineering approach of B+S(fr) for permanent roadways may need to be supplemented with longer fibers and probably the addition of mesh and cable bolts.

One must be prepared to reclassify and resupport if or when stress changes cause the need for rehabilitation due to observed deformation and cracking. The advancing mining fronts will tend to change the stress reduction factor (SRF), possibly to a dramatic level, causing apparent reductions to RQD and apparent or even real increases to  $J_n$  due to stress-fracturing effects. The addition of mesh and longer cable bolts for tolerating larger deformations

will usually be a part of this subsequent phase. Longer fibers from the start that tolerate larger strains would be a logical difference of approach between civil and mining applications of B+S(fr) that might delay rehabilitation requirements.

Increases of SRF due to increased ratios of  $\sigma_1/\sigma_c$  with the advancing mining front *might* follow the changes suggested by Grimstad and Barton [1993] for the case of mining drifts in massive rock surrounding an ore body. The 1993–1994 (slightly) updated SRF ratings for high stress are shown in Table 1. If, on the other hand, the high stresses caused by mining depths or advancing mining fronts are acting on distinctly jointed rock, as experienced for instance in Western Australia, then the equations proposed by Peck [2000] are recommended. These are based on the original SRF values of 1974.

The exponential relationship derived by Peck [2000] from the original SRF ratings of Barton et al. [1974] is as follows:

$$SRF = 34(\sigma_c/\sigma_1)^{-1.2} \quad (1)$$

For strongly anisotropic stress fields, if measured, Peck [2000] derived the following best-fit equation from the Barton et al. [1974] suggestion of downgrading of  $\sigma_c$  with strong stress anisotropy:

$$SRF = 31(\sigma_1/\sigma_3)^{0.3}(\sigma_c/\sigma_1)^{-1.2} \quad (2)$$

**Table 1.—Excerpt from updated SRF ratings based on Grimstad and Barton [1993], with additional notes from Barton [2002].**

Case	Competent rock, rock stress problems	$\sigma_c/\sigma_1$	$\sigma_0/\sigma_c$	Stress reduction factor (SRF)
H .....	Low-stress, near-surface, open joints.	>200	<0.01	2.5
J .....	Medium stress, favorable stress condition.	200–10	0.01–0.3	1
K .....	High-stress, very tight structure. Usually favorable to stability, may be unfavorable for wall stability.	10–5	0.3–0.4	0.5–2
L .....	Moderate slabbing after >1 hr in massive rock.	5–3	0.5–0.65	5–50
M .....	Slabbing and rock burst after a few minutes in massive rock.	3–2	0.65–1	50–200
N .....	Heavy rock burst (strain burst) and immediate dynamic deformations in massive rock.	<2	>1	200–400

### NOTES:

1. For strongly anisotropic virgin stress field (if measured): When  $5 \leq \sigma_1/\sigma_3 \leq 10$ , reduce  $\sigma_c$  to 0.75  $\sigma_c$ . When  $\sigma_1/\sigma_3 > 10$ , reduce  $\sigma_c$  to 0.5  $\sigma_c$ , where  $\sigma_c$  = unconfined compression strength,  $\sigma_1$  and  $\sigma_3$  are the major and minor principal stresses, and  $\sigma_0$  = maximum tangential stress (estimated from elastic theory).
2. Few case records available where depth of crown below surface is less than span width. Suggest an SRF increase from 2.5 to 5 for such cases (see case H).
3. Cases L, M, and N are usually most relevant for support design of deep tunnel excavations in hard massive rock masses, with RQD/ $J_n$  ratios from about 50 to 200.
4. For general characterization of rock masses distant from excavation influences, the use of SRF = 5, 2.5, 1.0, and 0.5 is recommended as depth increases from, say, 0–5 m, 5–25 m, 25–250 m, to >250 m. This will help to adjust Q for some of the effective stress effects, in combination with appropriate characterization values of  $J_w$ . Correlations with depth-dependent static deformation modulus and seismic velocity will then follow the practice used when these were developed.

## STANDUP TIME USING Q-RMR CONVERSION

There is such widespread use of RMR, often in parallel with Q, that it is appropriate to address a possible interrelationship between the two. This, of course, has been the subject of many publications. One camp uses the “ln” (natural logarithm) format shown in Equation 1 in Figure 12; the other uses the “log” format shown in Equation 2 in this figure. Since the latter format is simpler and probably gives a more logical range of RMR in relation to the Q-scale (avoiding the negative values that occur below  $Q = 0.01$ ), it has been used by the author also in relation to standup time and in relation to deformation modulus conversion between the two systems. Since we are engineers and not scientists, our craft is the ability to make realistic approximations, leaving unnecessary decimal places on the calculator.

The conversion between RMR and Q used to estimate standup time is based on Figure 12 (Equation 2). Figure 13 suggests that when the Q-value is as low as, for example, 0.01, or RMR is as low as 20, the standup time for a <1-m advance (beyond the last support) may be a matter of minutes, with collapse imminent or immediate if an advance of 2–3 m was made by an excessive length of blasting round.

## SOME CHARACTERIZATION LESSONS FROM SITE INVESTIGATIONS

Lessons learned and Q-logging techniques applied when investigating ground conditions and modeling planned excavation and support of a mine-size cavern will now be reviewed. The case record is the 62-m span Gjøvik Olympic cavern in Norway. Reference will also be made to some of the Q-correlations given earlier in this paper.

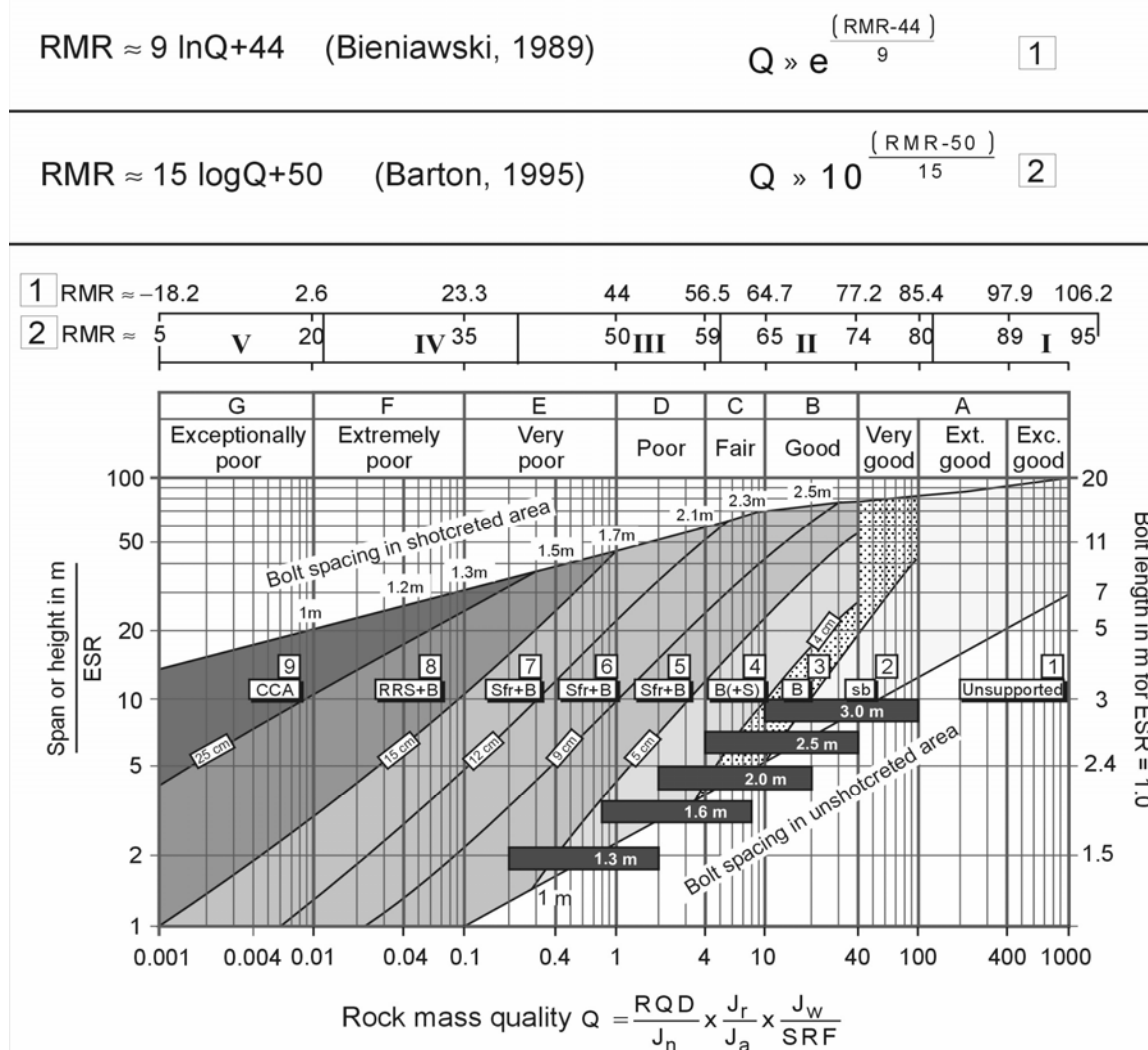


Figure 12.—The Q-support chart from the Grimstad and Barton [1993] update for  $S_{(fr)}$  in place of  $S_{(mr)}$ . (NOTE: Equation 2 (inset) avoids unwanted negative values of RMR when  $Q < 0.01$ .) ESR = excavation support ratio.

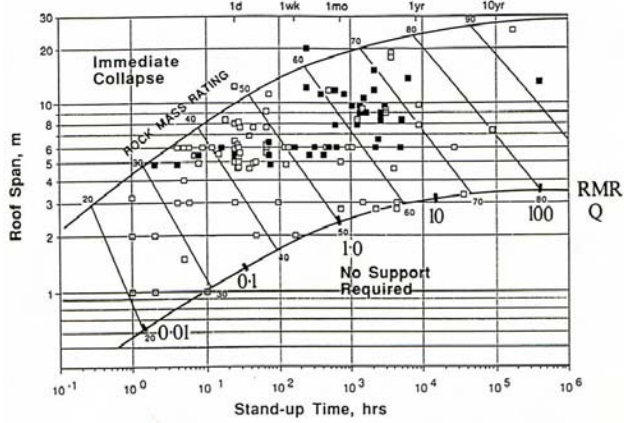


Figure 13.—Bieniawski [1989] standup time estimations. Note the Q-value approximations (large numbers next to small RMR numbers). “Roof span” refers to distance from the last support to the (new) tunnel face.

A start will be made with the comparison of Q-histogram-based core logging (see cross-hatched area in Figure 14) and the Q-logging performed in existing nearby excavations (see black area in Figure 14). Note the “tail” on the RQD distribution, as logged in the case of the core logging, and the lack of a tail when Q-logging in existing excavations. This was caused by lack of Q-parameter data where shotcrete covered the poorest rock when logging the existing excavations.

The boreholes used for core recovery were permeability tested ( $K$  mostly  $\approx 10^{-7}$  to  $10^{-8}$  m/s) and were also used for crosshole seismic tomography. Two examples are shown in Figure 15. The expected increase in velocity with depth, from about 3.5 to 5.0 km/s, is shown. What was

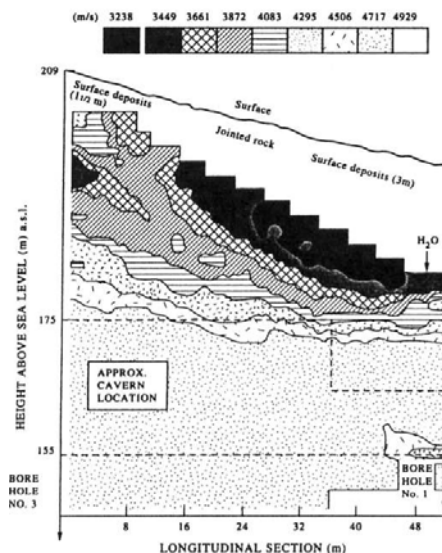


Figure 15.—Crosshole seismic tomography between two pairs of holes at the Gjøvik cavern site prior to cavern location decisions. An expected increase in velocity with depth is indicated, but in this particular case, the rock quality of the gneiss did not noticeably improve.

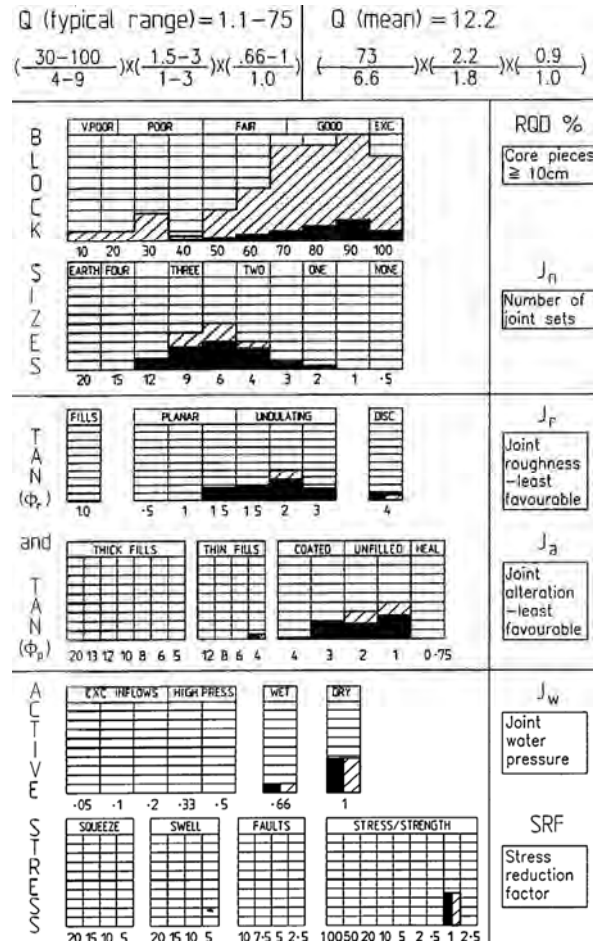
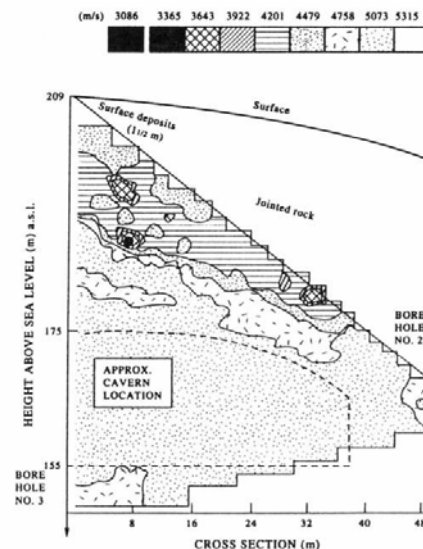
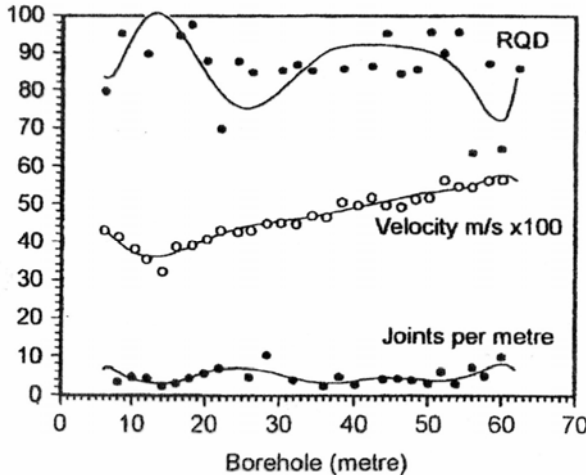


Figure 14.—Q-histogram logging of core (four holes) and existing local excavations (black), performed by different Norwegian Geotechnical Institute Q-loggers at different times [Barton et al. 1994].





**Figure 16.**—Note the lack of a general rock quality improvement with depth compared to the consistent rise in P-wave velocity. The Q-value logged down the holes mostly varied between 1 and 30, with a mean of 10–12 and showed no tendency for improved quality below about 5 m [Barton et al. 1994].

unexpected was that the rock quality (RQD,  $\text{Fm}^{-1}$ , and Q) did not show a corresponding general increase in quality, as can be ascertained by studying Figure 16, which shows the velocities interpreted close to one of the boreholes.

The Q– $V_p$  depth models shown earlier in Figures 10–12 indicated how velocity increase can occur without the need for Q-value increase. However, between 25 and 50 m, the predicted increase in velocity is relatively minor, such as 4.5–5.0 km/s. The increase of closer to 2 km/s between 10 and 60 m depth, shown in Figure 16, may be explained by the measured horizontal stress increase, which was as much as 5 MPa over this same limited depth range.

This increase, with little assumed change in rock quality, is possible due to the increased interlock of the rough conjugate jointing (high  $J_r$  and joint roughness coefficient (JRC)) and the relatively sound tectonized gneiss, with UCS about 90 MPa and joint compressive strength (JCS) about 75 MPa. In softer rock like chalk, acoustic closure (in relation to  $V_p$ ) would occur at much shallower depths than this [Barton 2006].

### INPUT DATA FROM ROCK MASS CLASSIFICATION

In the late 1960s, there was a movement in some rock mechanics circles to try to move beyond the confines of continuum modeling and focus on the possible effects of jointing on the performance and reinforcement needs of rock excavations, whether they be tunnels, slopes, or dam abutments. Thanks to the late-1960s modeling developments of R. E. Goodman and his colleagues with joint elements in finite-element codes, followed by P. A.

$E_n (\text{GPa}) = \left(1 - \frac{C}{2}\right) \sqrt{\frac{\sigma_{\text{eq}}}{100}} \times 10^{(\text{QCD} - 10)/4C}$	$E_m \approx 10 \times Q_c^{\frac{1}{3}}$
$\sigma_{\text{cm}} = \sigma_{\text{ci}} \times \frac{(m_b + 4a - a m_b - 8a )(m_b/4 + c)^{a-1}}{2(1+a)(2+c)}$	$\sigma_{\text{ce}} \approx \bar{\sigma} \sqrt{C_c^3}$
$\phi' = \arcsin \left[ \frac{6am_b(s+m_b\sigma_{\text{cn}})^{a-1}}{2(1+a)(2+a) + 6am_b(s+m_b\sigma_{\text{cn}})^{a-1}} \right]$	$\phi' \approx \tan^{-1} \left( \frac{J_r}{J_a} \times \frac{J_w}{1} \right)$
$C' = \frac{C_{\text{cl}}(1-2a)s + (1-a)m_b\sigma_{\text{cn}}(s-m_b\sigma_{\text{cn}})^{a-1}}{(1+a)(2+a)\sqrt{1 + \left( \frac{6am_b(s+m_b\sigma_{\text{cn}})^{a-1}}{(1+a)(2+a)} \right) / (1+a)(2+a)}}$	$C' \approx \left( \text{ROD} \times \frac{1}{\text{SFR}} \times \frac{C_c}{100} \right)$

**Figure 17.**—The extraordinarily complex formulas (left) for developing input data for some recent continuum models compared with some of the less developed and equivalent Q-based formulas.

Cundall in the early 1970s, first with  $\mu$ DEC, then UDEC, and later with 3DEC, this focus could be fulfilled by an increasing number of rock mechanics practitioners around the world. However, using these codes correctly, with realistic input data, needs experience, time, and therefore budgets to match. Ironically, input data for some continuum codes now seem to be considerably more complex than for discontinuum codes, as suggested in Figure 17.

GSI-based Hoek-Brown formulations for “simple” geotechnical input data for the rock mass, shown in Figure 17, such as deformation modulus, cohesion, and friction angle, have reached “black box” levels of complexity, which seems to be detrimental to the idea of rock engineering if engineering judgment is still to be exercised in this rewarding field of engineering.

There is no possibility to have any feel for the influence of local rock quality on the rock mass compression strength, friction angle, or cohesion when formulations require software rather than estimation for their evaluation. The formulas on the left of Figure 17 cannot be considered “empirical” anymore, with the exception of the first equation for estimating modulus.

Presumably as a result of time and budgetary pressures, as well as the developing need to model large-scale mining problems, there has been a marked trend for using “convenient” continuum codes, which also have particularly good graphic representation of results. Simple software packages for handling the complex input data calculations (Figure 17) are also provided so that a smart user might theoretically need only limited understanding of rock mechanics principles to use the codes successfully.

The author has often used the method of rapidly left-thumbing from the back of a consultant’s report to the front, whereby the colored appendices of endless stress distributions and deformation patterns can be read almost as in a film. Does all this color represent anything real?

**Table 2.—Five hypothetical rock masses with reducing quality from top to bottom of the table.**  
 (Note the difference between Q and  $Q_c$  due to normalization by  $\sigma_c/100$ . The sensitive, logical values of FC and CC already exist in the  $Q_c$  calculation, requiring no further empiricism.)

RQD	$J_n$	$J_r$	$J_a$	$J_w$	SRF	Q	$\sigma_c$	$Q_c$	FC, °	CC, MPa	$V_p$ , km/s	$E_{mess}$ , GPa
100.....	2	2	1	1	1	100	100	100	63	50	5.5	46
90.....	9	1	1	1	1	10	100	10	45	10	4.5	22
60.....	12	1.5	2	0.66	1	2.5	50	1.2	26	2.5	3.6	10.7
30.....	15	1	4	0.66	2.5	0.13	33	0.04	9	0.26	2.1	3.5
10.....	20	1	6	0.5	5	0.008	10	0.0008	5	0.01	0.4	0.9

Would the numerical modelers know how to input a neglected clay seam without “smoothing it out” in a continuum approximation? Would the complex estimates of  $c'$  and  $\phi'$  in Figure 17 change very much?

### CC AND FC: THE COHESIVE AND FRICTIONAL COMPONENTS OF $Q_c$

On the right side of Figure 17, simple Q-based equations for  $c$  and  $\phi$  are shown that are actually found to be composed of each half of the  $Q_c$ -formulation. They have the advantage of not requiring software for their calculation—they already exist in the calculation of the  $Q_c$  value. They are defined as follows:

$$\text{cohesive component (CC)} = \text{RQD}/J_n \times 1/\text{SRF} \times \sigma_c/100$$

$$\text{frictional component (FC)} = \tan^{-1}[J_r/J_a \times J_w]$$

Examples of these rock mass component strengths are given in Table 2 for a range of possible Q-values for increasingly jointed rock masses.

The P-wave velocity and (pseudostatic) deformation modulus estimates in Table 2 are from the central

diagonal, near-surface (25-m depth) interrelationships given in Figure 10. They could equally well be quoted for greater depths, if more relevant. Some physical examples of rock masses with different CC and FC characteristics are shown in Figure 18.

Plate loading tests taken to such high stress levels that rock mass failure occurs are rare. However, measurement of P-wave velocity at such sites may allow tentative extrapolation to other sites through a common rock mass quality estimate. Such data can then be a source of tentative rock mass strength ( $\sigma_{c\text{ mass}}$ ) estimation.

Table 3 suggests compressive (and cohesive) strengths in rock masses somewhat higher than those usually assumed. They also show some implicit variation from the values set up in Table 2 (from specific Q-parameter combinations), but reinforce the idea of potentially very high cohesive strengths (e.g., tens of MPa) in competent rock masses. This table of values seems to imply very different values of cohesion from some of the earlier RMR-based estimates of cohesion for rock masses, where  $c$  was generally given as <1 MPa for a wide range of RMR.



**Figure 18.—Examples of rock masses with particularly low CC (left) and particularly low FC (right).** These require relatively more shotcrete (left) and relatively more bolting (right). The original Q-system case records have apparently reflected these different needs, and the Q-parameter ratings developed have given the possibility of realistic CC and FC values.

**Table 3.—Plate load tests driven to failure, with corresponding velocity and modulus data for the different rock masses**  
 (Savich et al. [1974]; see Barton [2006] for other data sets)

Velocity $V_p$ (km/s) .....	2.3	3.7	4.0
Modulus $E_{\text{mass}}$ (GPa) .....	1	3	15
Rock mass $\sigma_{cm}$ (MPa) .....	4	20	50

## CONCLUSIONS

1. Q-system linkages to parameters useful for design are based on sound, simple empiricism that works because it reflects practice and that can be used because it can be remembered. It does not require black-box software evaluation.
2. The wide range of Q-values (0.001–1000) reflects to some degree the very wide range of geological conditions and is probably responsible for the fact that empirical equations based on the Q-value or on  $Q_c$  are particularly simple.
3. The Q-parameters  $J_n$  and  $J_r$  are very useful for evaluating overbreak potential and cavability in mining. When  $J_n/J_r \geq 6$ , significant overbreak will tend to occur, unless limited by timely support close to the excavation face. Caving is also likely to occur relatively unassisted. A modifying factor is, of course, the ratio  $J_r/J_a$ , representing frictional strength. Stress and water pressure are final modifiers.
4. An integration of the Q-value with seismic and permeability data has been developed because there is a limit to how many boreholes can be drilled, how many cores can be logged, and how many permeability tests can be performed. The ability to extrapolate these point sources of information helps to project rock quality classes along a tunnel or to different parts of a large cavern or mine.
5. Due to the effect of increased stress at greater tunnel or cavern depth, it must be expected that deformation modulus and seismic velocity will increase. Eventual sonic logging or crosshole tomography ahead of a tunnel face may therefore give a higher velocity than the rock quality may suggest.
6. Strength criteria of the form “ $c + \tan \phi$ ” used in continuum codes, with links to GSI, have recently acquired remarkable complexity and require software for evaluation of their components. The terms CC and FC from the Q-calculation show promise in giving a direct preliminary estimate of the magnitudes of rock mass cohesive and frictional strength. Logic would suggest that these components should also not be added in an eventual failure criterion.

## REFERENCES

- Barton N [1995]. The influence of joint properties in modelling jointed rock masses. Keynote lecture at the Eighth International Society for Rock Mechanics Congress (Tokyo, Japan), 3:1023–1032. Rotterdam, Netherlands: Balkema.
- Barton N [1988]. Project Oscar – LKAB/LuH: Estimation of shear strength parameters for mine design studies. Oslo, Norway: Norwegian Geotechnical Institute, NGI report 87659–1.
- Barton N [2002]. Some new Q-value correlations to assist in site characterization and tunnel design. Int J Rock Mech Min Sci 39(2):185–216.
- Barton N [2004]. Failure around tunnels and boreholes and other problems in rock mechanics [letter]. ISRM News J 8(2):12–18.
- Barton N [2006]. Rock quality, seismic velocity, attenuation and anisotropy. London and Netherlands: Taylor & Francis.
- Barton N, By TL, Chryssanthakis P, Tunbridge L, Kristiansen J, Løset F, et al. [1994]. Predicted and measured performance of the 62-m span Norwegian Olympic ice hockey cavern at Gjøvik. Int J Rock Mech Min Sci Geomech Abstr 31(6):617–641.
- Barton N, Lien R, Lunde J [1974]. Engineering classification of rock masses for the design of tunnel support. Rock Mech 6(4):189–236.
- Bieniawski ZT [1989]. Engineering rock mass classifications: a complete manual for engineers and geologists in mining, civil and petroleum engineering. John Wiley & Sons, Inc.
- Grimstad E, Barton N [1993]. Updating of the Q-system for NMT. In: Proceedings of the International Symposium on Sprayed Concrete – Modern Use of Wet Mix Sprayed Concrete for Underground Support. Oslo, Norway: Norwegian Concrete Association.
- Hutchinson DJ, Diederichs MS [1996]. Cable bolting in underground mines. Bitech Publishers, Ltd.: Richmond, British Columbia, Canada.
- Peck W [2000]. Determining the stress reduction factor in highly stressed jointed rock. Aust Geomech 35(2).
- Savich AI, Koptev VI, Zamakhaiev AM [1974]. In situ ultrasonic investigation of failure of limestone. In: Proceedings of the Third International Society for Rock Mechanics Congress (Denver, CO), IIA:418–423.
- Sjøgren B, Øfsthus A, Sandberg J [1979]. Seismic classification of rock mass qualities. Geophys Prospect 27: 409–442.



# MECHANIZED EXCAVABILITY RATING FOR HARD-ROCK MINING

By Z. T. Bieniawski, D.Sc. (Eng),<sup>1</sup> and Benjamín Celada, Ph.D.<sup>2</sup>

When you can measure what you are speaking about, and express it in numbers, you know something about it; but when you cannot measure it, when you cannot express it in numbers, your knowledge is of a meager and unsatisfactory kind.

—Lord Kelvin (1824–1907)

## ABSTRACT

After emphasizing the importance of quantitative rock mass classifications in mining, originally directed to selection of rock support measures, but subsequently to estimates of rock mass properties such as rock mass strength and rock mass modulus of deformation, current attention calls for a classification specifically for rock mass excavability by tunnel boring machines (TBMs), which are used extensively in tunneling as well as in the mining industry.

This paper introduces the Rock Mass Excavability (RME) index for predicting excavability of rock masses by TBMs using a quantification of machine performance and rock mass conditions. The RME index is based on five input parameters aimed at relating rock mass behavior and machine characteristics: (1) uniaxial compressive strength of the rock material, (2) drillability/abrasivity, (3) rock mass jointing at mine drift face, (4) standup time of the excavation, and (5) groundwater inflow.

Development of the RME index entailed the collection of extensive data from more than 28 km of tunnels and some 400 case records from projects in Spain involving double-shield TBMs. In the process, a number of statistical correlations have been established between RME and such output parameters as degree of machine utilization, advance and penetration rates, thrust and torque of the cutterhead, and the specific energy of excavation. It was found that the RME index provides a particularly significant correlation for predicting the average rate of advance (m/day).

In essence, the RME index is a classification system that features interaction of rock mass conditions with boring machine characteristics for use in the early stages of a project.

It should be noted that the RME index does not replace the Rock Mass Rating (RMR) or Q-systems as used in mining and tunneling; indeed, one of the RME input parameters, standup time, is determined from the RMR. However, the approach presented introduces a specialized tool relevant to excavating tunnels and drifts. Possible applications to hard-rock mining are explored.

## INTRODUCTION

Rock mass classifications, although originally developed for rock tunneling in civil engineering, have been used in mining for some 35 years, going back to RMR applications in South African hard-rock and coal mining [Bieniawski 1972; Laubscher 1976]. In the United States, research investigations by Kendorski et al. [1983] for hard-rock mining, based on RMR, as well as for coal mining by Unal [1983] for roof support and Kalamaras and Bieniawski [1995] for pillar design, also based on RMR, were highly innovative, and their results are used to this day.

More recently, attention has been paid to rock mass classifications aimed at determining rock mass properties, i.e., rock mass strength and the rock mass modulus of deformation. Examples of particularly useful charts for this purpose are presented in Appendix B of this paper.

Lately, as machine-bored excavations in tunneling become more common than drill-and-blast tunneling, a need emerged for predicting the performance of tunnel boring machines (TBMs) based on considerations of interaction of rock mass conditions and the TBM operational parameters. If successful, such findings would be of equal interest to mining applications.

## PREVIOUS STUDIES

When one considers the history of underground excavation technology, its development, and the major milestones, the emergence and increasing use of modern TBMs provided both spectacular advantages and achievements, as well as complex challenges and problems to designers and constructors who faced significant shortcomings in our understanding of the interaction of rock mass conditions and TBM design and performance.

In fact, when Terzaghi introduced his rock load concept in 1946, followed by Lauffer's standup time concept in 1958 and Deere's Rock Quality Designation (RQD) in 1964, these design approaches were directed to selection of rock reinforcement for tunnel construction by drilling and

<sup>1</sup>Professor, Superior School of Mines, University of Madrid, Spain, and President, Bieniawski Design Enterprises, Prescott, AZ.

<sup>2</sup>Professor, Superior School of Mines, University of Madrid, Spain, and President, Geocontrol, S.A., Madrid, Spain.

blasting. The equipment selected for tunnel excavation was left to the discretion of the contractor, with little input by the designer. Even subsequent modern rock mass classification methods [Bieniawski 1973; Barton 1974] were predominantly directed to drill-and-blast tunnels, independent of TBM characteristics.

Today, this is no longer the case. TBMs have increased in power, size, and type to such an extent that they directly influence tunnel design. Moreover, their selection is a source of tremendous satisfaction due to increased safety and higher performance, as well as deep despair when unexpected ground conditions are encountered and the TBM may be immobilized for months and sometimes has to be rescued by old-fashioned hand mining or conventional drill-and-blast excavation.

A major problem emerged: how to assess effectively the interaction between rock mass conditions, as described by the RMR or Q classification systems, and the design and performance characteristics of the TBM. Certainly, some attempts to solve this problem have been made, as reviewed below, but the state of the art still rests on the TBM manufacturers and tunnel contractors that must rely on their experience, ingenuity, and even the will to survive many adverse conditions.

## STATE OF THE ART IN ROCK EXCAVABILITY

Excavability is defined as the ease of excavation and was investigated as early as Kirsten [1982]. TBM excavability or performance prediction models were studied by Barton [2000], Alber [2001], Bieniawski [2004], Blindheim [2005], and others.

In essence, it is recognized that the choice between a TBM and drilling and blasting can be quantified based on rock mass quality and machine characteristics. An example of an interdependence function is the  $Q_{TBM}$  formulation [Barton 2000]:

$$Q_{TBM} = \frac{RQD_0}{J_n} \times J_r / J_a \times J_w / SRF \times \sigma_{MASS} / F \times 20 / CLI \times q / 20 \quad (1)$$

where CLI = cutter life index (Norwegian Institute of Technology), SRF = stress reduction factor, F = average cutter load (tnf), q = quartz content (%).

Equation 1 received much attention, but was also severely criticized [Blindheim 2005]. In this research, the above relationship was also tested, but without success because of the problem with the definition of rock mass strength,  $\sigma_{MASS}$ , which is based on “inversion of  $\sigma_c$  to a rock mass strength, with correction for density,” rendering it unacceptable. Nevertheless, Abrahão and Barton [2003] applied this equation with all 21 parameters (“for which no apology is made,” declared the authors), emphasizing that the rock-machine interaction in tunneling is very complex.

Subsequently, the key objection to  $Q_{TBM}$  was provided by a major study from Norway (where the Q-system was invented) published by Palmström and Broch [2006]. They concluded:

$Q_{TBM}$  is complex and even misleading and shows low sensitivity to penetration rate; the correlation coefficient with recorded data is even worse than conventional Q or RMR or with other basic parameters like the uniaxial compressive strength of the intact rock. It is recommended that the  $Q_{TBM}$  should not to be used.

This finding is clearly supported by Figure 1.

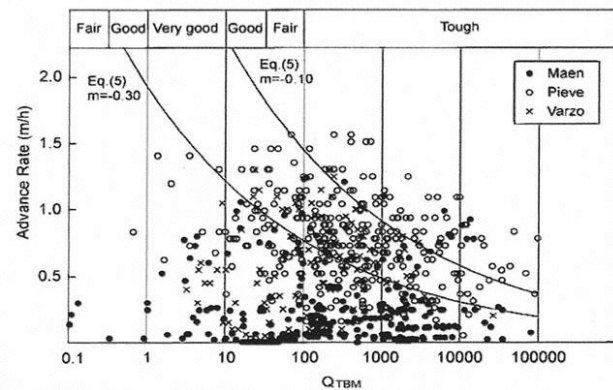


Figure 1.—Advance rates for three TBM tunnels plotted against  $Q_{TBM}$  [Sapigni et al. 2002].

Other attempts were reported by Alber [2001] concentrating on contracting practice and probabilistic estimates of advance rates and project economics. The RMR system was used by Grandori et al. [1995] to demonstrate ranges of effectiveness for TBM performance in different rock mass quality as a function of machine type: open TBM or double-shield. Bieniawski [2004] reviewed the concept of rock mass excavability based on the RMR as adjusted for TBMs.

However, there is convincing evidence that complex equations combining rock mass quality RMR or Q with additional parameters related to TBM characteristics are not an effective approach. In other words, it is doubtful that one formula can include all the factors pertinent to rock mass quality, as well as those influencing TBM choice and performance.

In fact, expert opinion holds that the RMR and Q-systems are most effective as they are commonly used, consistent with the purposes for which they were developed. Thus, adjusting these systems for TBM-sensitive parameters, such as rock abrasivity and cutter thrust, may be counterproductive and may only create confusion.

## THE CONCEPT OF THE ROCK MASS EXCAVABILITY (RME) INDEX

After much overwhelming evidence, such as shown in Figure 1, we concluded that modifying an existing rock mass quality classification, be it the RMR or Q, for determining rock mass excavability was not an effective approach for modern engineering practice. Accordingly, research devoted to rock mass excavability was initiated in 2004 with the objective of establishing an index, similar to the RMR, but which was specifically directed to predicting rock mass excavability, rather than rock mass quality. This work was aimed at selecting the appropriate method of tunnel excavation, having considered rock mass-machine interaction, using TBMs or conventional mechanized excavation. The RME concept proposed first by Bieniawski et al. [2006] was based on analyses of 387 sections of three Spanish tunnels comprising 22.9 km in length. In each case, the tunnels studied included detailed data on rock mass characteristics and TBM parameters, as shown in the RME input data form in Figure 2.

<b>INPUT DATA FORM for Rock Mass Excavability</b>	
Name of Tunnel .....	
Initial chainage of section:.....Final chainage of section:.....	
Length of section:.....m (should be > 40 m)	
Duration of excavation (days):..... (number + 1 decimal)	
Average Rate of Advance ARA = .....m/day	
Lithology:.....Average depth:.....m	
<b>ROCK MASS PARAMETERS</b>	
Uniaxial compressive strength of intact rock ( $\sigma_c$ ):..... MPa	
Drilling Rate Index DRI:..... Type of homogeneity at excavation face:.....	
N° of joints per meter:.....Rock Mass Rating RMR: range.....average.....	
Orientation of discontinuities with respect to tunnel axis (perpendicular, parallel or oblique):.....	
Stand up time:.....hours Groundwater inflow at tunnel face: .....liters/sec	
Rock Mass Excavability RME range .....average.....	
<b>TBM PARAMETERS</b>	
Average speed of cutterhead rotation: ..... rpm Applied Thrust:.....m . kN	
Specific Penetration:.....mm /rev	
Rate of Penetration:..... mm /min	
N° cutters changed:..... Rate of TBM utilization: .....% .....	

**Figure 2.—Input data form for determining the Rock Mass Excavability (RME) index.**

**Table 1.—Input ratings for Rock Mass Excavability (RME) index**

UCS OF INTACT ROCK (0–25 points)						
$\sigma_c$ (MPa).....	<5	5–30	30–90	90–180	>180	
Average rating .....	4	14	25	14	0	
DRILLABILITY (0–15 points)						
Drilling Rate Index ....	>80	80–65	65–50	50–40	<40	
Average rating .....	15	10	7	3	0	
DISCONTINUITIES AT TUNNEL FACE (0–30 points)						
Homogeneity			Number of joints per meter			Orientation with respect to tunnel axis
	Homo-geneous	Mixed	0–4	4–8	8–15	Perpendicular      Oblique      Parallel
Avg. rating	10	0	2	7	15	5      3      0
STANDUP TIME (0–25 points)						
Hours .....	<5	5–24	24–96	96–192	>192	
Average rating .....	0	2	10	15	25	
GROUNDWATER INFLOW (0–5 points)						
L/sec .....	>100	70–100	30–70	10–30	<10	
Average rating .....	0	1	2	4 <sup>1</sup>	5	

<sup>1</sup>Zero for argillaceous rocks.

## SELECTION OF RME INPUT PARAMETERS

The RME index is based on the five input parameters listed in Table 1, together with the ratings associated with each. Selecting the five parameters involved a Linear Discriminant Analysis using the R code developed by the Institute of Statistics and Probability Theory of the Vienna University of Technology, Austria. As a result of this analysis, it was found that the parameters with stronger influence in the average rate of advance (ARA), expressed in m/day, are: drillability/abrasivity, discontinuity spacing, and standup time. In addition, it was decided to include the two basic rock mechanics parameters: uniaxial compressive strength (UCS) of the rock material and water inflow because these two factors are known to strongly influence the TBM advance. Once the five parameters were selected, a weighted distribution was performed. These weights have been statistically analyzed, minimizing the error in the ARA prediction and resulting in the ratings shown in Table 1.

In practice, four of the input parameters are determined from standard site exploration programs: UCS of the rock material, rock drillability, rock mass jointing (spacing, orientation, and condition of discontinuities at the tunnel front), and groundwater inflow. The fifth parameter, standup time, is estimated from the well-known RMR chart (Figure 3), which depicts standup time versus unsupported active span as a function of RMR (after Bieniawski [1989]; see also Appendices A and B of this paper). As the case studies on that chart were derived from drill-and-blast tunnels, a correlation obtained by Alber [1993] is used for TBM tunnels. The following equation is applicable:

$$RMR_{TBM} = 0.8 \times RMR_{D\&B} + 20 \quad (2)$$

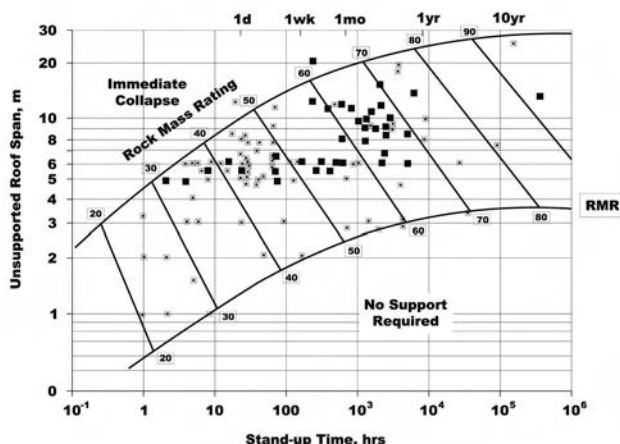


Figure 3.—Standup time as a function of RMR and unsupported span [Bieniawski 1989].

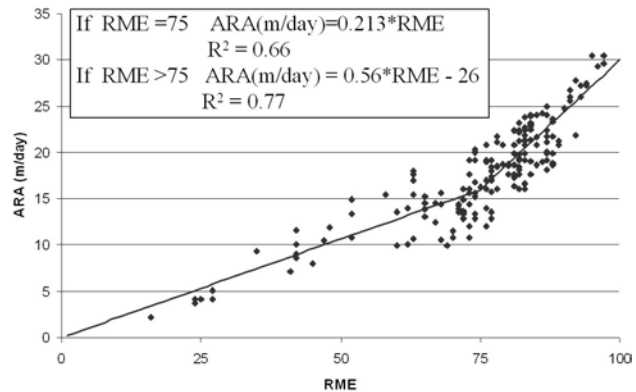


Figure 4.—Correlation between the RME index and the average rate of advance (m/day) for single- and double-shield TBMs.

## CORRELATION BETWEEN AVERAGE RATE OF ADVANCE (ARA) AND RME

The average rate of advance (ARA), expressed in m/day, is the most significant parameter to compare performances from several tunnel or drift construction projects. The statistical analyses carried out provided the correlation depicted in Figure 4 between the ARA and RME for single- and double-shield TBMs.

These findings were derived for tunnels with diameters close to 10 m. In order to take into account the influence of other tunnel diameters, D, the coefficient kD is used. The values of kD can be calculated from the following expression:

$$kD = -0.007D^3 + 0.1637D^2 - 1.2859D + 4.5158 \quad (3)$$

## CORRELATIONS OF RME WITH OTHER PARAMETERS

A number of significant correlations were obtained in this study in addition to those discussed above.

### Specific Energy of Excavation

The concept of specific energy of excavation ( $E_s$ ) for mechanized tunneling and mining is “borrowed” from the petroleum and gas drilling industry, where it has been used for many years [Teale 1965]. Most recently, this concept was applied to assess the ease of mechanical excavation involving this expression:

$$E_s = F/A + 2\pi N T / A \times ARA \quad (4)$$

where  $E_s$  = specific energy of excavation ( $\text{kJ}/\text{m}^3$ );  
 $F$  = total cutterhead thrust ( $\text{kN}$ );  
 $A$  = excavated face area ( $\text{m}^2$ );  
 $N$  = cutterhead rotation speed (rps);  
 $T$  = applied torque ( $\text{kN}\cdot\text{m}$ );  
and  $ARA$  = average rate of advance ( $\text{m}/\text{s}$ ).

The above equation consists of two terms. The first represents the specific energy of the cutterhead thrust from static loading, while the second is the specific energy of rotation incurred by the rotating cutterhead. In this study, the specific energy of rotation ( $E_r$ ) was related to the RME in Figure 5.

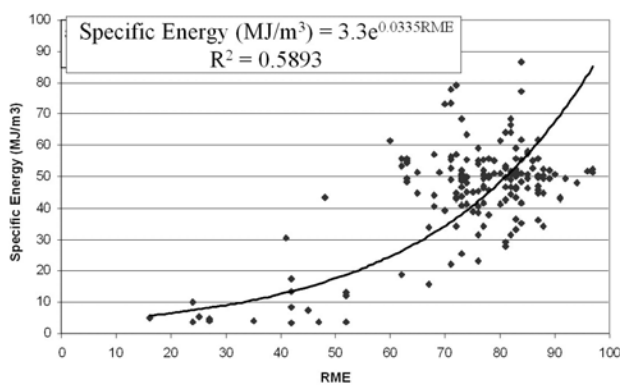


**Figure 5.—Correlation between the RME index and the specific energy of excavation.**

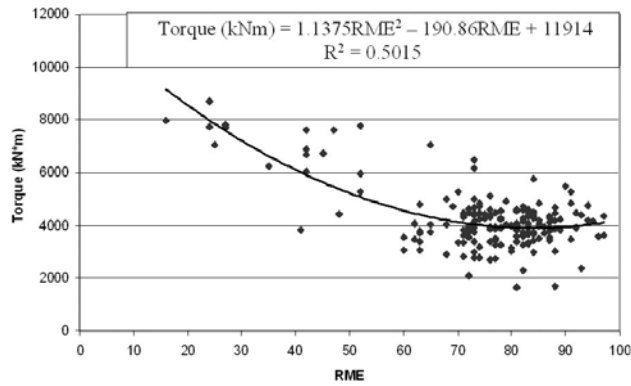


**Figure 6.—Correlation between the RME index and TBM torque.**

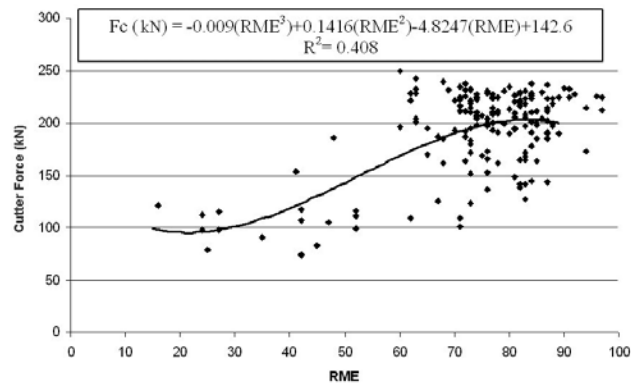


**Figure 7.—Correlation between the RME index and cutterhead thrust.**

### Cutterhead Thrust ( $F_C$ ) and Torque ( $T$ )

Figures 6–7 show the correlation of RME with both  $F_C$  and  $T$  values, providing acceptable coefficients of  $R=0.64$  and  $R=0.71$ , respectively, for single- and double-shield TBMs.

### LATEST FINDINGS

The construction of the famous Guadarrama tunnels involving two tubes, each 9.5 m in diameter and 28 km long, using four double-shield TBMs, led to the introduction of an adjustment to the predicted ARA obtained from a given RME, incorporating the effect of the length of the tunnel excavated and the influence of the crew skills when dealing with the TBM and the terrain. This can be represented as

$$ARA_T = \frac{ARA_R}{F_L \times F_C} \quad (5)$$

where  $ARA_T$  = predicted true value of ARA from the correlation with RME;  
 $ARA_R$  = recorded average rate of advance, m/day, achieved in a tunnel section;  
 $F_L$  = factor of experience as a function of tunnel length excavated;  
and  $F_C$  = factor of effectiveness by the crew handling the TBM and the terrain.

Based on the results obtained during construction of the Guadarrama and Abdalajís Tunnels, Tables 2–3 show the values appropriate for the coefficients  $F_L$  and  $F_C$ .

**Table 2.—RME adjustment factor ( $F_L$ )**

Tunnel length excavated (km)	Adjustment factor ( $F_L$ )
0.5.....	0.50
1.0.....	0.86
2.0.....	0.97
4.0.....	1.00
6.0.....	1.07
8.0.....	1.12
10.0.....	1.15
12.0.....	1.20

**Table 3.—RME adjustment factor ( $F_c$ )**

Effectiveness of the crew handling TBM and terrain	Adjustment factor ( $F_c$ )
Less than efficient.....	0.88
Efficient.....	1.00
Very efficient.....	1.15

This produces a refined RME<sub>07</sub> correlation depicted in Figure 8 devoted specifically to double-shield TBMs.

### SPECIAL CONSIDERATIONS FOR APPLICATIONS IN MINING

Applications of rock mass classifications in mining require some special considerations compared to civil engineering for a number of reasons. The three most important are—

1. The effect of in situ stresses, since mines are usually deeper than tunnels;
2. The effect of the induced stresses, because in mining the stress field changes as mining advances and also due to adjacent excavations; and

3. The effect of blasting damage, because in hard-rock mining drilling and blasting, unless smooth blasting is used, may have an adverse effect on stability compared to machine boring.

As a matter of fact, all of the above effects were incorporated into the Mining Basic RMR (MBR) classification proposed by Kendorski et al. [1983].

There are various types of excavating machines used in mining. In modern hard-rock mines, machine excavation is used to construct access drifts and chambers, while in coal mines, continuous miners and shearers are common. In each case, to access mineral deposit production, mines employ roadheaders and/or open-type TBMs.

The RME index can be applied directly to evaluate excavability of mine drifts and chambers. However, at the time of writing, work on correlations between the RME and ARA is still in progress for roadheaders and open TBMs. In fact, investigations to determine a correlation between the RME and ARA for open-type TBMs began last year, with results expected to be presented by June 2007.

As far as applications to roadheaders and similar machines are concerned, we are still in the process of data collection and would welcome any case histories of RME applications in this respect by interested parties. In

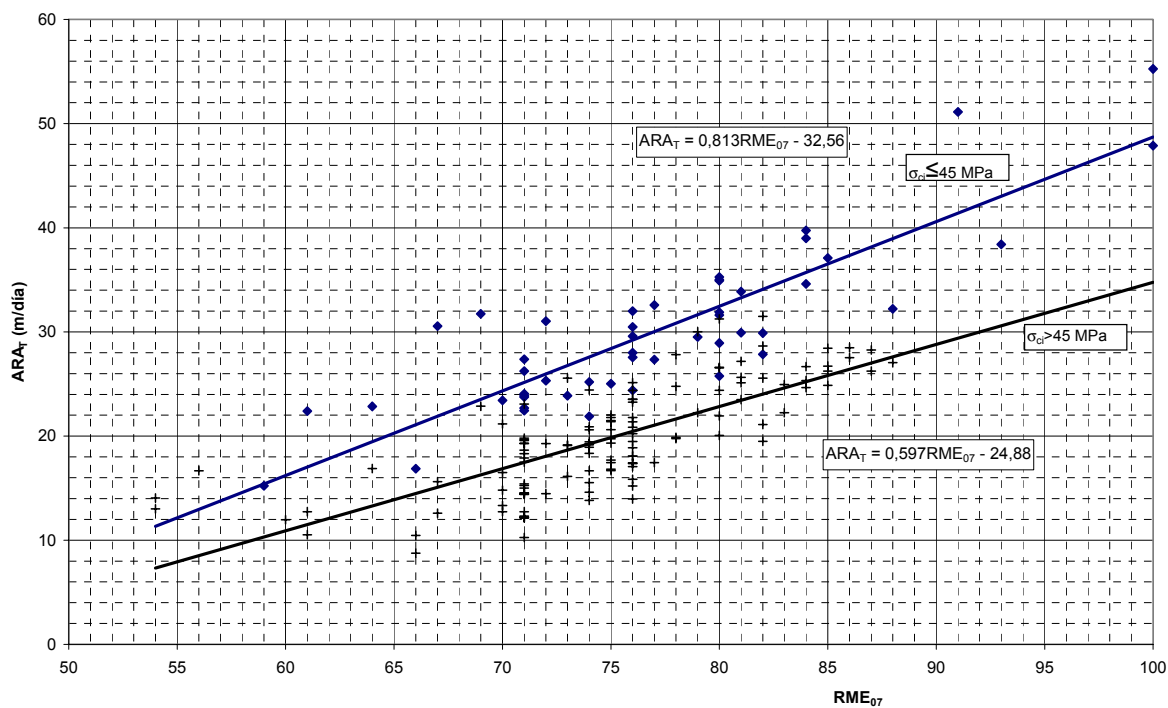


**Figure 8.—Correlation between the RME<sub>07</sub> and the average rate of advance for double-shield TBMs. For RME<50, TBMs in double-shield mode are not recommended.**

addition, applications in room-and-pillar and longwall mining will require modifications to the actual structure of the RME index due to the specific nature of such mining operations. For example, the ratings for the standup time parameter may require an adjustment factor due to the degree of fracturing in the roof strata and due to the effect of the induced stress in order to better assess the stability of the rock mass in these types of mining operations.

## CONCLUSIONS

After 3 years of studies and analyses of more than 400 case histories, RME seems to provide a tool that enables tunnel designers and constructors to estimate the performance of TBMs. Future work will focus on extending the RME to all types of TBMs and improving the existing correlations with the significant operational output parameters. Extending this work for more applications to mining provides challenging opportunities.

## ACKNOWLEDGMENTS

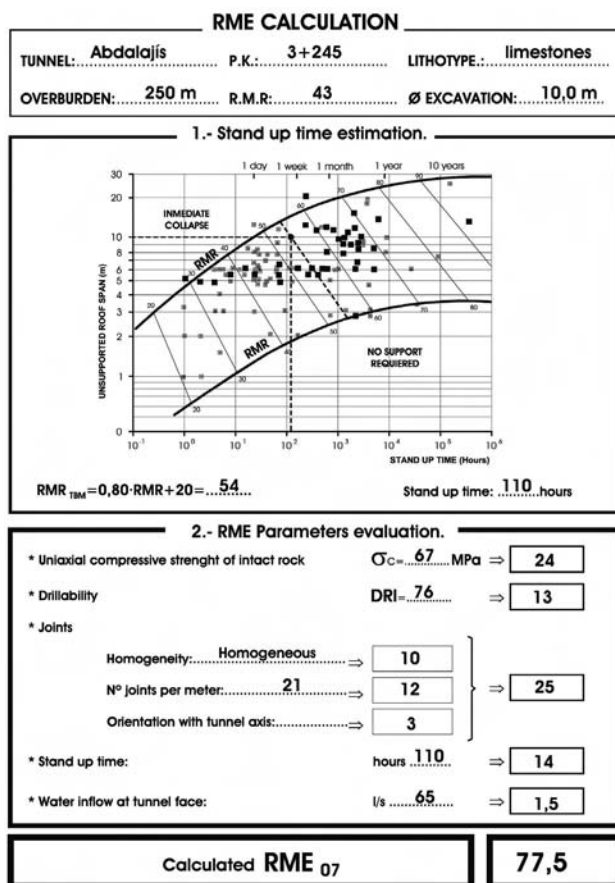
This paper was made possible by the dedicated work of the professional staff at Geocontrol, S.A., Madrid, Spain, including the first two recipients of the Bieniawski Scholarship for tunneling research at the Superior School of Mines, Universidad Politécnica de Madrid: Doña María Álvarez Hernández and currently Don José Carballo Rodríguez. These Bieniawski Scholarships were generously funded by Geocontrol, S.A.

## REFERENCES

- Abrahão RA, Barton N [2003]. Employing TBM prognosis model. *Tunnels & Tunnelling Int* 35(12):20–23.
- Alber M [1993]. Classifying TBM contracts. *Tunnels & Tunnelling Int Dec*:41–43.
- Alber M [2001]. Advance rates for hard-rock TBMs and their effects on project economics. *Tunnelling Undergr Space Technol* 15(1):55–60.
- Barton N [1974]. Engineering classification by the Q-system. *Rock Mech* 6(4):183–236.
- Barton N [2000]. TBM tunneling in jointed and faulted rock. Rotterdam, Netherlands: Balkema.
- Bieniawski ZT [1972]. Engineering classification for rock masses. Rep S Afr Coun Sci Ind Res, ME 327/Rock Mech, Pretoria, South Africa.
- Bieniawski ZT [1973]. Geomechanics classification of jointed rock masses. *J S Afr Inst Civ Eng Dec*:382–398.
- Bieniawski ZT [1989]. Engineering rock mass classifications: a complete manual. New York: John Wiley & Sons.
- Bieniawski ZT [2004]. Aspectos clave en la elección del método constructivo de túneles (in Spanish). In: Proceedings of Jornada Técnica (Madrid, Spain), pp. 1–37. Also in: Ingeopress, No. 126, pp. 50–68.
- Bieniawski ZT, Celada B, Galera JM, Álvares M [2006]. Rock mass excavability (RME) index: a new way to select the optimum tunnel construction method. In: Proceedings of the ITA World Tunnelling Congress (Seoul, South Korea).
- Blindheim OT [2005]. A critique of  $Q_{TBM}$ . *Tunnels & Tunnelling Int* 6:32–35.
- Grandori R, Jager M, Vigl, L [1995]. The Evinos TBM tunnel. In: Proceedings of the Rapid Excavation and Tunneling Conference. American Society of Civil Engineers, pp. 132–146.
- Kalamaras ES, Bieniawski ZT [1995]. A rock mass strength concept incorporating the effect of time. In: Proceedings of the ISRM Congress (Tokyo, Japan). Balkema, pp. 295–302.
- Kendorski FS, Cummings RA, Bieniawski ZT, Skinner EH [1983]. Rock mass classification for block caving mine drift support. In: Proceedings of the 15th ISRM Congress (Melbourne, Victoria, Australia). Balkema, pp. B101–B113.
- Kirsten HAD [1982]. A classification for excavation. *Civ Eng S Afr* 7:293.
- Laubscher DH, Taylor HW [1976]. The importance of geomechanics of jointed rock masses in mining operations. In: Proceedings of the Symposium on Exploration for Rock Engineering (Johannesburg, South Africa), pp. 119–128.
- Palmström A, Broch E [2006]. Use and misuse of rock mass classification systems with particular reference to the Q-system. *Tunnelling Undergr Space Technol* 21(6):575–593.
- Sapigni M, Berti M, Bethaz E, Bustillo A, Cardone G [2002]. TBM performance estimation using rock mass classifications. *Int J Rock Mech Min Sci* 39:771–788.
- Teale R [1965]. The concept of specific energy in rock drilling. *Int J Rock Mech Min Sci* 2:57–73.
- Unal E [1983]. Design guidelines and roof control standards for coal mine roofs [Dissertation]. University Park, PA: The Pennsylvania State University.

## APPENDIX A.—EXAMPLE OF RME CALCULATIONS

The figure below presents an example of the actual procedure for calculating  $RME_{07}$  for one of the case histories plotted in Figure 8.



## APPENDIX B.—GENERAL GUIDELINES ON ROCK MASS CLASSIFICATIONS (BASED ON THE RMR SYSTEM: 35 YEARS LATER)

The Rock Mass Excavability classification features one parameter—standup time—depicted in Figure 3, which is determined from the Rock Mass Rating (RMR), as shown in Appendix A. Since RMR was first introduced in 1972 and published internationally in 1973, it is appropriate to briefly summarize some of the lessons acquired about rock mass classifications after 35 years of use throughout the world.

The most important aspect to remember is that the main application of RMR is not just recommendations for rock support (because they change as technology changes), but estimation of rock mass properties for design and numerical purposes, i.e., the modulus of deformation of the rock mass, rock mass strength, and standup time. Figures A-1 and A-2 depict these strength and deformation relationships. In fact, the RMR case histories for these purposes still remain the prime data for analyses and correlations and are published in full [Bieniawski 1989].

There are three general guidelines to be observed for good engineering practice:

1. Rock mass classifications, either quantitative systems, such as RMR and Q, or descriptive methods (New Austrian Tunneling Method (NATM) or Geological Strength Index (GSI)), are most effective if not used on their own, but incorporated within the overall engineering design process.
2. Rock mass classifications on their own should only be used for preliminary planning purposes and not as final rock reinforcement. For preliminary design and planning purposes, the two quantitative RME and Q-systems are excellently suited. They quantify rock mass conditions, enable estimates of rock mass properties, and provide the reference bases for expected rock mass conditions.
3. The two predominant quantitative rock mass classifications, RMR and Q, are particularly essential for monitoring rock conditions during construction or mining to enable effective comparison of predicted conditions from site investigation with those encountered. For this purpose, descriptive classifications (those not based on quantitative input data) are deficient. They do not provide a continuous quantification of the encountered conditions, even if based on deformation measurements during construction, because contractual specifications in many countries prevent enough measurements to be taken since they interfere with the mining or tunneling schedule.

Most of all—users, please beware! It is not recommended to apply any rock mass classification system on its own, be it NATM, RMR, or Q. Instead, both RMR and Q should always be used to cross-check the results and compare recommendations, even if known correlations exist between these two systems, which sometimes turn out to be oversimplifications.

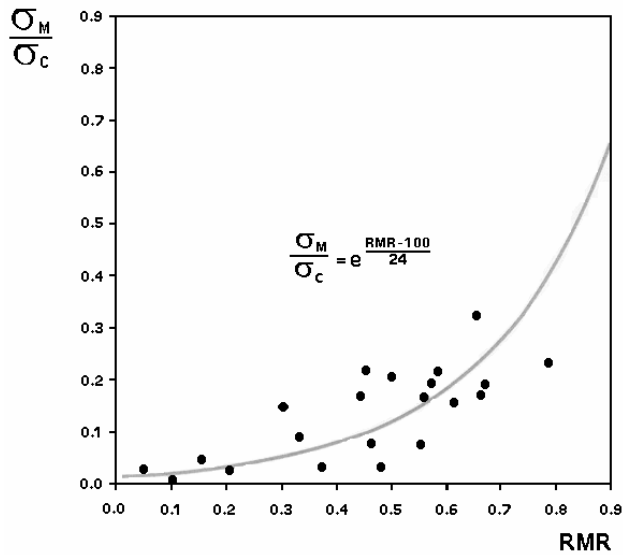


**Figure A-1.**—Correlation between the ratio of rock mass strength,  $\sigma_M$ , and UCS of rock material,  $\sigma_c$ , as a function of RMR [Kalamaras and Bieniawski 1995].

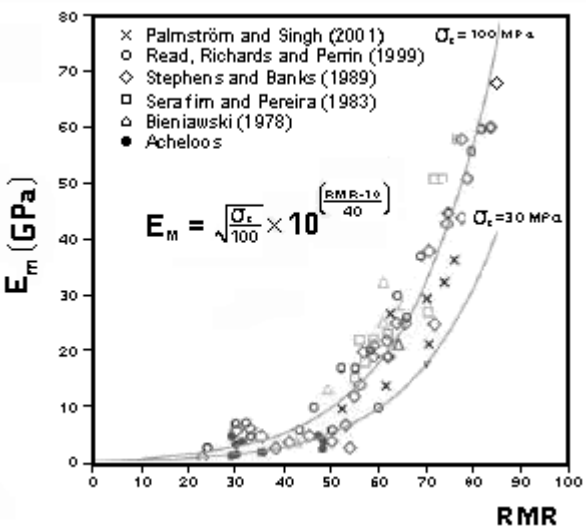


**Figure A-2.**—Correlation between the modulus of deformation,  $E_M$ , and RMR.



# ROCK MASS CHARACTERIZATION OF PRIMARY COPPER ORE FOR CAVING AT THE EL TENIENTE MINE, CHILE

By Andres Brzovic<sup>1</sup> and Ernesto Villaescusa, Ph.D.<sup>2</sup>

## ABSTRACT

Rock masses of the primary copper ore at the El Teniente Mine are very competent and massive. The rock mass contains almost no open discontinuities. Nevertheless, there is a high frequency network of small discontinuities coupled with widely spaced faults. A data collection campaign designed to characterize the rock structure was recently implemented. The results show that conventional analysis in terms of discontinuity frequency does not predict differences between two studied sectors. However, when an empirical definition of a weak discontinuity is applied, appreciable differences between the two sectors appear in terms of discontinuity frequency and predicted in situ block size distributions. These differences are in accordance with actual observations at the mine site. Due to the geological features of the primary copper ore, rock mass classification schemes cannot be readily applied to characterize these rock masses.

## INTRODUCTION

Rock mass classification systems have been developed and used since the 1950s as useful design tools in civil and mining projects. Initially developed for tunneling reinforcement [Terzaghi 1946], these have been extended to multiple civil engineering applications [Barton et al. 1974; Hoek et al. 1995; Laubscher 1993].

The rock mass classification schemes are based on the parameterization of the geological features of the rock mass. These systems simplify the rock mass into two main components: the intact rock properties and the discontinuity characteristics. The International Society for Rock Mechanics (ISRM) has suggested guidelines to characterize these geological features [ISRM 1978].

Following ISRM's guidelines, a data collection campaign designed to characterize the rock structure of the primary copper ore was implemented recently at the

El Teniente Mine. This paper presents some results of this current research [Brzovic 2005]. Some data analyses previously published [Brzovic et al. 2006; Brzovic and Villaescusa 2007] are used here since they are relevant to consider when the rock mass classification schemes are applied.

## El Teniente Mine Overview

The El Teniente Mine, located in the Andes Mountains in central Chile, 70 km south of Santiago (Figure 1), is one of the largest underground mine operations in the world. Since 1906, more than 1.1 billion tons of ore has been mined. The mine is a state-owned company (Codelco), and it is currently extracting 131,000 tons per day using block-caving methods. Panel (called conventional) and pre-undercut caving methods [Rojas et al. 2000b], variations of standard block caving, were introduced in 1982 and 1994, respectively, to exploit the primary copper ore (Figure 2).

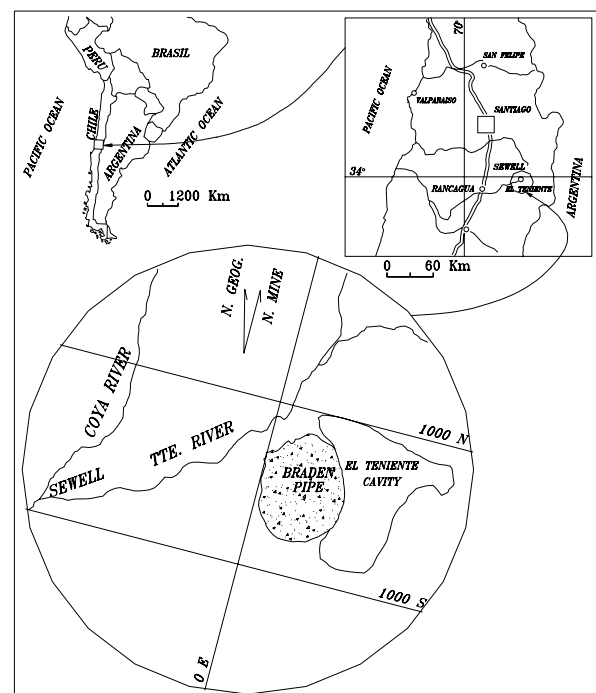


Figure 1.—Location of the El Teniente Mine.

<sup>1</sup>CRC Mining, Western Australian School of Mines, Kalgoorlie, Australia, and Codelco Division El Teniente, Millan, Rancagua, Chile.

<sup>2</sup>CRC Mining, Western Australian School of Mines, Kalgoorlie, Australia.

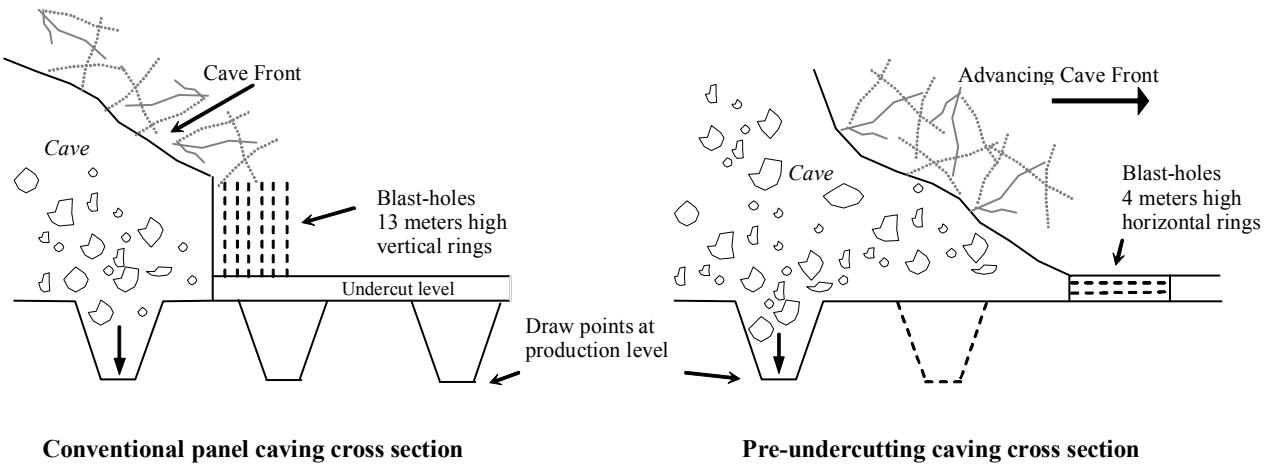


Figure 2.—Panel and pre-undercut caving methods at the El Teniente Mine.

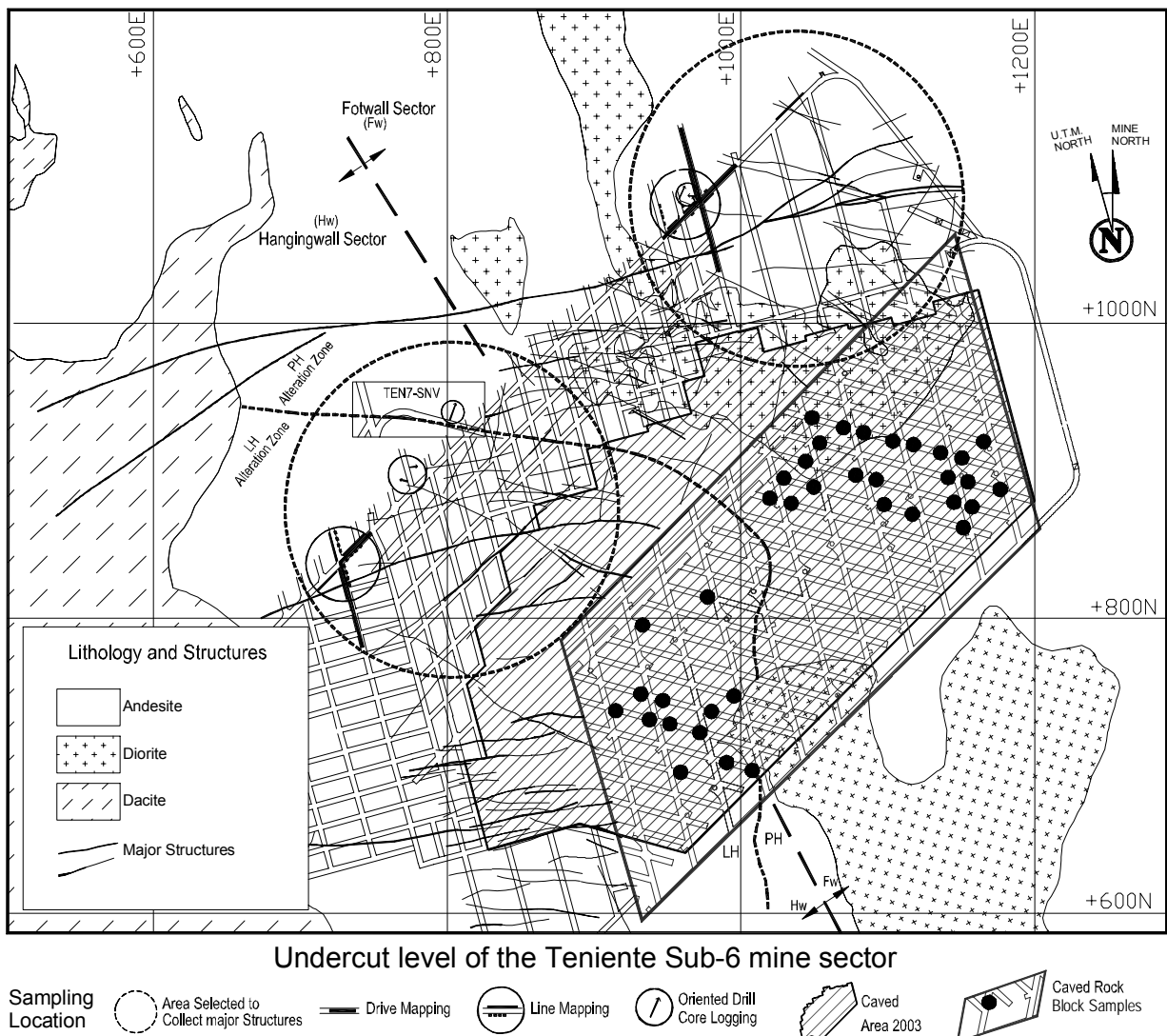


Figure 3.—Geology of the studied sectors and sampling locations for line sampling techniques and the collected caved rock blocks.



**Figure 4.**—Stockwork veins (most white lines) and faults (middle of the left photo) recognized within the primary copper ore. The right photo is rock block (1.4-m-long base) showing the stockwork veins, which is used as a monument in Rancagua, Chile.

Currently, almost all of the caving operations are being undertaken within primary copper ore. Such rock masses are very competent and massive, exhibiting brittle, often violent failure under high-stress conditions [Rojas et al. 2000a]. Caving generally results in large rock fragments. Despite these unfavorable rock mass conditions, high rates of production have been achieved since primary copper ore extraction by the conventional panel caving method began in 1982.

### Geology and Rock Mass Properties

El Teniente is the largest known copper-molybdenum deposit in the world [Skewes et al. 2006]. It is hosted in a copper porphyry system [Cannell et al. 2005]. The main rock types include a mafic intrusive complex (andesite for this paper), felsic porphyry intrusive (dacite and diorite) and hydrothermal breccias (Braden breccia) of the Miocene Era (Figure 3). Two main structure types are observed within the primary copper ore: a system of large-scale faults [Garrido et al. 1994] and a stockwork having a high frequency of small-scale vein features [Brzovic and Villaescusa 2007; Cuadra 1986], as shown in Figure 4.

The stockwork veins observed within primary copper ore are mainly filled and cemented (healed) with quartz, sulfides, and anhydrite (Figure 4). Different vein types have been identified, and these define alteration zones according to their local abundance. Main alteration zones

are referred to as shown in Figure 3: the late hydrothermal (LH) zone and the principal hydrothermal (PH) zone [Cuadra 1986].

Open joints are rarely found within the primary copper ore, and faults have a very low frequency of occurrence in line sampling ( $0.1 \text{ m}^{-1}$ ) [Brzovic 2001]. Joints and faults are the only open discontinuities at the El Teniente Mine. Thus, the primary copper ore rock mass prior to caving can be described as very competent, massive, and impermeable. Intact rock mass properties and rating of rock mass quality used in current mine planning, for main rock types, are presented in Table 1 [Celhay et al. 2005].

### Data Collection Design

In order to characterize the rock structure of the primary copper ore, line sampling techniques were undertaken in mine drives within two levels of the Teniente Sub-6 Mine sector (Figure 3). Two structural domains referred to as andesite Hw (hangingwall) and Fw (footwall) were characterized by applying different truncation and censoring biases [Brady and Brown 2003; Villaescusa 1990]. These sampling biases can be considered as different mapping scales (Table 2). A detailed description of the sampling regime adopted in this study is presented by Brzovic and Villaescusa [2007].

**Table 1.—Mean of the intact rock mass properties and rock mass quality used for main rock types [Celhay et al. 2005]**

Rock type	Intact rock properties				Rock mass rating		
	Density (ton/m <sup>3</sup> )	E (GPa)	v	UCS (MPa)	RMR <sub>L</sub>	Q'	GSI
Braden breccias.....	2.61	21	0.19	70	—	—	—
Dacite .....	2.63	30	0.18	90	59–66	22–32	75–95
Diorite .....	2.77	45	0.21	140	64	19	75–90
Andesite.....	2.77	56	0.20	115	53–59	19–22	70–85

NOTE.—E, Young's modulus; v, Poisson's ratio; RMR<sub>L</sub> from Laubscher [1993]; Q' adapted from Barton et al. [1974]; and Geological Strength Index (GSI) from Hoek et al. [1995].

**Table 2.—Censoring level, truncation biases, and sample length applied to different line sampling techniques**

Sampling method	Censoring level <sup>1</sup> (m)	Truncation bias (m)	Range of the horizontal sample length (m)
Major structure interpretation.....	—	30	150
Drive mapping .....	4.4–4.9	4	30–150
Line mapping .....	3.6–4	<sup>2</sup> 0.3	7–22
Oriented drill core logging.....	0.1–0.14	<sup>2</sup> 0.1	4–12

<sup>1</sup>Censoring level only considers the maximum high or width of the observation window.

<sup>2</sup>Some discontinuities longer than the threshold value could not be collected during data collection.

## ROCK STRUCTURE CHARACTERIZATION

Although 8 of the 10 suggested parameters by ISRM were fully characterized in both sectors [Brzovic 2005], only the relevant ones are detailed in the following sections.

### Discontinuity Occurrence at Different Mapping Scales

Taking into account the main geological discontinuities found within primary copper ore [Brzovic 2001; Cuadra 1986; Garrido et al. 1994], the occurrence for main discontinuity types observed in line mapping is presented in Table 3.

Although the occurrence of discontinuities does not consider the natural anisotropy of the rock structure, some relevant aspects are deduced from Table 3. This is considering the fact that, in most cases, a similar sampling orientation with respect to discontinuity orientation was used for all of the mapping scales [Brzovic and Villaescusa 2007]. Firstly, excluding faults, open joints are not found within the primary copper ore; instead, a large number of veins were recognized (Figure 4). Secondly, faults were better characterized using large-scale sampling. In contrast, veins were better characterized using small-scale sampling. In other words, faults and veins are present within the primary copper ore at different scales. These discontinuity characteristics do not depend on the sampling regime, as discussed by Brzovic and Villaescusa [2007].

**Table 3.—Discontinuity type occurrence observed for each data collection technique**

Sampling method	Sector	Data	Discontinuity occurrence (%)	
			Faults	Veins
Major structures interpretation.....	Hw	21	57.1	42.9
	Fw	22	77.3	22.7
Drive mapping .....	Hw	239	16.7	83.3
	Fw	206	30.5	69.5
Lines mapping .....	Hw	521	1.9	98.1
	Fw	319	7.2	92.8
Oriented drill core logging .....	Hw	606	0.3	99.7
	Fw	565	1.9	98.1

Hw Hangingwall. Fw Footwall.

### Discontinuity Orientation

Faults were found defining one or two subvertical sets at each sector (using large mapping scale). Although subhorizontal faults were not entirely defined by large-scale sampling, the fault data are in agreement with the strike-slip fault characteristics described at the mine scale [Garrido et al. 1994]. In contrast, data from small-scale sampling show that, for both sectors, the veins comprise at least three semiorthogonal discontinuity sets. Figure 5 shows examples of both fault and vein contour orientations from drive and line mapping at the Hw sector.

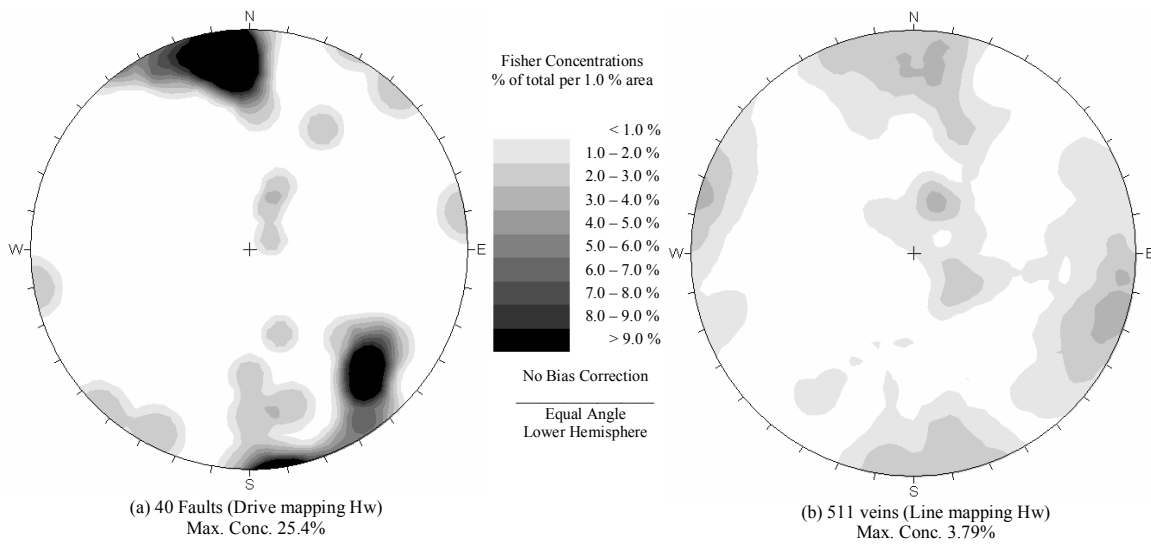


**Figure 5.—Fault (a) and vein (b) contour orientations plotted in lower hemisphere projections.**

### Discontinuity Spacing

The mean normal fault set spacing determined only by large-scale sampling ranges mainly between 5 and 10 m, which is in agreement with previous work [Brooks et al. 1996; Brzovic 2001]. Conversely, high vein frequency was found using small-scale sampling. However, the discontinuity spacing is strongly influenced by the truncation bias used, as Figure 6 shows. Assuming that each truncation level applied represents a mapping scale, the mean normal discontinuity set frequency may be represented as a fractal feature within the rock mass. Scaling law properties (fractal and lineal) for the spacing on other parameters of the geological discontinuities have been proposed by several authors [Cladouhos and Marrett 1996; Gillespie et al. 1993; Hobbs 1993; Scholz 2002], which are consistent with this finding. It is important to

recognize that the truncation bias used during data collection plays a relevant role in the spacing obtained, particularly if the rock mass classification schemes are applied.

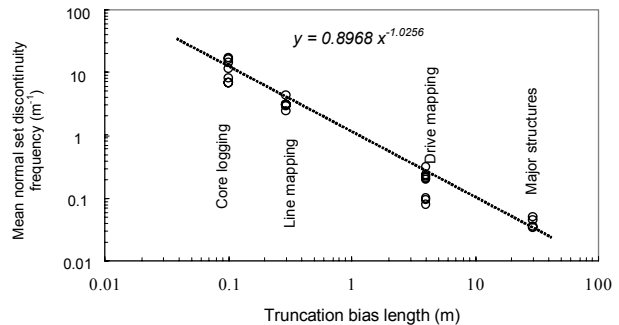


**Figure 6.—Discontinuity frequency and truncation bias length.**

**Table 4.—Extremes in values of discontinuity frequency and their orientation using three-dimensional loci [Hudson and Priest 1983]**

Sampling method	Global type	Andesite Hw		Andesite Fw	
		Discontinuity frequency ( $m^{-1}$ )	Trend/Plunge	Discontinuity frequency ( $m^{-1}$ )	Trend/Plunge
Line mapping	Maxima	6.53	062/48	8.82	064/34
	Minima	2.34	197/07	2.23	257/68
	Mean	4.97		5.74	
	Coefficient of variation	17%		25%	
Oriented drill core logging	Maxima	29.70	036/17	28.56	342/02
	Minima	8.69	280/05	4.61	225/65
	Mean	19.32		16.90	
	Coefficient of variation	26%		32%	

Hw Hangingwall. Fw Footwall.

Additionally, using the proposed discontinuity frequency diagram, three-dimensional loci [Hudson and Priest 1983], the global maxima and minima, and their orientations for discontinuity frequencies were estimated for both sectors (Table 4). This table also includes the mean discontinuity frequency as the average values obtained from more than 8,000 equidistant directions. This mean value would represent the discontinuity frequency normalized with respect to the orientation at this location.

Table 4 confirms the strong influence of the truncation bias in the discontinuity frequency gathered from a rock mass. It also shows that, in terms of structural anisotropy, both sectors are quite similar when considering the same mapping scale, but minor differences appear when comparing the same sectors at different mapping scales. Therefore, the data in Table 4 show negligible differences between the andesite sectors when all discontinuity types are considered.

### **Vein Infill**

The infill observed in veins was studied by a quantitative estimation of their mineral composition. For instance, a vein could be described as containing 25% quartz, 50%

chalcopyrite, and 25% anhydrite. This quantitative infill description was only undertaken at small sampling scales, i.e., line mapping and oriented drill core logging.

The results show that more than nine mineral species were present within the vein infill. Rarely was one mineral present in all veins, and rarely did this mineral maintain the same proportion of abundance as infill throughout all veins (Tables 5–6). In fact, some particular mineral compositions and associated alteration halos have been used to classify vein types at the El Teniente ore deposit [Cuadra 1986]. Nevertheless, four main mineral species were found to be the most common and abundant in all veins recognized during this study: chlorite, anhydrite, chalcopyrite, and quartz (Table 6).

In addition, in terms of veins infill, no substantial differences could be observed between discontinuity sets from the same mapping scale/sector. For example, Table 7 presents discrete data for the sets observed in Figure 5b. In this table, a similar infill pattern is observed for each set. The individual values are similar to the mean of the sector. However, the mineralogical composition was found to have some particular differences between andesite sectors.

**Table 5.—Mean of mineral species observed as vein infill, by data collection technique and sector**

Sampling method	Sector	Data	Mean of mineral specie observed as vein infill (%)						
			Chlorite	Biotite	Anhydrite	Chalcopyrite	Pyrite	Quartz	Other
Line mapping	Hw	511	6.8	1.7	17.4	13.0	0.2	56.5	4.4
	Fw	296	10.0	1.6	21.7	29.7	2.8	31.5	2.7
Drill core logging	Hw	604	5.5	5.0	2.6	13.0	0.3	68.9	4.7
	Fw	554	13.2	3.7	16.5	26.8	3.9	32.4	3.5

**Table 6.—Percentage of mineral species observed as infill within all veins, by data collection technique and sector**

Sampling method	Sector	Data	Proportion of veins having the mineral specie as infill (%)						
			Molybdenite	Chlorite	Biotite	Anhydrite	Chalcopyrite	Pyrite	Quartz
Line mapping	Hw	511	6.5	52.8	12.3	71.2	80.2	3.1	91.8
	Fw	296	6.4	58.4	12.8	84.8	94.6	17.9	86.8
Drill core logging	Hw	604	5.6	38.1	22.5	18.7	80.0	2.5	94.9
	Fw	554	3.1	67.5	25.4	70.6	96.6	31.9	86.3

**Table 7.—Mean of mineral species observed as vein infill for each family set (refer to Figure 5b) using line mapping at Hw sector**

Sampling method	Data	Mean of mineral specie observed as vein infill (%)						
		Chlorite	Biotite	Anhydrite	Chalcopyrite	Pyrite	Quartz	Other
Random	30	5.2	2.3	16.7	8.2	0.6	61.5	5.5
Set 1 (subvertical E–W)	173	6.1	1.5	17.0	13.6	0.2	55.8	5.8
Set 2 (subvertical N–S)	142	8.8	2.5	23.9	13.1	0.4	48.3	3.0
Set 3 (subhorizontal)	166	6.2	1.0	12.4	13.2	0.2	63.3	3.7
Total and mean	511	6.8	1.7	17.4	13.0	0.2	56.5	4.4

**Table 8.—Vein thickness distribution for each family set observed (refer to Figure 5b) using line mapping at Hw sector**

Family set	Data	Thickness distribution observed (%)					
		<1 mm	1 to <2 mm	2 to <3 mm	3 to <5 mm	5 to <10 mm	≥10 mm
Random	30	16.7	56.7	10.0	6.7	3.3	6.7
Set 1 (subvertical E–W)	172	13.4	40.1	19.8	18.6	7.0	1.2
Set 2 (subvertical N–S)	139	10.1	61.9	10.1	8.6	5.8	3.6
Set 3 (subhorizontal)	165	12.7	45.5	15.2	12.7	6.1	7.9
Total and mean	506	12.5	48.8	15.0	13.2	6.1	4.3

**Table 9.—Vein thickness distribution occurrence observed in veins for each data collection technique**

Sampling method	Truncation bias length	Data	Thickness distribution observed (%)					
			<1 mm	1 to <2 mm	2 to <3 mm	3 to <5 mm	5 to <10 mm	≥10 mm
Drive mapping	4 m	342	—	5.5	11.7	41.9	25.4	15.5
Line mapping	0.3 m	802	13.3	48.9	15.8	14.9	4.2	2.9
Drill core logging ( $\phi = 10\text{--}14$ mm)	0.1 m	1126	26.3	44.2	13.6	11.7	2.6	1.6
Drill core logging ( $\phi = 4.6$ mm)	<sup>1</sup> 0.03 m	Many <sup>2</sup>	64.0	21.5	7.7	4.3	1.8	0.7

<sup>1</sup>Although there was not a truncation bias length threshold criterion during drill core logging, the practical length threshold is estimated at around 0.03 m based on the ability to visually identify discontinuity during core logging.

<sup>2</sup>Mean obtained from 108 core section samples 6.1 m long collected from multiple directions [Brzovic 2005].

### Vein Thickness

Data analysis of the vein thickness distribution also showed that no differences between discontinuity sets from the same mapping scale at any sector could be observed. Similar to the vein infill, Table 8 shows almost the same vein thickness distribution for each set of data plotted in Figure 5b. The vein set thickness distribution is the same as the mean of the sector.

Nevertheless, similar to discontinuity spacing, Table 9 suggests that the distribution of vein thicknesses observed in line sampling was strongly affected by the truncation level applied. Additional (thinner) discontinuities appeared as the truncation length value was decreased. In this table, data collected by standard unoriented drill core (46-mm-diam) are included [Brzovic 2005] and confirm this finding. This vein characteristic is in agreement with the linear relationship observed between vein length and aperture in several different geological environments [Vermilye and Scholz 1995].

Therefore, two important facts can be deduced. Firstly, assuming a representative sample size, the observed vein thickness distributions (and also the vein infill pattern) can be considered to have an isotropic characteristic within the rock mass, i.e., a linear sampling scheme will define the same thickness distributions at any discontinuity orientation. Secondly, longer discontinuities recognized at the El Teniente Mine tend to be statistically thicker than shorter ones. Furthermore, data analysis indicated that the vein infill does not show changes as the vein thickness varies (Figure 7).

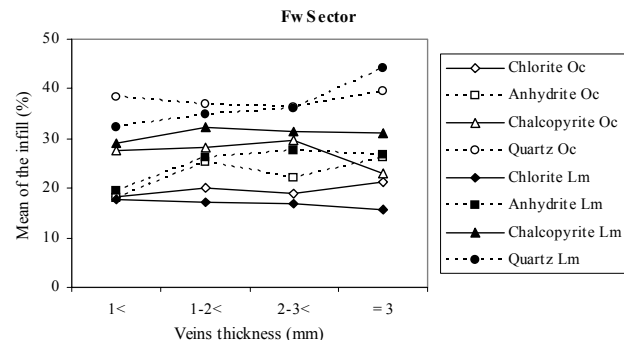


**Figure 7.—Relationship between thicknesses and the mean of the mineralogical infill in veins observed at the Fw sector. (Oc = oriented drill core; Lm = line mapping.)**

### In Situ Rock Block Size Distribution

In order to obtain the in situ rock block distribution and for illustrative purposes only, the data gathered from oriented drill core logging were simulated using a software program [Thompson 2002]. This program assumes a Fisher distribution for orientation, negative exponential distribution for spacing, and infinite trace length for discontinuities (Figure 8). Similar to the discontinuity frequency, Figure 8 shows that the in situ rock block size distributions are practically the same between the andesite sectors.

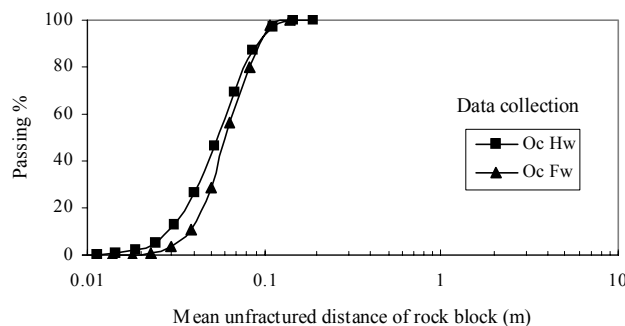


**Figure 8.—In situ block size distributions from rock structure simulation. (Oc = oriented drill core.)**

### WEAK DISCONTINUITIES AT THE EL TENIENTE MINE

The data analysis presented so far included all discontinuities recognized within the rock mass of primary copper ore. However, it is not expected that veins having intermediate- or high-tensile strength (veins having abundant quartz as infill) would be dominant during rock mass disassembly by caving.

Laubscher and Jakubec [2000] have incorporated the effect of healed veins in their proposed methodology to estimate the quality of a jointed rock mass. They described veins as cemented filled joints. However, because of the lack of data regarding the mechanical properties of veins, they proposed the use of the Mohs scale of hardness [Laubscher and Jakubec 2000] to define their frictional properties. In this proposed methodology, veins filled with quartz are ignored due to their strong strength. However, this work does not specify how to proceed when a vein is filled with more than one mineral having different hardnesses, as is the case for most discontinuities recognized at the El Teniente Mine (Tables 5–7).

The lack of experimental determination of the vein infill strength [Willoner 2000] led the authors to study the characteristics of caved rock blocks at the draw points. The objective was to find a common mineralogical association ensemble in veins that defined caved rock block faces during the rock mass disassembly by caving.

This study was carried out at the production level of the Teniente Sub-6 Mine sector (Figure 3), and its major finding was explained in detail by Brzovic et al. [2006] and Brzovic and Villaescusa [2007]. The main conclusion reached was an empirical definition of weak discontinuities, which are those veins having less than 35% of hard minerals as infill. A hard mineral was particularly defined as having a Mohs scale of hardness greater than 4 [Hurlbut 1941]. This finding was gathered from the commonly observed characteristics in 639 veins forming caved rock block faces (Figure 9). These veins were significant weaknesses within the rock mass during the caving and subsequent fragmentation process.

The following comparisons of the El Teniente rock structure are made, taking into account the overwhelming effect of weak discontinuities.

### ROCK STRUCTURE CHARACTERIZATION USING ONLY WEAK DISCONTINUITIES

The cumulative frequency of veins collected using oriented drill core logging in terms of their abundance of hard minerals as infill is shown in Figure 10. This figure shows that for the threshold value adopted here (veins filled up to 35% of hard infill), the weak discontinuities represent 16.3% and 49.9% of all discontinuities observed in andesite Hw and andesite Fw, respectively. Figure 10 also shows that appreciable differences between these sectors still appear if a different threshold value of hard infill would be adopted.

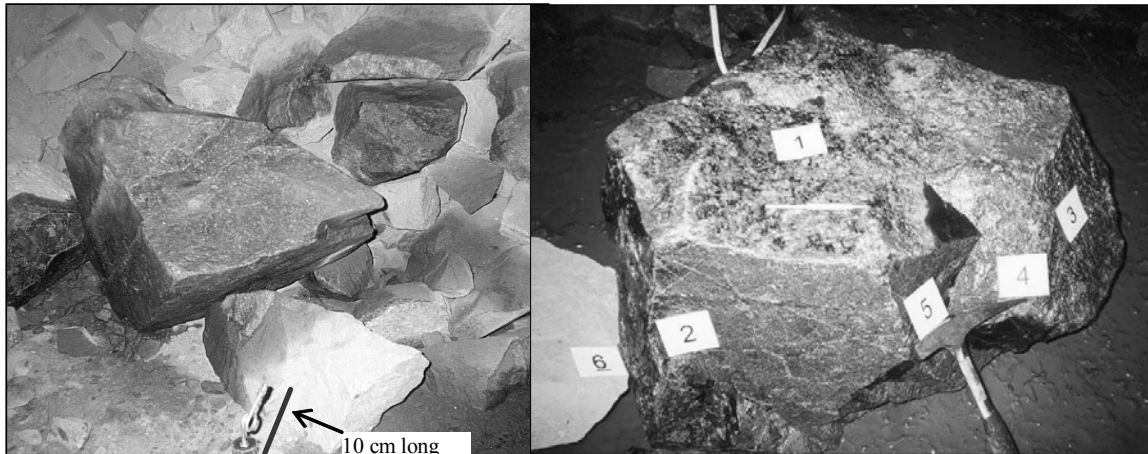


**Figure 9.—Veins as faces of polyhedral caved rock blocks in draw points showing mineralogical infill such as chalcopyrite and quartz.**

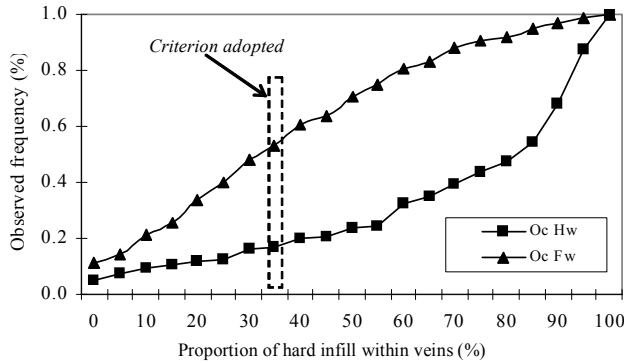


**Figure 10.**—Cumulative frequency of veins collected using oriented drill core logging (Oc) in terms of the hard minerals as infill. Dashed line shows the criterion of weak discontinuities used in this study.

### Weak Discontinuity Spacing

Since weak discontinuities are a subgroup of all discontinuities, the mean normal weak discontinuity set spacing was estimated using the same set definition. Using the three-dimensional loci [Hudson and Priest 1983], the global maxima and minima and their orientations for weak discontinuity frequencies were estimated for both sectors (Table 10). No appreciable differences in structural anisotropy can be determined when only the weak discontinuities are considered and compared to when all discontinuities are considered. This can be concluded by comparing Tables 4 and 10. These conclusions reveal two important things. First, they confirm the isotropic characteristic of the vein infill within the rock mass. Second, the different thickness distributions observed at both mapping scales do not affect the vein infill characteristics, as suggested by Figure 7.

Table 10 clearly shows that at any mapping scale the andesite rock type from the Fw sector has a larger frequency of weak discontinuities. According to drill core data, the normalized frequency of weak discontinuities within the Fw sector is nearly three times that of the Hw sector.

**Table 10.**—Extremes in values of discontinuity frequency and their orientation of weak discontinuities using three-dimensional loci [Hudson and Priest 1983]

Sampling method	Global type	Andesite Hw		Andesite Fw	
		Discontinuity frequency ( $\text{m}^{-1}$ )	Trend/Plunge	Discontinuity frequency ( $\text{m}^{-1}$ )	Trend/Plunge
Line mapping	Maxima	3.29	066/47	4.88	062/36
	Minima	0.80	197/07	1.41	257/68
	Mean	2.44		3.24	
	Coefficient of variation	23%		24%	
Oriented drill core logging	Maxima	5.62	027/06	15.40	340/00
	Minima	1.04	280/05	2.88	225/65
	Mean	3.46		9.11	
	Coefficient of variation	35%		31%	

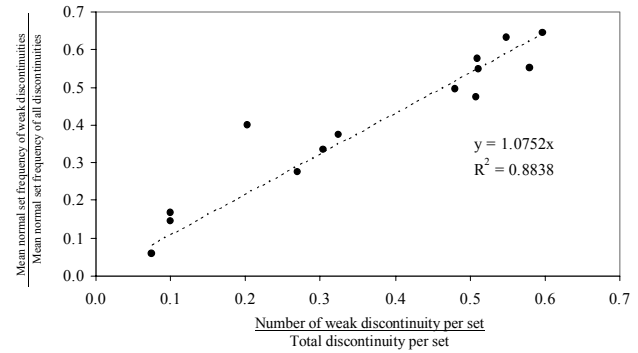


**Figure 11.**—Ratio between weak and all discontinuities.

In addition, using only data collected by oriented drill core and line mapping from both sectors, the ratio between weak discontinuities and all discontinuities per each discontinuity set is calculated and presented in Figure 11. The data shown in this figure suggest that weak discontinuities are homogeneously distributed within any discontinuity set.

### Weak Discontinuity Persistence

The discontinuity trace length features were only studied using line mapping at mine drives. Data analysis of the weak discontinuity trace length distribution showed that no differences between discontinuity sets could be observed (Table 11). This finding is consistent with a circular shape of discontinuities, which always present the same distribution pattern at any rock exposure [Warburton 1980]. Then, the mean value of the trace length distribution for the whole sector can be calculated. Table 11 also shows that the trace length distribution of any set of the Hw sector (plotted in Figure 5b) is almost the same as the mean of the sector. Moreover, Figure 12 reveals that the mean trace length distribution of each sector for weak and all discontinuities are practically the same.

**Table 11.—Weak discontinuity trace length distribution for each family set observed (refer to Figure 5b) using line mapping at Hw sector**

Family set	Data	Trace length distribution observed (%)						
		<0.5 m	0.5 to <1.0 m	1.0 to <1.5 m	1.5 to <2.0 m	2.5 to <3.0 m	3.0 to <4.0 m	≥4 m
Set 1 (subvertical E-W)	52	3.8	23.1	15.4	11.5	21.2	11.5	13.5
Set 2 (subvertical N-S)	44	4.5	15.9	29.5	18.2	11.4	9.1	11.4
Set 3 (subhorizontal)	34	5.9	8.8	14.7	17.6	11.8	11.8	29.4
Total and mean of Hw sector	134	4.5	17.2	20.1	15.7	15.7	10.4	16.4

NOTE.—Data collection by line mapping used a threshold value of 0.3 m as truncation bias.

**Table 12.—Weak discontinuity thickness distribution for each family set observed (refer to Figure 5b) using line mapping at Hw sector**

Family set	Data	Thickness distribution observed (%)					
		<1 mm	1 to <2 mm	2 to <3 mm	3 to <5 mm	5 to <10 mm	≥10 mm
Set 1 (subvertical E-W)	53	13.2	35.8	24.5	13.2	9.5	3.8
Set 2 (subvertical N-S)	46	4.3	65.2	17.4	8.8	—	4.3
Set 3 (subhorizontal)	33	6.1	39.4	24.2	21.2	6.1	3.0
Total and mean	136	9.6	46.3	22.1	13.2	5.0	3.7

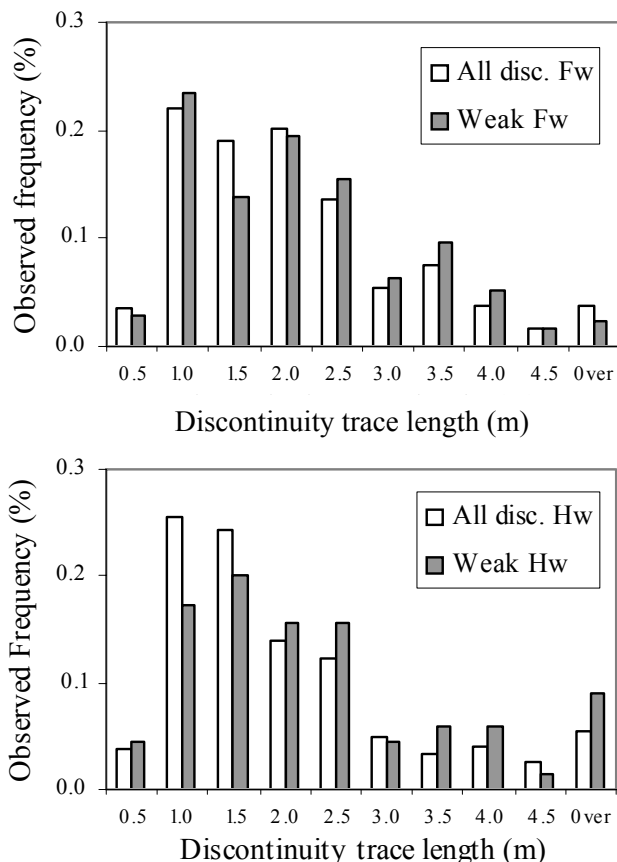


**Figure 12.—Discontinuity trace length from data collected in line mapping.**

Therefore, the observed persistence distributions of the discontinuities irrespective of their infill features can be considered to have an isotropic characteristic within the rock mass.

### Weak Discontinuity Thickness

Data analysis of the weak vein thickness distribution also showed that no differences between discontinuity sets from the same mapping scale at any sector could be observed. For example, Table 12 shows almost the same weak vein thickness distribution for each set of the data plotted in Figure 5b, which do not differ from when all discontinuities are considered (Tables 8–9). Therefore, the observed thickness distributions can also be considered to have an isotropic characteristic within the rock mass.

### Block Size

The weak discontinuity data set from oriented drill core logging was used to stochastically simulate the rock structure and to determine in situ block size distributions [Thompson 2002]. The results are presented in Figure 13. The figure clearly shows that when the strength of the discontinuities is taken into account, the andesite rock type from the Hw sector has a coarser in situ rock block size distribution than the Fw sector. These predicted differences shown in Figure 13 are in accordance with the actual observations at the mine site. However, these differences could not be established by applying rock mass classification schemes (see Table 1).

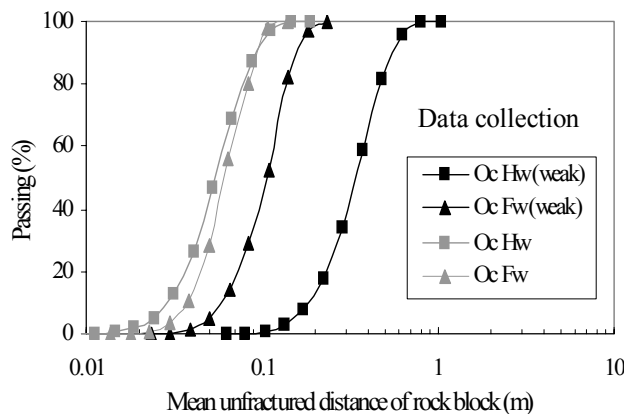


**Figure 13.**—In situ block size distributions from rock structure simulation for weak discontinuities using oriented drill core logging (Oc). Light gray data are from Figure 8.

## DISCUSSION

Since conventional rock mass classification systems parameterized mainly open joints to assess rock mass quality [Barton et al. 1974; Hoek et al. 1995; Laubscher 1993], these schemes cannot be readily applied to the rock masses of the primary copper ore at the El Teniente Mine. Even the last upgrade of the Mining Rock Mass Rating (MRMR) [Laubscher and Jakubec 2000] cannot be applied because it does not take into account the multiple mineral ensembles of the vein infill.

Moreover, other discontinuity characteristics that are not clearly included in the classification schemes seem to play a relevant role during rock mass behavior. This is the case for discontinuity thicknesses, which have been found to control rock mass disassembly during caving and the fragmentation process [Brzovic et al. 2006; Brzovic and Villaescusa 2007].

In addition, the discontinuity trace length plays a relevant role in rock mass characterization when a truncation bias length during data collection is adopted. This characteristic must be taken into account if comparisons between different mines are made.

The discontinuity features that have been found to be variable between mine sectors at the El Teniente Mine are the occurrence of veins and their infill characteristic. These particular geological characteristics combined with the in situ rock block distribution seem to be enough to characterize the rock masses of the primary copper ore.

## CONCLUDING REMARKS

A data collection campaign designed to characterize the rock structure of the primary copper ore was recently implemented at the El Teniente Mine in central Chile. The results indicated that mainly faults and veins are present within the rock mass. Subvertical faults were defined as

widely spaced, while veins were present in high frequencies in at least three semiorthogonal orientations. Almost no joints were found within the rock mass. Moreover, negligible differences were observed in terms of in situ rock block distributions between the two studied sectors.

A definition of weak discontinuities has been adopted [Brzovic et al. 2006; Brzovic and Villaescusa 2007], which is based on the analysis of rock mass behavior during caving. Only when weak discontinuities are used, the rock mass characterization predicts differences between the two studied sectors. These differences, which are represented in terms of discontinuity frequency and in situ rock block distributions, are in accordance with actual observations at the mine site.

Truncation biases applied during data collection strongly affected the discontinuity set parameters, such as spacing and distribution of thicknesses, and in situ block size distribution. Some discontinuity parameters such as trace length and thicknesses have been found to have an isotropic characteristic within the rock mass. The discontinuity infill has also been found to have an isotropic characteristic, but only within each location, because it changes between sectors. It has also been found that longer discontinuities are statistically thicker than shorter ones, and the infill compositions do not change with their thicknesses. Most of these discontinuity characteristics were found for both weak and all discontinuities.

In conclusion, due to the geological features of the primary copper ore, rock mass classification schemes cannot be readily applied to characterize rock masses at the El Teniente Mine.

## ACKNOWLEDGMENTS

The authors wish to acknowledge the financial support of Codelco and the Western Australian School of Mines. Permission to publish this paper by Codelco-Chile, El Teniente Division, is also acknowledged. The authors also gratefully acknowledge the superintendence geology personnel for their collaboration, in particular, David Benado and José Seguel.

## REFERENCES

- Barton N, Lien R, Lunde J [1974]. Engineering classification of rock masses for the design of tunnel support. *Rock Mech* 6(4):189–236.
- Brady BGH, Brown TE [2003]. Rock mechanics for underground mining. 3rd ed. London: Kluwer Academic Publisher.
- Brooks BA, Allmendinger R, Garrido I. [1996]. Fault spacing in the El Teniente mine, central Chile: evidence for nonfractal fault geometry. *J Geophys Res* 101(B6): 13633–13653.
- Brzovic A [2001]. Fundamentos geológicos para un sistema de clasificación geotécnico del macizo rocoso

- primario, mina El Teniente (in Spanish). Internal report SGL-187/2001 of the Superintendence Geology, CODELCO-Chile, El Teniente Division.
- Brzovic A [2005]. Characterization of the primary copper ore for caving at the El Teniente mine, Chile [Draft Dissertation]. Western Australian School of Mines.
- Brzovic A, Villaescusa E [2007]. Rock mass characterization and assessment of block-forming geological discontinuities during caving of primary copper ore at the El Teniente mine, Chile. *Int J Rock Mech Min Sci* 44(4): 565–583.
- Brzovic A, Villaescusa E, Figueroa C [2006]. Characterization of block-forming geological discontinuities during primary ore caving at El Teniente mine, Chile. In: Yale DP, Holtz SC, Breeds C, Ozbay U, eds. Proceedings of the 41st U.S. Rock Mechanics Symposium (Golden, CO, June 17–21, 2006). Alexandria, VA: American Rock Mechanics Association, paper 980.
- Cannell J, Cooke D, Walshe JL, Stein H [2005]. Geology, mineralization, alteration, and structural evolution of the El Teniente porphyry Cu-Mo deposit. *Econ Geol* 100: 979–1005.
- Celhay F, Pereira J, Burgos AL [2005]. Geología y recursos para el nuevo nivel mina: etapa ingeniería conceptual (in Spanish). Internal report SGL-I-030/2005 of the Superintendence Geology, CODELCO-Chile, El Teniente Division.
- Cladouhos T, Marrett R [1996]. Are fault growth and linkage models consistent with power-law distributions of fault lengths? *J Struct Geol* 18(2/3):281–293.
- Cuadra P [1986]. Geocronología K-Ar del yacimiento El Teniente y áreas adyacentes (in Spanish). *Revista Geologica de Chile* 27:3–26.
- Garrido I, Riveros M, Cladouhos T, Espineira D, Allmendinger R [1994]. Modelo geológico estructural yacimiento El Teniente (in Spanish). In: Proceedings of VII Congreso Geológico Chileno 2:1533–1558.
- Gillespie PA, Howard CB, Walsh JJ, Watterson J [1993]. Measurement and characteristic of spatial distribution of fractures. *Tectonophysics* 226:113–141.
- Hobbs BE [1993]. The significance of structural geology in rock mechanics. In: Hudson J, ed. Comprehensive rock engineering. Vol. 1. Pergamon Press, pp. 25–62.
- Hoek E, Kaiser PK, Dawden WF [1995]. Support of underground excavations in hard rock. Rotterdam, Netherlands: Balkema.
- Hudson JA, Priest SD [1983]. Discontinuity frequency in rock masses. *Int J Rock Mech Min Sci Geomech Abstr* 20(2):73–89.
- Hurlbut C [1941]. Dana's manual of mineralogy. 15th ed. John Wiley & Sons.
- ISRM [1978]. Commission on standardization of laboratory and field test. Suggested methods for the quantitative description of discontinuities in rock masses. *Int J Rock Mech Min Sci Geomech Abstr* 15:319–368.
- Laubscher D [1993]. Planning mass mining operations. In: Hudson J, ed. Comprehensive rock engineering. Vol. 2. Pergamon Press, pp. 547–583.
- Laubscher D, Jakubec J [2000]. The MRMR rock mass classification system for jointed rock masses. In: Hustrulid WA, Bullock R, eds. Underground mining methods: engineering fundamental and international case studies. Littleton, CO: Society for Mining, Metallurgy, and Exploration, Inc.
- Rojas E, Cavieres P, Dunlop R, Gaete S [2000a]. Control of induced seismicity at the El Teniente mine, Codelco Chile. In: Chitombo G, ed. Proceedings of MassMin 2000 (Brisbane, Queensland, Australia, October 29–November 2, 2000). Australasian Institute of Mining and Metallurgy (AusIMM), pp. 775–781.
- Rojas E, Molina R, Cavieres P [2000b]. Preundercut caving in El Teniente Mine, Chile. In: Hustrulid WA, Bullock R, eds. Underground mining methods: engineering fundamental and international case studies. Littleton, CO: Society for Mining, Metallurgy, and Exploration, Inc., pp. 417–423.
- Scholz CH [2002]. The mechanics of earthquakes and faulting. 2nd ed. Cambridge, U.K.: Cambridge University Press.
- Skewes MA, Arevalo A, Floody R, Zuniga P, Stern CR [2006]. The El Teniente megabreccia deposit: the world's largest deposit. In: Porter TM, ed. Super porphyry copper and gold deposits: a global perspective. Linden Park, South Australia: PGC Publishing.
- Terzaghi K [1946]. Theoretical soil mechanics. John Wiley & Sons.
- Thompson AG [2002]. Stability assessment and reinforcement of block assemblies near underground excavations. In: Hammah R, Bawden W, Curran J, Telesnicki M, eds. Proceedings of the NARMS-TAC Conference (July 7–10, 2002). Vol. 2. Toronto, Ontario, Canada: University of Toronto Press, pp. 1439–1446.
- Vermilye J, Scholz CH [1995]. Relation between vein length and aperture. *J Struct Geol* 17(3):423–434.
- Villaescusa E [1990]. A three-dimensional model of rock jointing [Dissertation]. Brisbane, Australia: University of Queensland.
- Warburton PM [1980]. A stereological interpretation of joint trace data. *Int J Rock Mech Min Sci Geomech Abstr* 17(4):181–190.
- Willoner A [2000]. Characterization of rock mass quality and prediction of mass behaviour: an investigation into the parameters which influence the strength of healed joints in hypogene mineralized andesite at El Teniente copper mine, Chile [Thesis]. Leeds, U.K.: University of Leeds, School of Earth Sciences.

# STOPE DESIGN CONSIDERATIONS USING ROCK MASS CLASSIFICATION TOOLS AT THE XSTRATA ZINC GEORGE FISHER MINE

By Geoff W. Capes,<sup>1</sup> Jeremy P. Doolan,<sup>2</sup> and Leigh B. Neindorf<sup>3</sup>

## ABSTRACT

The development and use of rock mass classification tools have been a key component for improving stope design over the past 4 years at the Xstrata Zinc George Fisher Mine in northern Queensland, Australia. In 2003, stope extraction data from 3 years of open-stope mining provided an excellent situation to review the assumptions in the feasibility study. Extracted stope profile information, drillhole geotechnical data, underground observations, and oral and written communication were used to develop a thorough stope reconciliation performance database. Without collecting the back analysis data and presenting the data in a usable format, engineers are left to debate opinion instead of engineered judgment. This can lead to biased and uninformed design parameter choices with the potential to repeat poor design. This paper demonstrates some effective, practical examples of empirical data collection where rock mass classifications tools were developed and used to create improved confidence in predicting stope stability and failure profiles. The work contributed to design changes that resulted in a reduction in stope hangingwall dilution and an increase in head grade while continuing to ramp up production from 2003–2005.

## INTRODUCTION

This paper describes the development and use of rock mass classification tools in stope design over the past 4 years at the George Fisher (GF) North Mine. The deposit is located 22 km north along strike from the Mount Isa Lead Mine. A joint stope dilution study between the Xstrata Zinc George Fisher Mine (Figure 1) and the University of Saskatchewan, Canada, began in October 2003. The objective was to create a thorough understanding of hangingwall (HW) overbreak using a sound geological engineering approach that focused on data

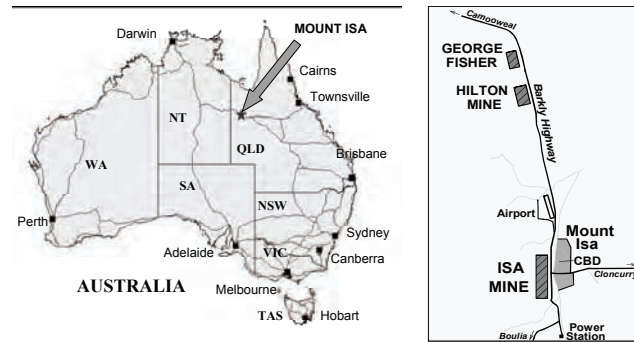


Figure 1.—Location of George Fisher Mine.

collection of historic stope performance, rock mass classification, and underground observations of D ore body. The evolution of the work has created a better understanding of stope HW stability and created a change in mining methodology. The work contributed to a reduction in annual stope dilution from 14.4% (2003) to 6.3% (2005), an increase in zinc grade from 7.4% to 8.7%, and an increase in production from 2.1 to 2.6 Mt [Capes et al. 2006].

## BACKGROUND

### Geology

The George Fisher Mine contains two similar deposits located approximately 2 km apart with an estimated total resource of 127 Mt at 100 g/t silver, 5.3% lead, and 9.2% zinc (June 2005). The GF North deposit makes up approximately two-thirds of the current production, with the remaining ore coming from GF South (previously known as Hilton). The GF North deposit, the focus of this study, is composed of a series of stratiform ore bodies striking near north-south and dipping west between 30° to 70°. The sphalerite-pyrite-galena-pyrrhotite type mineralized areas are separated by various thicknesses of bedded shales and siltstones [Forrestal 1990].

D ore body is currently the key area of extraction, grading at approximately 5% lead, 9% zinc, and 100 g/t silver with the mineralization being unequally distributed through the ore body, including a high-grade massive sulfide layer sometimes defining the ore/HW contact. Typically, the D ore body HW rock is composed of a siltstone marker rib followed by a package of pyritic shales

<sup>1</sup>Ph.D. candidate, Department of Civil and Geological Engineering, University of Saskatchewan, Saskatoon, Canada, and senior planning engineer, Xstrata Zinc, George Fisher Mine, Mount Isa, Queensland, Australia.

<sup>2</sup>Rock mechanics engineer, Xstrata Zinc, George Fisher Mine, Mount Isa, Queensland, Australia.

<sup>3</sup>Project manager, Xstrata Zinc, Mount Isa, Queensland, Australia.

(5%–20% fine-grained pyrite) and a series of very fissile black shales (Figure 2). This is topped off with a variably thick mineralized lead-zinc lens. A section of siltstone separates this lens from the massive pyrite marker and massive sulfides, which define the start of C ore body. The thickness and rock mass quality of each package between D ore body and C ore body vary quite significantly along strike and dip as a result of past brittle and ductile deformation from faulting and folding events. A large number of geological structures affect the George Fisher deposit with varying degrees of offset, ore body rotation, drag folding, and metal redistribution [Grenfell and

Haydon 2006]. The two main types of faults are cross-cutting north-east trending faults and bedding parallel faults having their own individual characteristics and zone of influence.

### Stope Layout and Design

The mining method at GF consists mainly of transverse open-stope mining where the ore bodies are greater than 10 m in thickness. Transverse stopes are mined from a footwall drive access either on a 30- or 60-m sublevel spacing giving consideration to the local rock mass quality and stope shape relationship. Primary stopes are mined until uneconomic conditions exist and then are filled with either a cement aggregate fill or a paste fill material. A secondary stope is typically mined once the adjacent primaries have been mined to one 30-m sublevel higher than the secondary stope and the fill has been allowed to sit for 28 days and gain sufficient strength to act as a sidewall during extraction (Figure 3). The original “15–20” design (17.5-m crosscut centers), primary and secondary stope strike lengths, respectively, was changed in 2003 to a “10–20” design (15-m crosscut centers). This eventually became a floating design based on local rock quality where primary stopes could be up to 15 m on strike considering the cost of cemented backfill, local ore body width, HW stability, and effects on the mining cycle. In addition, the drill design of stopes within the George Fisher Mine underwent a change in 2003 when D ore body HW drives were eliminated and transverse stope crosscuts were used as the only access for D ore body extraction. One of the main motives behind this design change was

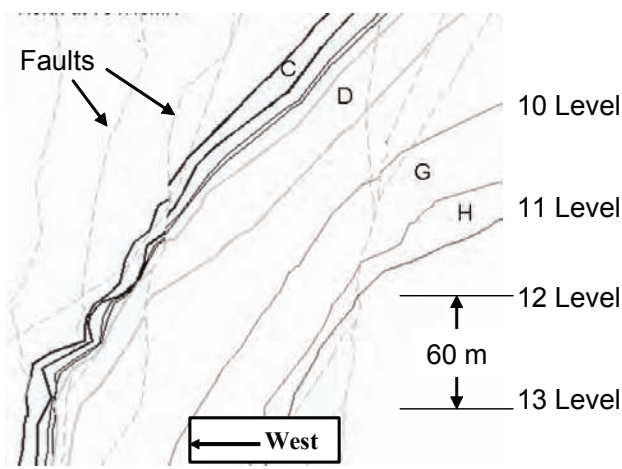


Figure 2.—Typical cross-section of George Fisher ore bodies.

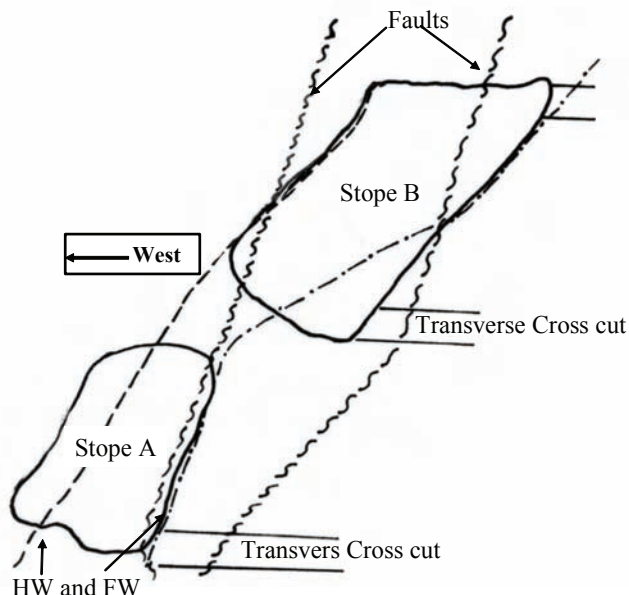
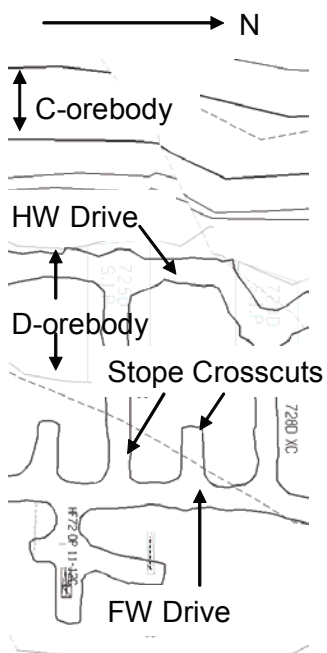


Figure 3.—George Fisher mining layout (plan and cross-section views).

the existence of problems with the stope hangingwalls and adjacent hangingwall drive failures as a response to stoping. The elimination of HW drives created the need for additional diamond drilling of the ore body to delineate the stope extraction wireframes. This addition of drilling and subsequent geotechnical logging has provided substantial relevant information for stope design and reconciliation purposes.

Numerical modeling provided an adequate set of rules for mine-wide sequencing [Beck 2003], which, when adhered to, lead to a sustainable mining method. The suggested guidelines included minimizing overbreak in primaries to avoid connection of voids when mining secondaries, tight-filling stopes, eliminating triple-lift pendant pillars, decreasing stope cycle time, and creating a better sequence to minimize stress effects on extraction. However, even with the mine-wide changes and mine-wide sequencing rules, a set sublevel spacing and crosscut width in poor-quality HW rock mass continued to result in unpredicted major individual stope HW failures and subsequent production inefficiencies. Thus, a thorough understanding of individual stope performance was required in order to achieve further positive design change.

## DEVELOPMENT AND USE OF ROCK MASS CLASSIFICATION TOOLS AND EMPIRICAL METHODS FOR DESIGN

### Overview

During late 2003, stope extraction data from 3 years of mining provided an excellent situation to review the assumptions in the feasibility study. Stope profile information based on data acquired using the cavity monitoring system [Miller et al. 1992], drillhole (BQ size) geotechnical data, underground observations, and oral and written communication was used to develop a thorough stope reconciliation performance database. On-site research, coupled with subsequent design trial and implementation, resulted in the development of a model that showed a relationship between rock mass quality, span, and resultant extraction profile. The goal of this model was to use it as a template and continually update the knowledge with underground observations and reconciliations of case histories. The model represented significant time, discussion, and research, but with more data, the model would evolve and lead to continued improvements in the understanding of HW behavior and design of stopes.

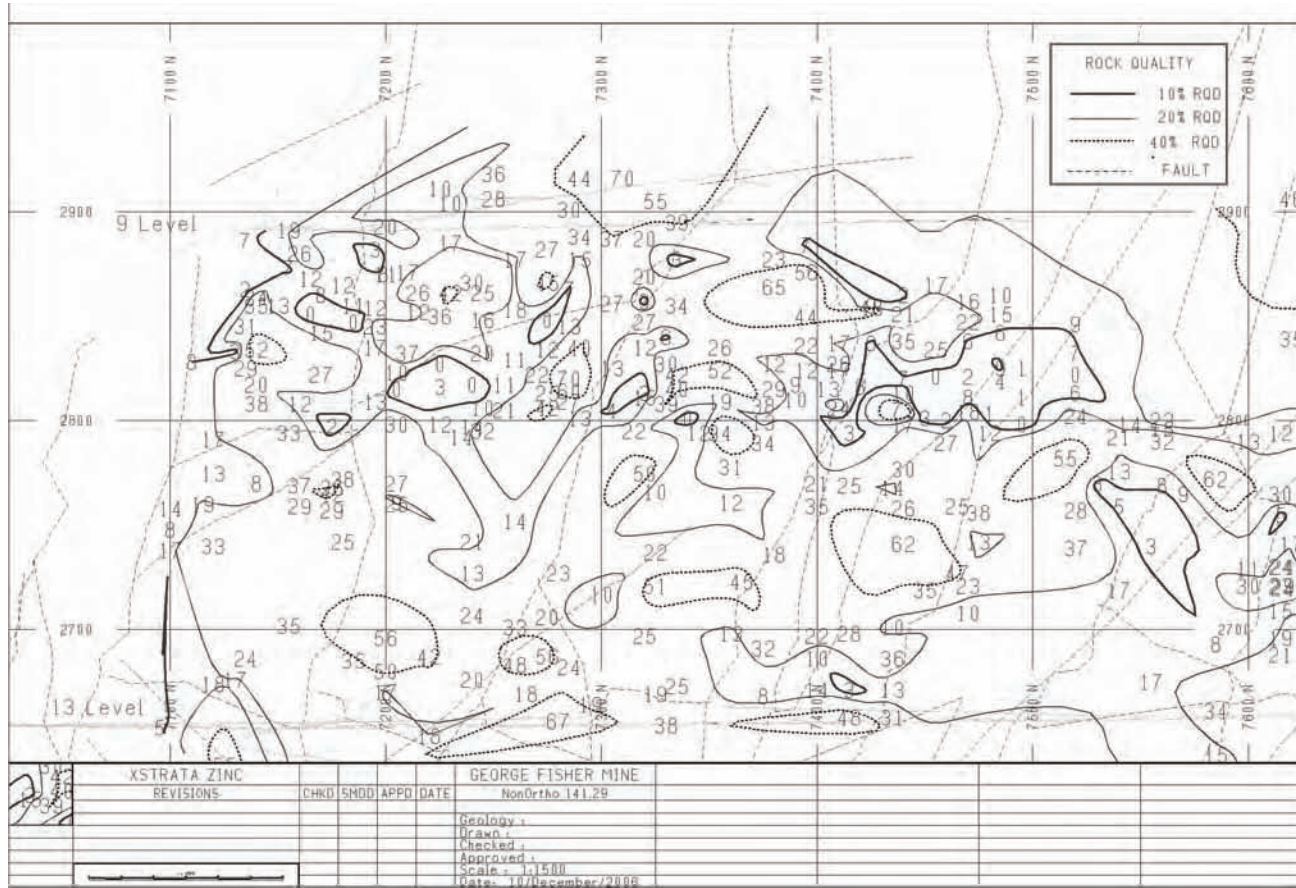


**Figure 4.—RQD long section contoured.**

## Phase 1: RQD Long Section

The first step of the study was to create a long section of the available geotechnical data. The comprehensiveness and density of geotechnical data depend on the year in which the drillhole was logged. Most holes after 1999 have RQD data available (BQ: 36.5–40.7 mm) as recommended by Hadjigeorgiou [1999]. Rock Quality Designation (RQD) [Deere 1964] was originally developed for drill core  $\geq 54$  mm, although the “BQ RQD” is used to compare site data. The RQD data were averaged for the first 5 and 10 m of rock into the hangingwall and placed on a long section showing significant variation along strike and dip. The 5-m average RQD long section (Figure 4) has evolved from a scrappy, hand-contoured, coffee-stained desk map to a sharable plan able to be accessed by the technical services team on the mine design software. The original section was hand-contoured while the up-to-date section was contoured by triangulating the RQD values on the mine software as topographic surfaces between points and joining equal elevation points as contours. There is a substantial increase in RQD data density above the 2,800 elevation due to the removal of the HW drives and requirement for diamond drilling and subsequent geotechnical logging.

## Phase 2: Empirical Methods

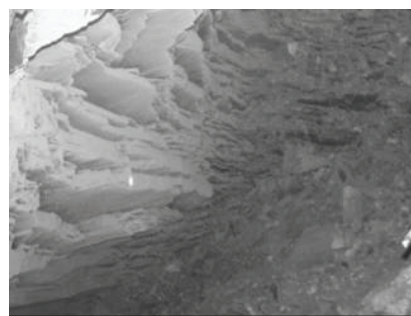
The next step was to gather additional averaged data for use in empirical design methods, such as the modified stability graph method [Potvin 1988] and dilution graph method [Clark and Pakalnis 1997], which require a single estimate of rock mass properties for the surface being analyzed. This involved acquiring geotechnical parameters such as joint condition, joint alteration, and joint roughness used in the Q-system [Barton et al. 1974]. Based on many underground observations and stope reconciliations, the rock in the HW area was assigned three broad categories (Figure 5). Each stope was assigned values within a category and plotted with actual ELOS values using the dilution graph format. ELOS (“equivalent linear overbreak/slough”) is defined as the volume of the HW overbreak divided by the stope HW surface area [Clark and Pakalnis 1997]. ELOS is a useful tool for mine planning because it provides the ability to quantify a diluted stope shape to enhance mine scheduling purposes. The dilution graph was modified with new ELOS lines calibrated to data collected for stoping in poor-quality rock masses where minimal data have been presented except for Capes et al. [2005] and Brady et al. [2005] (Figure 6). The “calibrated” curves on the modified dilution graph (Figure 6, right) have been used to predict HW overbreak in both GF North and South operations for the last few years. The calibrated curves, which need to be statistically verified as a final part of the study, are an effective tool for local stope design as they contain a large amount of data in

the required hydraulic radius (H.R.), modified stability number ( $N'$ ) ranges.

However, further work was required to examine why some cases did not agree with the design approach based on the average rock mass conditions. When Category 3 rocks ( $RQD < 10\%-20\%$ ,  $N' < 1$ ) were analyzed, the failure prediction did not seem to correlate with the ELOS predictions based on a 5-m average of HW conditions. Two such examples included having a 6-m ELOS in a primary stope where  $<0.5$  m was expected ( $N' = 0.5$ , H.R. = 3) and an 13-m ELOS where approximately 4 m was expected ( $N' = 0.8$ , H.R. = 7). For category 1 (RQD  $> 40\%$ ,  $N' > 6$ ) and category 2 (RQD 20%–40%,  $N' = 1\text{--}4$ ) rocks, the majority of cases of ELOS prediction were within acceptable error for stope prediction requirements, but an improved model was desired to examine the cases that did not fit.



- Category 1  
RQD  $> 40\%$   
(for at least 1-2m)  
 $Jn < 6\text{--}9$   
 $Jr = 1$   
 $Ja = 1$   
 $Q' = 4.4$   
 $A = 1, B=0.3, C= 4\text{--}7$   
 $N' > 6$



- Category 2  
RQD = 20-40%  
(5m average)  
 $Jn = 12$   
 $Jr = 1$   
 $Ja = 2$   
 $Q' = 0.8\text{--}1.6$   
 $A = 1, B=0.3, C= 4\text{--}7$   
 $N' = 1\text{--}4$



- Category 3  
RQD<10-20%  
(5m average)  
 $Jn = 12\text{--}15$   
 $Jr = 1\text{--}2$   
 $Ja = 2\text{--}4$   
 $Q' = 0.3\text{--}0.8$   
 $A = 1, B=0.3, C= 4\text{--}7$   
 $N' < 1$

Figure 5.—Examples of HW rock categories at George Fisher Mine.

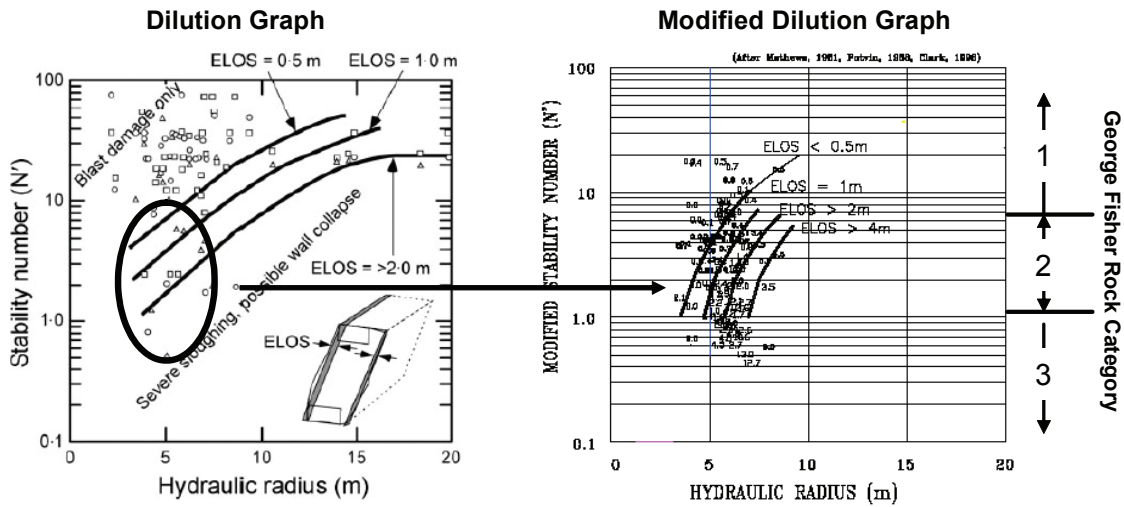


Figure 6.—Dilution graph (from Brady et al. [2005]) and modified dilution graph with additional data from poor-quality rock masses (after Capes et al. [2005]).

### Phase 3: Rock Category and Failure Profile Relationships

The next step was to investigate the additional factors that have been documented to relate to HW overbreak from a comprehensive literature review and studies conducted at the George Fisher Mine. These additional factors, including faulting, stress, blasting, undercutting, and time, were identified to examine how or if they played a role in erroneous ELOS prediction. During this next phase of the study, interesting relationships were observed between failure shape, rock quality, and span when the RQD drillhole data were overlain as logged intervals on HW failure profiles in the mine design software. Thus, the methodology was changed to first investigate these novel relationships before examining the additional factors.

RQD cross-section plots were created for individual stopes and provided valuable data for understanding the variability of rock quality near the HW/ore boundary (Figure 7). The RQD plots coupled with underground observations created the idea of different failure profiles (Figure 7) for the different rock mass categories shown in Figure 5. Areas where the RQD < 10%–20% typically failed into the next rock mass category without arching. Areas with RQD 20%–40% would arch to become stable within span constraints or would change profile when a different rock category was intersected. Stability existed in other stopes where the stope failed to a composite beam or plate of rock in which the RQD > 40% for at least 1 m. These relatively thin zones of higher RQD rock define a more stable domain, and the position of this domain was found to define the extent of failure, within span constraints. These stable domains were not always a consistent lithology, but could often be defined as pyritic shales, siltstone beds, or a narrow mineralized area. Data were collected to create a design tool demonstrating the

stability relationship between the composite beam thickness (meters of BQ core >40% RQD) and span (Figure 8). Figures 9–12 demonstrate four case histories of the model incorporating the three rock categories. Recognizing the changing rock mass condition with

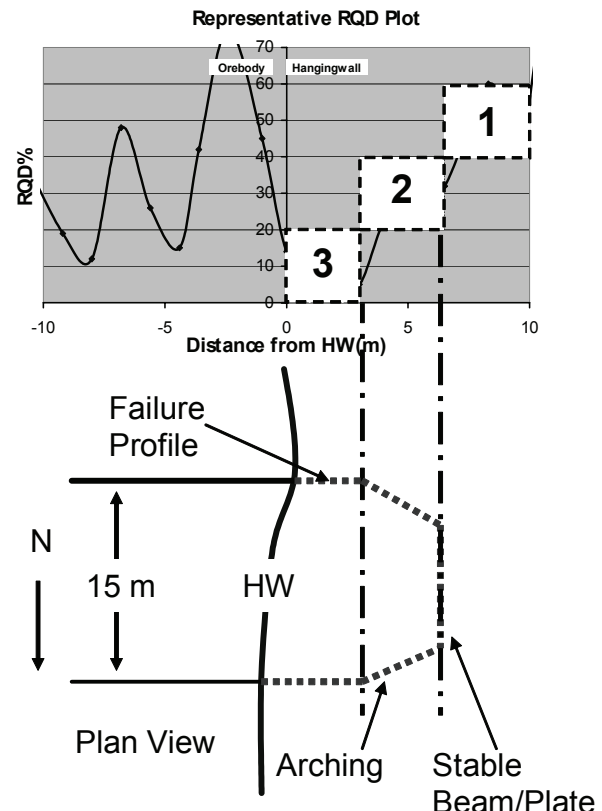


Figure 7.—RQD plot and representative failure shape profiles based on rock category and span.

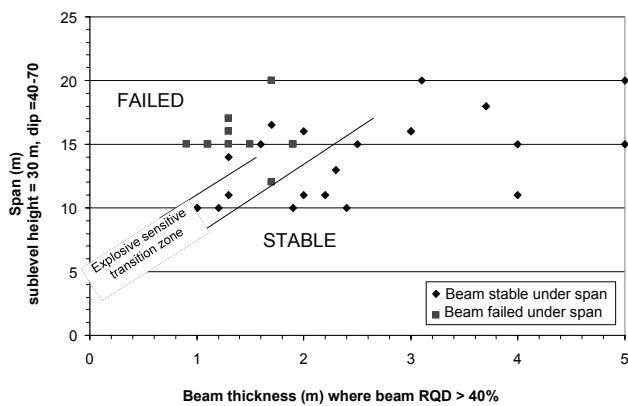


Figure 8.—Composite beam thickness versus span stability graph.

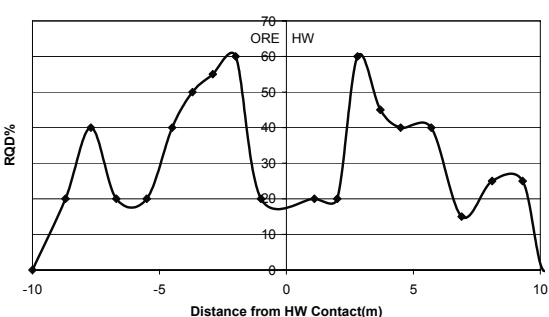
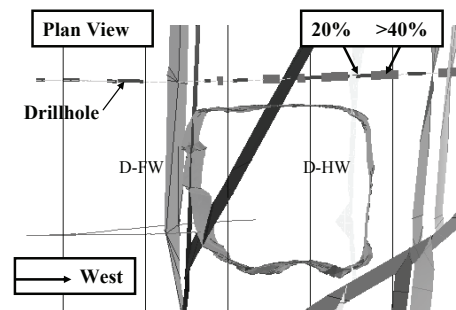
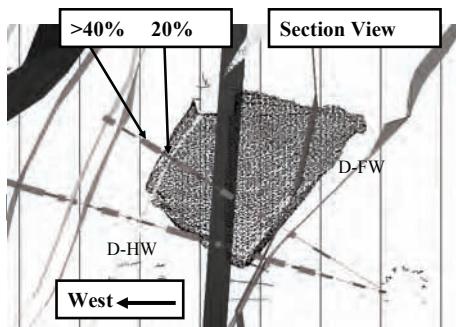


Figure 9.—716D 12C-11L. Secondary stope where a major failure was expected using predicted stress conditions. Local rock mass conditions limited depth of failure to 2–3 m as stope failed through category 3 rock to the category 1 composite beam (February 2004).

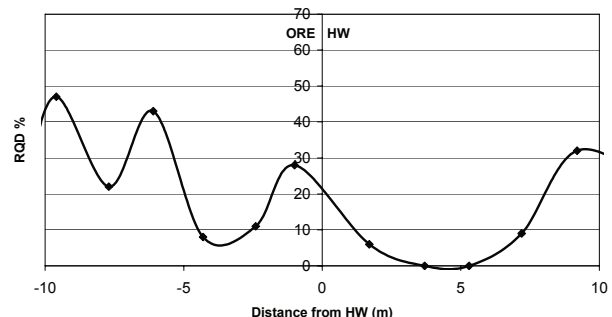
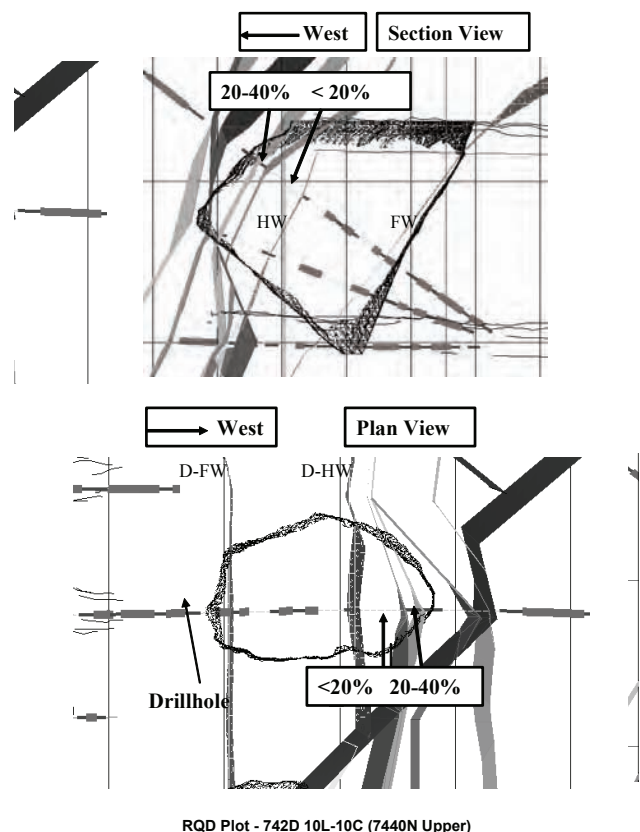
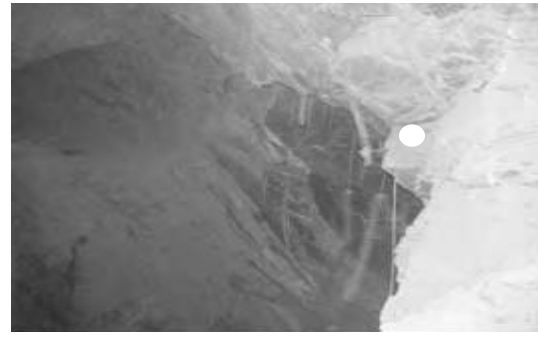


Figure 10.—742D 10L-10C. Primary stope where 6- to 8-m depth of HW failure was predicted. Failure depth was 8–10 m. Stope failed without arching through first 5 m of category 3 rock, then arched off to a stable profile through category 2 rock (September 2006).

distance from the hangingwall contact enabled an improved and accurate method of estimating HW dilution. RQD was noted as the most significant contributor as a geotechnical input into stope design and is the most available and most easily obtained data. Stope performance prediction now includes a cumulative overbreak prediction where the extraction profile is estimated through the different domains to create an expected stope shape for mine planning. Further work is being conducted to look at correlations between arching failure angle, span, and RQD. This may be difficult to quantify due to the lack of available data to estimate bedding perpendicular joint spacing for individual stopes.



11-m HW span



17-m HW span

NOTE: Dot represents similar position under each span. Span was increased in the upper left of photo.

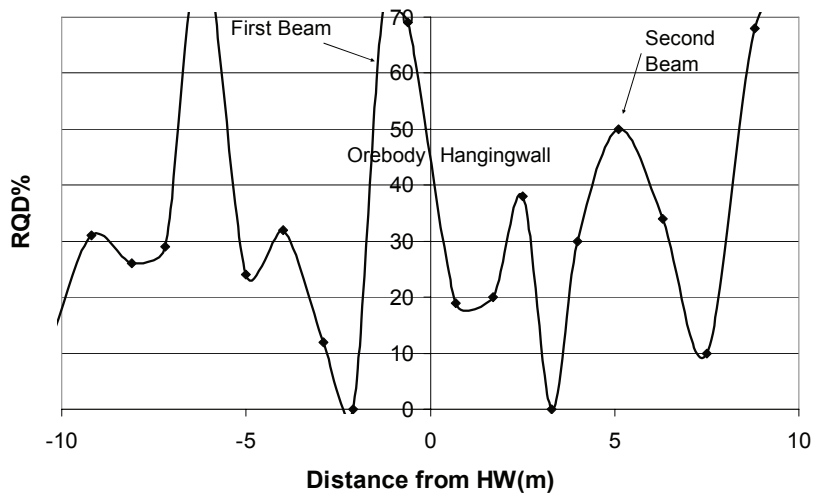
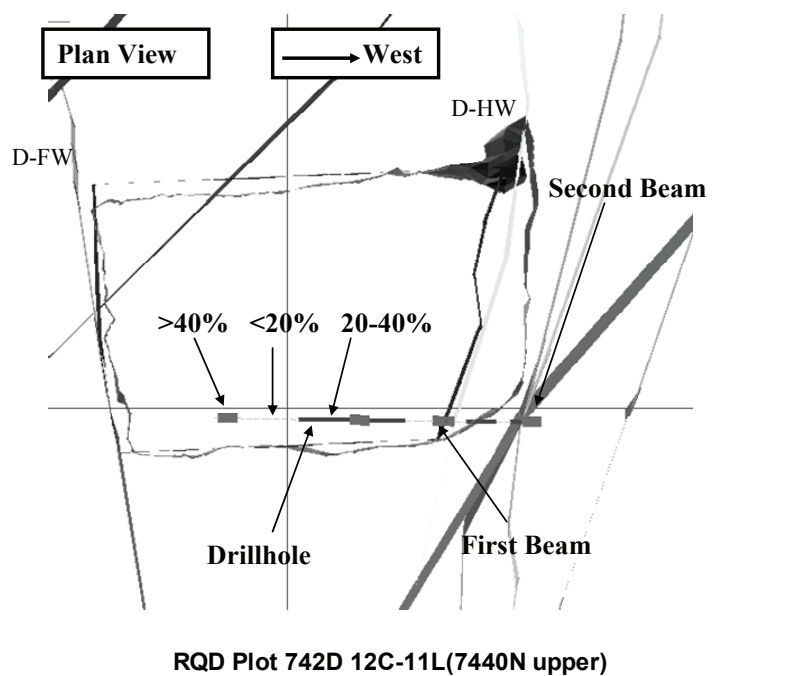
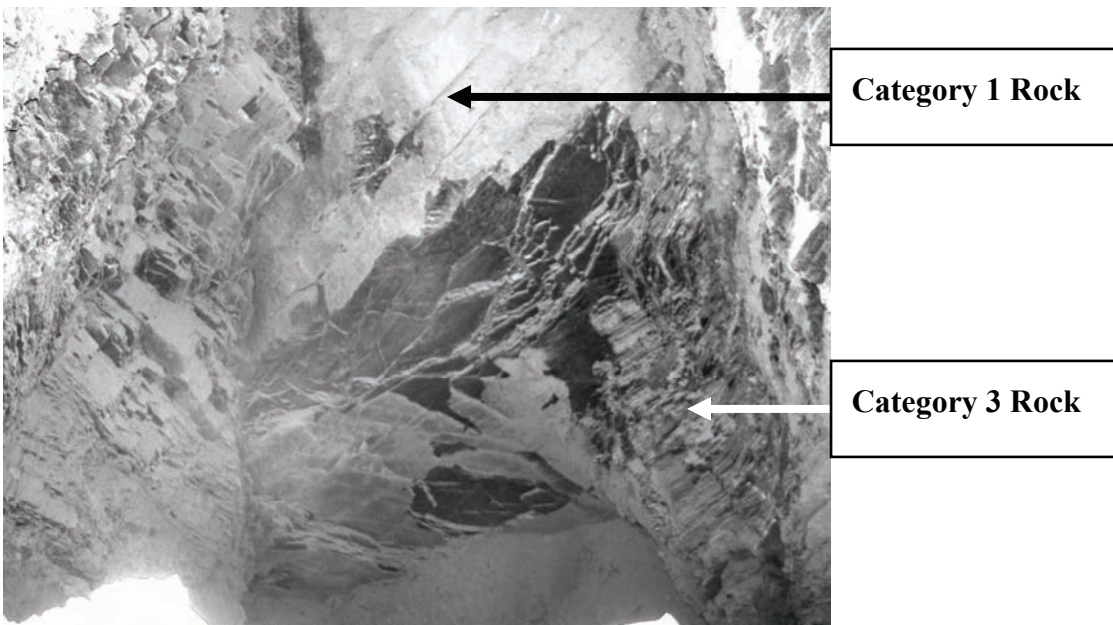


Figure 11.—742D 12C-11L. First composite beam (category 1) was stable under 11-m span, but failed under a 17-m span, arching through the category 2 rock to the second composite beam (May 2004).



**Figure 12.—**Looking west through the open stope. Photo shows failure through category 3 to category 1 rocks.

#### Phase 4: Additional Factors

With the improved model for predicting HW performance developed, the effect of faulting, blasting, stress, undercutting, and time were then investigated to examine how much of a role they played in stope HW stability.

The effect of faults at the mine was debated, as some stopes with faults passing through had major overbreak, while others remained stable under similar stoping conditions. Some trends between faulting and lower RQD values were evident, but were not consistent. The RQD long section showed that RQD and stope stability could not consistently be related to the location of faulting, although poor rock quality can be associated with some of the faults (Figure 5). For example, there has been failure next to the S73 fault on the majority of levels where the stopes have been mined to the north of the fault (Figure 13). This correlation cannot be seen with all the north-east trending faults and agrees with the geological descriptions that the major faults show variable dextral offset, displacement and features [Grenfell and Haydon 2006].

Blasting has not been analyzed to the same degree as the other factors. This is due to the consideration of a 25-m-wide ore body, the failures are occurring at a depth much greater than the influence of ANFO higher-density explosive (approximately 0-2 m back break based on local opinion) or ISANOL lower-density explosive (approximately 0- to 0.5-m back break) in the HW ring of an 89-mm-diam production hole, and that the majority of HW rings have been charged with low-density explosive. The study has only touched on a few areas where data have been

available to show the effect of using low- or high-density explosive near a category 1 rock mass. This is shown as the explosive-sensitive zone on the composite beam versus span stability plot (Figure 8).

The performance of primary and secondary stopes was compared to examine the effect of the different stress conditions under which the stopes were mined. There were no consistently observed trends to indicate that stress levels influenced stope HW behavior on a mine-wide scale based on a comparison of depth of HW failure in primary stopes and secondary stopes in the same area of the mine. The comparison of depth of failures averaged 4.2 m for secondary stopes (58 samples) and 4.3 m for primary stopes (75 samples). However, secondary stopes have most often either performed in a stable manner or had >5-m depth failure, with significantly fewer cases in the 0- to 5-m depth of failure category (Figure 14). The sizes of primary and secondary stopes have varied through the life of the mine, providing a good spread of data for comparison. Stope HW performance can be seen as a function of individual stope design choices, where the stope depth of failure is plotted on a long section with rock quality (Figure 13). Secondary stopes extracted with adequate sequencing have performed well under larger HW spans than primary stopes where the HW RQD in the secondary stope has been better than that of the primary. On the other hand, there have been additional HW and back failures in secondary stopes where mining has been conducted out of sequence (triple-lift pendants), where cemented fill has failed in primaries, and some areas where primary stopes in the lift above were not filled for up to 8 months, resulting in additional fall-off and a subsequently worse

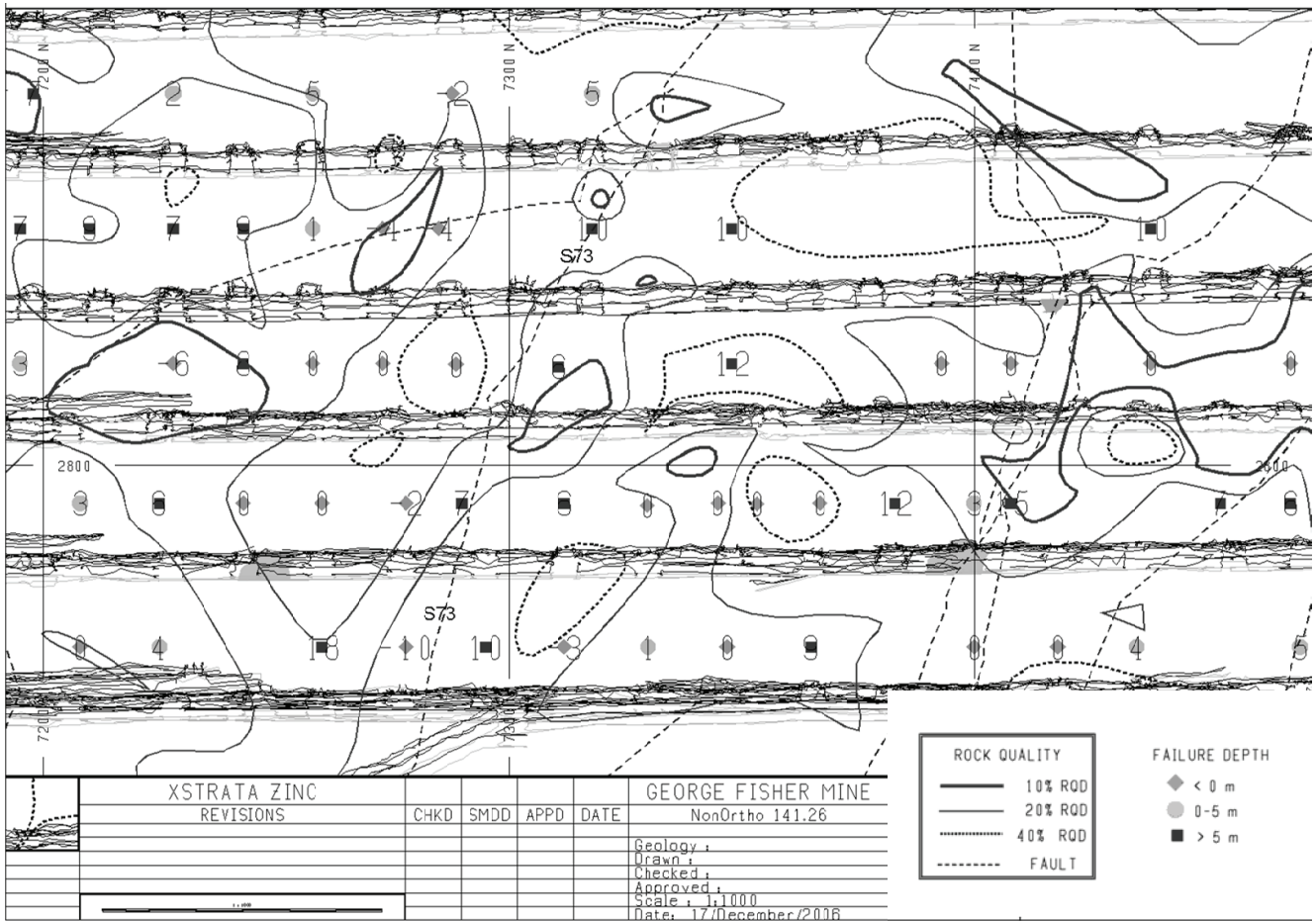


Figure 13.—Long section with faults, stopes, and depth of failure (plotted at stope centerlines).

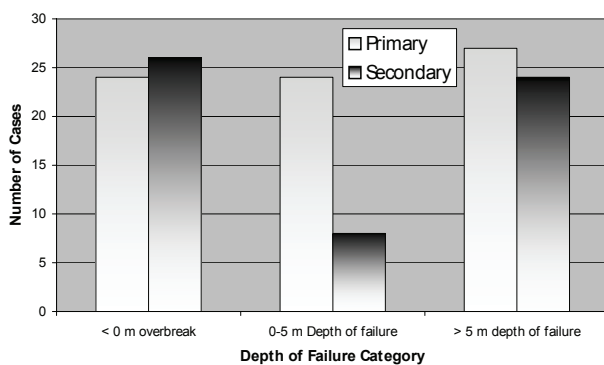


Figure 14.—Comparison of failures in primary and secondary stopes.

stress condition for mining the secondaries. During 2006, significant delays in cement filling and/or lack of tight filling of previous lifts of the primaries were experienced. Three of the four secondary stopes (719D, 723D, 730D 10L–10C) experienced large back failure/caving above the designed stope level. One particular stope had 10 m of HW

failure and caved 20 m above the designed stope level when it was predicted to have 2–3 m of HW failure based on the cumulative overbreak model. The primary stopes had all been mined at a 15-m strike span to access the tonnes sooner and were left open for up to 254 days, during which time sidewall failures occurred off of the secondary stope pillars, resulting in a stope <15 m wide. It is important to capture such information to verify the limits to which the design model can be applied and to reiterate the potential downstream mining-influenced effects where sequencing and backfill conflict with meeting production targets.

Current work is being completed to determine the effects of producing stopes adjacent to voids that have remained open for extended periods of time. The mining cycle, from firing to filling, is being analyzed with respect to stope behavior prediction and performance, with emphasis on time-related failure of the stopes. Analysis to date has shown that relaxation/failure of the secondary pillar seems to be reduced by the timely filling of the primary stopes on the same level as well as the next lift above.

Being able to recognize potential poor stope performance at an early stage in the design process will allow for more efficient mine planning and extraction, with manageable dilution. So far, telltale signs of poor-performing stopes have been mining difficulties when establishing secondary crosscuts, such as arching failure of the crosscut profiles, and difficulty installing ground support and reinforcement. HW and/or back overbreak from the previous lift must also be considered to determine stope HW design choices for the next lift. In conjunction with the model, the time-related failure study, together with observational data, should give the planning team more insight into predicting future stope performance and managing stope stability.

### **Summary: Results of Trials and Methodology**

Management and operational support to implement changes to individual stope designs was very positive, and many ideas were discussed to improve mine performance based on the understanding of HW behavior. Based on the cumulative overbreak model where the rock mass conditions meet the specific criteria, these design choices include the verticalization of HWs, use of cabled and non-cabled ore chocks for HW stability, use of ore skins where mining consequences from HW failure are high, and an effective rock mass management strategy [Capes et al. 2005]. The development and use of the model resulted in significant research and development benefits to the company. Figure 15 shows the contribution of the stoping methodology change as a reduction in annual stope dilution from 14.4% (2003) to 6.3% (2005), an increase in zinc grade from 7.4% to 8.7%, and an increase in production from 2.1 to 2.6 Mt [Capes et al. 2006].

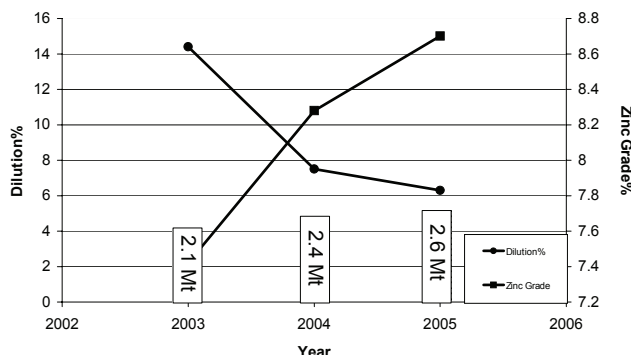


**Figure 15.—George Fisher North stope dilution percent, total mine tonnes, and zinc grade versus time.**

### **CONCLUSIONS**

Dedicated on-site research using a sound geological engineering approach of data collection, communication, underground observations, analysis, and implementation of ideas resulted in a thorough understanding of HW

overbreak. This was achieved by creating a model for design based on historical performance, understanding why it worked and why it did not work, appreciating it for the insights it provided, and continually reanalyzing as more information became available. The study has reemphasized the belief in understanding relevant factors for individual stope design. The averaging approach for estimating rock mass properties for design methods does not always provide the best answer based on available information. Many considerations must be given to design individual stopes. Generalizing all stope designs into one category can lead to poor design. Individual fault characteristics play a role in stope stability. There is no discernible difference in average HW depth of failure between primary and secondary stopes, although mining out of sequence, triple-lift pendants, and poor cement fill quality or lack of tight fill and/or delayed fill in primary stopes may lead to greater HW failure and create subsequent stope back failure. The model created the ability to develop innovative empirical stope design tools to control and reduce dilution in conjunction with following a set of mine-wide extraction rules developed from numerical modeling. The development and use of the model resulted in significant research and development benefits to the company. The confidence in prediction created individual stope design changes that contributed to a reduction in dilution and an increase in head grade while continuing to ramp up production from 2003–2005.

### **ACKNOWLEDGMENTS**

The authors would like to thank Xstrata Zinc and the University of Saskatchewan for their support, as well as the various technical services and operations personnel and consultants who have shared their thoughts during their time at George Fisher Mine Operations.

### **REFERENCES**

- Beck DA [2003]. Stress influences on rockmass damage and stope stability at GF mine-calibrated model criteria. Consultant report for Xstrata Zinc, George Fisher mine.
- Barton N, Lien R, Lunde J [1974]. Engineering classification of rock masses for the design of tunnel support. Rock Mech 6(4):189–236.
- Brady TM, Pakalnis R, Clark L [2005]. Design in weak rock masses: Nevada underground mining operations. SME preprint 05–43. Littleton, CO: Society for Mining, Metallurgy, and Exploration, Inc.
- Capes GW, Grant DR, Neindorf LB [2006]. George Fisher: sustainable mine design. Paper presented at the Second International Seminar on Strategic Versus Tactical Approaches in Mining (Perth, Australia).
- Capes GW, Milne DM, Grant DR [2005]. Stope hangingwall design approaches at the Xstrata Zinc, George

Fisher mine, North Queensland, Australia. In: Chen G, Huang S, Zhou W, Tinucci J, eds. Proceedings of the 40th U.S. Rock Mechanics Symposium (Anchorage, AK, June 25–29, 2005). Alexandria, VA: American Rock Mechanics Association.

Clark L, Pakalnis R [1997]. An empirical design approach for estimating unplanned dilution from open stope hangingwalls and footwalls. Presented at the 99th Canadian Institute of Mining Annual Conference (Vancouver, British Columbia, Canada).

Deere DU [1964]. Technical description of rock cores for engineer-purposes. *Rock Mech Eng Geol* 1(1).

Forrestal PJ [1990]. Mount Isa and Hilton silver-lead-zinc deposits. In: Hughes FE, ed. *Geology of the mineral deposits of Australia and Papua New Guinea*. AusIMM Monogr 14:927–934.

Grenfell K, Haydon M [2006]. Challenges in modelling large complex orebodies at the George Fisher north mine. In: *Proceedings of the Sixth International Mining Geology Conference* (Darwin, Northern Territory, Australia, August 21–23, 2006).

Hadjigeorgiou J [1999]. Memorandum of March 11, 1999, from John Hadjigeorgiou, Laval University, Quebec, Canada: a discussion document on geotechnical rock mass characterisation for Mount Isa.

Miller F, Jacobs D, Potvin Y [1992]. Laser measurement of open stope dilution. *CIM Bull* 85:Jul-Aug.

Potvin Y [1988]. *Empirical open-stope design in Canada* [Dissertation]. Vancouver, British Columbia, Canada: University of British Columbia.



# AN INTEGRATED APPROACH TO SUPPORT DESIGN IN UNDERGROUND COAL MINES

By Murali M. Gadde,<sup>1</sup> John A. Rusnak,<sup>2</sup> and Christopher Mark, Ph.D., P.E.<sup>3</sup>

## ABSTRACT

Rock mass classification systems are extremely useful for site characterization and have been employed by the rock mechanics community for several decades. While empirical in nature, the classification systems provide a viable means to quantify the nature of rock mass, which is necessary for stability analyses. In U.S. coal mines, the Coal Mine Roof Rating (CMRR) is the most widely used classification system for several purposes, including support selection, chain pillar design, assessing the stability of extended face cuts, etc. The Analysis of Roof Bolt Systems (ARBS) is an empirical method developed from the CMRR to guide selection of roof bolts as the primary support system in U.S. coal mines. In this paper, the experience of Peabody Energy in applying ARBS to support design is discussed. In general, data from the Peabody mines show that ARBS predictions match well with field conditions. Peabody, however, does not use ARBS as the stand-alone methodology for support selection. Peabody uses a two-pronged approach in which the support requirement is initially estimated from the classification method, and then numerical modeling is used to select the proper reinforcement system. Such an integrated approach is necessary, as ARBS suggests only the “amount of steel” that may be used to support the roof and does not specify which type of roof bolt to use. A case study is used to demonstrate the usefulness of ARBS and Peabody’s integrated approach to support design. Also, the application of ARBS at several Peabody mines showed a very good correlation with support cost. The correlation indicated a direct relation between bolting cost and the ARBS value.

## INTRODUCTION

A rock mass is an extremely complex material to deal with quantitatively. This is further so when one attempts to describe its “quality” in relation to its engineering behavior. Several factors influence rock mass behavior, including the number, nature, and spatial distribution of discontinuities traversing through it; compressive strength

of the rock matrix; presence of water; etc. Despite the complexity, efforts have been made to provide quantitative descriptions of rock mass quality, which are indispensable for engineering analyses.

During the past 4 decades, significant progress has been made in quantitative rock mass site characterization, especially through the development of rock mass classification systems. The most notable of these systems are Bieniawski’s [1973] Rock Mass Rating (RMR) and the Rock Mass Quality Index (Q) proposed by Barton et al. [1974]. Common to these and other classification systems is the selection of a few significant variables that have the most bearing on rock mass engineering behavior. Each of these variables are assigned numerical values that reflect their importance in controlling such behavior. After individual ratings are assigned to the significant parameters, they are mathematically manipulated to obtain one final number, which provides a quantitative description of the nature of the rock mass.

Both the RMR and Q were developed mainly based on case histories from tunnels driven in “hard rock.” As a result, they cannot be directly extended for use with coal measure rocks, as the parameters that influence the response of the rock mass are different. Several classification schemes applicable for coal measure rocks have been developed by various researchers, the most popular of which is the Coal Mine Roof Rating (CMRR) developed by the U.S. Bureau of Mines [Molinda and Mark 1994]. This system follows Bieniawski’s RMR format with values ranging from 0 to 100 to indicate the quality of the strata. The CMRR is most widely used in the United States and Australia; it has also been employed in South Africa, Canada, and the United Kingdom. The most recent of the coal mine classification systems is the Coal Measure Classification (CMC) proposed by Whittles et al. [2007].

Over the years since its inception, the CMRR has been used for several purposes in coal mine strata control. Correlations have been developed to select roof bolts as the primary support system, in sizing longwall chain pillars, to forecast if extended face cuts will work or not, and several others [Mark and Molinda 2005]. The main interest of this paper is the usefulness of the CMRR and its offshoot, the Analysis of Roof Bolt Systems (ARBS) [Mark et al. 2001], for roof bolt design as they are applied to Peabody Energy mines. Also, the limitations of ARBS are pointed out, and the integrated approach that Peabody has developed to overcome some of the problems is discussed.

<sup>1</sup>Senior engineer, Peabody Energy, St Louis, MO.

<sup>2</sup>Vice president of engineering, Peabody Energy, St. Louis, MO.

<sup>3</sup>Principal research mining engineer, Pittsburgh Research Laboratory, National Institute for Occupational Safety and Health, Pittsburgh, PA.

## THE COAL MINE ROOF RATING (CMRR)

The CMRR has two different versions: field [Molinda and Mark 1994] and drill core [Mark et al. 2002]. The field CMRR is estimated from underground observations where the roof is exposed mainly by roof falls and overcasts. Since visual observations play a key role in the field CMRR, it is somewhat subjective. Two different persons are likely to come up with different field CMRR values for the same site, although experience has shown that they will usually differ by no more than about five points. In contrast, drill core CMRR is derived from laboratory-determined parameters and measurements on cores, which are less subjective, but are subject to their own variability.

In both the field and drill core CMRR, the following parameters are weighed to estimate the roof competence:

- Compressive strength
- Discontinuities

In the field CMRR, the discontinuities are characterized by their cohesion, roughness, spacing, and persistence. In the core version, discontinuity ratings are determined by the fracture spacing and diametral point load strength.

The process of computing CMRR starts by dividing the roof into structural “units.” Strength and discontinuity ratings are then determined and added together to calculate the “unit ratings.” The unit ratings are then corrected for the number of discontinuity sets and the moisture sensitivity. Next, the overall CMRR of the roof is obtained by thickness-weighted averaging of the unit ratings within the “bolted interval.” Adjustments are then applied to the average CMRR for the following factors to determine the final rating:

- Strong bed in the bolted interval
- Number of units
- Groundwater
- Overlying beds

The structure of the CMRR as given above seems to work well in quantifying the quality of roof for most situations. One important assumption in the development of the CMRR is that the bedding plane is the major discontinuity in a coal mine. Since bedding planes are almost always horizontal to subhorizontal, their orientation is not a key factor in determining the roof stability. This is the reason why the orientation of a discontinuity has not been accounted for in the CMRR. The presence of other discontinuities, such as slickensides, is considered in the CMRR, but the orientation of those features is not.

There are situations, however, where practical experience indicates that the orientation of these features may be a critical factor in determining the support requirements, as indicated by the rock fall shown in Figure 1. This photo

was taken at a mine that has frequently occurring slickensided slip planes, which intersect at unfavorable angles to create wedge failure conditions. The immediate roof at the mine is made of black shale overlain by a very competent limestone. The CMRR for this roof was estimated to be over 60. Despite this high CMRR, several rock falls have occurred at the mine mainly because of the unfavorably oriented slickensided slip planes.



Figure 1.—Roof fall initiated by unfavorably oriented slip planes.

In cases like these, a discontinuity orientation adjustment to the CMRR can help to make it more general. This additional correction, however, is not essential for every application. It may be applied only if the instability is governed by the orientation of the discontinuity and occurs very frequently in a panel to make it a “general” feature rather than an isolated abnormality. Further, the correction is needed only if it is intended to deal with any instability originating from the discontinuity orientation by the primary support system. Even though several possibilities exist theoretically, practical experience in coal mines indicates that orientation-related rock falls are unlikely unless multiple features intersect at adverse angles. Based on the experience at the one case history mentioned above, the tentative suggestion in Table 1 is made to account for the discontinuity orientation in the CMRR. The adjustment shall be applied only to the unit ratings of the units that are intersected by the discontinuities.

Table 1.—Adjustment in the CMRR for the unfavorable discontinuity orientation

Condition	CMRR adjustment
Multiple discontinuities (joints, slip planes, etc.) intersecting at adverse angles to create sliding or wedge failure conditions .....	-5

## ROOF BOLT DESIGN USING ARBS AND THE CMRR

One of the most important applications of the CMRR is to design roof bolts as the primary support system. This is accomplished through an empirical approach called the ARBS [Mark et al. 2001]. Roof fall rates from 37 U.S. coal mines formed the necessary database for the logistic regression analyses conducted in ARBS. The final guidelines help in the selection of roof bolt pattern, bolt length, and intersection span based on the CMRR and other geomining inputs. ARBS is valid, however, only if the bolts work in beam building or supplementary support mode. A discriminant equation in terms of depth and CMRR was developed to determine which support mechanism was applicable for a given mining condition [Mark et al. 2001]. In ARBS, the required bolt density is given by a parameter,  $PSUP_G$ , as given below:

$$PSUP_G = (SF) [0.3 (Is_G - Is)] [(5.7 \log_{10} H) - (0.35 CMRR) + 6.5] \quad (1)$$

where SF = stability factor,  
 $Is_G$  = suggested intersection span, ft,  
 $Is$  = actual intersection span, ft,  
 $H$  = depth of cover, ft,  
and CMRR = coal mine roof rating.

The key advantages of ARBS are that it is simple to use and it is based on actual case histories. Therefore, a large number of uncertainties associated with coal mine ground control designs are inherently included in the statistical analyses conducted for ARBS. However, just like any other empirical tool, ARBS has its own limitations. First, the design equations cannot be extrapolated with confidence beyond the range of the original data. Second, some critical equations were developed from rather limited amount of data and thus should be used with caution. Third, and most importantly, ARBS does not specify which type of bolt to use in providing the bolt density given by Equation 1.

In U.S. coal mines, several different types of roof bolts are used, and each one works on a different mechanism [Dolinar and Bhatt 2000]. For example, the reinforcing action in fully grouted bolts is different from resin-assisted mechanical bolts. Unfortunately, the selection of bolt type is an extremely complex problem that cannot be addressed by a simple approach like ARBS. For this reason, Peabody uses an integrated approach wherein the support requirement is first estimated by ARBS, then the bolt type is chosen with the help of numerical modeling.

In the following sections, Peabody's experience with the application of ARBS and details on the Integrated Support Design Methodology (ISDM) are presented.

## PEABODY EXPERIENCE

Roof bolt design at most Peabody mines has evolved over the years by trial and error and limited engineering studies. Bolt pattern, bolt type, entry width, etc., were changed until each operation found the best system that worked for its conditions. Therefore, this database would form a very reliable check on the validity of the CMRR and ARBS. Data have now been collected from several operating Peabody mines located throughout the major U.S. coalfields. The number and location of the mines covered in this study are listed in Table 2. Some details relevant to the estimation of the CMRR and ARBS for the studied mines are provided in Table 3. The data were collected from both the mains and the panels at each operation. In the areas of adverse roof conditions, some secondary supports were also installed. The number of MSHA-reportable roof falls per 10,000 ft of development was collected from the mines that had noticed some instability. The data are given in Table 4 and plotted in Figure 2 against the CMRR. Five mines, with CMRR values ranging from less than 30 to nearly 50, have experienced roof fall rates less than 0.2 per 10,000 ft of development. The roof fall rates at three other mines were significantly higher.

**Table 2.—Number of mines by coalfield used in the study**

Coalfield/State	No. of mines
Interior Province: Eastern Region (Illinois Basin) .....	8
Appalachian.....	4
Colorado.....	1

**Table 3.—Different variables relevant to the CMRR and ARBS at the case study mines**

Depth, ft.....	150–1,400
Entry width, ft.....	16–22
Actual intersection span, ft .....	27–35
Steel grade, ksi.....	40, 50, 60, 75
No. of bolts per row .....	3–6
Bolt row spacing, ft .....	3.5–5
Bolt length, ft.....	3.5–10
Bolt diameter, in.....	0.625–0.875
Bolt type.....	RAM, FGR, TT
Accessories .....	Wood boards, square steel plates, straps, and wire mesh

RAM = resin-assisted mechanical. FGR = fully grouted rebar.

TT = torque tension.

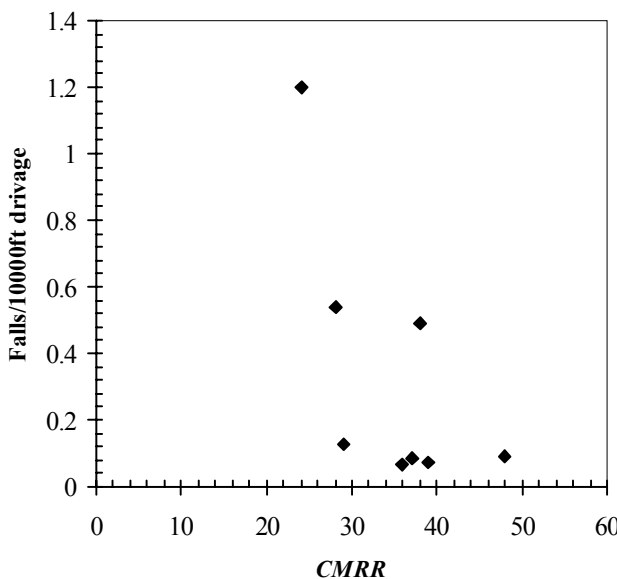


Figure 2.—Roof fall rate against CMRR for some case study mines.

At each of the studied operations, the CMRR was estimated from either underground observations or drill core data. Then, the suggested ARBS from Equation 1 was computed and compared with the actual value based on the successful roof bolting system. In estimating the suggested ARBS value, the stability factor was set to 1.0 in Equation 1. The derived numbers are given in Table 4 and plotted in Figure 3.

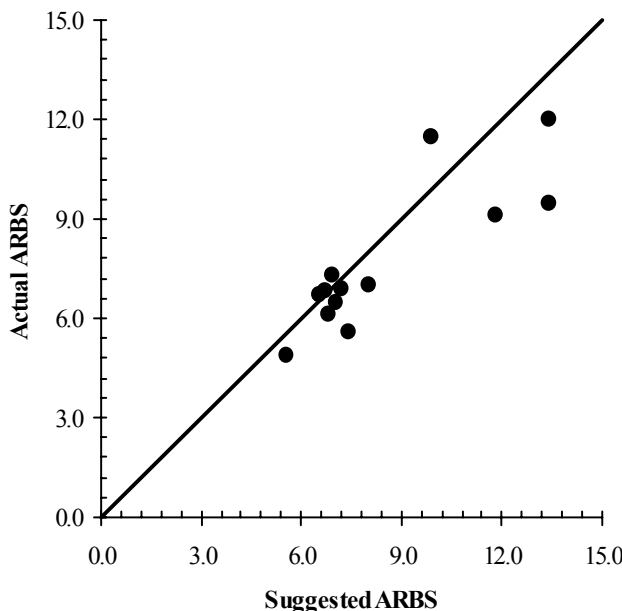


Figure 3.—Suggested versus actual ARBS values at the case study mines.

Table 4.—Suggested and actual ARBS values at the case study mines

Mine	CMRR	Suggested ARBS	Actual ARBS	Actual-to-suggested ARBS ratio	No. of roof falls per 10,000 ft of development
A.....	39	5.6	4.9	0.88	0.074
B.....	37	7.1	6.5	0.92	0.082
C ....	40	6.5	6.7	1.03	—
D ....	40	6.8	6.1	0.89	—
E.....	38	7.4	5.6	0.75	0.490
F.....	28	11.8	9.1	0.77	0.540
G....	24	13.4	9.5	0.71	1.200
H....	36	7.2	6.9	0.96	0.069
I.....	29	13.4	12.0	0.90	0.130
J.....	44	8.0	7.0	0.88	—
K.....	48	6.7	6.8	1.01	0.089
L.....	46	7.0	7.3	1.05	—
M....	43	9.9	11.5	1.16	—

The data in Table 4 show that the CMRR values at the studied mines varied from 24 to 48. Further analysis indicated that all eight Illinois Basin mines had CMRR values equal to or below 40, while all of the Appalachian mines, except one from the northern Appalachian coalfields, had CMRR values that exceeded 40.

Table 4 and Figure 3 further show that, in general, there is excellent agreement between the suggested and actual ARBS values at the studied mines. The three mines (E, F, and G) with the lowest ARBS stability factors also have the highest roof fall rates. These data support the validity and usefulness of ARBS in predicting the primary support requirements.

Since ARBS is an indirect measure of the amount of steel installed for roof support, it is logical to expect a good correlation with the support cost. To verify this, data

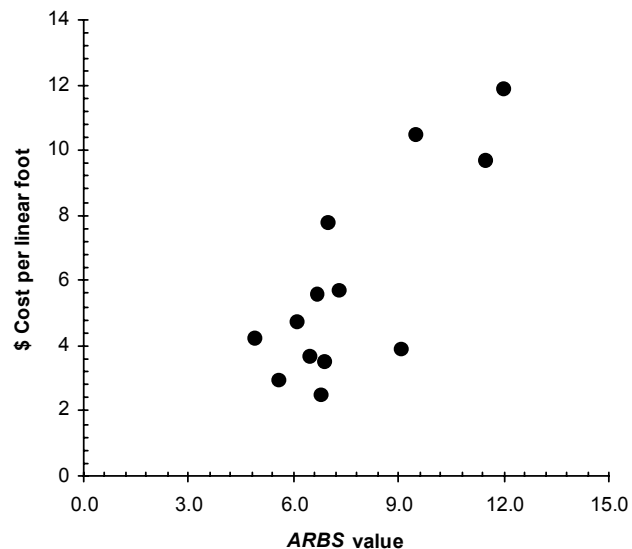


Figure 4.—Relation between the ARBS value and the average cost per linear foot of advance over a 6-month period.

were collected from the same mines in Table 4, which are plotted in Figure 4. A direct linear relation between ARBS value and the support cost can be seen from this figure. Note that the cost shown is the average value for a 6-month period for each mine and includes only the steel (bolt + plate) used for the primary support. This analysis shows that ARBS will also serve as an indicator of the support cost incurred in installing the bolt density suggested by it.

### INTEGRATED SUPPORT DESIGN METHODOLOGY (ISDM)

Within the confines of the original database, discussions in the preceding section have shown the effectiveness of ARBS in estimating the required support density. For complete roof bolt design, however, it is also necessary to know which type of bolt to use for any given mining conditions. While providing the same support resistance, different types of bolts will provide different levels of reinforcement depending on how harmonious the

bolt type is with the roof conditions. Any incompatibility may lead to instability or uneconomic designs.

Unfortunately, no scientific guidelines exist that help determine the matching bolt type for a given roof. The best available alternative is to use numerical modeling wherein the specific geomining conditions are simulated with different types of bolts to determine the best one. Therefore, a very effective roof bolt design can be achieved by combining the positive aspects of ARBS with those of numerical modeling. In fact, achieving such a fusion is the essence of Peabody's Integrated Support Design Methodology (ISDM). The individual steps in this process are shown in Figure 5. With some site-specific alterations, this methodology is being implemented in all of the new support design exercises at Peabody mines.

The ISDM process clearly recognizes the intractability of strata control designs by any single approach. The ISDM aims to maximize the benefits of empirical and analytical methods, neither of which alone can provide answers to all of the questions in support design. As Figure 5 indicates, one of the most critical elements of the

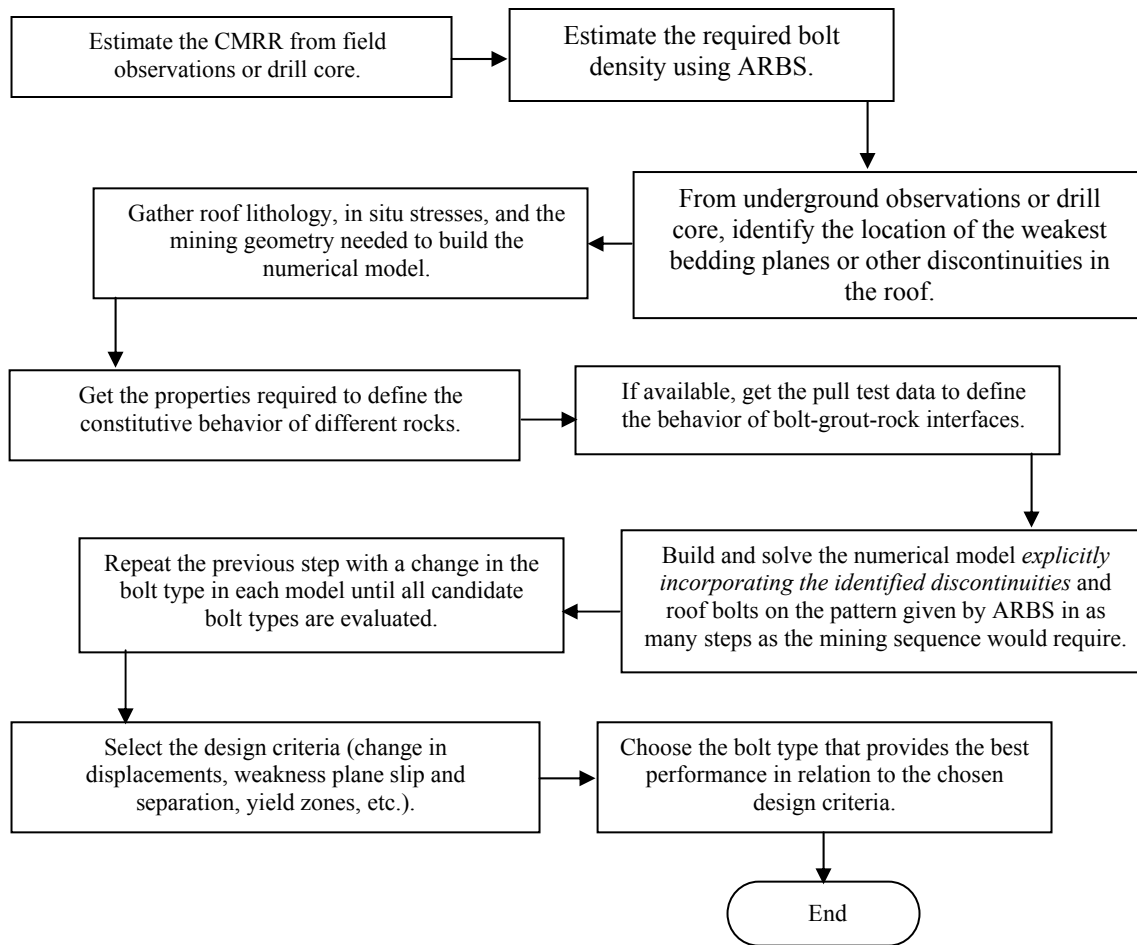


Figure 5.—Individual steps in Peabody's ISDM.

ISDM is to identify the weakest bedding planes in the roof and explicitly include those features in numerical models. Such detailed analysis is not possible any other way but through numerical modeling. Also, different types of roof bolts could easily be simulated with numerical methods. More details on the individual steps in Figure 5 are provided below with the help of a recent support design exercise carried out for a Peabody mine.

### ISDM EXAMPLE

The mine in this case study will extract a coal seam of variable thickness with a final mining height of about 7 ft. The immediate roof at the mine is predominantly shale. At a few places, where the coal seam is thicker than 7 ft, a rider coal forms the immediate roof. Although over the bulk of the reserve the bolted horizon consists mainly of shale, at a few locations sandstone comes close enough to the seam to be a part of the bolting horizon. The average depth of the seam is about 680 ft. Exploratory drill core was available from 11 boreholes with all of the necessary rock strength information to estimate the CMRR.

The following discussion illustrates each step involved in arriving at the recommended support design using the ISDM:

#### **Step 1: Estimate the CMRR.**

From the available 11 core holes, the CMRR was estimated and the numbers are shown in Figure 6.

#### **Step 2: Use ARBS to determine the required bolt density.**

Since the CMRR is reasonably consistent (as seen from Figure 6), the average value of 41 was used as the input for ARBS. Based on this and other mining inputs, it was found that for the proposed 18-ft-wide entry at the mine, four 6-ft-long #6, grade 60 bolts on 3.5-ft row spacing will provide a stability factor of 1.25. Since this bolt pattern will provide a stability factor in excess of the one recommended in ARBS, the design has been accepted. It may be mentioned that this is just one of the several support patterns suggested for different geomining conditions at the study mine.

#### **Step 3: Gather necessary inputs for modeling.**

The next step in ISDM is to conduct numerical modeling to determine the proper bolt type. Based on physical observations on the recovered cores, no major discontinuities other than bedding planes were discovered at the case study mine. Although core breakage was noticed at several locations, the only discontinuities considered for the modeling were those between distinct lithologic units or those that were not related to core handling. For instance, one hole that has been used for modeling has rider coal in the immediate roof and shale above it. From core

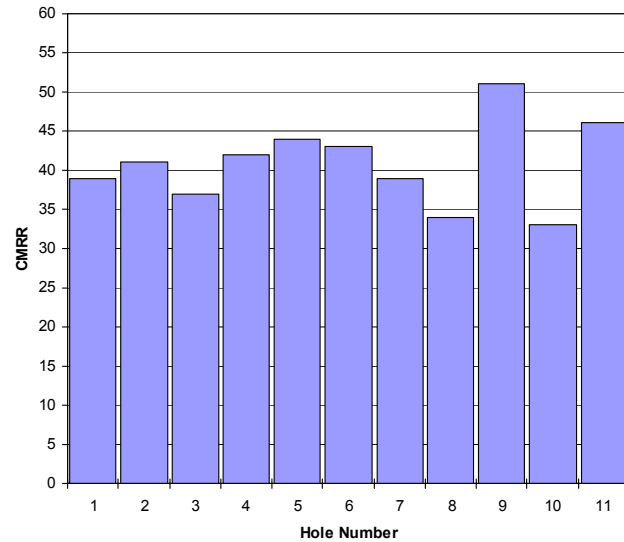


**Figure 6.—CMRR variation at the case study mine.**

examination, it was found that there were seven different weakness planes within the first 7 ft of the roof that need to be considered in the modeling. All these seven contacts were explicitly included in the models for this type of roof lithology.

In all of the models, the rock was treated as an elastic material. The necessary data required to define this constitutive behavior were available from laboratory testing on cores. The contacts, however, were simulated using inelastic Mohr-Coulomb behavior. Even though the bedding planes were not tested for their properties, the assumed numbers will not significantly alter the modeling outcome, as the objective here is to compare the relative performance of different types of bolts under otherwise identical conditions. Any errors in the input data will most likely affect all of the models to the same extent.

Since the case study mine is a new venture, field pull tests on roof bolts were not conducted to determine the required inputs for the bolt simulation. However, actual pull test data from a different mine on #6, grade 60 fully grouted rebar were used to estimate the shear stiffness of the bolt system.

#### **Step 4: Build and solve the models with different bolt types.**

Two different bolt types were considered for the case study mine: fully grouted and torque-tension type. In the case of the torque-tension bolt, only the top 4 ft was grouted. The models for each bolt type were run in two stages. In the first stage, the model was solved to create the premining stresses; in the second, the mine entries were created with bolts installed on the pattern suggested by ARBS. In each model, the bedding planes identified in step 3 were explicitly included.

In previous modeling studies reported in the literature, roof bolts were typically simulated in one of two ways: either the bolts were built “physically,” or mathematically equivalent bolts were used. In the first approach, the roof bolt, resin, and drill hole are explicitly made in a numerical model. Inputs are then provided to define the constitutive behavior of each element separately along with the interface properties for bolt-resin and resin-rock contacts. Ideally, this seems to be the most accurate way to model roof bolts. Difficulties, however, arise for several reasons. First, the roof bolts are dimensionally two or three orders smaller than the mine entry and, therefore, achieving a proper mesh density becomes extremely difficult even with the best of the available computing resources. Second, the constitutive behavior of the bolt-resin and resin-rock interfaces has never been tested in situ to provide all of the inputs needed for modeling. Third, problems in numerical solutions will easily occur because of the several awkwardly intersecting contact planes in this approach. Finally, it is extremely time-consuming to build and solve a model that has all of the complications of “physically” including roof bolts. To make the problem solvable in a reasonable amount of time and within the limits of available computing resources, several assumptions and simplifications must be made. As a result, even though the explicit inclusion of bolts may provide a sense of precision, the benefits of such a tedious approach may be more illusory than real. In any case, explicit modeling of roof

bolts may perhaps be justified for research work, but is certainly not a feasible option for routine support design.

In the second approach, mathematically equivalent roof bolt elements are created whose constitutive behavior will provide an accurate representation of the roof bolt action. Since many of the complications involved with the first approach are eliminated, it is much easier to model a large number of bolts in a single model with little effort. Also, the assumptions involved in formulating the bolt elements are probably no worse than those required to make physically built roof bolts “work” numerically. For the obvious advantages, in this study the second approach has been chosen for bolt modeling using a finite difference-based code, FLAC3D<sup>4</sup> [Itasca Consulting Group 2005]. This software is by far the most commonly used modeling tool in rock engineering. FLAC solves the dynamic equation of motion in time-domain to provide pseudostatic solutions. The explicit solution scheme adopted in FLAC3D makes it an ideal tool for simulating nonlinear behaviors [Itasca Consulting Group 2005].

**Step 5: Examine the model results and choose the final bolt type.**

Roof bolts are point-acting-type structures whose radius of influence is rather limited. As a result, there may not be a significant difference in the stress state of the

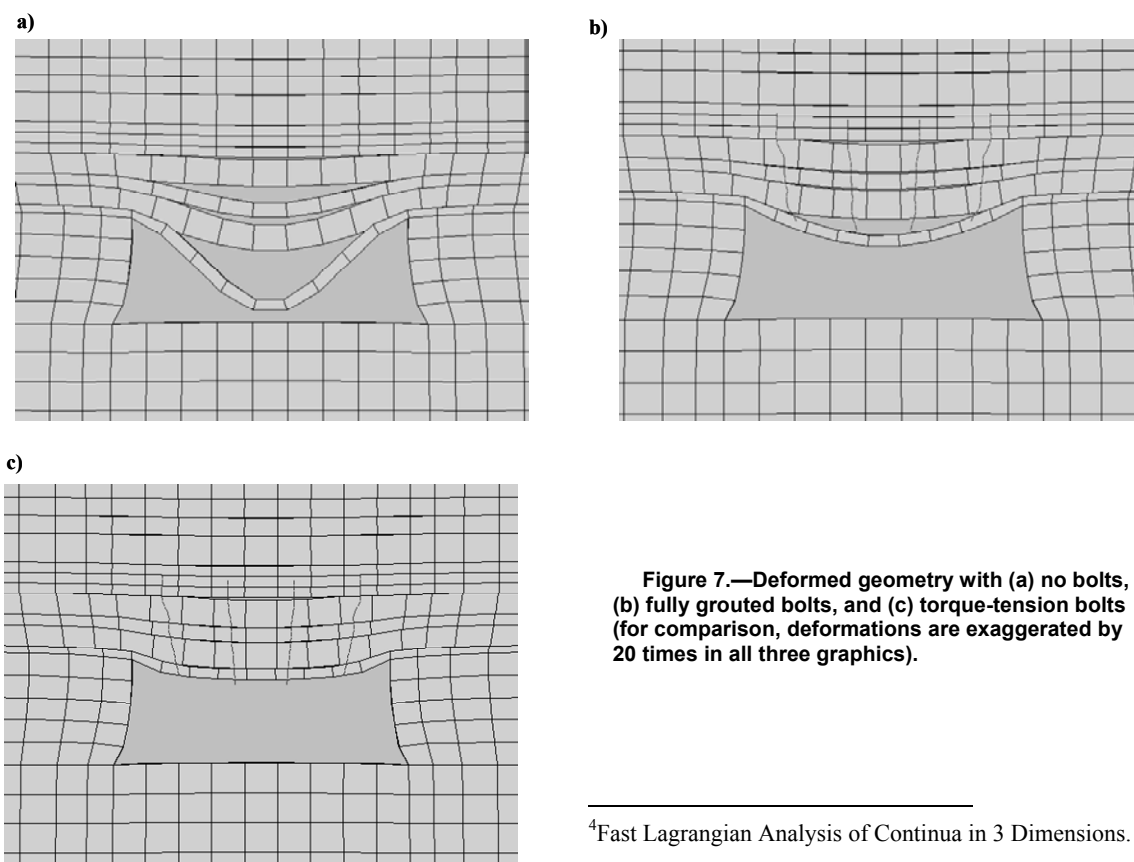


**Figure 7.—Deformed geometry with (a) no bolts, (b) fully grouted bolts, and (c) torque-tension bolts (for comparison, deformations are exaggerated by 20 times in all three graphics).**

---

<sup>4</sup>Fast Lagrangian Analysis of Continua in 3 Dimensions.

immediate roof to make a substantial difference to the extent of yield zones or to the magnitude of local safety factors. For this reason, in this study, the criterion used for bolt performance comparison was vertical displacement. If a bolt keeps individual layers in the immediate roof tightly bundled together, then the bolt will most likely perform well. Based on this criterion and the layered nature of the immediate roof, torque-tension rebar was found to be the best bolt type, as shown by the modeling results in Figures 7–8.

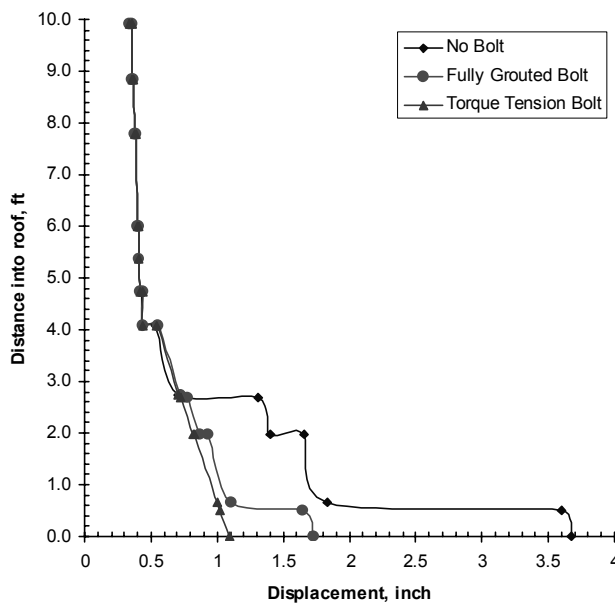


**Figure 8.—Vertical displacement at the middle of the entry with distance into roof.**

Without roof bolts, Figure 7 shows that the first three layers will separate from the layers above, and the resulting deformations are so large that these layers will most likely fail. Even with fully grouted roof bolts, the first layer's movement is considerable, and thus some skin failures cannot be ruled out. The torque-tension bolts, however, substantially reduce the separations and slips across the first three bedding planes. This can be seen more clearly from a plot of vertical displacement at the middle of the entry shown in Figure 8.

In a different part of the reserve at the case study mine, the immediate roof has shale and sandstone within the bolting horizon. By a similar numerical modeling exercise, the models found that fully grouted roof bolts could stabilize the roof as effectively as torque-tension bolts. For the obvious cost benefits, fully grouted bolts were recommended for this area.

## CONCLUSIONS

Empiricism and coal mine strata control are inseparable. The contributions of empirical rock mass classification systems and their derivatives for successful roof

support designs are considerable. Notwithstanding the ground-breaking advancements in numerical modeling, empirical tools will continue to play a critical role in strata control designs. This fact has been demonstrated by the success of the CMRR and ARBS, as shown in this paper.

Much can be achieved by synthesizing the benefits of empirical and analytical tools, which indeed is the crux of Peabody's ISDM. As demonstrated by the case study in this paper, this integrated approach can provide very detailed information on the performance of different types of roof bolts under the same roof conditions. Also, the modeling helps to explain the failure mechanics, and this knowledge will substantially aid in devising proper support measures.

## REFERENCES

- Barton N, Lien R, Lunde J [1974]. Engineering classification of rock masses for the design of tunnel support. *Rock Mech* 6(4):189–236.
- Bieniawski ZT [1973]. Engineering classification of jointed rock masses. *Trans S Afr Inst Civ Eng* 15:335–344.
- Dolinar DR, Bhatt SK [2000]. Trends in roof bolt application. In: Mark C, Dolinar DR, Tuchman RJ, Barczak TM, Signer SP, Wopat PF, eds. *Proceedings: New Technology for Coal Mine Roof Support*. Pittsburgh, PA: U.S. Department of Health and Human Services, Public Health Service, Centers for Disease Control and Prevention, National Institute for Occupational Safety and Health, DHHS (NIOSH) Publication No. 2000-151, IC 9453, pp. 43–51.
- Itasca Consulting Group [2005]. *Fast Lagrangian analysis of continua in 3 dimensions, version 3.0*. Minneapolis, MN: Itasca Consulting Group, Inc.
- Mark C, Molinda GM [2005]. The coal mine roof rating (CMRR): a decade of experience. *Int J Coal Geol* 64(1–2):85–103.
- Mark C, Molinda GM, Barton TM [2002]. New developments with the coal mine roof rating. In: Peng SS, Mark C, Khair AW, Heasley KA, eds. *Proceedings of the 21st International Conference on Ground Control in Mining*. Morgantown, WV: West Virginia University, pp. 294–301.
- Mark C, Molinda GM, Dolinar DR [2001]. Analysis of roof bolt systems. In: Peng SS, Mark C, Khair AW, eds. *Proceedings of the 20th International Conference on Ground Control in Mining*. Morgantown, WV: West Virginia University, pp. 218–225.
- Molinda GM, Mark C [1994]. Coal mine roof rating (CMRR): a practical rock mass classification for coal mines. Pittsburgh, PA: U.S. Department of the Interior, Bureau of Mines, IC 9387.
- Whittles DN, Reddish DJ, Lowndes IS [2007]. The development of a coal measure classification (CMC) and its use for prediction of geomechanical parameters. *Int J Rock Mech Min Sci* 44(4):496–513.

# A ROCK MASS RATING SCHEME FOR CLASTIC SEDIMENTS BASED ON GEOPHYSICAL LOGS

By Peter J. Hatherly, Ph.D.,<sup>1</sup> Terry P. Medhurst, Ph.D.,<sup>2</sup> and Stuart A. MacGregor<sup>3</sup>

## ABSTRACT

In addition to fractures and joints, compositional factors and bedding influence the strength of clastic sedimentary rocks. Rock mass rating schemes must therefore consider all of these factors.

In this paper, a rating scheme for clastic sediments based on geophysical measurements is described. Geophysical logging allows an approximation of rock composition to be obtained and an assessment of bedding frequency and laminations. Velocity measurements incorporate the effects of fracturing.

The rating requires scores for the intact rock, bedding/cohesion, and defects. These are combined to yield a Geophysical Strata Rating (GSR). Determination of the GSR is objective and repeatable. GSR values are typically between 20 and 80 and can be related to the Coal Mine Roof Rating.

## INTRODUCTION

Analysis of geophysical borehole logs provides one of the best approaches to characterizing rocks within boreholes. The techniques have been developed mainly for use in petroleum exploration, but there are also established applications in coal mining, metalliferous mining, groundwater investigations, and civil engineering. For mining, the main application is to provide information on ore quality, geological correlations, and geotechnical properties.

This paper concerns the geotechnical applications in underground coal mining where the characterization of roof and floor strata is important for understanding caving behavior and roof support requirements. The results relate to Australian coal mining conditions where the coals are mainly of Permian age and depths of mining are usually less than 500 m. Roof and floor strata are mainly sandstones, siltstones, and claystones with occasional tuff beds and bands of siderite. Limestones are absent. Given the mainly clastic nature of these strata, the techniques of geophysical log analysis developed for the characterization of petroleum reservoirs are particularly useful.

On the basis of these techniques, Medhurst and Hatherly [2005] proposed the Geophysical Strata Rating (GSR). In this paper, we further develop the GSR and provide examples of its application. The GSR mainly relies upon sonic logging. In this regard, it can be viewed as a refinement of UCS/sonic relationships frequently employed in Australian coal mining. It also has similarities with the approach developed by Barton [2002, 2006] for determining Q-values from sonic, porosity, and depth information. The GSR delivers results on a linear scale similar to the Coal Mine Roof Rating (CMRR) of Molinda and Mark [1994]. It combines separate ratings for the intact rock mass and defects. Beyond consideration of velocity, porosity, and depth, it also considers clay content (shaliness).

Owing to the widespread interest in using sonic velocity in geotechnical investigations, this paper begins with a review of the geotechnical significance of sonic velocity.

## SONIC LOGGING

The sonic velocity obtained by sonic logging is a compressional seismic wave (P-wave) with velocity,  $V_p$  given by

$$V_p = \sqrt{\frac{k - 4/3\mu}{\rho}} \quad (1)$$

where  $k$  is the bulk modulus (incompressibility),  $\mu$  is the shear modulus, and  $\rho$  is the density.

In an isotropic and homogeneous rock body, seismic velocity responds to the elastic properties and density of the medium as might be measured in a rock mechanics laboratory. If the strength of the rock were related to its elastic properties, then the velocity would also be related to the strength. However, when inhomogeneities due to factors such as compositional variations and defects are present in the rock mass, as well as anisotropy in the form of bedding and other directional features,  $k$ ,  $\mu$ , and  $\rho$  are variable and the interpretation of  $V_p$  becomes more difficult. To understand the significance of a velocity measurement, it is necessary to understand the influence of the various causes of inhomogeneity and anisotropy.

In fresh igneous rocks where the porosity is low and the crystals have similar elastic properties, the velocity is largely controlled by fractures and joints. Barton [2006] makes frequent reference to the work of Sjøgren et al. [1979], who correlated RQD with measurements of  $V_p$ .

<sup>1</sup>CRC professor of mining geophysics, University of Sydney, Sydney, New South Wales, Australia.

<sup>2</sup>Principal geotechnical consultant, AMC Consultants Pty. Ltd., Brisbane, Queensland, Australia.

<sup>3</sup>Senior geological engineer, SCT Operations Pty. Ltd., Wollongong, New South Wales, Australia.

from shallow seismic refraction surveys in Norwegian igneous and metamorphic rocks. As is also reported by Barton [2006], Deere et al. [1967] found a relationship between RQD and the square of the ratio of  $V_p$  measured in the field and in the laboratory on intact samples. However, when igneous rocks weather, compositional changes occur and pore spaces develop. Other factors will then influence the velocity.

In sedimentary rocks, particularly those that form petroleum reservoirs, there has been considerable attention given to understanding the relationship between  $V_p$  and composition and porosity. Pressure is also an important factor because of its influence on the porosity. While it is not possible to determine exact expressions for  $V_p$ , laboratory studies allow development of empirical relationships. For example, Han et al. [1986] report on a study of sandstone samples with fractional porosities,  $\phi$ , ranging from 0.02 to 0.3 and clay contents,  $V_{Shale}$ , ranging from 0.03 to 0.5. Results are given for a number of confining pressures. For example, at 5-MPa confinement,  $V_p$  is given by

$$V_p = 5.26 - 7.08\phi - 2.02V_{Shale} \quad (2)$$

with a correlation coefficient of 0.969.

While this equation shows that porosity has 3.5 times the effect on the velocity compared to clay, the clay content does have a measurable effect. This is illustrated in Figure 1, which shows how velocity varies over the compositional range investigated by Han et al. [1986]. As Han et al. point out, the velocity in a rock with very near-zero porosity and low clay content is significantly lower than the velocity of 6.05 km/s true for quartz aggregates. This implies that just small amounts of clay are able to soften the sandstone matrix and produce a reduction in velocity.

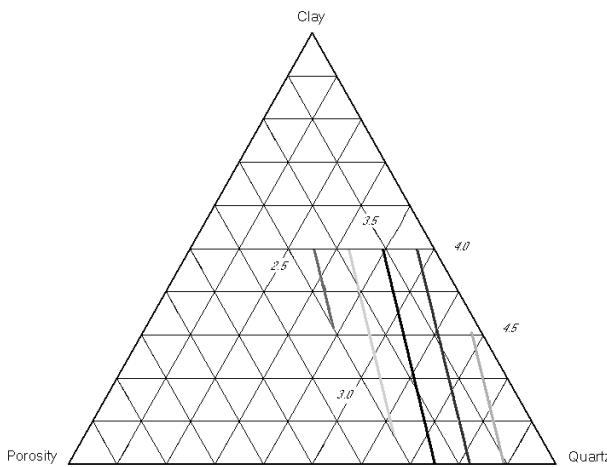


**Figure 1.**—Ternary diagram showing changes in  $V_p$  in sandstone according to porosity, clay, and quartz content at 5-MPa confinement. Velocities are in km/s. Quartz content =  $1 - V_{Shale} - \phi$ .

Han et al. [1986] also suggest that for clay to have an effect on the velocity, it has to be either structural (i.e., bonding grains) or laminar (forming discrete layers between grains). If the clay were simply suspended between pores, then negligible affects would be expected. Dvorkin and Brevik [1999] use the separate influence on  $V_p$  of clay in the form of cements and interstitial clays to infer the strength and permeability of reservoir-forming sandstones. Similar observations were made in another study by Eberhart-Phillips et al. [1989], who obtained empirical relationships between  $V_p$  and  $\phi$ ,  $V_{Shale}$  and effective pressure,  $p_e$  (confining pressure minus the pore pressure). They observed systematic departures for some sandstones from normal trends, which they attributed to factors such as the shape and size of grains and pores, as well as the degree of compaction.

As an empirical relationship between  $V_p$ , composition and  $p_e$ , Eberhart-Phillips et al. [1989] derived the equation:

$$V_p = 5.77 - 6.94\phi - 1.73\sqrt{V_{Shale}} + 0.446(p_e - e^{-16.7p_e}) \quad (3)$$

By calculating velocity, this equation can be used to provide confirmation of clay content and porosity determinations from natural gamma, neutron porosity, and density logs. It also allows velocity measurements to be checked against the results from these other logging data.

## ROCK CHARACTERIZATION FROM SONIC VELOCITY

From Equation 1 it follows that there are relationships between  $V_p$  and modulus. If density is known and measurements are also made of shear wave velocity, it is possible to solve for  $k$  and  $\mu$ . However, the strains involved in the measurement of  $V_p$  are of the order of microstrains, whereas in rock testing the strains are of the order of millistrains. With these very different orders of strain, it is found that different values of the modulus are obtained.

Both Barton [2006] and Wang [2000] review and discuss these issues and present numerous results. The reason for the difference is attributed to the behavior of pore and crack boundaries. At low strains, these are stiff, but they deform elastically at higher strains and the rock appears softer. In materials such as steel and solid quartz, there is little difference between values. This is also the case at depth (pressures greater than 100 MPa), when pores and cracks are closed. Closer to the Earth's surface, the so-called dynamic modulus obtained by seismic measurements in sedimentary rocks may be twice the laboratory values (static modulus). Wang [2000] also reports that Winkler [1979] found, for the same reasons, there is a strain dependence for  $V_p$ .

In the case of the UCS, there is no theoretical basis for relating it to  $V_p$ . However, because it is generally observed that stiffer rocks are stronger, empirical estimates of UCS

can be made from  $V_p$ , provided fracturing is not strongly influencing  $V_p$ . Barton [2006] presents comparisons between  $V_p$  and UCS and reference is made to a  $V_p^3$  relationship, one that also provides a reasonable first estimate of UCS in Australian coalfields.

As discussed by Medhurst and Hatherly [2005], many Australian coal mines use empirical relationships to estimate UCS from  $V_p$ . If a relationship is established for a specific situation where strength does vary with modulus and there is proper consideration of the effects of pressure and fracturing on velocity, this approach can be followed. Situations where  $V_p$  is not particularly sensitive to UCS include those involving poorly cemented cohesionless rocks and also shales where moisture conditions influence strength.

For purposes of rock mass characterization, Barton [2002, 2006] developed a graphical approach for determining a Q-value and modulus from  $V_p$ , porosity, and depth. As a basis, it uses the hard-rock relationship:

$$V_p \approx 3.5 + \log_{10} Q \quad (4)$$

which Barton derived from results of numerous investigations involving unweathered rocks such as granites, gneisses, volcanic ignimbrite, and competent sandstones, all at depths to about 25 m. To allow for the influence of depth and porosity and to extend the application to other rock types, a normalized value  $Q_c$  is introduced whereby

$$Q_c = \frac{Q}{100} \text{UCS} \quad (5)$$

The physical basis for this approach is evident from the preceding discussion on the relationship between  $V_p$ , RQD, pressure, modulus, and UCS. Variations in  $V_p$  due to compositional factors such as the clay content in clastic rocks are not explicitly included. However, Equation 5 does make some allowance for compositional variation because of the relationship between  $V_p$  and UCS and because of the strength reduction factors involved in the determination of Q.

The GSR for clastic rocks that is described below similarly uses information on  $V_p$ , porosity, and depth to determine a rock mass rating. However, it is based on direct geomechanical considerations of rock strength and includes explicit consideration of the clay content. To determine GSR, geophysical logging data are analyzed. As a minimum, sonic, density, and natural gamma logs are required. Neutron porosity logs can also provide alternative estimates of shaliness and porosity, which will help improve the analysis. A basis for the geophysical log interpretation procedure is given by Medhurst and Hatherly [2005] and Hatherly et al. [2006].

## GEOPHYSICAL STRATA RATING (GSR)

Like soil classification systems, sedimentary rocks are amenable to characterization via a description of the grain size and type, amount of pore space, and moisture content. Fortunately, geophysical logs provide a reliable and repeatable measure of such parameters. As discussed, sonic velocity is a key measure that reflects rock stiffness and to some extent rock strength and fracturing, provided changes in mineral composition and porosity can be detected via other log data. At its core, the GSR is based on providing ratings for the quality of the individual beds, their contacts, and frequency.

### Rock Score

The rock score attempts to provide a measure of the quality of the individual beds and has three components: strength score, porosity score, and moisture score. The strength score is calculated using sonic velocity and is used as the basic measure of rock competency. Adjustments are then applied to take into account the influence of high-porosity, poorly consolidated materials and the influence of high moisture content. Using an empirical approach, the following relationships have been developed:

$$\text{Strength score} = 20 * V_p - 45 \quad (6)$$

where  $V_p$  is in km/s and is corrected for effective pressure via Equation 3.

$$\text{Porosity score} = -5 * X * Y \quad (7)$$

where  $X$  relates to the clay content,  $V_{Shale}$ , and  $Y$  relates to the porosity,  $\phi$ . If  $V_{Shale} > 0.35$ ,  $X = 0$ . If  $V_{Shale}$  is between 0.25 and 0.35,  $X$  is linear between 1 and 0. When  $V_{Shale} < 0.25$ ,  $X = 1$ . If  $\phi < 0.05$ ,  $Y = 0$ . When  $\phi$  is between 0.05 and 0.2,  $Y$  is linear between 0 and 3. When  $\phi > 0.2$ ,  $Y = 3$ .

Essentially, the maximum adjustment of -15 occurs when  $V_{Shale} < 0.25$  and  $\phi > 0.2$  and reduces to zero when  $V_{Shale} > 0.35$  or  $\phi < 0.05$ .

$$\text{Moisture score} = -5 * X * Y \quad (8)$$

where  $X$  relates to  $V_{Shale}$  and  $Y$  relates to  $\phi$ . If  $V_{Shale} < 0.65$ ,  $X = 0$ . If  $V_{Shale}$  is between 0.65 and 0.75,  $X$  is linear between 0 and 1. When  $V_{Shale} > 0.75$ ,  $X = 1$ . If  $\phi < 0.025$ ,  $Y = 0$ . When  $\phi$  is between 0.025 and 0.075,  $Y$  is linear between 0 and 2. When  $\phi > 0.075$ ,  $Y = 2$ .

Essentially, the maximum adjustment of -10 occurs when  $V_{Shale} > 0.75$  and  $\varphi > 0.075$  and reduces to zero when  $V_{Shale} < 0.65$  or  $\varphi < 0.025$ .

The final estimate of rock score is therefore given by

$$\text{Rock score} = \text{Strength score} + \text{Porosity score} + \text{Moisture score} \quad (9)$$

### **Bedding Contact/Cohesion Score**

In the Australian coalfields, stronger rocks tend to have stronger bedding. This allows a bedding/cohesion score to be given on the basis of sonic velocity. High-quartz sandstones are assumed to have strongly bound and/or cemented bedding surfaces, whereas mudstones are assumed to have smooth, planar, and weaker bedding surfaces.

$$\text{Cohesion score} = 10 + 5 * X \quad (10)$$

where  $X$  relates to  $V_p$ , again corrected for effective pressure. If  $V_p < 2.75$ ,  $X = 0$ . When  $V_p$  is between 2.75 and 3.25,  $X$  is linear between 0 and 2. When  $V_p > 3.25$ ,  $X = 2$ .

In the case of hard sandstones, i.e., quartz contents greater than 0.57 and  $V_p > 3.25$ , an additional component applies:

$$\text{Cohesion score} = \text{Cohesion score} + 5 * X * Y \quad (11)$$

where  $X$  again relates to  $V_p$  and  $Y$  relates to the quartz content. If  $V_p$  is between 3.25 and 3.5,  $X$  is linear between 0 and 1. If  $V_p > 3.5$ ,  $X = 1$ . If the quartz content is between 0.57 and 0.67,  $Y$  is linear between 0 and 1. When quartz  $> 0.67$ ,  $Y = 1$ .

### **Initial GSR (GSRI)**

$$\text{Initial GSR (GSRI)} = \text{Rock score} + \text{Cohesion score} \quad (12)$$

The initial GSR (GSRI) provides a measure of variation in the rock quality of individual beds. In doing so, it not only provides a bed rating, but by the contrast between beds, it also reflects the variation between beds. It is thus possible to obtain measures of bed frequency in laminated strata or to determine the thickness of so-called geotechnical strata units in thicker strata sequences where lithological boundaries are less significant.

### **Defect Score**

In keeping with other rock mass rating schemes, the GSR also needs to reflect the state of the defects introduced by fracturing and bedding. When cores and direct rock exposures are available, ratings are provided by manual logging—an intensive and potentially subjective

process. With geophysical logs, acoustic scanner data also allow direct mapping of defects provided they are evident in the borehole wall. However, this is also an intensive and potentially subjective process.

For the GSR, defect information is extracted from the results of the analysis of the geophysical logs. The variability in these is taken to be the indicator of defects. Specifically, rapid changes in  $V_{Shale}$  are likely to indicate changes in lithology, while changes in GSRI are likely to indicate that defects in the form of fractures and changes in lithology are present. The variability is thus determined on the basis of the rate of change of GSRI and  $V_{Shale}$ .

The *bedding score* is based on the variability in  $V_{Shale}$  and is designed to capture the transitions between sandstones and siltstones/mudstones and also the variability within fine-grained units. The mean value and standard deviation of the variability is established over the interval of interest, and a bedding score between 0 and 10 is assigned. A score of 10 indicates that there is no change occurring in  $V_{Shale}$ . A score of 0 indicates that the maximum changes in  $V_{Shale}$  are occurring at the point in question.

The *fracture score* is based on the variability in the GSRI. The GSRI provides an overall estimate of the state of the rock mass from all available geophysical logging data and therefore captures any influences on the logs of the bedding as well as fractures. Following the work of Priest [1993] on joint frequency, an exponential relationship is used to describe the variability and from this, the likelihood that any particular value of variability is due to a defect is predicted. At each point, a linear score between 0 and 10 is applied on the basis of this probability.

### **Final GSR**

$$\text{GSR} = \text{GSRI} + \text{Bedding score} + \text{Fracture score} \quad (13)$$

### **EXAMPLES**

#### **Implementation**

Most geophysical logging data are recorded in the standard LAS (Log ASCII Standard) format.<sup>4</sup> Files begin with a header containing log and borehole information, and point-by-point log data are then supplied in column format. Being an ASCII format, LAS files can be read using standard text editors and imported into databases and spreadsheets such as Microsoft Excel. Visual Basic macros within Excel have been written to interpret the geophysical

---

<sup>4</sup>An exception arises with image and other data intensive logs, such as acoustic scanners and full waveform sonic logs. For these, binary data formats are used, but unfortunately standard file formats have not been accepted by the logging industry. Proprietary formats prevail.

logs and to calculate the GSR. All data contributing to the GSR are tabulated and can be examined in their own right.

### Southern Coalfield, New South Wales, Australia

Figure 2 shows an example of a result from the Southern Coalfield, 60 km south of Sydney. The geophysical logs were initially obtained at 0.01-m spacings up the borehole. To reduce statistical uncertainty, especially in the natural gamma log, the logs were smoothed and resampled at 0.05-m spacings. Data are shown over a 4-m interval near the top of the working seam.

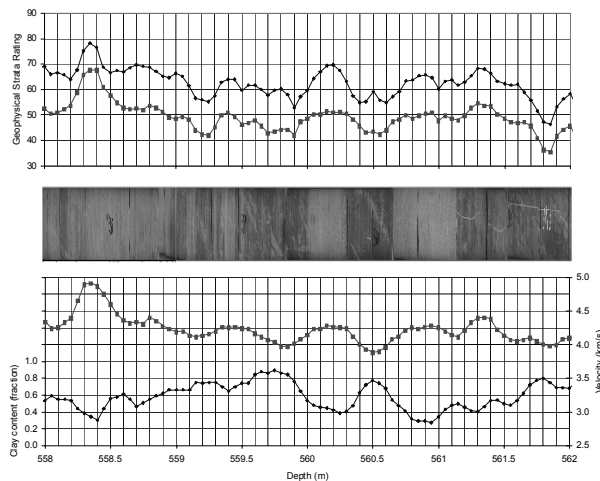


**Figure 2.**—**Top:** GSR (black) and GSRI (gray). **Center:** Core photograph showing a sequence of sandstones (white) and siltstones (gray). **Bottom:** Sonic velocity (gray) and interpreted clay content (black).

At the base of Figure 2, the interpreted clay content is shown together with the sonic data. Core photos are shown immediately above. There are no fractures evident, and the variations in clay content and velocity can be seen to be due to the changing lithology. In the gray silt bands, velocities are lower and clay content increases. Some of the bands have distinct margins (e.g., the siltstone band between 560.3 and 560.65 m).<sup>5</sup> In other sections, there are gradational changes in properties. For example, there is an increase in clay content and decrease in velocity between 558.8 m and 559.8 m. Here the strata are coarsening upward. At 558.35 m there is a band of high velocity, which is due to siderite. Siderite bands show up in the geophysical logs as thin zones of abnormally high density and velocity. There is also a minor siderite band interpreted to be present at 561.3 m.

<sup>5</sup>Geophysical logs necessarily sample the rock mass over a finite interval of about 10–20 cm. For this reason, none of the rock boundaries appear abrupt.

At the top of Figure 2 are shown the GSRI and GSR. As expected, the GSRI shows the trends evident in the log data and core. Where there are distinct bands, they are evident as discrete layers. The sandstones have a GSRI of about 50. For the siderite it is 68; in the siltstones, it is about 42. Similarly, the gradational changes in lithology are represented by gradational changes in GSRI. There is also a region of low GSRI at 561.8 m, which is due to low velocity affecting the strength and cohesion score, and high shaliness and porosity, which influence the moisture score.

When the defect score is added to the GSRI to obtain the GSR, the gradational units remain gradational, the GSR at the boundaries of the discrete beds is enhanced (GSR goes relatively lower), and the GSR at the center of the discrete beds is enhanced. Lithological and bedding effects can thus be seen to be incorporated into the rating.

### Newcastle Coalfield, New South Wales, Australia

The second example (Figure 3) comes from the Newcastle Coalfield 100 km north of Sydney. Here, results for the 2-m-thick immediate roof of the working seam are shown. From the core, five lithological units were identified and assigned separate CMRR ratings based on their discontinuities and intact strength. The lithologies, discontinuity spacing rating, UCS, and overall CMRR ratings for each unit are shown. The mudstones have lower UCS values than the sandstones. There is a low discontinuity spacing rating in the muddy sandstone in the immediate roof.

Figure 3 also shows the GSRI, GSR, and various defect scores determined from the geophysical logs. From the GSRI, it can be seen that the mudstones tend to have lower values than the sandstones. The fracture score established from the variability of the GSRI tends to be low at the bed boundaries and also in the immediate muddy sandstone with the low discontinuity spacing rating. For the bedding score, lows occur in the vicinity of the bed boundaries. When the bedding and fracture scores are added to the GSRI to produce the GSR, it can be seen that the relativity between the various beds is maintained and there are decreases in GSR at the bed boundaries and in the fractured muddy sandstone. While the absolute values of the GSR differ from the CMRR unit ratings in the sandstones, there is quite reasonable overall correlation between the CMRR unit rating and the GSR.

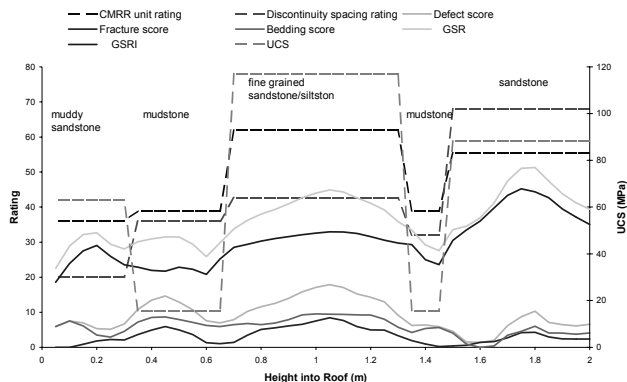


**Figure 3.—Comparison of GSR and CMRR. The sample interval in the geophysical logs is 0.05 m.**

## DISCUSSION AND CONCLUSIONS

The GSR is designed to be a rock mass rating system based on geophysical logging data for clastic strata typical of coal mining regions. It has some similarities to the method proposed by Barton [2002, 2006] for determining Q-values from geophysical data, but it allows for the variations in seismic velocity that can occur as a result of changes in lithology from clay-rich rocks to sandstones. Such changes in lithology also change the geotechnical properties of the strata, and the GSR is designed to accommodate these.

The elements of the geophysical log interpretation behind the application of the GSR have been confirmed through the analysis of many geophysical logs from the coalfields of Australia, and the main structure of the GSR is in place. Fine-tuning of the various scores, particularly the two defect scores, is now underway through comparisons with independent geotechnical ratings. The CMRR is the obvious scheme against which these comparisons can be made. Once these are completed, a more definitive GSR is likely.

Another area where work is under way concerns the effect of clay on rock properties. Earlier reference [Dvorkin and Brevik 1999; Eberhart-Phillips et al. 1989] was made to the effects of interstitial clay and clay in the form of a cement on seismic velocity. Following the work of Katahara [1995], it is possible to identify from natural gamma and porosity logs in shaly sandstones the presence of interstitial clay, clay cements, and laminar clay. On the basis of these considerations, refinements to the moisture and porosity scores are likely.

As a rating scheme, the GSR assigns a single value to every depth point. However, the component scores and interpreted geophysical data leading to the GSR have direct geotechnical and geological significance. Examination of these provides insights into the geotechnical

properties of the strata and could also be used as input into numerical modeling investigations.

Geophysical log analysis and the GSR are not expected to totally replace manual geotechnical logging. As with any form of remote sensing, there will always be the need to provide ground truth. Anomalous regions identified by the GSR analysis should also be independently investigated to verify geotechnical conditions.

The benefits of the GSR should also be obvious. It is objective, repeatable, inexpensive to conduct, and representative of the state of the rocks as they are in the ground. Data from holes drilled for exploration purposes are also potentially available for analysis, thus supplementing the geotechnical database. By virtue of the fact that the GSR delivers a continuous assessment, it also provides insights into characteristics of rock units that may not be evident from manual logging, where properties are assigned across discrete geotechnical units. Bed and defect boundaries are also highlighted through the process.

## ACKNOWLEDGMENTS

Development of the GSR has been funded by the Australian Coal Association Research Program, CRC Mining, and CSIRO Exploration and Mining. We thank Centennial Coal, BHP Billiton Illawarra Coal, and David Hill of Strata Engineering for the data used in the examples. Discussions with Christopher Mark, Ph.D., and Gregory M. Molinda of the NIOSH Pittsburgh Research Laboratory and Winton J. Gale, Ph.D., of SCT Operations helped to provide clarity.

## REFERENCES

- Barton N [2002]. Some new Q-value correlations to assist in site characterization and tunnel design. *Int J Rock Mech Min Sci* 39(2):185–216.
- Barton N [2006]. Rock quality, seismic velocity, attenuation and anisotropy. London and Netherlands: Taylor & Francis.
- Deere DU, Hendron AJ, Patton FD, Cording EJ [1967]. Design of surface and near-surface construction. In: Fairhurst C, ed. *Rock failure and breakage of rock*. New York: Society of Mining Engineers of AIME.
- Dvorkin J, Brevik I [1999]. Diagnosing high-porosity sandstones: strength and permeability from porosity and velocity. *Geophysics* 64(3):795–799.
- Eberhart-Phillips D, Han D-H, Zoback MD [1989]. Empirical relationships among seismic velocity, effective pressure, porosity and clay content in sandstone. *Geophysics* 54:82–89.
- Han D-H, Nur A, Morgan D [1986]. Effects of porosity and clay content on wave velocities in sandstones. *Geophysics* 51:2093–2107.
- Hatherly P, Thomson S, Armstrong M [2006]. Geophysical log analysis for the southern Sydney basin. In:

- Hutton A, Griffin J, eds. Proceedings of the 36th Sydney Basin Symposium (Wollongong, New South Wales, November 27–29, 2006), pp. 59–70.
- Katahara KW [1995]. Gamma ray log response in shaly sands. *Log Analyst* 36(4).
- Medhurst T, Hatherly P [2005]. Geotechnical strata characterization using geophysical borehole logs. In: Peng SS, Mark C, Tadolini SC, Finfinger GL, Khair AW, Heasley KA, eds. Proceedings of the 24th International Conference on Ground Control in Mining. Morgantown, WV: West Virginia University, pp. 179–186.
- Molinda GM, Mark C [1994]. Coal mine roof rating (CMRR): a practical rock mass classification for coal mines. Pittsburgh, PA: U.S. Department of the Interior, Bureau of Mines, IC 9387.
- Priest SD [1993]. Discontinuity analysis for rock engineering. London: Chapman & Hall.
- Sjøgren B, Øfsthus A, Sandberg J [1979]. Seismic classification of rock mass qualities. *Geophys Prospecting* 48:815–834.
- Wang Z [2000]. Dynamic versus static elastic properties of reservoir rocks. In: Wang Z, Nur A, eds. Seismic and acoustic velocities in reservoir rocks. Vol. 3: Recent developments. Tulsa, OK: Society of Exploration Geophysicists, pp. 531–539.
- Winkler K [1979]. Effects of pore fluid and frictional sliding on seismic attenuation [Dissertation]. Stanford, CA: Stanford University.



# PRACTICAL EXPERIENCES WITH APPLICATION OF THE COAL MINE ROOF RATING (CMRR) IN AUSTRALIAN COAL MINES

By David Hill<sup>1</sup>

## ABSTRACT

The Australian underground coal mining industry has made extensive use of the Coal Mine Roof Rating (CMRR) classification system for a diverse range of purposes in recent years. These include mining method selection, and coal pillar and roof support design. This paper outlines a series of case histories, from large-scale feasibility studies to local support design investigations, that collectively illustrate the broad applicability, advantages, and usefulness of the methodology, as well as some of the current limitations.

The key role of the CMRR in an overall hazard definition methodology is demonstrated for a major Australian project, and some ideas with regard to the future application of the CMRR, in the context of geotechnical risk management within a progressive, highly productive extractive industry, are put forward.

## BACKGROUND

The Coal Mine Roof Rating (CMRR) is a measure of roof quality or structural competency for bedded roof types typical of underground coal mines. The CMRR was developed by the former U.S. Bureau of Mines (of which the health and safety research component was transferred to NIOSH) and has been widely applied in Australia since the mid-1990s. It was derived from the South African Council for Scientific and Industrial Research's Rock Mass Rating (RMR) system, which has been used in the mining and tunneling industries for over 30 years [Bieniawski 1974].

The CMRR was initially based on field observations at surface highwalls and portals, as well as underground air crossings and roof falls [Molinda and Mark 1994]. Later, a methodology was developed for assessing the CMRR from drill core, to assist where underground exposures were limited or unavailable [Mark and Molinda 1996]. The system was revised in 2003 to incorporate experiences gained since 1994 [Mark and Molinda 2003].

The CMRR considers the following factors:

- Thickness of the individual roof beds
- Shear strength properties of the bedding/planes of weakness

- Compressive strength of the rock material
- Moisture sensitivity of the rock material
- Number of different units (i.e., the degree of homogeneity of the roof)
- Presence of groundwater
- Presence of a particularly strong bed or weaker overlying beds

Essentially, the CMRR is calculated by deriving unit ratings for individual geotechnical units and then determining a weighted average for the bolted horizon. The CMRR is therefore specific to roof bolt length and can change, for example, if the bolt length is increased to anchor into an overlying relatively competent horizon or if a particularly incompetent unit in the immediate roof is cut down during drivage. Unit ratings can range from 0 to 100; the typical range encountered in Australia is 15–70.

Molinda and Mark [1994] suggest the following categorization of roof competency:

CMRR < 45	Weak roof
CMRR = 45–65	Moderate roof
CMRR > 65	Strong roof

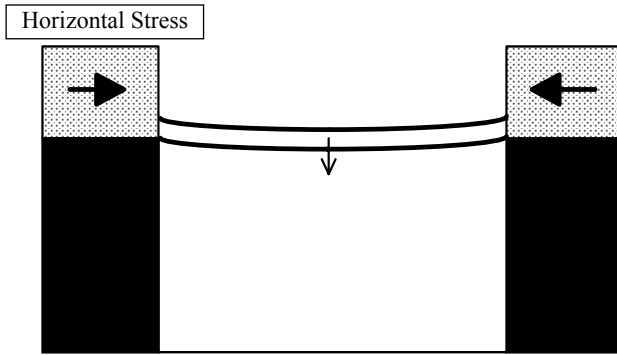
At the time of the original U.S. research, 75% of the data fell into the "weak" or "moderate" categories, with an average CMRR of around 53. By contrast, Australian coal industry research in the late 1990s indicated a lower average CMRR for longwall mines of 50, with 86% of the data falling into the "weak" or "moderate" categories [Colwell 1998]. The issue of typically lower roof competencies in Australia will be explored later in this paper.

## POSITIVE ASPECTS OF THE CMRR

With particular regard to the underground coal mining geotechnical environment, the CMRR system is considered to incorporate a number of positive technical features and to offer the rock mechanics engineer several practical advantages over alternative approaches.

The major positive technical aspect is that the CMRR system focuses on characterizing the structural competency of a bedded, sedimentary rock mass and effectively its propensity for deformation due to buckling under the action of horizontal stress, noting that in Australian collieries, this is the main cause of roof deterioration (see Figure 1). The propensity for roof buckling is a function of the excavation span, bed thickness, and the material stiffness properties. A roof that remains intact, without any

<sup>1</sup>Principal, Strata Engineering (Australia) Pty. Ltd., New South Wales, Australia.



- Tensile/shear failure occurs along bedding planes
- Roof measures subdivide into thinner discrete units
- Increased displacements

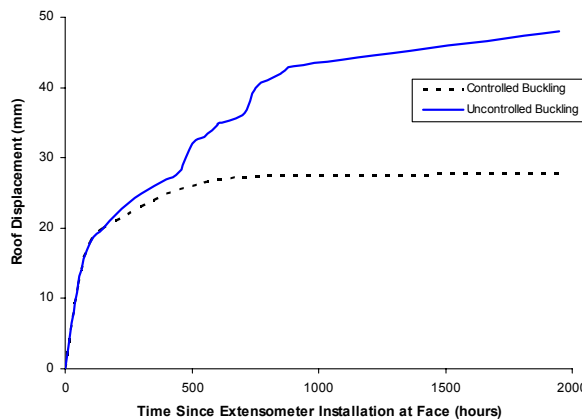


**Figure 1.—Schematic of roof buckling under the action of horizontal stress and typical roof displacement data.**

appreciable delamination under the action of horizontal stress, can be referred to as “static.”

The CMRR drill core methodology typically ascribes approximately two-thirds of the overall rating to the discontinuity rating, which is related directly to bed thickness and the potential for delamination (i.e., reducing bed thickness). This discontinuity rating is defined as the lower of two parameters: the discontinuity spacing rating (defined from RQD and/or the fracture spacing) and the diametral point load test (PLT) rating. The diametral point load testing aids in identifying a material that is prone to delamination (e.g., fissile), which may be otherwise unbroken in the core tray. The relatively humble diametral PLT on vertically orientated core is highly relevant to assessing the potential for roof buckling due to horizontal stress.

The practical advantages of the CMRR relate very largely to its widespread application and the extensive databases that link the parameter to a range of mining situations (i.e., the CMRR is used as a primary input in a

number of coal pillar and roof support design scenarios). Over the last decade, the CMRR has effectively become a common universal language for engineering geologists and geotechnical engineers operating in the U.S. and Australian coal industries. This has come about by a process of technology transfer, which has been particularly aided by the emphasis on the part of NIOSH on publishing associated research outcomes, including the underpinning databases. This availability and transparency of data has enabled other practitioners to interrogate the empirical findings and rapidly develop experience and confidence in the associated applications. As with all empirical methodologies, understanding the limitations and nature of the underpinning database is vital. Extrapolating technical findings, such as regression relationships, beyond the limits of a database can be highly problematic, requiring both caution and wisdom.

In practice, engineers have been able to take published research outcomes, derive their own local data, and interrogate that data in the context of the published work. This aids in understanding the local situation, including the extent to which local circumstances may vary from those previously encountered elsewhere, with associated caveats on the confidence that can be placed in the analysis.

The position of the CMRR within the coal industry has become akin to that of Microsoft Windows within the software industry—there may be a better commonly available and applicable operating system, but the CMRR has become entrenched. Furthermore, as the use of the CMRR spreads, the barriers to entry of alternative methodologies increase at a disproportionate rate. In the medium term (the next 10 years), it is considered highly unlikely that the CMRR will be displaced by any new innovation. A more likely outcome is that current technical initiatives will develop “calibrations” with the CMRR, such that the latter remains the lingua franca.

## CURRENT ISSUES WITH USING THE CMRR

A number of issues associated with using the CMRR warrant mention, as they can influence the technical result and associated design outcomes.

### Methodology Aspects

Firstly and probably most significantly, it should be noted that the three published and accepted methodologies (i.e., the original exposure observation method, the initial drill core method, and the revised drill core procedures) can yield very different outcomes in specific circumstances. An extreme example is the massive conglomerate roof that is typical of the Great Northern Seam in the Lake Macquarie (Newcastle Coalfield) area of New South Wales. The original observation method would be guided by the general lack of discontinuities within the unit and would produce a rating of around 90. By contrast, both the

original and revised drill core procedures would recognize the moderate strength of the material (commonly  $\leq 60$  MPa and controlled by the nature of the cementation of the matrix between the pebbles), resulting in a typical unit rating of 60–65. In practice, the Teralba Conglomerate will typically span  $\geq 50$  m practically indefinitely, unsupported and with localized skin failures only.

In this case, the variance in the CMRR has no appreciable operational impact, as in the prevailing geotechnical environment (and in an Australian regulatory framework), even a CMRR of 60 will result in effectively minimum design outcomes (i.e., in this case, it does not particularly matter if the roof is better than suggested by a CMRR of 60). However, it does have negative implications in that it can reduce confidence in the reliability of the technique and hinder effective communication (i.e., it is unhelpful to categorize a unit as “moderate” if, for all practical purposes, it behaves as “strong”). Furthermore, the variance would be operationally significant if the CMRR were to be used as a guide to cavability, in which case vastly different expectations would tend to be associated with a CMRR of 60 as opposed to 90.

Also, the old and current drill core methods tend to produce different outcomes. The current method is considered an overall improvement in that it more systematically accounts for the influence of bedding and jointing, such that structurally affected areas are less likely to be overrated (essentially, the original method defaulted to the diametral PLT strength rating and ignored the discontinuity rating). However, in the current system, the maximum discontinuity spacing rating has been downgraded significantly from 70 to 48 (22 points). This tends to reduce the significance in the rating system of thickly bedded/massive sandstones and conglomerates, such that more conservative results are obtained.

Obviously, such a major change in a rating system requires careful consideration, as these systems are only useful in the context of their derived databases. Adjusting the input to these databases necessarily alters the outcomes in terms of the relationships between parameters and the derived equations. The impact of the changes is reduced in this case by the fact that the underpinning NIOSH CMRR databases are derived very largely from underground observations as opposed to drill core.

In fact, the use of the CMRR in the United States is understood to be based largely on underground observations, whereas in Australia the drill core method is most commonly applied. This change in emphasis also needs to be understood, as it materially impacts the way in which the CMRR is applied. As an example, a number of major Australian coal projects have used the CMRR to investigate spatial variations in roof competency across resource areas in recent years, which is only viable given the availability of adequate exploration borehole data.

Since the revision of the drill core method in 2003, Strata Engineering has on several occasions cross-checked the results obtained using the various published procedures. An example is illustrated in Figure 2, which summarizes the outcomes of a CMRR survey based on 30 drill cores across the resource area for a major longwall project in New South Wales. The following comments are made with regard to the results:

1. On average, the CMRR values obtained using the revised procedure were reduced by 10% compared to those obtained using the old drill core method (i.e., a slightly more conservative result was generally obtained).
2. 50% of the data points varied within only  $\pm 10\%$ .
3. The percentage variation trend line crossed zero at a CMRR value of 45, which, as noted, marks the category transition from “weak” to “moderate” roof. Practically, the revised procedure tended to have limited overall effect for CMRR values of  $< 55$ .
4. A variation of  $>20\%$  was only noted in two circumstances. Firstly, in fault-affected areas, the revised procedure was more sensitive to jointing, with reduced CMRR values (note the three outlying data points in Figure 2). This was considered an improved, more realistic outcome. Secondly, the impact of reducing the maximum discontinuity rating from 70 to 48 was most pronounced in cases where the original methodology would generate particularly high CMRR values ( $> 65$ ).

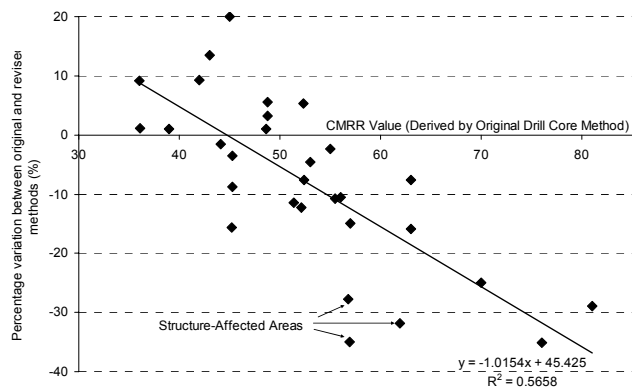


Figure 2.—Example of the effect of the revision to CMRR drill core procedures.

Other surveys and comparisons have produced similar results, although it is common to find that there is still some reduction in the unit ratings between the old and current methodologies, even in the CMRR  $< 40$  range. In practice, experience suggests that it is virtually impossible to obtain a CMRR of  $> 70$  with the revised drill core procedure.

It is important to note that the great bulk of the Australian coal mining industry is currently operating at CMRRs of 35–55. This is the area of greatest significance for mine design and operational practice. It is also the zone of closest agreement between the various CMRR procedures, such that the impact of any discrepancies is reduced. Also, Australian experience suggests that roof behavior tends to become generally benign and insensitive to CMRR fluctuations at values of  $\geq 55$  (i.e., these values tend to be associated with static roof behavior, which is essentially self-supporting and the most stable roof condition attainable). Therefore, the disparities between the CMRR methodologies in stronger roof types tend to have minimal practical consequence.

Overall, the variances are currently tolerated, given that the modified procedures tend to be more conservative (in the case of areas of geological structure, appropriately so). However, in a different geotechnical environment or industry, the discrepancies could potentially be of more concern.

### **Coal Roof**

Approximately 50% of the Australian longwall mining industry operates under a roof wholly or at least partly composed of coal. Australian coals tend to be weak, bedded, and cleated (jointed), resulting in low CMRR values (typically 30–40). Nevertheless, in the absence of persistent, weak partings (commonly associated with thin mudstone or tuff bands), these coal roof units tend to perform relatively well, for example, under tailgate loading conditions. Historically, this has tended to be attributed largely to the low modulus of the material attracting reduced levels of horizontal stress (i.e., a specific gravity of 1.3–1.5, versus typically 2.5 for adjacent strata).

As a consequence, it has become common to apply adjustment factors to coal ratings. Although there is no generally agreed adjustment process, these adjustment factors typically range up to an additional 20% of the raw rating, depending on the extent to which the unit is clean (i.e., the prevalence of thin “dirt” bands), as well as the practical experiences of mining under the given roof type.

### **Human Error**

Although the CMRR is considered a relatively straightforward and uncomplicated system of rock mass classification, the potential for human error remains. A common error is the failure to distinguish between geological and geotechnical units. This is particularly true for gradational roof types (e.g., dark gray mudstone grading upward into gray siltstone, or bands of fine alternating with medium-grained sandstone). It is common for a roof material that visually is reasonably uniform to be logged by a geologist as a single lithological unit, whereas in practice the structural competency of the unit can vary markedly. This is especially true over short distances

directly relevant to ground behavior (i.e., the first 2 m of roof). Unless the individual conducting the geotechnical logging is aware of the need to gather sufficient detail to define the homogeneity of a particular unit, valuable information can be lost.

When using the drill core method in the absence of visibly distinct roof units, PLTs (diametral plus axial) at a maximum of a 0.5-m spacing in the bolted interval will normally generate sufficient data to enable a reasonable analysis. Evaluation of a combined RQD, fracture spacing, and PLT data set then often facilitates subdivision of preliminary roof units, producing a more meaningful overall CMRR outcome.

### **Horizontal Stress**

A common feature of the Australian coal mining geotechnical environment is a level of horizontal stress that is much higher than the vertical, often with appreciable stress anisotropy. Major principal horizontal stresses two to four times the vertical stress are typical, along with minor horizontal stresses one to three times the vertical. Elevated horizontal stress magnitudes and stress field rotation can be associated with major geological structures, such as reverse faults. The stress regime often manifests itself in roof behavior that is strongly directionally dependent (i.e., an unfavorable roadway orientation with respect to the major horizontal stress is frequently associated with increased roof displacement).

The relatively high levels of horizontal stress are a cause for prudence in applying any empirical relationships involving the CMRR and parameters related to stress (e.g., depth) derived from the U.S. coal mining industry, which does not seem to experience the phenomena described previously (at least not to the same degree).

An example is the use of the CMRR as a guide to the probability of stability of extended cuts (i.e., temporarily unsupported heading lengths of greater than 6 m) in “cut-and-flit” (place-changing) development operations, based on U.S. research [Mark 1999]. There are at least two known Australian cases of the failure of extended-cut drivage systems in strongly anisotropic horizontal stress fields due to instability of the unsupported cut in the unfavorable roadway direction.

## **USE OF THE CMRR IN AUSTRALIA: PRACTICAL EXAMPLES**

### **Drivage Method Selection**

Following directly from the comments made in the “Horizontal Stress” section above, it is useful to consider the Australian experience of cut-and-flit mining in the context of the overall knowledge base. The relationship between the CMRR, depth, and stability of extended cuts taken during cut-and-flit operations is shown in Figure 3 [Mark 1999], together with the Australian data.

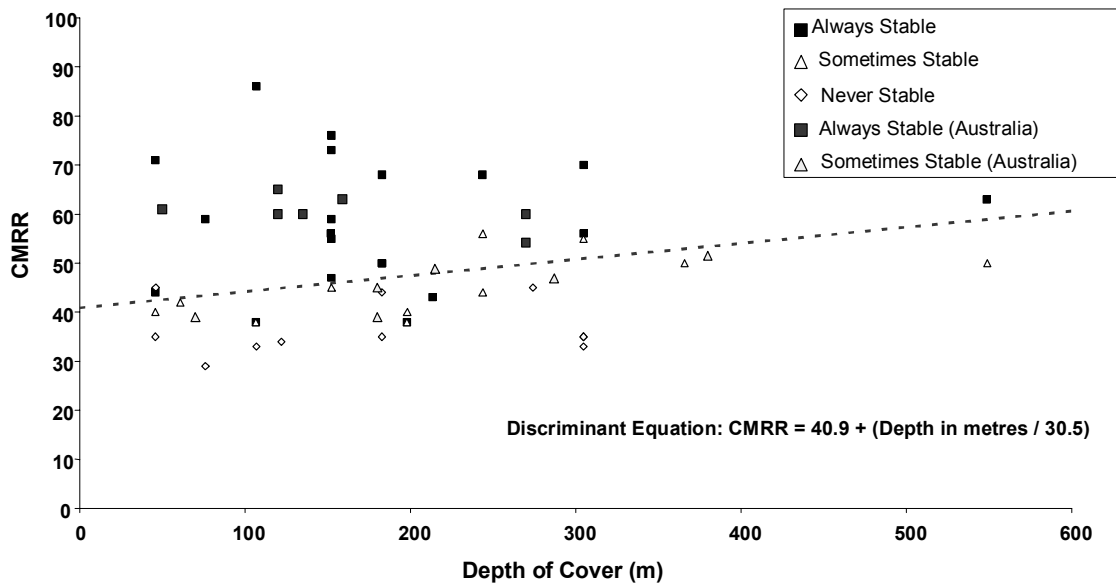


**Figure 3.—CMRR extended-cut database.**

The U.S. database derives from a survey of place-changing operations requesting mine operators to rank their experiences with regard to extended-cut stability. Also shown in Figure 3 is the discriminant equation trend line derived by Mark [1999], which is the line that best splits the “always stable” from the “sometimes stable/never stable” cases.

The line of the discriminant equation is given by

$$CMRR = 40.9 + H/30.5 \quad (1)$$

where  $H$  is the depth of cover (m).

Effectively, the higher the CMRR, the more likely place-changing is to be a success and the more likely the roof is to retain static behavior, depending in part on depth of cover (and the associated levels of in situ stress).

The following comments are made with regard to Figure 3:

1. It is evident that Australian cut-and-flit experience is generally consistent with that of the United States in terms of the distribution of the data with respect to the discriminant equation.
2. The Australian “always stable” cases are characterized by CMRRs of >50 and depths of <300 m.
3. The transition from “always” to “sometimes stable” is commonly marked by a progressive increase in the severity of skin failure (i.e., detachment of the first 0.5 m of roof in the unsupported cut, often associated with a bed with a low unit rating in the immediate roof), as opposed to massive roof failure.
4. The “sometimes stable” Australian case at a 380-m depth was characterized by directionally dependent roof behavior.

5. The two “sometimes stable” Australian cases involving CMRRs of 39 both involved a coal roof.

The CMRR extended-cut relationship has been used, in conjunction with cover depth data, to delineate areas of potential cut-and-flit development as part of the planning process for new mines. However, cut-and-flit has never been the preferred method of gate road drivage in Australia, and the use of this process has declined since the 1990s.

More recently, the CMRR extended-cut relationship has been used as a guide as to the likely transition point from static to buckling roof behavior when using conventional cut-and-bolt (or “in-place”) drivage techniques. This transition point is associated with a marked increase in roof support requirements and a need to restrict the unsupported span at the face, which even with conventional development can vary between 2 and 15 m, depending on the configuration of the miner bolter.

Therefore, although a mine may not be contemplating using cut-and-flit, use can be made of the fact that the successful application of this technique depends on the roof behaving in a largely self-supporting fashion (such that cuts >6 m will tend to stand unsupported, often for extended periods prior to bolting). This has ramifications for continuous miner selection, particularly regarding the distance from the face at which bolts are installed.

## Roof Characterization

The support system designer is required to have an appreciation of expected ground conditions in an area to be mined, as well as the likely range of ground conditions (e.g., the propensity for zones of poor roof). In this regard, characterization of likely roof competency at the planning

stage, backed up with hazard mapping during subsequent mine development, are key components of the strata management process.

New projects place increased emphasis on mapping roof competency using drill core data and, in particular, the CMRR. The information generated is usually combined with the available knowledge of the in situ stresses and geological structure in the area of interest to arrive at initial estimates of ground conditions and likely associated ground support needs. At the operational stage, this information is combined with mapping of geological structure and roof behavior to produce composite hazard plans, which are progressively extrapolated into adjacent mining areas.

Increasingly, the focus of these activities is not on drawing copious "lines on plans," but on producing color-coded hazard information (e.g., green – yellow – red) that can be readily assimilated by mining personnel.

An example of CMRR contouring for planning purposes is shown in Figure 4. This particular plan is based on 50 CMRR results from an area of approximately 16 km<sup>2</sup> (an exploration borehole spacing of around 500 m). Subsequent mining has borne out the general strength trends depicted in the example.

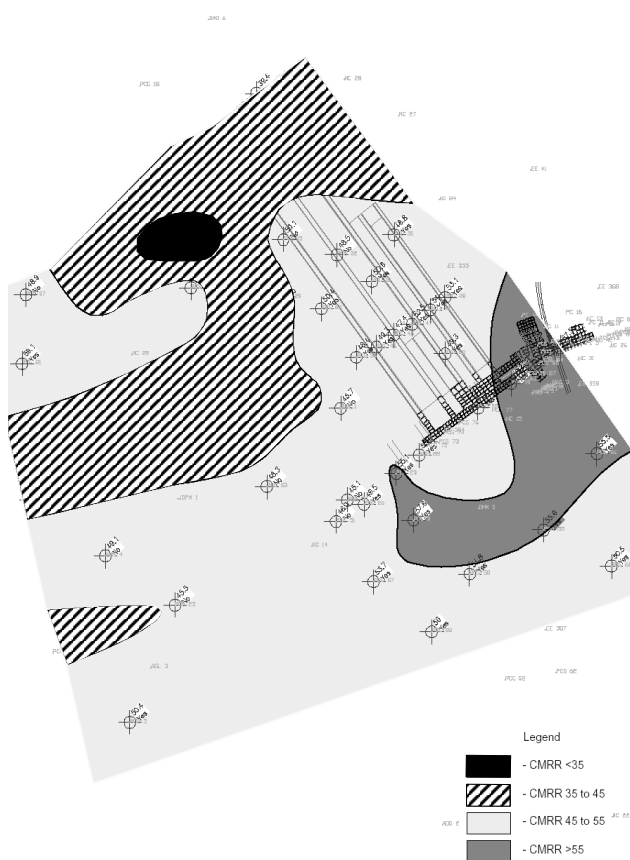


**Figure 4.—Example of CMRR contouring.**

From Australian experience, the following refinement of the CMRR classification is considered appropriate. This particularly focuses on the CMRR 35–55 rating zone, which is of most practical interest:

CMRR < 35	Very weak roof
CMRR ≥ 35, but < 45	Weak roof
CMRR ≥ 45, but < 55	Moderate roof
CMRR ≥ 55, but < 65	Strong roof
CMRR ≥ 65	Very strong roof

It is understood that less success has been had in the United States regarding the development of spatial trends of roof strength, although the exercises known to date [Mark et al. 2004] have involved significantly greater borehole spacings (i.e., typically >2 km).

The successful application of this technique in Australia in recent years has generally been based on the following:

1. Exploration borehole spacings of ≤ 500 m.
2. Drawing interpretations also from complementary geological data sets (e.g., structure and sedimentology information).
3. Adoption of a pragmatic approach as to the quality of the information generated versus practical project needs.
4. An example of the interpretation of a CMRR data set is given in Figure 5. Although there is no overall trend linking the CMRR to depth, if the northwestern area (bounded by a seam convergence zone and characterized by a distinct thickening of the seam) is isolated, then it is apparent that over the major part of the resource area, roof quality improves gradually with depth. Within this area, it is not necessary or appropriate to attempt to define the CMRR to two decimal places for a given depth; it is enough to be aware that very weak roof can be expected at depths of <150 m, with weak/moderate roof at greater depths.

Spatial trends for the CMRR can be used in conjunction with other relevant information and parameters (e.g., structural and sedimentology data, depth, and drivage orientation with respect to the major horizontal stress) to produce preliminary hazard plans. The plans are then progressively refined as actual mining information becomes available. An example of a preliminary hazard plan for a major mining project is shown in Figure 6.

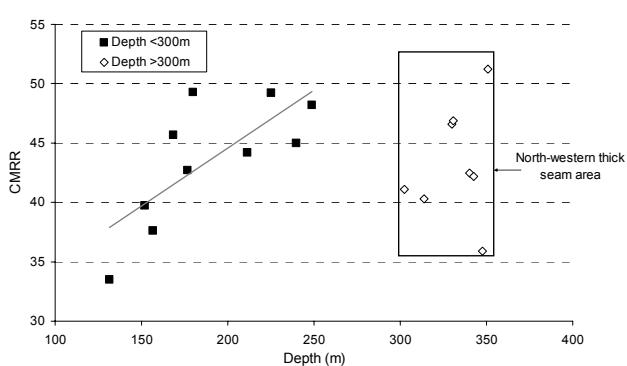


Figure 5.—Example of spatial trends from a CMRR data set.

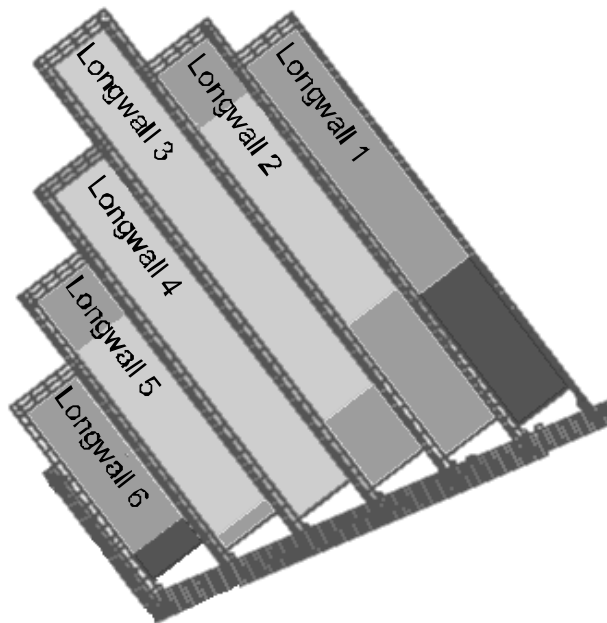


Figure 6.—Preliminary hazard plan for a major mining project.

### Design Optimization

Information regarding spatial trends of the CMRR has been used in a number of recent Australian projects to optimize the design of the layout and/or ground support system. An example is tapered longwall chain pillars (Figure 7), which were first used at the South Bulga Mine in New South Wales in 2001. A tapered pillar design is feasible wherever the mining layout is unconstrained by existing development and there is a reasonably consistent change in one or more variables, such as the CMRR or depth, from one end of a panel to the other. The dimensions of the longwall block itself do not change, such that the panel will be rotated by a fractional amount (the

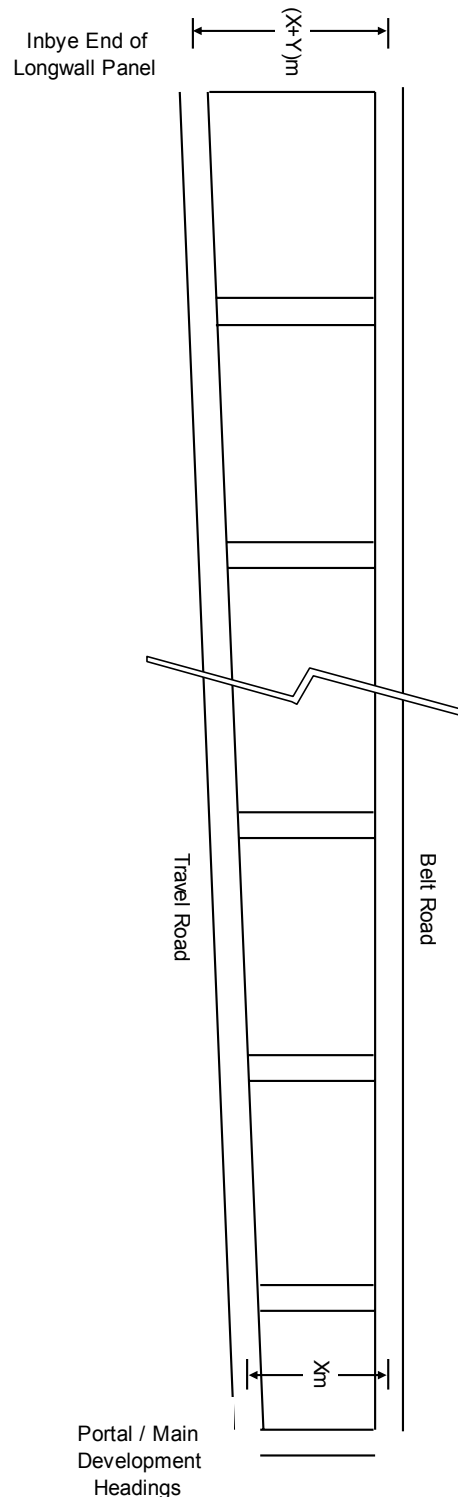


Figure 7.—Splayed chain pillar concept.

“splay” angle is typically  $<1^\circ$ , which is practically imperceptible underground). Gate road drivage savings of several kilometers have been achieved by optimizing pillars widths using this approach.

## CONCLUDING REMARKS

A number of applications of the CMRR in Australia have been outlined. Although the CMRR is not considered a perfect rock mass classification system (several current issues have been highlighted), it is generally well suited to the Australian coal mine geotechnical environment and practical ground control issues facing the industry. Accordingly, the CMRR is increasingly accepted and its applications continue to extend, such that the scope and potential for the use of alternative systems is restricted.

It should not be implied, however, that the CMRR is used exclusively. There are several technical areas, mainly in the design of ground support, in which the CMRR and its associated empirical relationships are very commonly used in conjunction with other methodologies, including alternative rock mass classification schemes (specifically, Q and RMR), as well as numerical, analytical, and experiential approaches. This is most evident at the feasibility stage of a mining project. In the absence of meaningful local experience, design outcomes pertaining to alternative methodologies are often compared and cross-checked; inconsistencies can then be scrutinized.

It is expected that, in Australia at least, there will be an increasing focus on the use of the CMRR for defining spatial roof strength trends across resource areas, as this is an area in which the geotechnical engineer can add considerable value to a mining project, provided that the data are used rationally.

## REFERENCES

- Bieniawski ZT [1974]. Geomechanics classification of rock masses and its application in tunnelling. In: Proceedings of the Third International Congress on Rock Mechanics (Denver, CO), ISRM, *IIA*:27–32.
- Colwell MG [1998]. Chain pillar design: calibration of ALPS. Australian Coal Association Research Program, final report: ACARP project C6036.
- Mark C [1999]. Application of coal mine roof rating (CMRR) to extended cuts. *Min Eng* *51*(4):52–56.
- Mark C, Molinda GM [1996]. Rating coal mine roof strength from exploratory drill core. In: Ozdemir L, Hanna K, Haramy KY, Peng S, eds. Proceedings of the 15th International Conference on Ground Control in Mining. Golden, CO: Colorado School of Mines, pp. 415–428.
- Mark C, Molinda GM [2003]. The coal mine roof rating in mining engineering practice. In: Aziz N, Kininmonth B, eds. Proceedings of the Fourth Underground Coal Operators' Conference. Carlton, Victoria, Australia: Australian Institute of Mining and Metallurgy.
- Mark C, McWilliams LJ, Pappas DM, Rusnak JA [2004]. Spatial trends in rock strength: can they be determined from coreholes? In: Peng SS, Mark C, Finfinger GL, Tadolini SC, Heasley KA, Khair AW, eds. Proceedings of the 23rd International Conference on Ground Control in Mining. Morgantown, WV: West Virginia University, pp. 177–182.
- Molinda GM, Mark C [1994]. Coal mine roof rating (CMRR): a practical rock mass classification for coal mines. Pittsburgh, PA: U.S. Department of the Interior, Bureau of Mines, IC 9387.

# USE OF THE MINING ROCK MASS RATING (MRMR) CLASSIFICATION: INDUSTRY EXPERIENCE

By Jarek Jakubec, C.Eng.,<sup>1</sup> and Gabriel S. Esterhuizen, Ph.D.<sup>2</sup>

## ABSTRACT

In 2000, Laubscher's Mining Rock Mass Rating (MRMR) classification system was updated and published. The new system brought a few fundamental changes that were in direct response to the challenges and problems encountered when applying the classification system in the mining environment, specifically caving operations. The fundamental changes introduced into the MRMR system in 2000 were the abandonment of the Rock Quality Designation (RQD) as an input parameter, accounting for healed and cemented joints, and the concept of rock block strength.

The objective of this paper is not to discuss the role and usefulness of classification systems; the fact that classification systems are widely used in every stage of mining projects speaks for itself. This paper discusses some of the experiences gained with the MRMR 2000 system in various mining projects and shows how the changes to the system have resulted in improved assessment of rock mass conditions. Issues related to core logging for rock mass assessment are also presented.

## INTRODUCTION

Laubscher's Mining Rock Mass Rating (MRMR) system was introduced in 1975 [Laubscher 1975] and has been modified and expanded several times since then [Laubscher 1990, 1993; Laubscher and Taylor 1976]. The last update was released in 2000 [Laubscher and Jakubec 2001]. The principal changes in the new In Situ Rock Mass Rating (IRMR) included the concept of rock block strength, which accounts for the effect of cemented joints and veins. All of the changes were in direct response to the challenges encountered when applying the classification system in the mining environment, specifically caving operations in Chile and Australia.

If rock mass classification is to reflect reality, it is important that all of the critical parameters influencing the rock mass behavior are accounted for. Ignoring strength reduction due to microfractures or ignoring the presence of

cemented joints could result in the misclassification of the rock mass competency and can have serious safety and/or economic consequences.

As with any empirically based system, it is important that experiences from new projects are analyzed and the classification system is further refined and calibrated. Although some of the rules and relationships used in MRMR and its applications are "crude," it is our view that it is better to use a simplistic method than to ignore the issues. To quote John Maynard Keynes: "It is better to be roughly right than precisely wrong."

Unfortunately, in the real world, the rock masses are inherently variable and do not conform to an ideal pattern. The issue of appropriate site-specific geotechnical evaluation of rock masses was recently discussed by Murphy and Campbell [in press]. In order to ensure that rock mass classification reflects reality, a certain amount of engineering judgment/interpretation is required. A classification system can provide guidelines for design, but the mining practitioner must ensure that the system is applied correctly. The role of the classification system as a communication tool between operation, engineering, geology, and management cannot be stressed enough. Unfortunately, a failure in communication is often one of the root causes of the problem.

This paper discusses some of the experience with Laubscher's IRMR/MRMR system as introduced in 2000.

## THE MRMR CLASSIFICATION SYSTEM: AN OVERVIEW

There are currently three main classification systems used in the metal mining industry: Bieniawski's RMR [Bieniawski 1973], Barton's Q [Barton et al. 1974], and Laubscher's MRMR [Laubscher and Jakubec 2001]. A rough comparison of these systems in terms of required input parameters is shown in Table 1. The main differentiators of the MRMR 2000 system compared to previous versions of the MRMR, Q-system, and Bieniawski RMR systems are:

- Scale concept in material strength (intact rock > rock block > rock mass)
- Inclusion of cemented joints and veinlets
- Abandonment of the Rock Quality Designation (RQD) as an input parameter
- Mining adjustments (in comparison to Q)

<sup>1</sup>Principal rock mechanics engineer, SRK Vancouver, Vancouver, British Columbia, Canada.

<sup>2</sup>Senior research fellow, Pittsburgh Research Laboratory, National Institute for Occupational Safety and Health, Pittsburgh, PA.

**Table 1.—Comparison of main classification systems used in the mining industry**

Category	Parameters	Beniawski RMR	Barton Q	Laubscher 90	Laubscher 2000
Intact rock strength	UCS	x	x	x	x
Open joint frequency	RQD	x	x	x	-
	FF/m	x	-	x	x
	Joint set (Jn)	x	x	x	x
Open Joint strength	Roughness (Jr)	x	x	x	x
	Alteration (Ja)	x	x	x	x
	Infill (Ja)	x	x	x	x
Cemented joints quantity and strength	CJ/m	-	-	-	x
	CJ strength	-	-	-	x

Another system that is occasionally encountered in metal-mining projects is the Geological Strength Index (GSI) [Hoek et al. 1995]. Since this system cannot be easily “decoded” and individual parameters assessed separately, it was not used for comparison in Table 1. The objective of this paper is not to discuss which system is more suitable, nor is it to describe every detail of the MRMR system. It is recommended that the reader refer to Laubscher and Jakubec [2001], where the MRMR 2000 system is fully discussed. Flowsheets illustrating the different parts of the MRMR 2000 system are shown in Figures 1–2. Figure 1 illustrates the parameters used to determine the IRMR, and mining adjustments that produce the final MRMR value are presented in Figure 2.

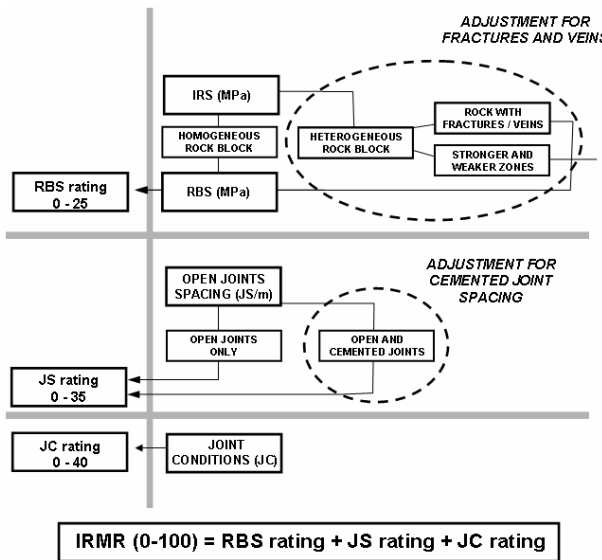


**Figure 1.—IRMR 2000 flowsheet.**

The application of the MRMR system in mine design is presented in the paper “Planning Mass Mining Operations” [Laubscher 1993]. The main design recommendations and guidelines include:

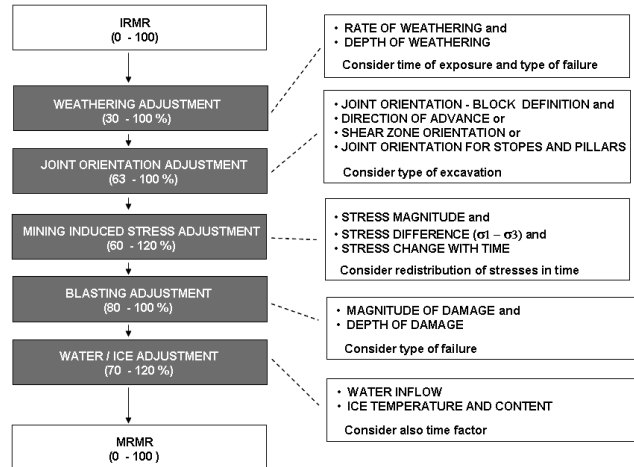


**Figure 2.—Mining adjustments.**

- Support design
- Cavability diagrams and stability of open stopes
- Extent of cave and failure zones
- Caving fragmentation
- Caving rates and mining sequence
- Pit slope guidelines

The design charts and associated recommendations are based on experience gained in mining projects around the world and have found wide acceptance within the mining industry.

## THE CONCEPT OF A ROCK BLOCK

The MRMR 2000 system accounts for the effect of scale in its assessment of rock strength, recognizing that small-scale intact rock samples do not necessarily reflect the strength of the larger rock blocks bounded by through-going joints. The concept of a rock block is illustrated in Figure 3. A rock block is defined as the rock material bounded by throughgoing joints and can contain discontinuous fractures and veinlets. It is important to separate continuous “block-bounding” joints from discontinuous fractures and veinlets, especially for mass mining methods where cavability and fragmentation assessment are fundamental to the design.

The scale concept, which addresses the material strength from small intact rock samples that can be tested directly in the laboratory, through rock block strength that is influenced by discontinuous fractures and veinlets, to the full-scale rock mass strength, is illustrated in Figure 4.

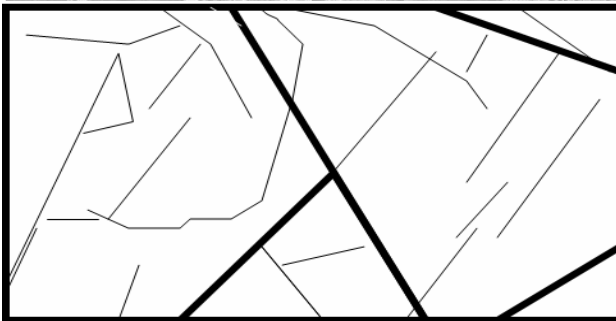


**Figure 3.**—Example of a rock mass that contains throughgoing joints (thick lines) as well as discontinuous fractures (thin lines). Rock blocks are bounded by the throughgoing joints.

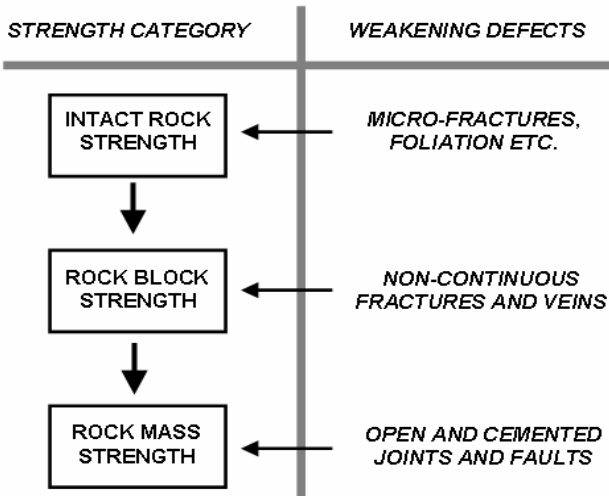


**Figure 4.**—Scale concept used in MRMR classification.

The challenge is to assign appropriate strength reduction factors to account for the cemented joints (Figure 5), fractures, and veinlets that may be present in rock blocks. It is clear that if a classification system ignores such features, the rock mass strength is overestimated, or if they are forced into the open joint category, the rock mass is underestimated.

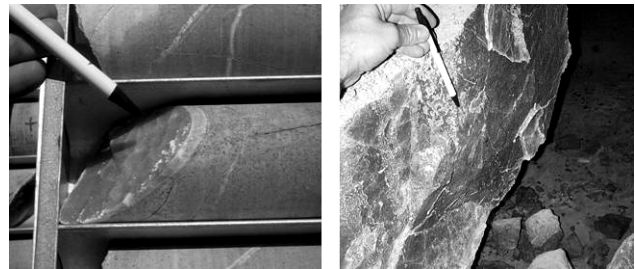


**Figure 5.**—Cemented joints in the core (left) could significantly influence rock block strength and fragmentation in a caving environment (right).

### ACCOUNTING FOR CEMENTED JOINTS AND VEINLETS

The MRMR 2000 system introduced empirical charts where the impact of the quantity and quality of cemented joints and veinlets on rock block strength can be assessed. The method is based on the Mohs hardness number of the infill materials and the frequency of the filled joints and veinlets.

It should be noted that the suggested Mohs hardness number for estimating the strength of the infill is only a field guideline, and effort should be made to better define the strength of such defects. The use of laboratory tests, back analysis, and numerical models (such as Itasca's Particle Flow Code (PFC)) could be very useful in better understanding the role of healed discontinuities with regard to rock block strength.

The effect of cemented joints and veinlets can have a significant impact on the caving process in block caving or sublevel caving operations. Figure 6 illustrates the difference in the predicted fragmentation for a rock mass that contains healed, calcite-filled veinlets based on two methods of assessing the IRMR value. The Block Cave Fragmentation (BCF) [Esterhuizen 2003] software package was used to conduct the analyses. The software makes use of joint set data, uniaxial compressive strength of the rock, stress field, and characteristics of small-scale fractures and veinlets to estimate rock fragmentation during block caving. The rock block strength is calculated as part of the process and affects stress-related fracturing. The lower curve in Figure 6 shows the predicted fragmentation if the presence of fractures and cemented veinlets is ignored in the assessment of rock strength. These results indicate very coarse fragmentation, with about 25% of the rock fragments being less than  $2 \text{ m}^3$  in size. The upper curve shows the results if the fractures and veinlets are accounted for. In this case, the predicted fragmentation is good, with about 90% of the rock fragments predicted to be less than  $2 \text{ m}^3$ . The difference in predicted fragmentation is largely due to the effect of the field stress on the rock blocks. If the fractures and veinlets are ignored, the rock block strength is overestimated, and coarse fragmentation is predicted.

When the effects of these features are included, the assigned rock block strength is reduced, which in turn dramatically reduces the predicted fragmentation. The expected fragmentation has a significant impact on the likely production rates, mine layout, and operational cost of a block-caving operation.

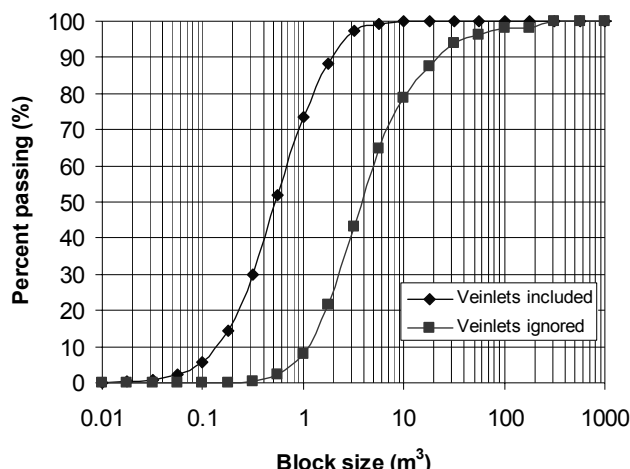


Figure 6.—Effect of calcite-filled veinlets on predicted fragmentation in block caving.

## RQD AND FRACTURE FREQUENCY

The other major difference of MRMR compared to other classifications is in the utilization of RQD. The RQD system was originally developed for tunneling conditions and was published in 1967. The fact that it is still used today is a good testimony to Deere, who introduced it 40 years ago.

RQD is a very simple, effective, and quick method to assess the rock mass competency in certain types of rocks. However, besides the lack of accountability for the basic rock mass parameters such as intact rock strength and strength of defects, the tradeoff against its simplicity is its poor reliability in highly fractured, massive, or highly anisotropic conditions. The method simply does not have the resolution that may be required for a more accurate assessment of fragmentation, cavability, and other mine design aspects. Figure 7 illustrates some of the issues related to RQD as a rock mass descriptor, and the RQD is compared to the IRMR obtained from fracture frequency.

If the rock mass character is such that RQD does not reflect the conditions accurately, then, of course, any classification system that uses RQD is exposed to problems. Figure 8 illustrates an example from one of the major block-caving projects in Chile, where the difference in IRMR values obtained by the fracture frequency (FF/m) method versus the RQD method is quite obvious. The comparison was made from drill core logging for a block-caving project in which an accurate assessment of rock

mass conditions has a significant impact on the choice of mine layout, operating procedures, and financial investment. In this case, the IRMR calculated from the FF/m was considered to be more representative of the actual rock mass conditions than the values based on the RQD. Third-party review of the outcomes, inspection of exposures in the current open-pit mine, and comparison to values estimated from the GSI rating confirmed this conclusion.

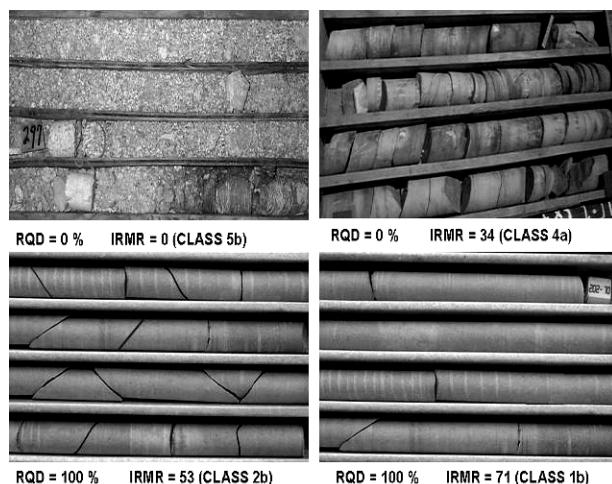


Figure 7.—Example of the problems with RQD assessment of highly fractured or massive rock masses.

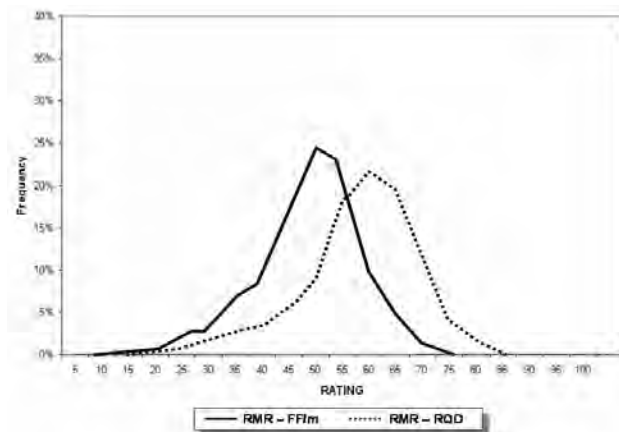


Figure 8.—Example of difference between RQD and fracture frequency-based IRMR. The IRMR based on fracture frequency (solid line) is considered more representative of actual rock mass conditions.

## PRACTICAL PROBLEMS WITH ROCK MASS ASSESSMENT RELATED TO DATA COLLECTION METHOD

As discussed above, the difference between the reality and the rock mass competency models could be due to the lack of ability to include specific geological features in our classification systems, e.g., cemented joints and veinlets.

However, if only drill core is used for rock mass assessment, we are exposed to a whole range of biases, and the resulting description of the rock mass could be significantly skewed. The potential problems and pitfalls were described by Laubscher and Jakubec [2001] and Murphy and Campbell [in press]. It is important to realize that rock mass assessment based on drill core only can easily be off by 50%.

The main challenges in rock mass assessment based on core logging, regardless of the classification system used, are:

- *Differentiation between artificially induced breaks and natural defects.* In situ borehole scanners can help to assess in situ conditions.
- *Assessment of discontinuities in foliated or highly laminated rocks.* In such rock masses, the borehole scanner may not be effective.
- *Differentiation between continuous joints and discontinuous fractures.* This problem cannot be successfully resolved without rock mass exposures (see Figure 9).
- *Drilling orientation bias.* Missing or underestimating discontinuity sets subparallel to the drill-hole. Different orientation of the drillholes can mitigate the problem.

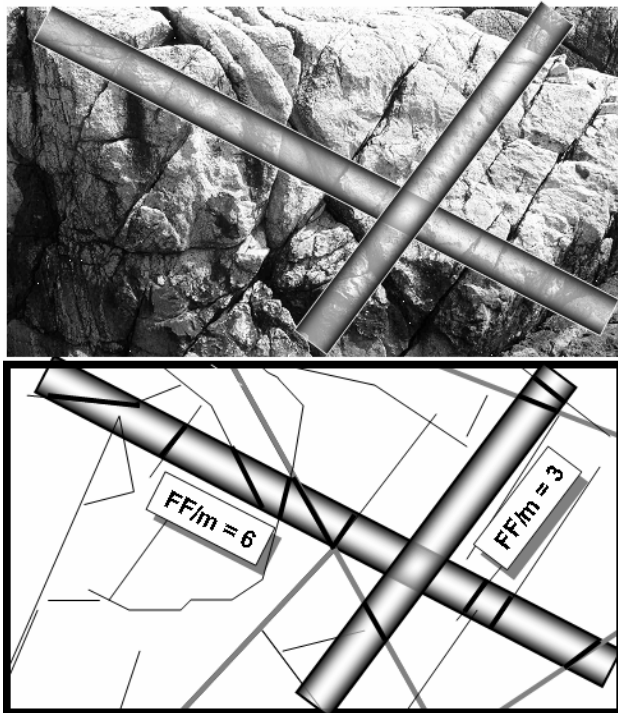


**Figure 9.—Picture illustrating the bias that could be introduced by borehole orientation. Also, it is difficult from the core to judge which discontinuities represent continuous joints and which are small-scale fractures.**

- *Accurate assessment of weak joint infill* that is washed out in most drilling processes. Triple tube techniques can help to alleviate this problem.
- *Rock strength assessment in weathered/ altered sensitive rock types such as kimberlites and mudstones.* Using specialized drilling fluids, very careful sample collection/preservation programs, and speedy delivery to the laboratory can partly mitigate these problems.
- *Material anisotropy.* Assessment of both intact rock strength and discontinuity strength anisotropy from the drill core could be a problem. The core cross-section is simply too small to capture joint geometry. (See the example shown in Figure 10.)

Any of the points mentioned above can have a significant impact on the rock mass assessment, and it is necessary that data be scrutinized in that respect.



**Figure 10.—Joint geometry may not be obvious from the drill core unless the joint is intersected at a very shallow angle.**

## DISCUSSION AND CONCLUSIONS

Some of the challenges in assessing rock mass conditions have been addressed by the MRRM 2000 system. These include the abandonment of RQD as a parameter, accounting for healed and cemented joints, and the introduction of the concept of rock block strength. This paper shows how these modifications have resulted in improved assessment of critical aspects of rock mass behavior for mine design.

When assessing rock mass behavior (by any method), it is important to remember that we cannot rely only on exact science. The inherent variability of nature does not allow the development of a universal, rigorous rock mass classification system that would be practical at the same time. It is therefore necessary to keep the system flexible and open to adjustments. This raises the issue of whether

we should strictly follow the letter of the classification systems or whether we should treat classification systems as a guideline to be used together with engineering judgment. The authors believe that spirit is more important than the letter and that field observations must be accounted for in the final judgment.

Unfortunately, the trend in the mining industry is to shift focus from the field to the office and solve problems "remotely." As our computational skills have increased dramatically, it seems that our observational skills have decreased at the same rate. Also, the discipline and somewhat rigorous process of data collection, visualization, and analysis have broken down. Despite the fact that most of today's projects have rendered three-dimensional models of geology (or at least an artist's image), it is very rare these days to find a proper set of working plans and sections where a "creative thinking" process was applied and geological and geotechnical concepts are tested prior to computerization. We would like to quote Dr. Scott-Smith—"the answers are in the rocks"—to remind us that "reality" checks should be constantly performed on our models.

### ACKNOWLEDGMENT

The authors would like to thank Dr. Dennis Laubscher for reviewing this paper and for his valuable comments.

### REFERENCES

- Barton N, Lien R, Lunde J [1974]. Engineering classification of rock masses for the design of tunnel support. *Rock Mech* 6(4):189–236.
- Bieniawski ZT [1973]. Engineering classification of jointed rock masses. *Trans S Afr Inst Civ Eng* 15:335–344.
- Esterhuizen GS [2003]. Block cave fragmentation (BCF) user's manual. Unpublished.
- Hoek E, Kaiser PK, Bawden WF [1995]. Support of underground excavations in hard rock. Rotterdam, Netherlands: Balkema.
- Laubscher DH [1975]. Class distinction in rock masses. *Coal gold base min S Afr* 23(Aug).
- Laubscher DH [1990]. A geomechanics classification system for the rating of rock mass in mine design. *Trans S Afr Inst Min Metal* 9(10).
- Laubscher DH [1993]. Planning mass mining operations. In: Hudson J, ed. *Comprehensive rock engineering*. Vol. 2. Pergamon Press, pp. 547–583.
- Laubscher DH, Jakubec J [2001]. The MRMR rock mass classification for jointed rock masses. In: Hustrulid WA, Bullock RL, eds. *Underground mining methods: engineering fundamentals and international case studies*. Littleton, CO: Society for Mining, Metallurgy, and Exploration, Inc., pp. 475–481.
- Laubscher DH, Taylor HW [1976]. The importance of geomechanics of jointed rock masses in mining operations. In: *Proceedings of the Symposium on Exploration for Rock Engineering* (Johannesburg, South Africa), pp. 119–128.
- Murphy BA, Campbell JR [in press]. Establishing a site specific mining geotechnical atlas. In: *Proceedings of the First Canada-U.S. Rock Mechanics Symposium*, Vancouver, British Columbia, Canada.

# CLASSIFICATION-BASED PROBABILISTIC DESIGN OF GROUND SUPPORT

By Radford B. Langston,<sup>1</sup> Dr. Hendrik A. D. Kirsten,<sup>2</sup> Dr. Graham C. Howell,<sup>3</sup> and John A. Marjerison<sup>4</sup>

## ABSTRACT

Probabilistic design is gaining wider acceptance in the rock engineering community since it allows more rigorous determination of risk relating to ground fall or excavation instability. Risk analysis can be conducted by various means, but the basis is formed by either objectively or subjectively determining probability of occurrence of an event. In the case of rock engineering, this event is either instability or excavation failure. Rock mass classification systems provide objective analysis of data collected on a typically subjective basis that also relate closely to excavation stability. A probabilistic analysis technique is presented that uses statistical distributions of rock mass and material properties, ground support fixture specifications, stress conditions, opening geometry, and ground support installation quality to more rigorously determine probability of failure for an underground opening and the subsequent risk to personnel.

## INTRODUCTION

The philosophy governing much ground support practice in underground excavation relies on the concept of constructing a support arch by harnessing the frictional and cohesive strength inherent in the rock mass through reinforcement. Rock masses, in some cases, are self-supporting and need few, if any, additional elements to mobilize their strength. However, in instances where the rock mass requires added elements to be stable, three essential components must be present in order to effectively construct an arch. The first two components are rock reinforcement and surface support. Presence of competent abutments for the support arch to stand upon is the third vital component.

Field data collection systems are useful tools to gauge the effectiveness of these three components in creating a stable support arch. These systems typically are intimately tied to empirical design methods, design graphs, and deterministic approaches, as are the principles of the geomechanical concepts put forth in this paper. However, with the technique described herein, both objective and

subjective probabilistic methods are suggested to derive a basis for design, as well as an overall picture of system integrity and risk analysis.

In the course of rock mass data collection, reduction, and design, varying degrees of uncertainty exist concerning all input parameters. Ignorance or simply the unknowability of specific values for often critical design factors makes a probabilistic approach to rock mass classification and ground support design a useful tool. Empirical and deterministic design approaches do not incorporate uncertainty into the process aside from ad hoc methods or simply by pure overdesign. Probabilistic methods also allow the production of more objective end products from input variables that are frequently quite subjective. Objective products resulting from the design process make their contribution in a risk, financial, or other decision-making analysis more rigorous. If little or no geotechnical data exist, this process can be also be used to conduct "what if" or sensitivity analysis for specified components of a feasibility study.

## BASIC PROBABILITY CONCEPTS

Some basic probability concepts as they apply to this particular problem are outlined below.

### Cause and Effect

Human interaction is a world of complex cause and effect. Causes to effects that we pursue are often effects of lesser-order causes. A cause of an effect is an effect of one or more identifiable underlying causes. Human shortcomings, in principle, constitute the lowest order of causes because humans ultimately hold the initiative to all action.

*Cause:* underlying factor that leads to a particular event  
*Effect:* outcome resulting from a particular event

### Independent and Dependent Causes

Two separate types of causes are considered in this paper. Independent causes take place separately from other causes and are represented by a logical "OR" statement. Dependent causes require other factors in order to occur and are represented by a logical "AND" statement. Probabilities of occurrence of independent causes are added with each other to exclude joint occurrences, and those for dependent causes are multiplied together.

<sup>1</sup>Consulting engineer, Red Lodge, MT.

<sup>2</sup>Consulting engineer, Fontainebleau, South Africa.

<sup>3</sup>Steffen, Robertson, and Kirsten, Cape Town, South Africa.

<sup>4</sup>Stillwater Mining Co., Nye, MT.

## Thresholds for Probability

International thresholds for probability of loss are given after Cole [1993] in Table 1 in terms of total losses of life, property, and money. Total loss of life denotes fatality, whereas property denotes fixed assets and money, and business ventures. Thresholds are selected in terms of voluntary and involuntary exposure of the affected aspects to the hazards. They apply to the overall probability of loss, which includes the probabilities of failure and exposure.

The thresholds are expressed in terms of lifetime frequencies, which are defined as the probable unit number of times that a hazard would occur during the life of the person affected. A natural lifetime is on average 70 years and a working lifetime is 50 years, which corresponds to  $250 \times 8$  working hours per annum or  $250 \times 8 \times 50 = 100,000$  total working hours. Expressed as a percentage, the lifetime probability of loss is equal to one-tenth of the fatality accident rate. The fatality accident rate is equal to the number of deaths from 1,000 people who are involved in a hazardous activity for their entire lives. The upper limit of lifetime probability of loss is equal to 7,000%, which by definition is the product of 70 as the average lifetime in years and 100% as the probability of occurrence of an event that will certainly occur in every year. The probabilities of failure that may be determined for engineering systems represent lifetime frequencies because they represent the unit number of times that the systems may fail in the conceivable future.

Cole [1993] determined the threshold probabilities of losses in Table 1. They are generally much more stringent than those recommended in the literature prior to 1987, but are substantially in agreement with recommendations of

various authors since. The “Acceptable and Tolerable Risk Criteria” given in Appendix H of the *Landslide Risk Management Concepts and Guidelines* published by the Australian Geomechanics Society [2000] correspond accurately with these thresholds.

## Assignment of Probabilities

Probabilities of failure can be derived from randomly sampled distributions of input variables to generate a distribution of end product capacity versus demand values. They can also be subjectively assigned through experience, engineering judgment, and use of the eight-point scale shown in Table 2.

### Objective Assignment of Probability

The likely occurrence of an event may be objectively determined by the following process. First, random sampling of the distributions for the governing input parameters produces a population of rock mass values that are translated into ground support demand. Next, a second group of values of ground support capacity is generated in the same manner. Values from both of these distributions are then randomly sampled to generate a distribution of capacity versus demand. The probability of failure is then the area under the probability density function left of the value where capacity equals demand. Distributions can be derived from statistical analysis of the input data or from predetermined functions if the statistical parameters are not well established. Figures 1–3 are normal, triangular, and uniform probability density functions commonly used for these purposes.

**Table 1.—Acceptable lifetime probabilities of total losses [Cole 1993]**

Degree of risk	Attitude to reliability		Probability (%) of total loss of		
	Voluntary	Involuntary	Life	Property	Money
Very risky .....	Very concerned	Totally unacceptable	70 (–) (deep-sea diving or rock climbing)	700 (–) (volcano or avalanche)	7,000 (–) (gambling)
Risky .....	Concerned	Not acceptable	7 (1.60) (deep-sea diving or rock climbing)	70 (–) (volcano or avalanche)	700 (–) (gambling)
Some risk.....	Circumspect	Very concerned	0.7 (2.50) (car, airplane, or home accident)	7 (1.60) (undermining or earthquake)	70 (–) (small business failure)
Slight chance ....	Of little concern	Concerned	0.07 (3.22) (car, airplane, or home accident)	0.7 (2.50) (undermining or earthquake)	7 (1.60) (small business failure)
Unlikely .....	Of no concern	Circumspect	0.007 (3.82) (public transport accident)	0.07 (3.22) (flooding)	0.7 (2.50) (company failure)
Very unlikely ....	Of no concern	Of little concern	0.0007 (4.35) (fatality in public place)	0.007 (3.82) (failure of foundation on soil)	0.07 (3.22) (failure of banks or building societies)
Practically impossible.....	Of no concern	Of no concern	0.00007 (4.83) (failure of nuclear powerplant)	0.0007 (4.35) (failure of foundation on rock)	0.007 (3.82) (collapse of National Savings)

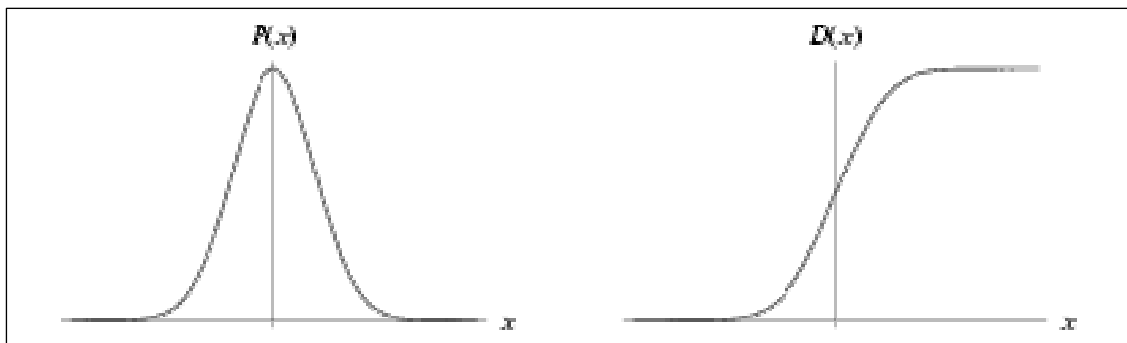


Figure 1.—Normal probability density function and cumulative distribution function [MathWorld 2007].

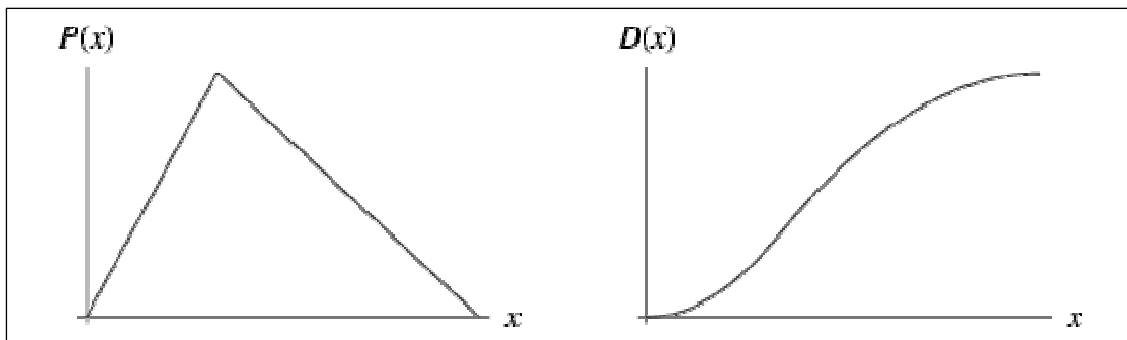


Figure 2.—Triangular probability density function and cumulative distribution function [MathWorld 2007].

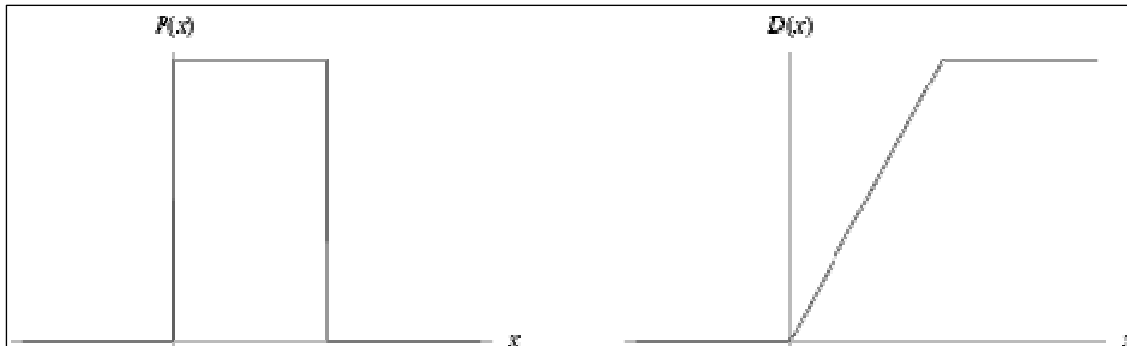


Figure 3.—Uniform probability density function and cumulative distribution function [MathWorld 2007].

### SUBJECTIVE ASSIGNMENT OF PROBABILITY

The eight-point scale described below was developed for evaluating operational safety in South African coal mines. It can consistently evaluate operational safety, system integrity, economic viability, process reliability, and environmental protection and rehabilitation in a wide

range of engineering systems [Kirsten 1999]. The six-point scale Risk Assessment Table published by the Institution of Civil Engineers and the Faculty and Institute of Actuaries [1998] in the United Kingdom is identical in concept. The six-point scale in Appendix G of the *Landslide Risk Management Concepts and Guidelines* published by the Australian Geomechanics Society [2000]

is almost identical to Table 2 in both qualitative and quantitative levels of probability.

**Table 2.—Classes for probability of occurrence**

Qualitative evaluation	Quantitative evaluation
Certain.....	Every time
Very high.....	1 in 10
High.....	1 in 100
Moderate.....	1 in 1,000
Low.....	1 in 10,000
Very low.....	1 in 100,000
Extremely low.....	1 in 1 million
Practically zero.....	1 in 10 million

## GEOMECHANICAL DATA

Rock mass parameters are closely tied and most often differ with variations in rock type, which usually also defines the spatial relationships of the parameters and the excavation. The system used in this paper for assessing rock mass quality is the Q-system developed by Barton et al. [1974]. The methods described in this paper would work equally well for virtually any rock mass classification system.

Rock mass quality, Q, varies on a logarithmic scale from 0.001 to 1,000 and is determined by Equation 1:

$$Q = (RQD/J_n) \times (J_r/J_a) \times (J_w/SRF) \quad (1)$$

RQD/J<sub>n</sub> is an estimate of block size. J<sub>r</sub>/J<sub>a</sub> generally represents the strength of the discontinuities demarcating the blocks. J<sub>w</sub>/SRF is a measure of the active stress present in the rock mass [Barton et al. 1974].

All of the inputs for the equation can be defined as random variables and, as such, may belong to populations easily defined by statistical distributions. Five of the six parameters needed to define rock mass quality (Q) listed below can be sampled from their own distribution. The last, stress reduction factor (SRF), can be either chosen from a distribution of SRF or calculated from the UCS and depth, each of which can also be picked from a specific distribution [Kirsten 1988]. Any one of these random variables can also be held to a constant value. The rock mass input parameters are listed below.

- RQD is a measure of the degree of fracturing in the rock mass;
- J<sub>n</sub> represents the total number of discrete joint sets in the rock mass;
- J<sub>r</sub> is a measure of friction and, to a somewhat lesser degree, cohesion of a discontinuity;
- J<sub>a</sub> represents the amount of both cohesion and friction of a discontinuity;
- J<sub>w</sub> is the amount of water inflow affecting the rock mass; and
- SRF quantifies the effect of the excavation on the rock mass.

Other geomechanical parameters that can be selected out of specified distributions are—

- UCS;
- Angle of internal friction;
- Unit weight;
- Maximum principal primitive stress;
- Minimum principal primitive stress;
- Maximum principal primitive stress direction;
- Depth below surface;
- Span variation;
- Excavation support ratio; and
- Geologic structure variations.

All of these rock mass and geomechanical properties combine with excavation size and geometry to place a demand of some magnitude on the ground support system. The designed ground support system must reinforce and confine the rock mass to the point that the effects of this demand are counteracted in order to provide excavation stability.

## SUPPORT COMPONENTS

Variation in ground support elements is typically less pronounced than rock mass properties because they are produced by a relatively well controlled manufacturing process. However, the installation process, design layout, and excavation profile often vary widely. For a specified rock-reinforcing fixture, any of the following support component parameters can be sampled randomly from an appropriate distribution:

- Fixture length;
- Angle from normal;
- Material properties;
- Fixture specifications;
- Hole diameter;
- In-plane spacing;
- Out-of-plane spacing;
- Plate properties; and
- Properties of the fixture rock interface(s).

Statistical distributions can represent the shotcrete properties listed below:

- Thickness;
- Span-thickness ratio;
- Compressive strength;
- Shear strength; and
- Reinforcement properties.

Surface support elements also conform to this process. These are:

- Area per meter;
- Catenary rise;
- Strand tensile strength;
- Mesh anchor shear area;
- Weld strength; and
- Strand spacing.

When the distribution of rock mass and geomechanical demand has been generated, it is compared to a distribution of ground support capacity. This comparison results in a distribution of capacity versus demand. The probability of failure determined from the capacity versus demand distribution is the area under the best-fit curve left of the point where capacity equals demand. This represents probability of structural failure ( $p_{sfw}$ ), and the process of deriving the probability is applied to each wall of the excavation in turn. Probability of failure for each wall will then be combined with the probabilities for the other walls by a logical “OR” statement since failure can occur in any wall independent of the others. From this point, the other aspects determining total probability failure and overall threat may now be applied.

Failure of ground support subsystems such as installation quality increase the overall probability of failure, but due to the difficulty in objective measurement, the probabilities of failure are best subjectively applied. These probabilities of the factors listed below are subjectively assessed and applied to each wall separately. The subjective application of the probabilities should be derived from the eight-point scale in Table 2. In general terms, the subsystems are described by the following list:

- Fixtures installed per manufacturer’s specifications and standard industry practice
- Proper anchorage for the specified fixture
- Rock bolt plates tight against the rock face
- Angle of the installed fixture as close to normal to the bearing surface as possible
- Significant structures or weak contacts crossed and locked together
- Systematic and regular support installation
- Adherence to specified design or ground support standard
- Installed support adequate for the ground type
- Rock not excessively damaged due to blasting
- Blast holes drilled on line and not out into the walls or up into the back
- The walls have relatively smooth profile
- No excessive loading of ground support elements
- Surface support elements secured tightly against the rock surface

## DISCUSSION

Each of these subjectively assigned probabilities of subsystem failure can now be combined with the probability of structural failure for a given wall with a logical “OR” statement, giving a probability of overall structural failure ( $p_{osfw}$ ) calculated by:

$$P_{osfw} = 1 - [(1 - p_{sfw}) * (1 - p_{ss1}) * (1 - p_{ss2}) * (1 - p_{ssn+1})] \quad (2)$$

where  $p_{osfw}$  = P(overall structural failure wall);  
 $p_{sfw}$  = P(probability of structural failure wall);  
 $p_{ss1}$  = P(probability of subsystem failure 1);  
 $p_{ss2}$  = P(probability of subsystem failure 2);  
and  $p_{ssn+1}$  = P(probability of subsystem failure n).

Three additional aspects needed in determining total probability of failure and overall threat to personal injury must now be considered. The first of these is probability of ejection freedom. This concept is based on the degree of confinement or restraint against spontaneous block ejection resulting from a gravitational or seismic acceleration provided to the rock mass as the level of ground support increases. As the number of ground support elements multiply, the probability that a block of rock can spontaneously be ejected, taking a worker by surprise, decreases. The probability of surprise or ejection freedom with no support installed is 100%, or certain. As the support quantity increases, the probability of ejection freedom decreases by an order of magnitude as shown in Table 3.

**Table 3.—Probability of ejection freedom**

Support level	Probability of ejection freedom
No support.....	Every time
Light support.....	1 in 10
Moderate support.....	1 in 100
Heavy support.....	1 in 1,000
Very heavy support.....	1 in 10,000
Extremely heavy support.....	1 in 100,000

The next facet of the overall threat to consider is the probability of personnel appearance. This probability can be calculated as the percentage of the entire work shift that personnel spend exposed to potential excavation instability. It can also be referenced from Table 4.

**Table 4.—Probability of personnel appearance**

Personnel appearance	Probability
Continuous.....	1.0
Very regular.....	0.3
Regular.....	0.03
Occasional.....	0.003
Very occasional.....	0.0003
Rare.....	0.00003

The final variable needed to complete this calculation is the probability of personnel coincidence. Coincidence is essentially calculated by a 0.5-m width of a person divided by the total length of excavation that exposes that person to a rock fall hazard. Thus, for one person in 50 m of tunnel, the personnel coincidence is 0.5/50, or 0.1.

In order to now determine total probability of failure, the probability of overall structural failure for each wall is “OR” gated to the other walls to obtain the probability of failure for the entire excavation.

$$P_{osfe} = 1 - [(1 - p_{osfw1}) * (1 - p_{osfw2}) * (1 - p_{osfw3})] \quad (3)$$

where  $p_{osfe}$  = P(overall structural failure excavation);  
 $p_{osfw1}$  = P(overall structural failure wall 1);  
 $p_{osfw2}$  = P(overall structural failure wall 2);  
and  $p_{osfw3}$  = P(overall structural failure wall 3).

In order to calculate the overall threat of injury for the entire excavation, the overall probability of structural failure for the excavation is “AND” gated with the probability of ejection freedom, probability of personnel appearance, and probability of personnel coincidence, as shown in Equation 4:

$$T = p_{osfe} * p_{ejec} * p_{app} * p_{coin} \quad (4)$$

where  $T$  = overall threat of injury;  
 $p_{osfe}$  = P(overall structural failure excavation);  
 $p_{ejec}$  = P(ejection freedom);  
 $p_{app}$  = P(personnel appearance);  
and  $p_{coin}$  = P(personnel coincidence).

When the overall threat is calculated, it can be compared to the thresholds shown in Table 1. If the overall threat is below an acceptable level, the design can stand. If it is not, a number of methods can be employed to reduce the threat. Rock mass variable distributions should be checked for plausibility or appropriate application and assumptions regarding input variables recalibrated. The design can be reconsidered and altered to increase ground support capacity, thereby reducing the possibility of structural failure. Subsystem shortfalls found to contribute significantly to the probability of structural failure can be remediated. The probability of ejection freedom decreases with an increase in support quantity, and the probability of personnel appearance and coincidence can be reduced by limiting access to the area.

Another methodology that has been employed is to conduct a survey of numerous excavations at a project such as a large mining operation and apply this process to each excavation. When the overall threat for an appropriate number of workings have been calculated, the distribution of threats can be plotted, as shown in Figure 4.

An appropriate design level of threat for work in underground excavations is less than  $10^{-4}$ , or 1 chance in

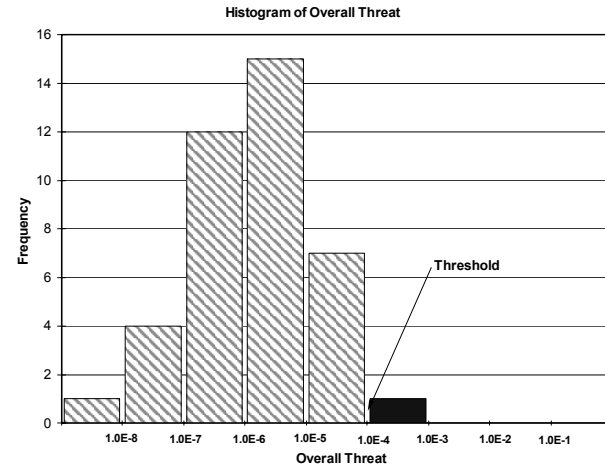


Figure 4.—Example histogram of threat.

10,000. As a basis for comparison, this probability of occurrence is equivalent to acceptable risk of injury on a public transport system [Kirsten 1999]. Values above this threshold indicate a need to promptly address conditions, while values below this indicate acceptable level of threat or risk. Probabilities that are several orders of magnitude below the threshold indicate less than optimal ground support economy. Figure 4 shows an example distribution of threat from 42 hypothetical cases.

As previously stated, when overall threat exceeds the threshold, access by personnel to the area can be limited until ground support remediation has been completed. It is advisable to install remedial ground support only from under supported ground that has an overall threat below a threshold acceptable to operations management. Prohibiting access to an area effectively decreases exposure so that the threat is reduced to below the acceptable level of threat. A reasonable goal is to not let more than 5% of headings exceed an acceptable threshold of  $10^{-4}$  at any instant of time.

## SUMMARY

Typical rock mass classification design systems involve data collection, data reduction, and then plotting the reduced data on empirical design curves. From this step, empirical or deterministic criteria are applied and a final design proposed. This type of process is quite adequate for many rock engineering problems. Some, however, lend themselves to probabilistic analysis due to the inhomogeneous nature of the rock mass and inherent uncertainty of its characterization.

Rock mass data collection, reduction, and design involve varying degrees of uncertainty due to the variability of all input parameters. Parameters collected during the course of rock mass classification and excavation design are random variables and, as such, belong to populations naturally expressed by statistical distributions.

Unknowns regarding specific values needed in ground support allow a probabilistic design approach to provide inputs that can be used with a known degree of confidence. That degree of confidence may be low or high, but it is known and was systematically derived. This process can also produce more objective end products from frequently subjective input variables. Objective products resulting from the design process make their contribution in a risk, financial, or other decision-making analysis more rigorous. If little or no geotechnical data exist, this process can be also be used to conduct “what if” or sensitivity analysis for specified components of a feasibility study.

Probability of loss thresholds are specified for total loss of life, property, and money. Thresholds are chosen with regard to voluntary and involuntary exposure to hazards and expressed in terms of lifetime frequencies. Probabilities of failure determined for engineering systems represent lifetime frequencies, since they correspond to the unit number of times the systems could fail in a potential lifetime.

After generation of a rock mass and geomechanical demand distribution, it is compared to a ground support capacity distribution that gives rise to a capacity versus demand distribution from which the probability of structural failure is calculated. Subjectively derived probabilities of failure for ground support subsystems are added to the probability of structural failure to give a probability of overall structural failure. The probability of ejection freedom, personnel appearance, and personnel coincidence are multiplied with the overall probability of structural failure to give the overall threat of injury.

When the overall threat of injury is above an acceptable threshold, several approaches can be taken to lessen the threat, from recalibrating input variables to increasing the quantity of ground support and remediating ground support subsystem shortfalls. Increasing support quantity decreases the probability of ejection freedom, and limiting access to the area lowers the probability of personnel appearance and coincidence.

## REFERENCES

- Australian Geomechanics Society [2000]. Landslide risk management concepts and guidelines. *Aust Geomech Mar*:49–92.
- Barton N, Lien R, Lunde J [1974]. Engineering classification of rock masses for the design of tunnel support. *Rock Mech* 6(4):189–236.
- Cole K [1993]. Building over abandoned shallow mines. Paper 1: Considerations of risk and reliability. *Ground Engineering*, pp. 35–37.
- Hoek E [1994]. Acceptable risks and practical decisions in rock engineering. Short course notes for 12th Annual Canadian Conference on Tunneling.
- Holton GA [2004]. Defining risk. *Financ Analysts J* 60(6):19–25.
- Institution of Civil Engineers and the Faculty and Institute of Actuaries [1998]. Risk analysis and management for projects (RAMP). London: Thomas Telford, Ltd.
- Kirsten HAD [1988]. Norwegian Geotechnical Institute or Q-system by N. Barton. Discussion contribution. Symposium on Rock Classification Systems for Engineering Purposes D-18, ASTM STP 984, ASTM, Cincinnati, OH, pp. 85–88.
- Kirsten HAD [1999]. Course on evaluation of risk as a decision-making criterion. SRK Consulting, 15 sections.
- MathWorld [2007]. Continuous distributions. [<http://mathworld.wolfram.com/topics/ContinuousDistributions.html>]. Date accessed: March 2007.



# THE GEOLOGICAL STRENGTH INDEX (GSI): A CHARACTERIZATION TOOL FOR ASSESSING ENGINEERING PROPERTIES FOR ROCK MASSES

By Paul G. Marinos, Ph.D.,<sup>1</sup> Vassilis Marinos,<sup>2</sup> and Evert Hoek, Ph.D.<sup>3</sup>

## ABSTRACT

The Geological Strength Index (GSI) is a system of rock mass characterization that has been developed in engineering rock mechanics to meet the need for reliable input data related to rock mass properties required as input for numerical analysis or closed-form solutions for designing tunnels, slopes, or foundations in rocks. The geological character of the rock material, together with the visual assessment of the mass it forms, is used as a direct input for the selection of parameters for predicting rock mass strength and deformability. This approach enables a rock mass to be considered as a mechanical continuum without losing the influence that geology has on its mechanical properties. It also provides a field method for characterizing difficult-to-describe rock masses. Recommendations on the use of GSI are given and, in addition, cases where the GSI is not applicable are discussed.

## INTRODUCTION

A few decades ago, the tools for designing tunnels started to change. Numerical methods were being developed that offered the promise for much more detailed analysis of difficult underground excavation problems.

Numerical tools available today allow the tunnel designer to analyze progressive failure processes and the sequentially installed reinforcement and support necessary to maintain the stability of the advancing tunnel until the final reinforcing or supporting structure can be installed. However, these numerical tools require reliable input information on the strength and deformation characteristics of the rock mass surrounding the tunnel. As it is practically impossible to determine this information by direct in situ testing (except for back analysis of already constructed tunnels), there was an increased need for estimating the rock mass properties from the intact rock properties and the characteristics of the discontinuities in the rock mass. This resulted in the development of the rock mass failure criterion by Hoek and Brown [1980]. A brief history of the

development of the Hoek-Brown criterion is to be published in the first issue of a new international journal entitled *Soils and Rocks* [Hoek and Marinos, in press].

The present paper is an update and extension of the paper by Marinos et al. [2005].

## THE GEOLOGICAL STRENGTH INDEX (GSI)

Hoek and Brown recognized that a rock mass failure criterion would have no practical value unless it could be related to geological observations that could be made quickly and easily by an engineering geologist or geologist in the field. They considered developing a new classification system during the evolution of the criterion in the late 1970s, but they soon gave up the idea and settled for the already published RMR system. It was appreciated that the RMR system (and the Q-system) [Bieniawski 1973; Barton et al. 1974] were developed for the estimation of underground excavation and support and that they included parameters that are not required for estimating rock mass properties. The groundwater and structural orientation parameters in RMR and the groundwater and stress parameters in Q are dealt with explicitly in effective stress numerical analyses, and the incorporation of these parameters into the rock mass property estimate results is inappropriate. Thus, it was recommended that only the first four parameters of the RMR system (intact rock strength, RQD rating, joint spacing, and joint conditions) should be used for the estimation of rock mass properties if this system had to be used.

After several years of use, it became obvious that the RMR system was difficult to apply to rock masses that are of very poor quality. The relationship between RMR and the constants "m" and "s" of the Hoek-Brown failure criterion begins to break down for severely fractured and weak rock masses.

Additionally, since RQD in most of the weak rock masses is essentially zero, it became necessary to consider an alternative classification system. The required system would place greater emphasis on basic geological observations of rock mass characteristics; reflect the material, its structure, and its geological history; and would be developed specifically for the estimation of rock mass properties rather than for tunnel reinforcement and support. This new classification, now called GSI, started life in Toronto, Canada, with engineering geology input from David Wood [Hoek et al. 1992]. The index and its use for the Hoek-Brown failure criterion was further developed by Hoek

<sup>1</sup>Professor, National Technical University of Athens, School of Civil Engineering, Athens, Greece.

<sup>2</sup>Research assistant, National Technical University of Athens, School of Civil Engineering, Athens, Greece.

<sup>3</sup>Consultant, Vancouver, British Columbia, Canada.

[1994] and presented in Hoek et al. [1995] and Hoek and Brown [1997], but it was still a hard-rock system roughly equivalent to RMR. Since 1998, Evert Hoek and Paul Marinos, dealing with incredibly difficult materials encountered in tunneling in Greece, developed the GSI system to its present form to include poor-quality rock masses (Figure 1) [Hoek et al. 1998; Marinos and Hoek 2000, 2001]. Today, GSI continues to evolve as the principal vehicle for geological data input for the Hoek-Brown criterion.

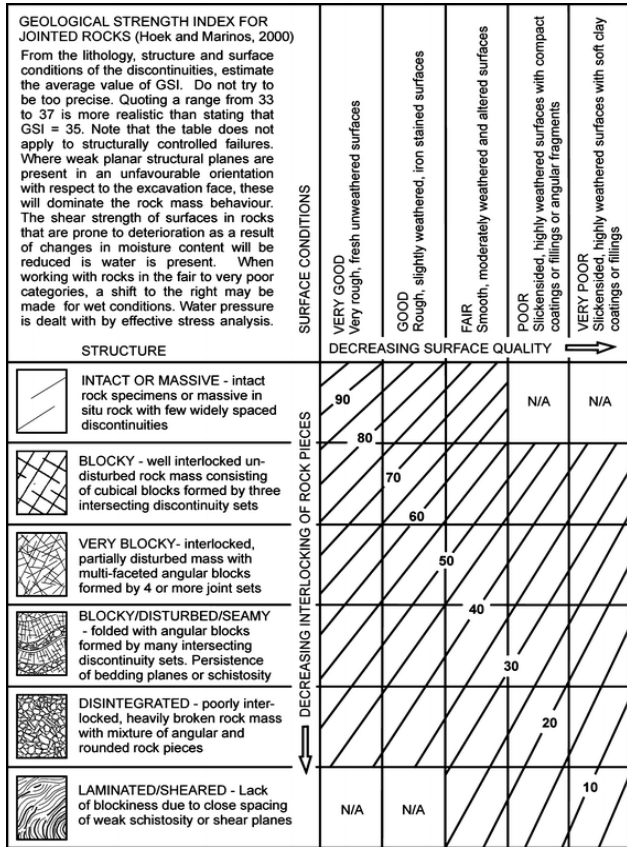


**Figure 1.—General chart for GSI estimates from geological observations.**

## FUNCTIONS OF THE GEOLOGICAL STRENGTH INDEX

The heart of the GSI classification is a careful engineering geology description of the rock mass, which is essentially qualitative, because it was believed that numbers on joints were largely meaningless for weak and complex rock masses. Note that the GSI system was never intended as a replacement for RMR or Q, as it has no rock mass reinforcement or support design capability. GSI alone is not a tunnel design tool; its only function is the estimation of rock mass properties. It is intimately linked

with the intact rock strength and should never be used independently of this parameter.

This index is based on an assessment of the lithology, structure, and condition of discontinuity surfaces in the rock mass, and it is estimated from visual examination of the rock mass exposed in outcrops, in surface excavations such as road cuts, and in tunnel faces and borehole cores. The GSI, by combining the two fundamental parameters of the geological process—the blockiness of the mass and the conditions of discontinuities—respects the main geological constraints that govern a formation. It is thus a geologically sound index that is simple to apply in the field.

Note that attempts to “quantify” the GSI classification to satisfy the perception that “engineers are happier with numbers” [Cai et al. 2004; Sonmez and Ulusay 1999] are interesting, but have to be applied with caution in order not to lose the geologic logic of the GSI system. The quantification processes used are related to the frequency and orientation of discontinuities and are limited to rock masses in which these numbers can easily be measured. These quantifications do not work well in tectonically disturbed rock masses in which the structural fabric has been destroyed. In such rock masses, the authors recommend the use of the original qualitative approach based on careful visual observations. Thus, the “quantification” system is only valid in the range of, say,  $35 < \text{GSI} < 75$ , when the rock mass behavior depends on sliding and rotation of intact rock pieces, and where the spacing and condition of discontinuities that separate these pieces and not the intact rock strength control the behavior. When the intact rock pieces themselves can fail, then the quantification is no longer valid.

Once a GSI “number” has been decided upon, this number is entered into a set of empirically developed equations to estimate the rock mass properties that can then be used as input into some form of numerical analysis or closed-form solution. The index is used in conjunction with appropriate values for the unconfined compressive strength (UCS) of the intact rock,  $\sigma_{ci}$ , and the petrographic constant,  $m_i$ , to calculate the mechanical properties of a rock mass, in particular the compressive strength of the rock mass ( $\sigma_{cm}$ ) and its deformation modulus ( $E$ ). Updated values of  $m_i$  can be found in Marinos and Hoek [2000] or in the RocLab program [Rocscience, Inc. 2007]. Basic procedures are explained by Hoek and Brown [1997], but a refinement of the empirical equations and the relationship between the Hoek-Brown and Mohr-Coulomb criteria have been addressed by Hoek et al. [2002] for appropriate ranges of stress encountered in tunnels and slopes. Hoek and Diederichs [2006] recently presented new equations for estimating rock mass deformation modulus incorporating measured or estimated intact modulus.

## SUGGESTIONS FOR USING GSI

After more than a dozen of years of application of the GSI and its variations for the characterization of the rock mass, this paper attempts to answer questions that have been raised by users about the appropriate selection of the index for various rock masses under various conditions.

### When Not to Use GSI

The GSI classification system is based on the assumption that the rock mass contains a sufficient number of "randomly" oriented discontinuities such that it behaves as a homogeneous isotropic mass. In other words, the behavior of the rock mass is independent of the direction of the applied loads. Therefore, it is clear that the GSI system should not be applied to those rock masses in which there is a clearly defined dominant structural orientation or structurally dependent gravitational instability. However, the Hoek-Brown criterion and the GSI chart can be applied with caution if the failure of such rock masses is not controlled by such anisotropy (e.g., in the case of a slope when the dominant structural discontinuity set dips into the slope and failure occurs through the rock mass). For rock masses with a structure such as that shown in the bottom row of the GSI chart (Figure 1), anisotropy is not a major issue, as the difference in the strength of the rock and that of the discontinuities within it is often small. Anisotropy in cases of stress-dependent instability is discussed later in this paper.

It is also inappropriate to assign GSI values to excavated faces in strong hard rock with a few discontinuities spaced at distances of similar magnitude to the dimensions of the tunnel or slope under consideration. In such cases, the stability of the tunnel or slope will be controlled by the three-dimensional geometry of the intersecting discontinuities and the free faces created by the excavation. Obviously, the GSI classification does not apply to such cases.

### Geological Description in the GSI Chart

In dealing with specific rock masses, it is suggested that the selection of the appropriate case in the GSI chart should not be limited to the visual similarity with the sketches of the structure of the rock mass as they appear in the charts. The associated descriptions must also be read carefully, so that the most suitable structure is chosen. The most appropriate case may well lie at some intermediate point between the limited number of sketches or descriptions included in the charts.

### Projection of GSI Values Into the Ground

Outcrops, excavated slopes, tunnel faces, and borehole cores are the most common sources of information for

estimating the GSI value of a rock mass. How should the numbers estimated from these sources be projected or extrapolated into the rock mass behind a slope or ahead of a tunnel?

Outcrops are an extremely valuable source of data in the initial stages of a project, but they suffer from the disadvantage that surface relaxation, weathering, and/or alteration may have significantly influenced the appearance of the rock mass components. This disadvantage can be overcome by trial trenches but, unless these are machine-excavated to considerable depth, there is no guarantee that the effects of deep weathering will have been eliminated. Judgment is therefore required in order to allow for these weathering and alteration effects in assessing the most probable GSI value at the depth of the proposed excavation.

Excavated slope and tunnel faces are probably the most reliable source of information for GSI estimates, provided that these faces are reasonably close to and in the same rock mass as the excavation under investigation.

Borehole cores are the best source of data at depth, but it must be recognized that it is necessary to extrapolate the one-dimensional information provided by the core to the three-dimensional in situ rock mass. However, this is a problem common to all borehole investigations, and most experienced engineering geologists are comfortable with this extrapolation process.

For stability analysis of a slope, the evaluation is based on the rock mass through which it is anticipated that a potential failure plane could pass. The estimation of GSI values in these cases requires considerable judgment, particularly when the failure plane can pass through several zones of different quality. Mean values may not be appropriate in this case.

For tunnels, the index should be assessed for the volume of rock involved in carrying loads, e.g., for about one diameter around the tunnel in the case of tunnel behavior or more locally in the case of a structure such as the elephant foot of a steel arch. In more general terms, the numerical models may include the variability of GSI values over the tunnel in "layers." Drs. Edmund Medley and Dimitrios Zekkos are currently considering developing a function defining the variation of GSI with depth for a specific case.

### Anisotropy

As discussed above, the Hoek-Brown criterion (and other similar criteria) assumes that the rock mass behaves isotropically and that failure does not follow a preferential direction imposed by the orientation of a specific discontinuity or a combination of two or three discontinuities. In these cases, the use of GSI to represent the whole rock mass is meaningless, as the failure is governed by the shear strength of these discontinuities and not of the rock mass.

However, cases where the criterion and the GSI chart can reasonably be used have been discussed above.

However, in a numerical analysis involving a single well-defined discontinuity such as a shear zone or fault, it is sometimes appropriate to apply the Hoek-Brown criterion to the overall rock mass and to superimpose the discontinuity as a significantly weaker element. In this case, the GSI value assigned to the rock mass should ignore the single major discontinuity. The properties of this discontinuity may fit the lower portion of the GSI chart or they may require a different approach, such as laboratory shear testing of soft clay fillings.

In general terms, when confinement is present, the stress-dependent regime is controlled by the anisotropy of the rock masses (e.g., slates, phyllites, etc.). A discussion of anisotropy rock mass behavior in tunneling beyond the commonly used classification systems is presented by Button et al. [2004]. In these cases, it would be necessary to develop an orientation-dependent GSI. This is a recent idea to try to simplify the treatment of anisotropic problems. However, in view of the potential for complicating the understanding of GSI, an alternative approach may be to use an orientation-dependent UCS. This is more logical from a physical point of view and, being almost completely interchangeable with GSI from a mathematical point of view, should work just as well. The GSI value in this case would be high, and the rock mass strength would be determined by the orientation-dependent  $\sigma_{ci}$  value.

With the capacity of present-day microcomputers, it is also possible to model anisotropy by superimposing a large number of discontinuities on an isotropic rock mass which is assigned a higher GSI value. These discontinuities can be assigned shear strength and stiffness characteristics that simulate the properties of the schistosity, bedding planes, and joints in the rock mass. Such models have been found to work well and give results that compare well with more traditional anisotropic solutions.

### Aperture of Discontinuities

The strength and deformation characteristics of a rock mass are dependent on the interlocking of the individual pieces of intact rock that make up the mass. Obviously, the aperture of the discontinuities that separate these individual pieces has an important influence on the rock mass properties.

There is no specific reference to the aperture of the discontinuities in the GSI chart, but a “disturbance factor” D has been provided in the most recent version of the Hoek-Brown failure criterion [Hoek et al. 2002] and is also used in the Hoek and Diederichs [2006] approach for estimating deformation modulus. This factor ranges from D=0 for undisturbed rock masses, such as those excavated by a tunnel boring machine, to D=1 for extremely disturbed rock masses, such as open-pit mine slopes that have

been subjected to very heavy production blasting. The factor allows for the disruption of the interlocking of the individual rock pieces as a result of opening of the discontinuities. The influence of this factor is of great significance to the calculated factors of safety.

At this stage, there is relatively little experience in the use of this factor, and it may be necessary to adjust its participation in the equations as more field evidence is accumulated. However, the experience so far suggests that this factor does provide a reasonable estimate of the influence of damage due to stress relaxation or blasting of excavated rock faces. Note that this damage decreases with depth into the rock mass and, in numerical modeling, it is generally appropriate to simulate this decrease by dividing the rock mass into a number of zones with decreasing values of D being applied to successive zones as the distance from the face increases. On the other hand, in very large open-pit mine slopes in which blasts can involve many tons of explosives, blast damage has been observed up to 100 m or more behind the excavated slope face. This would be a case for D=1 and there is a very large reduction in shear strength associated with damage. Hoek and Karzulovic [2000] have given some guidance on the extent of this damage and its impact on rock mass properties. For civil engineering slopes or foundation excavation, the blast damage is much more limited in both severity and extent, and the value of D is generally low.

This problem becomes less significant in weak and tectonically disturbed rock masses, as excavation is generally carried out by “gentle” mechanical means and the amount of surface damage is negligible compared to that which already exists in the rock mass.

### Geological Strength Index at Great Depth

In hard rock at great depth (e.g., 1,000 m or more) the rock mass structure is so tight that the mass behavior approaches that of the intact rock. In this case, the GSI value approaches 100 and the application of the GSI system is no longer meaningful.

The failure process that controls the stability of underground excavations under these conditions is dominated by brittle fracture initiation and propagation, which leads to spalling, slabbing, and, in extreme cases, rock bursts. Considerable research effort has been devoted to the study of these brittle fracture processes, and Diederichs et al. [2004] provide a useful summary of this work.

When tectonic disturbance is important and persists with depth, these comments do not apply and the GSI charts may be applicable, but should be used with caution.

### Discontinuities With Filling Materials

The GSI charts can be used to estimate the characteristics of rock masses with discontinuities with filling

materials using the descriptions in the columns for “poor” or “very poor” condition of discontinuities. If the filling material is systematic and thick (e.g., more than a few centimeters) or shear zones are present with clayey material, then the use of the GSI chart for heterogeneous rock masses (discussed below) is recommended.

### Influence of Water

The shear strength of the rock mass is reduced by the presence of water in the discontinuities or filling materials when these are prone to deterioration as a result of changes in moisture content. This is particularly valid in the “fair” to “very poor” categories of discontinuities, where a shift to the right may be made for wet conditions. The shift to the right is more substantial in the low-quality range of rock mass (last rows and columns of the chart).

Water pressure is dealt with by effective stress analysis in design, and it is independent of the GSI characterization of the rock mass.

### Weathered Rock Masses

The GSI values for weathered rock masses are shifted to the right of those of the same rock masses when these are unweathered. If the weathering has penetrated into the intact rock pieces that make up the mass (e.g., in weathered granites), then the constant  $m_i$  and the unconfined strength of the  $\sigma_{ci}$  of the Hoek-Brown criterion must also be reduced. If the weathering has penetrated the rock to the extent that the discontinuities and the structure have been lost, then the rock mass must be assessed as a soil and the GSI system no longer applies.

### Heterogeneous and Lithologically Varied or Complex Rock Masses

GSI has been extended to accommodate the most variable of rock masses, including extremely poor quality sheared rock masses of weak schistose materials (such as siltstones, clay shales, or phyllites) often interbedded with strong rock (such as sandstones, limestones, or quartzites). A GSI chart for flysch, a typical heterogeneous lithological

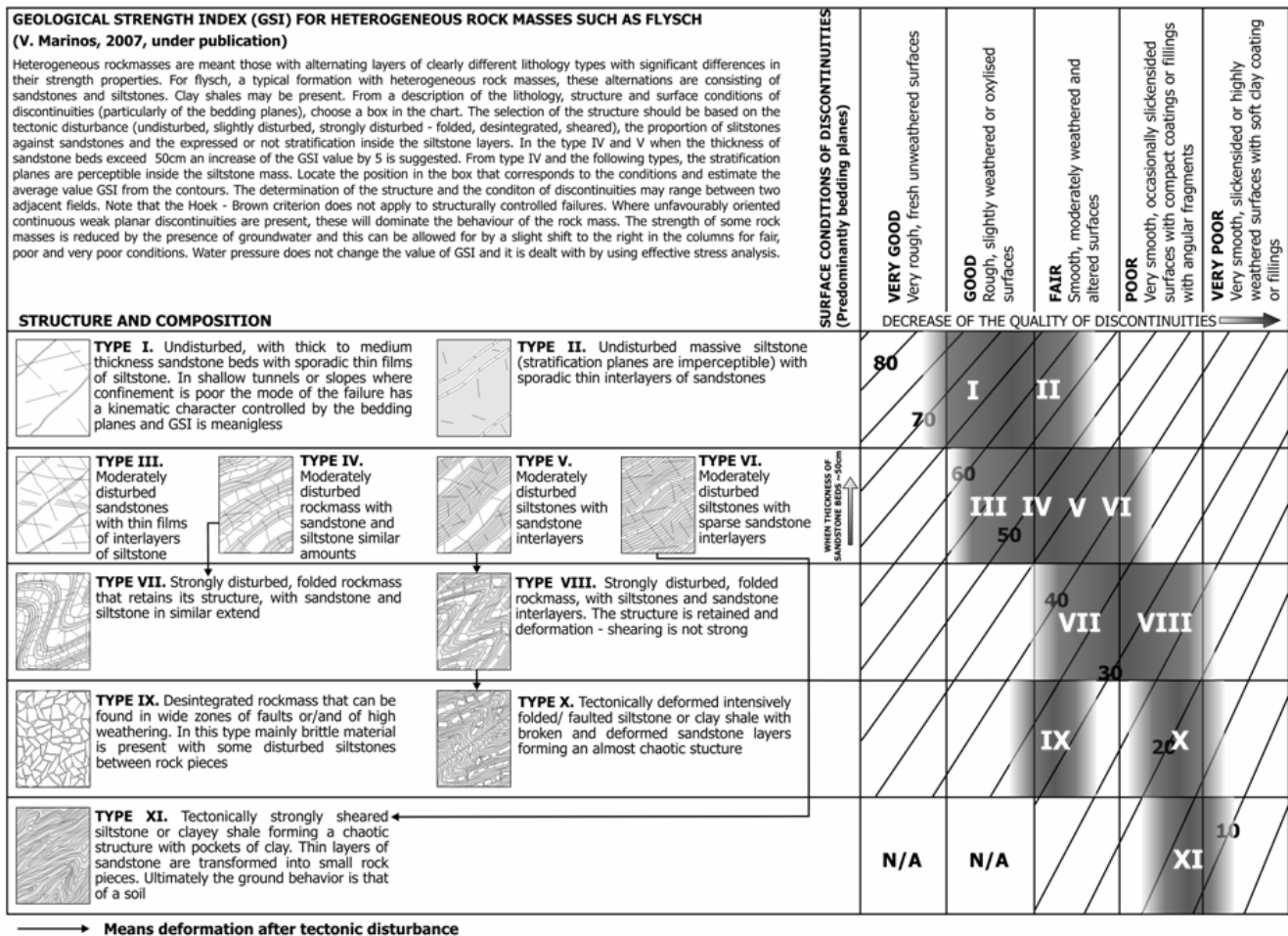


Figure 2.—Geological Strength Index for heterogeneous rocks such as flysch.

formation with tectonic disturbance, was published by Marinos and Hoek [2001]. This chart has recently been revised and is reproduced in Figure 2. This revision is based on recent experience from a number of tunnels constructed in Greece. It includes cases of siltstones with little disturbance and a variety of cases of siltstones alternating with good rock (e.g., sandstone).

For lithologically varied but tectonically undisturbed rock masses, such as the molasses, a new GSI chart was presented by Hoek et al. [2005] (Figure 3). For example, molasse consists of a series of tectonically undisturbed sediments of sandstones, conglomerates, siltstones, and marls produced by the erosion of mountain ranges after the final phase of an orogeny. The molasses behave quite differently from flysch, which has the same composition but was tectonically disturbed during the orogeny. They behave as continuous rock masses when they are confined at depth, and the bedding planes do not appear as clearly defined discontinuity surfaces. Close to the surface the layering of the formations is discernible, and only then similarities may exist with the structure of some types of flysch.

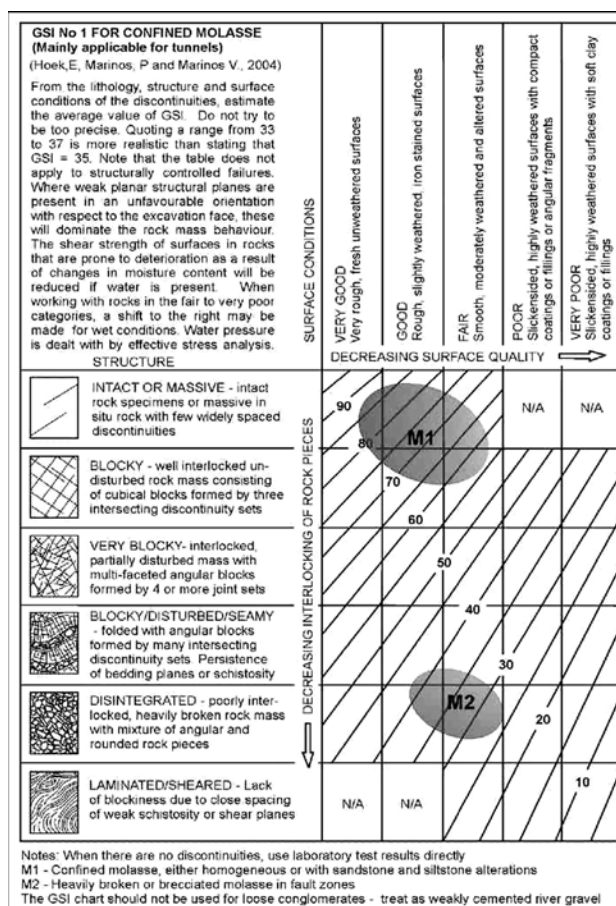
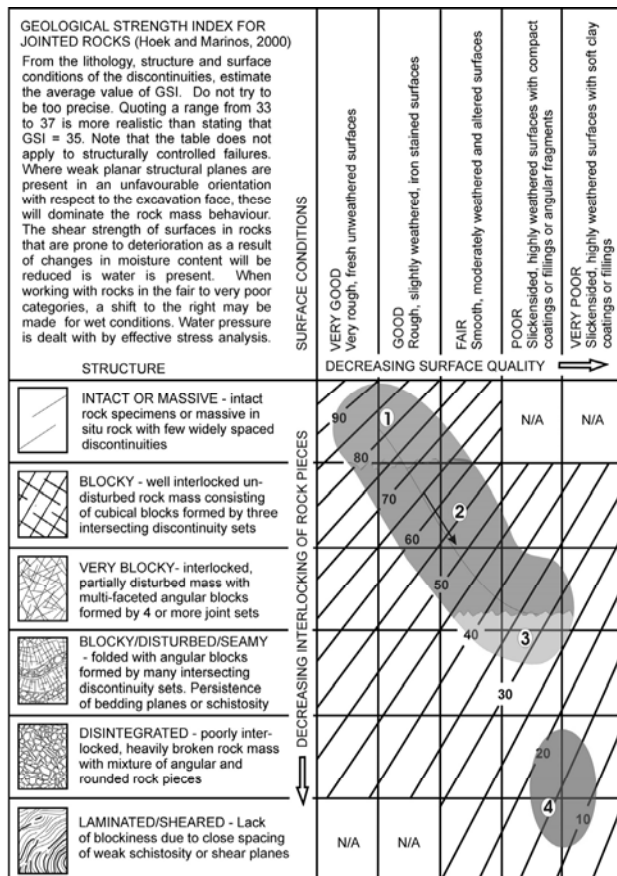


Figure 3.—Chart for confined molasse (mainly applicable for tunnels).

In design, the intact rock properties  $\sigma_{ci}$  and the  $m_i$  must also be considered. A “weighted average” of the properties of the strong and weak layers should be used.

Marinos et al. [2006] recently presented a quantitative description, using GSI, for rock masses within an ophiolitic complex. Included are types with large variability due to their range of petrographic types, their tectonic deformation, and their alternation (Figure 4). The structure of the various masses include types from massive strong to sheared weak, while the conditions of discontinuities are, in most cases, fair to very poor due to the fact that they are affected by serpentinization and shearing. This description allows the estimation of the range of properties and the understanding of the dramatic change in tunneling, from stable conditions to severe squeezing within the same formation at the same depth.



1. Massive strong peridotite with widely spaced discontinuities. The conditions of discontinuities are poorly only affected by serpentinisation
  2. Good to fair quality peridotite or compact serpentinite with discontinuities which may be severely affected from alteration.
  3. Schistose serpentinite. Schistosity may be more or less pronounced and their planes altered.
  4. Poor to very poor quality sheared serpentinite. The fragments are also consisting from weak materials
- Increase of presence of serpentines or other weak material (e.g talc) in joints or schistosity

Warning: The shaded areas indicate the ranges of GSI most likely to occur in these type of rocks. They may not be appropriate for a particular site specific case.

Figure 4.—Ranges of GSI for various qualities of peridotite-serpentinite rock masses in ophiolites.

## Rocks of Low Strength of Recent Age

When rocks such as marls, claystones, siltstones, and weak sandstones are developed in geologically stable conditions in a posttectonic environment, they usually present a simple structure with no or few discontinuities. When these rocks form continuous masses with no discontinuities, the rock mass can be treated as intact with engineering parameters given directly by laboratory testing. In such cases, the GSI classification is not applicable.

In cases where discontinuities are present, the use of the GSI chart for "blocky" or "massive" rock masses (Figure 1) may be applicable. The discontinuities in such weak rocks, although they are limited in number, cannot be better than "fair" (usually "fair" or "poor"); thus, the GSI values tend to be in the range of 45–65. In these cases, the low strength of the rock mass results from low intact strength  $\sigma_{ci}$ .

## PRECISION OF THE GSI CLASSIFICATION SYSTEM

The "qualitative" GSI system works well for engineering geologists since it is consistent with their experience in describing rocks and rock masses during logging and mapping. In some cases, engineers tend to be uncomfortable with the system because it does not contain parameters that can be measured in order to improve the precision of the estimated GSI value.

The authors do not share this concern, as they believe that it is not meaningful to attempt to assign a precise number to the GSI value for a typical rock mass. In all but the very simplest of cases, GSI is best described by assigning it a range of values. For analytical purposes, this range may be defined by a normal distribution with mean and standard deviation values assigned on the basis of common sense. GSI, with its qualitative principles of geological descriptions, is not restrained by the absence of good exposures or the limitations of quantitative core descriptions.

Although GSI is a totally independent system, in the earlier period of its application it was proposed that correlation of "adjusted" RMR and Q values with GSI be used for providing the necessary input for the Hoek-Brown criterion. Although this procedure may work with the better-quality rock masses, it is unreliable in the range of weak (e.g.,  $GSI < 35$ ), very weak, and heterogeneous rock masses, where these correlations are not recommended.

Whenever GSI is used, a direct assessment, based on the principles and charts presented above, is recommended. Fortunately, most GSI users have no difficulty in thinking of it as a totally independent system. However, in cases of comparisons or back analysis where other classification systems have been used, some kind of correlation with these other systems is needed. In such cases, it may be useful to consult the paper by Tzamos and Sofianos [in press]. The four classification-characterization systems

(RMR, Q, RMi [Palmström 1996], and GSI) were investigated, and all systems ratings are grouped in a common fabric index chart. The reader is reminded not to lose sight of the real geological world in considering such correlations.

## GSI AND CONTRACT DOCUMENTS

One of the most important contractual problems in rock construction and particularly in tunneling is the issue of "changed ground conditions." There are invariably arguments between the owner and the contractor on the nature of the ground specified in the contract and that actually encountered during construction. In order to overcome this problem, there has been a tendency to specify the anticipated conditions in terms of tunneling classifications. More recently, some contracts have used the GSI classification for this purpose, and the authors are strongly opposed to this trend.

As discussed earlier in this paper, GSI was developed solely for the purpose of estimating rock mass properties. Therefore, GSI is only one element in a tunnel design process and cannot be used, on its own, to specify tunneling conditions. It must be associated with the intact rock strength, the petrographic constant  $m_i$ , and all of the characteristics (such as anisotropy) of the rock mass that may impose a different mode of failure than that of a stressed homogeneous isotropic rock mass.

The use of any classification system to specify anticipated tunneling conditions is always a problem as these systems are open to a variety of interpretations, depending on the experience and level of conservatism of the observer. This can result in significant "changes" in excavation or support type and can have important financial consequences.

The geotechnical baseline report [Essex 1997] was introduced in an attempt to overcome some of the difficulties and has attracted an increasing amount of international attention in tunneling.

## CONCLUSIONS

Rock mass characterization has an important role, not only to define a conceptual model of the site geology, but also for the quantification needed for analyses "to ensure that the idealization (for modeling) does not misinterpret actuality" [Knill 2003]. If it is carried out in conjunction with numerical modeling, rock mass characterization presents the prospect of a far better understanding of the mechanics of rock mass behavior [Chandler et al. 2004]. The GSI system has considerable potential for use in rock engineering because it permits many characteristics of a rock mass to be quantified, thereby enhancing geological logic and reducing engineering uncertainty. Its use allows the influence of variables, which make up a rock mass, to be assessed and thus the behavior of rock masses to be explained more clearly. One of the advantages of the GSI is that the geological reasoning it embodies allows adjust-

ments of its ratings to cover a wide range of rock masses and conditions, but it also allows us to understand the limits of its application.

## ACKNOWLEDGMENTS

The paper is the result of a project cofunded by the European Social Fund (75%) and Greek National Resources (25%) – Operational Program for Educational and Vocational Training II (EPEAEK II) and particularly the Program PYTHAGORAS.

## REFERENCES

- Barton N, Lien R, Lunde J [1974]. Engineering classification of rock masses for the design of tunnel support. *Rock Mech* 6(4):189–236.
- Bierniawski ZT [1973]. Engineering classification of jointed rock masses. *Trans S Afr Inst Civ Eng* 15:335–344.
- Button E, Riedmueller G, Schubert W, Klima K, Medley E [2004]. Tunnelling in tectonic melanges: accommodating the impacts of geomechanical complexities and anisotropic rock mass fabrics. *Bull Eng Geol Env* 63:109–117.
- Cai M, Kaiser PK, Uno H, Tasaka Y, Minami M [2004]. Estimation of rock mass strength and deformation modulus of jointed hard rock masses using the GSI system. *Int J Rock Mech Min Sci* 41(1):3–19.
- Chandler RJ, de Freitas MH, Marinos P [2004]. Geotechnical characterization of soils and rocks: a geological perspective. In: Proceedings of the Advances in Geotechnical Engineering: The Skempton Conference. Vol 1. London: Thomas Telford, pp. 67–102.
- Diederichs MS, Kaiser PK, Eberhardt E [2004]. Damage initiation and propagation in hard rock during tunnelling and the influence of near-face stress rotation. *Int J Rock Mech Min Sci* 41(5):785–812.
- Essex RJ. [1997]. Geotechnical baseline reports for underground construction. Reston, VA: American Society of Civil Engineers.
- Hoek E [1994]. Strength of rock and rock masses. *News J ISRM* 2(2):4–16.
- Hoek E, Brown ET [1980]. Underground excavations in rock. London: Institution of Mining and Metallurgy.
- Hoek E, Brown ET [1997]. Practical estimates of rock mass strength. *Int J Rock Mech Min Sci Geomech Abstr* 34:1165–1186.
- Hoek E, Diederichs MS [2006]. Empirical estimation of rock mass modulus. *Int J Rock Mech Min Sci* 43:203–215.
- Hoek E, Karzulovic A [2000]. Rock mass properties for surface mines. In: Hustrulid WA, McCarter MK, van Zyl DJA, eds. Slope stability in surface mining. Littleton, CO: Society for Mining, Metallurgy, and Exploration, Inc., pp. 59–70.
- Hoek E, Marinos P [in press]. A brief history of the development of the Hoek-Brown failure criterion. *Int J Soils Rocks*.
- Hoek E, Caranza-Torres CT, Corkum B [2002]. Hoek-Brown failure criterion. In: Bawden HRW, Curran J, Telsenicki M, eds. Proceedings of the North American Rock Mechanics Society (NARMS-TAC), Mining Innovation and Technology (Toronto, Ontario, Canada), pp. 267–273.
- Hoek E, Kaiser PK, Bawden WF [1995]. Support of underground excavations in hard rock. Rotterdam, Netherlands: Balkema.
- Hoek E, Marinos P, Benissi M [1998]. Applicability of the geological strength index (GSI) classification for weak and sheared rock masses: the case of the Athens schist formation. *Bull Eng Geol Env* 57(2):151–160.
- Hoek E, Marinos P, Marinos V [2005]. Characterization and engineering properties of tectonically undisturbed but lithologically varied sedimentary rock masses under publication. *Int J Rock Mech Min Sci* 42:277–285.
- Hoek E, Wood D, Shah S [1992]. A modified Hoek-Brown criterion for jointed rock masses. In: Hudson JA, ed. Proceedings of the Rock Mechanics Symposium (Eurock '92). London: British Geotechnical Society, pp. 209–214.
- Knill J [2003]. Core values (first Hans-Closs lecture). *Bull Eng Geol Env* 62:1–34.
- Marinos P, Hoek E [2000]. GSI: a geologically friendly tool for rock mass strength estimation. In: Proceedings of GeoEng 2000 at the International Conference on Geotechnical and Geological Engineering (Melbourne, Victoria, Australia). Lancaster, PA: Technomic Publishers, pp. 1422–1446.
- Marinos P, Hoek E [2001]. Estimating the geotechnical properties of heterogeneous rock masses such as flysch. *Bull Eng Geol Env* 60:82–92.
- Marinos P, Hoek E, Marinos V [2006]. Variability of the engineering properties of rock masses quantified by the geological strength index: the case of ophiolites with special emphasis on tunnelling. *Bull Eng Geol Env* 65:129–142.
- Marinos V, Marinos P, Hoek E [2005]. The geological strength index: applications and limitations. *Bull Eng Geol Environ* 64:55–65.
- Palmström A [1996]. Characterizing rock masses by the RMI for use in practical rock engineering. Part 1: the development of the rock mass index (RMI). *Tunnelling Undergr Space Technol* 11(2):175–88.
- Rocscience, Inc. [2007]. RocLab v1.0: rock mass strength analysis using the generalized Hoek-Brown failure criterion. [<http://www.rocscience.com/products/RocLab.asp>]. Date accessed: April 2007.
- Sonmez H, Ulusay R [1999]. Modifications to the geological strength index (GSI) and their applicability to the stability of slopes. *Int J Rock Mech Min Sci* 36:743–760.
- Tzamos S, Sofianos AI [in press]. A correlation of four rock mass classification systems through their fabric indices. *Int J Rock Mech Min Sci*.

# DEVELOPMENT AND APPLICATION OF THE COAL MINE ROOF RATING (CMRR)

By Christopher Mark, Ph.D., P.E.,<sup>1</sup> and Gregory M. Molinda<sup>2</sup>

## ABSTRACT

The Coal Mine Roof Rating (CMRR) was developed 10 years ago to fill the gap between geologic characterization and engineering design. It combines many years of geologic studies in underground coal mines with worldwide experience with rock mass classification systems. Like other classification systems, the CMRR begins with the premise that the structural competence of mine roof rock is determined mainly by the discontinuities that weaken the rock fabric. However, the CMRR is specifically designed for bedded coal measure rock. Since its introduction, the CMRR has been incorporated into many aspects of mine planning, including longwall pillar design, roof support selection, feasibility studies, extended-cut evaluation, and others. It has also become truly international, with involvement in mine designs and funded research projects in South Africa, Canada, and Australia. This paper discusses the sources used in developing the CMRR, describes the CMRR data collection and calculation procedures, and briefly presents a number of practical mining applications in which the CMRR has played a prominent role.

## INTRODUCTION

Roof falls continue to be one of the greatest hazards faced by underground coal miners. In 2006, there were 7 fatalities from roof falls and nearly 500 rock fall injuries in the United States. In addition, more than 1,300 major roof collapses were reported to the Mine Safety and Health Administration. These roof falls can threaten miners, damage equipment, disrupt ventilation, and block critical emergency escape routes.

One reason roof falls have proven so difficult to eradicate is that mines are not built of manmade materials like steel or concrete, but rather of rock, just as nature made it. The structural integrity of a coal mine roof is greatly affected by natural weaknesses, including bedding planes, fractures, and small faults. The engineering properties of rock cannot be specified in advance with adequate precision and can vary widely from mine to mine and even within individual mines.

Engineers require quantitative data on the strength of rock masses for design. Traditional geologic reports contain valuable descriptive information, but few engineering properties. Laboratory tests, on the other hand, are inadequate because the strength of a small specimen is only indirectly related to the strength of the rock mass.

## ROCK MASS CLASSIFICATION

Rock mass classification schemes were developed to address these concerns. The most widely known systems, including Deere's Rock Quality Designation (RQD), Bieniawski's Rock Mass Rating (RMR), and Barton's Q-system, have been used extensively throughout the world [Deere and Miller 1966; Bieniawski 1973; Barton et al. 1974]. Rock mass classifications have been successful [Bieniawski 1988] because they—

- Provide a methodology for characterizing rock mass strength using simple measurements;
- Allow geologic information to be converted into quantitative engineering data;
- Enable better communication between geologists and engineers; and
- Make it possible to compare ground control experiences between sites, even when the geologic conditions are very different.

This last point highlights an extremely powerful application of rock mass classification systems, which is their use in empirical design methods. Empirical designs are based on mine experience—on the real-world successes and failures of actual ground control designs. By collecting a large number of case histories into a single database and subjecting them to statistical analysis, reliable and robust guidelines for design can be developed. A key advantage of empirical techniques is that it is not necessary to obtain a complete understanding of the mechanics to arrive at a reasonable solution. Rock mass classifications play an essential role in empirical design because they allow the overwhelming variety of geologic variables to be reduced to a single, meaningful, and repeatable parameter.

Unfortunately, the standard rock mass classification systems are not readily applicable to coal mining because—

- They tend to focus on the properties of joints, whereas bedding is generally the most significant discontinuity affecting coal mine roof.

<sup>1</sup>Principal research mining engineer.

<sup>2</sup>Research geologist.

Pittsburgh Research Laboratory, National Institute for Occupational Safety and Health, Pittsburgh, PA.

- They rate just one rock unit at a time, whereas coal mine roof often consists of several layers bound together by roof bolts.

In addition, the dimensions and stability requirements of tunnels are often very different from those of mines.

## COAL MINE GROUND CONTROL

The Coal Mine Roof Rating (CMRR) was developed more than 10 years ago to meet the needs of mine planners for a simple, repeatable, and meaningful classification system [Molinda and Mark 1994]. It employs the familiar format of Bieniawski's RMR, summing the individual ratings to obtain a final CMRR on a 0–100 scale. It is also designed so that the CMRR/unsupported span/standup time relationship is roughly comparable to the one determined for the RMR.

In determining the specific rock mass attributes and weightings to use, the CMRR built upon the rich vein of experience with coal mine ground control during the past 30 years. These sources can be divided into two groups. The first are papers describing specific geologic features, such as faults, clay veins, sandstone channels, kettle-bottoms, and others. A summary of this work was reported by Molinda [2003]. The second group, which includes efforts to generalize results for specific mines, regions, or countries, was more directly relevant to the development of the CMRR. In effect, these papers describe rock mass classification systems, although most are qualitative rather than quantitative. Table 1 provides a list of the coal mine roof classification systems consulted in the development of the CMRR, along with the significant geologic factors that they identified as being important to ground control. Following is a discussion of some of these factors and the issues involved with incorporating them into the CMRR.

**Bedding:** Bedding was the factor that was most consistently cited as causing roof problems in coal mines. The two most common examples were weak laminations in shale and thinly interbedded sandstone and shale (stackrock). In both examples, it is not just that the bedding planes are closely spaced, but also that the bedding surfaces are very weak. Indeed, several authors included “massive shale” as one of the more stable rock types [Moebs and Ferm 1982].

The issue of bedding (or grain alignment) is further complicated because some shales may appear massive, particularly to untrained eyes, but are actually highly laminated. The CMRR therefore emphasizes testing of the rock material to determine bedding plane strength even when the bedding is not visible. The approach is similar to that proposed by Buddery and Oldroyd [1992] and used successfully in South African coal mines.

**Strong Bed:** A problem unique to horizontally layered sedimentary rocks is that the roof structure often consists of several layers with different engineering characteristics. In developing the CMRR, two key questions had to be answered:

1. How far up into the roof should the evaluation extend?
2. How should the different layers be combined into a single rating? Should they be averaged together, or should the weakest or strongest layers be given precedence?

Few answers were available in the literature. Buddery and Oldroyd [1992] evaluated the first 2 m of roof, but weighted the layers nearest the roof line more heavily. Several authors seemed to imply that a weak layer can be very important by their emphasis on rider coal seams [Karmis and Kane 1984; Stingelin et al. 1979; Miller 1984].

The CMRR started with the insight that the *roof bolt length* largely determines the thickness of the mine roof structure. All coal mine roof in the United States must be bolted, and the bolts bind the different layers together. Generally, the layers above the bolts have much less influence than the units that are penetrated by the roof bolts.

Moreover, experience in many U.S. coalfields has clearly established that roof stability is greatly enhanced when the roof bolts anchor in a strong layer. This effect is most evident in the Illinois Basin, where roof falls are almost unknown when the bolts anchor in a limestone that is at least 0.6 m thick [Kester and Chugh 1980; Schaffer 1985; Damberger et al. 1980]. The strong bed effect has also been recognized in Alabama [Martin et al. 1988] and central Appalachia [Hylbert 1978]. Indeed, even the Code of Federal Regulations implies a strong bed effect when it states at 30 CFR 75.204(f)(1) that “roof bolts that provide support by suspending the roof from overlying stronger strata shall be long enough to anchor at least 12 inches into the stronger strata.”

**Moisture Sensitivity:** Moisture sensitivity is another factor that has been ignored by traditional rock mass classification systems, but is extremely important to coal mine ground control. Two roof shales may initially have very similar properties, but one may be essentially impermeous to moisture while the other completely disintegrates when exposed to groundwater or even humid mine air (Figure 1).

The presence of moisture-sensitive mudrocks may be just a nuisance, or it can severely damage the roof by reducing rock strength, generating swelling pressures, or compromising support effectiveness by causing sloughing around roof bolt plates. While the Slake Durability Test (SDT) has been widely used to evaluate moisture sensitivity [Hoek 1977], the CMRR employs a modified version of the simpler immersion test described by Sickler [1986].

**Table 1.—Rock mass classification systems for coal mines**

Author	Location	Rock strength	Bedding	Strong bed	Moisture sensitivity	Sandstone channels	Slickensides	Minor structures	No. of beds	Ground-water	Lineaments/ faults	Rider coals	Joints
Buddery and Oldroyd [1992]; Lattia et al. [2002] .....	South Africa	x			x								
Damberger et al. [1980] .....	Illinois Basin	x	x							x			
Ealy et al. [1979] .....	S. West Virginia	x									x		
Hylbert [1978] .....	E. Kentucky	x	x			x	x	x					
Karmis and Kane [1984] .....	Virginia	x				x		x			x		
Kester and Chugh [1980] .....	Illinois Basin	x	x			x				x			
Martin et al. [1988] .....	Alabama	x		x					x				
Milici et al. [1982] .....	Virginia	x				x		x			x		
Miller [1984] .....	Central Appalachia	x				x	x	x	x	x	x	x	
Moebs and Ferm [1982]; Ferm et al. [1978] .....	Virginia, S. West Virginia	x	x			x		x		x			
Moebs and Stateham [1985] .....	United States	x	x			x	x	x	x	x			
Newman and Bieniawski [1986] .....	United States	x	x			x		x	x	x		x	
Schaffer [1985] .....	Illinois Basin							x					
Sinha and Venkateswarlu [1986]; Venkateswarlu et al. [1989] .....	India	x	x			x	x	x	x	x	x		
Stingelin et al. [1979] .....	N. Appalachia	x							x			x	
Zhou et al. [1988] .....	United States	x	x	x				x	x	x	x	x	
Coal Mine Roof Rating (CMRR) .....	United States	x	x	x		x	x	x	x	x	x	x	x



**Figure 1.—Effect of water on a moisture-sensitive shale.**

**Slickensides and Other Discontinuities:** While bedding is generally the most significant weakness in the fabric of coal measure rocks, often some other type of discontinuity is present. Slickensides, which are small-scale (<2-m) fault surfaces of highly aligned clay minerals distinguished by glassy, grooved surfaces, are frequently cited as greatly reducing the competence of coal measure mudrocks (for example, see Moebs and Stateham [1985]). Jointing is encountered in Virginia [Karmis and Kane 1984] and occasionally elsewhere. In sandstones, coal spars and crossbeds can be significant. The original RMR rates only the most significant discontinuity set and largely ignores the others. The CMRR contains a “multiple discontinuity adjustment” so that the weakening effects of slickensides and other discontinuities can be explicitly included.

**Large-scale Features:** Large-scale features include sandstone channel margins, lineaments, faults, and some medium-scale features such as seam rolls and clay veins. These types of features are not included directly in the CMRR, although in some cases one CMRR value can be determined for “typical conditions” and another for “fracture zones” or “sandstone channel margin areas,” and these can then be plotted on hazard maps. However, the CMRR is not designed to rate conditions impacted by a major throughgoing discontinuity such as a fault. Such features normally require specially designed support systems.

#### DATA COLLECTION AND CALCULATION OF THE CMRR

The data required for the CMRR can be determined either from underground exposures, such as roof falls and overcasts, or from exploratory drill core. In either case, the main parameters measured are the—

- *Uniaxial compressive strength (UCS)* of the intact rock;
- *Intensity (spacing and persistence)* of bedding and other discontinuities;
- *Shear strength (cohesion and roughness)* of bedding and other discontinuities;
- *Moisture sensitivity* of the rock; and
- Presence of a *strong bed* in the bolted interval.

Other secondary factors include the *number of layers*, the presence of *groundwater*, and *surcharge* from overlying weak beds.

The CMRR is calculated in a two-step process. First, the mine roof is divided into *structural units*, and Unit Ratings are determined for each. A structural unit generally contains one lithologic layer, but several rock layers may be lumped together if their engineering properties are similar. In the second step, the CMRR is determined by averaging all the Unit Ratings within the bolted interval (with the contribution of each unit weighted by its thickness) and applying appropriate adjustment factors. This second step is the same regardless of whether the Unit Ratings were from data collected underground or from core. Figure 2 illustrates the process.

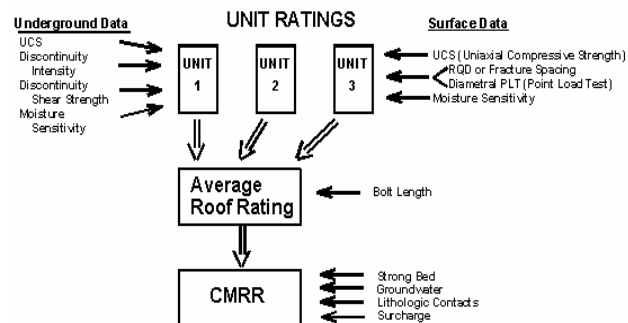


**Figure 2.—Flowchart for the CMRR.**

The procedures for gathering data and calculating the CMRR from underground exposures have remained essentially unchanged since they were first proposed in 1993. The underground data sheet is shown in Figure 3. Procedures to determine Unit Ratings from drill core have now been streamlined and updated based on new research [Mark et al. 2002]. Calculating the CMRR has been greatly simplified by the development of a CMRR computer program that can be obtained free of charge.

The sections below discuss each of the input parameters used in the CMRR.

CMRR

LOCATION DATE MINE PAGE OF CMRR

NAME \_\_\_\_\_  
TYPE OF EXPOSURE \_\_\_\_\_

DISCONTINUITÉS  
LINIEN

**Figure 3.—Underground data sheet for the CMRR.**

## Uniaxial Compressive Strength (UCS)

The UCS of the rock material influences roof strength in several ways. First, it determines the ease with which new fracturing (as opposed to movement along preexisting discontinuities) will take place. Second, the compressive strength of the rock is a factor in the shear strength of discontinuities. Approximately one-third of the CMRR is determined by the compressive strength rating, which is approximately twice the weight given to the UCS in the original RMR.

Laboratory testing is generally considered the standard method of determining the UCS. Unfortunately, laboratory tests are expensive because the samples must be carefully prepared. The variability in the results is also high, with the standard deviation typically about one-third of the mean for coal measure rocks [Rusnak and Mark 2000].

As an alternative, the CMRR recommends the point load test (PLT) for drill core. The PLT has been accepted in geotechnical practice for nearly 30 years [Hoek 1977]. An advantage of the PLT is that numerous tests can be performed because the procedures are simple and inexpensive. The apparatus is also inexpensive and portable. The International Society for Rock Mechanics has developed standard procedures for testing and data reduction [ISRM 1985].

Another advantage of the PLT is that both *diametral* and *axial* tests can be performed on core. In a diametral test, the load is applied parallel to bedding (Figure 4). The diametral test is therefore an indirect measure of the lateral strength, or bedding plane shear strength, and is further discussed later.

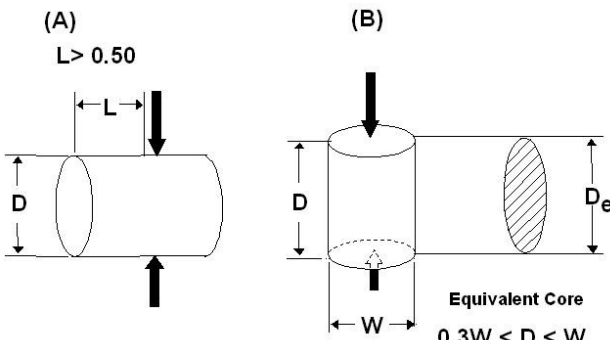


Figure 4.—Diametral and axial point load tests.

When the axial PLT is used to estimate the UCS, the Point Load Index ( $Is_{50}$ ) is converted using the following equation:

$$UCS = K (Is_{50}) \quad (1)$$

where  $K$  is the conversion factor. A comprehensive study involving more than 10,000 tests of coal measure rocks from six states [Rusnak and Mark 2000] found that  $K=21$

fit the data well for the entire range of rock types and geographic regions (Figure 5). The study also found that the variability of the PLT measurements, as measured by the standard deviation, was no greater than for UCS tests. The UCS rating scale used in the CMRR program is shown in Figure 6.

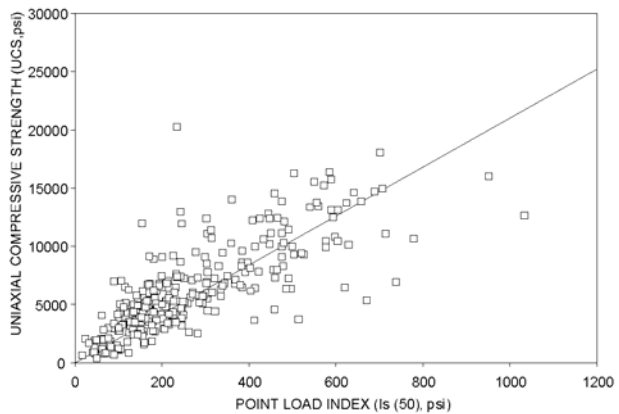


Figure 5.—Relationship between axial PLT and UCS test for shale (Rusnak and Mark [2000]).

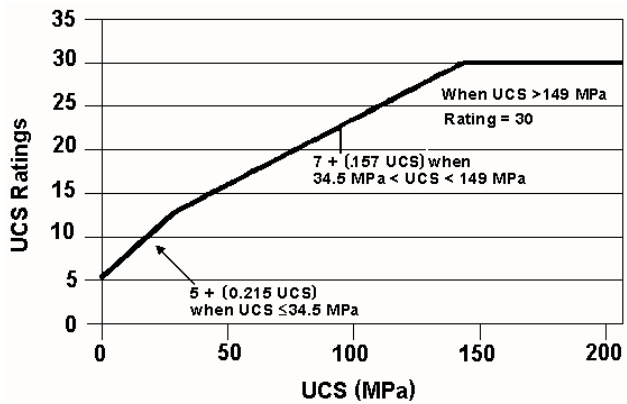


Figure 6.—CMRR rating scale for UCS tests.

Underground, the CMRR employs an indentation test proposed by Williamson [1984] to estimate UCS. The exposed rock face is struck with the round end of a ball peen hammer, and the resulting characteristic impact reaction is compared to the drawings shown on the left side of Figure 3. It is the *nature* of the reaction (indentation), not its magnitude, that is important.

A study was conducted to compare the UCS ratings derived from the Ball Peen Test with the PLT. In 17 of the 23 sites studied (or 74% of the cases), the difference between the two measurements was 4 points or less (Figure 7). The analysis resulted in slight changes to the Williamson rock strength classes, as shown in Table 2.

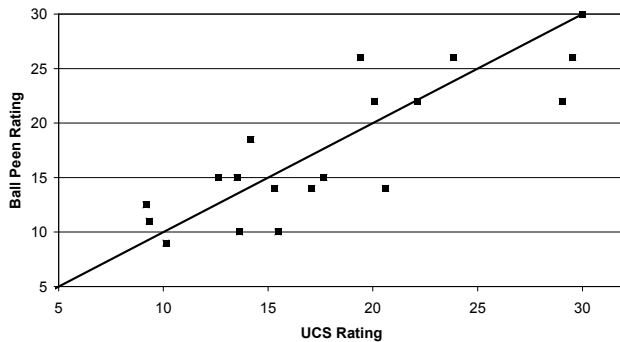


Figure 7.—Comparison between UCS and Ball Peen Tests.

Table 2.—Approximate UCS ranges from Ball Peen Hammer Tests

Ball peen hammer class	Williamson UCS range (MPa)	CMRR UCS range (MPa)	CMRR rating
Molds .....	<7	<14	5
Craters .....	7–21	14–35	10
Dents .....	21–56	35–70	15
Pits .....	56–105	70–120	22
Rebounds .....	>105	>120	30

### Discontinuity Intensity

Intensity is determined by the *spacing* between bedding planes or other discontinuities and the *persistence*, or extent, of each individual discontinuity. The more closely spaced a set of discontinuities, the greater the weakening effect on the rock mass. Persistence is more important for discontinuities that are widely spaced. Like UCS, intensity accounts for about one-third of the total CMRR.

Underground, both spacing and persistence can be measured directly using the standard methods for rock mass characterization [ISRM 1982]. Table 3 shows the Bedding/Discontinuity Rating Scale for underground data. The matrix shows what point value is added for each combination of spacing and persistence of discontinuities.

Table 3.—Bedding/discontinuity intensity rating table for underground data

Persistence	Spacing				
	>1.8 m	0.6–1.8 m	0.2–0.6 m	60–200 mm	<60 mm
0–1 m .....	35	30	24	17	9
1–3 m .....	32	27	21	15	9
>1 m .....	30	25	20	13	9

Most standard geotechnical core logging procedures include some measure of the natural breaks in the core. The two most commonly employed are the *fracture spacing* and the *RQD*. Fracture spacing is easily determined by counting the core breaks in a particular unit and

then dividing by the thickness of the unit. The RQD is obtained by dividing combined length of core pieces that are greater than 4 in long by the full length of the core run.

Both measures have their advocates in the geotechnical community. Priest and Hudson [1976] suggested that the two can be related by the following formula:

$$RQD = 100 e^{-0.1L} (0.1L+1) \quad (2)$$

where L = number of discontinuities per meter.

As input, the CMRR uses either the RQD or the fracture spacing. When the fracture spacing is greater than about 1 ft, the RQD is not very sensitive, so the fracture spacing is used directly. At the other extreme, when the core is highly broken or lost, the RQD seems to be the better measure. Either measure may be used in the intermediate range.

The program uses the equations shown in Figure 8 to calculate the Discontinuity Spacing Rating (DSR) of core from RQD or the fracture spacing. The equations were derived from the original CMRR rating tables. The minimum value of the DSR is 20; the maximum is 48 (see Figure 8).

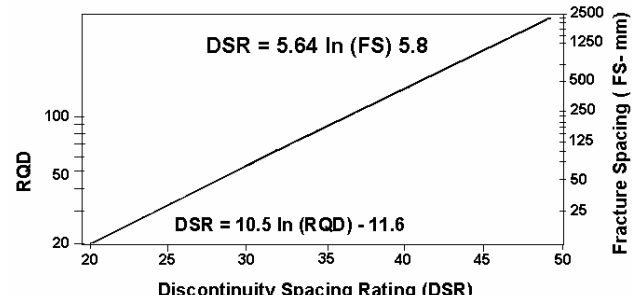


Figure 8.—CMRR rating scale for fracture spacing or RQD.

### Shear Strength of Discontinuities

Bedding plane shear strength is a critical parameter for coal mine ground control because the most severe loading applied to coal mine roof is normally lateral, caused by horizontal stress [Mark and Barczak 2000]. Molinda and Mark [1996] found that the lateral strength of some shales are just one-sixth of their axial strength.

Underground, the cohesion of bedding surfaces is evaluated by using a 9-cm mason chisel and a hammer to split hand samples of rock. Weaker, less cohesive surfaces require fewer chisel blows to split (see Figure 3). Cohesion can also be estimated by observing the nature of the fractured wall of a roof fall. If the wall "stairsteps," with most of the roof failure occurring along bedding, then the cohesion is probably low. On the other hand, if most of the

failure surfaces cut across bedding, then the strength of the bedding is most likely equal to or greater than that of the intact rock. Slickensided surfaces are already planes of failure and receive the minimum rating.

The roughness along a discontinuity surface is the other component of the surface's shear strength. In the CMRR, roughness of a surface is estimated visually and classified as *jagged*, *wavy*, or *planar*, using the system proposed by Barton et al. [1974]. This measure is to be applied on a scale that ranges from hand sample size to several feet across a fall exposure. The CMRR assumes that roughness significantly affects shear strength only when cohesion is in the middle range (see Table 4).

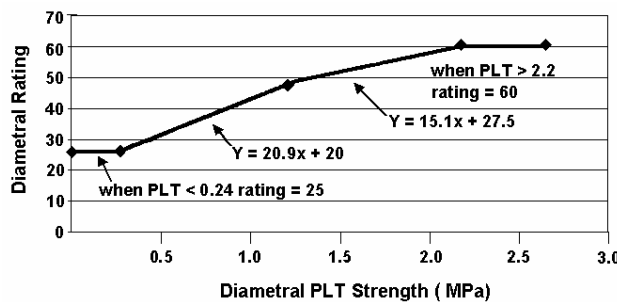


Figure 9.—CMRR rating scale for diametral point load tests.

Table 4.—Bedding/discontinuity shear strength rating table for underground data<sup>1</sup>

Roughness	COHESION			
	Strong	Moderate	Weak	Slickensided
Jagged .....	35	29	24	10
Wavy .....	35	27	20	10
Planar.....	35	25	16	10

<sup>1</sup>If unit has no bedding/discontinuities, then apply test to the intact rock.

When drill core is available, strength testing can be conducted. The diametral PLT is a convenient index test that provides a substitute for bedding plane shear testing. Because the precise relationship between bedding plane shear strength and the PLT is not known, and since it seems unlikely that the same K-factor used to convert the axial test to the UCS would apply, the CMRR uses the Point Load Index ( $IS_{50}$ ) directly. The diametral PLT rating values were derived from the original CMRR tables and the data presented by Molinda and Mark [1996] and are shown in Figure 9.

If the diametral test results show that the rock fabric or laminations are low-strength, it would be illogical to give the rock high marks for discontinuity spacing. In fact, both the fracture spacing and the RQD also actually measure the strength of discontinuities as well as their spacing, because strong discontinuities might withstand the rigors of the

IMMERSION TEST			
Mine: _____ Date: _____			
Unit No.: _____ Tester: _____			
Sample Description (Lithology, bedding, etc.): _____			
<b>Immersion</b>		<b>Breakability</b>	
<u>Observation</u> Appearance of Water	<u>Rating</u>	<u>Observation</u>	<u>Rating</u>
Clear = 0 Misty = -1 Cloudy = -3	_____	No Change 0 Small Change -2 Large Change -6	_____
Talus Formation	<i>Breakability Index</i> _____		
None = 0 Minor = -1 Major = -3	_____		
Cracking of Sample			
None = 0 Minor/Random = -1 Major/Preferred Orientation = -3 Specimen Breakdown = -9	_____		
<i>Total Immersion Index</i> _____			
<b>Procedure for Immersion Test</b>			
<ol style="list-style-type: none"> <li>Select sample(s) ~ hand sized</li> <li>Test for hand breakability.</li> <li>Rinse specimen (to remove surface dirt, dust, etc.)</li> <li>Immerse in water for 1 hour</li> <li>Observe and rate water appearance, talus formation, and cracking of sample</li> <li>Sum Rating for Immersion Index.</li> <li>Retest for hand breakability.</li> <li>Determine Breakability Index</li> <li>The final Immersion Test Index is the greater of the Breakability Index or the Immersion Index.</li> </ol>			

Figure 10.—Data sheet for the Immersion Test.

drilling process while weak ones break apart. Therefore, the *discontinuity rating* is the *lower* of the Diametral PLT Rating or the Discontinuity Spacing Rating.

### Moisture Sensitivity Deduction

In the CMRR, the maximum deduction for moisture sensitivity is 15 points. The data sheet for the Immersion Test is shown in Figure 10. If Immersion Test results are not available, moisture sensitivity can sometimes be estimated visually in underground exposures.

Usually, some time is required for contact with humid mine air to affect rock strength. In short-term applications, therefore, it may not be appropriate to apply the moisture sensitivity deduction. The CMRR program reports both the Unit Rating and the CMRR *with* and *without* the moisture sensitivity deduction.

Research was conducted to explore the relationship between the Slake Durability Test (SDT) and the Immersion Test. In the SDT, 10 lumps of rock, each weighing about 0.1 lb, are oven-dried, weighed, and then rotated through a water bath for 10 min. The repeated wetting and drying, together with the mild abrasion that takes place during the test, causes moisture-sensitive rocks to break down. The Slake Durability Index is the final dry weight of the sample expressed as a percentage of the original dry weight [Hoek 1977].

To compare the two tests, rock samples were collected underground from a variety of mine settings, carefully wrapped to maintain in situ moisture content, and tested in the laboratory. A total of 96 tests were run on 16 distinct rock types from 9 mines. The results are shown in Figure 11. From the testing conducted to date, there is a good correlation between the two tests for the “not sensitive” and “slightly sensitive” classes. The correlation is less reliable for distinguishing “moderately sensitive” rocks from “severely sensitive” rocks. Table 5 indicates how the results from either test can be used for input to the CMRR.

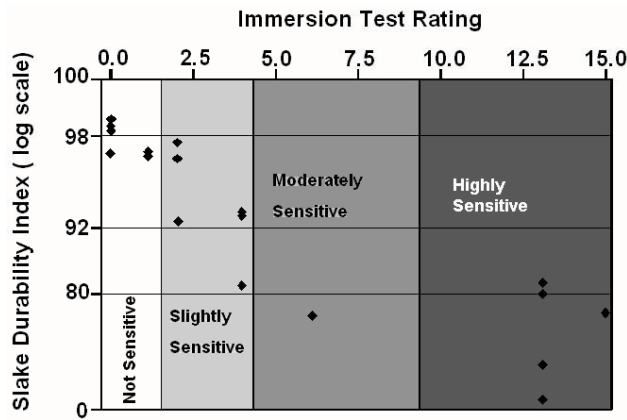


**Figure 11.—Comparison of the Stake Durability and Immersion Tests.**

**Table 5.—Moisture sensitivity classes and ratings from both Immersion and Stake Durability Tests<sup>1</sup>**

Moisture sensitivity class	Rating adjustment	Immersion Index	Stake Durability Index
Not sensitive.....	0	0–1	100–98
Slightly sensitive.....	-3	2–4	98–92
Moderately sensitive..	-7	5–9	92–80
Severely sensitive.....	-15	>9	<80

<sup>1</sup>Apply rating adjustment to Unit Rating only when unit forms the immediate roof or if water is leaking through the bolted interval.

### Calculation of the Unit Rating

When using underground data, the equation for calculating the Unit Rating is—

$$\begin{aligned} \text{Unit Rating} = & \text{UCS Rating} + \text{Discontinuity Intensity} \\ & \text{Rating} + \text{Discontinuity Shear Strength Rating} \\ & + \text{Multiple Discontinuity Adjustment} \\ & + \text{Moisture Sensitivity Deduction} \end{aligned}$$

For drill core data, the equation is even simpler:

$$\begin{aligned} \text{Unit Rating} = & \text{UCS Rating} + \text{Discontinuity Rating} \\ & + \text{Moisture Sensitivity Deduction} \end{aligned}$$

### Thickness-weighted Average Roof Rating

The next step in calculating the CMRR is to determine the thickness-weighted average of the Unit Ratings of all the units within the bolted interval. For example, assume that the roof consists of three units (from top down):

- 2-m sandstone, Unit Rating = 60
- 0.8-m siltstone, Unit Rating = 50
- 0.4-m shale, Unit Rating = 40

If the length of the roof bolts is 1.8 m, then the thickness-weighted average (RRW) is:

$$\text{RRW} = \frac{[(0.4 * 40) + (0.8 * 50) + (0.6 * 60)]}{1.8} = 51.1 \quad (3)$$

Note that even though the uppermost layer was 2 m thick, only the lowest 0.4 m (the distance to the top of the bolts) was used in the calculation.

The CMRR is now determined by applying several adjustment factors to the RRW.

### Strong Bed Adjustment (SBADJ)

One of the most important concepts in the CMRR is that the strongest bed within the bolted interval often determines the performance of mine roof. The strong bed's effect on the CMRR depends first upon how much stronger it is than the other units. Second, the strong bed must be at least 0.3 m thick before it can provide any additional support, and the amount of the adjustment is maximum when the bed is at least 1.2 m thick. Third, the roof bolts must obtain at least 0.3 m of anchorage in the strong bed for the adjustment to be considered. Finally, the higher into the roof that the strong bed is located, the less its positive effect will be.

In the original CMRR, the SBADJ was determined using a table. For improved accuracy and to facilitate implementation of the table in the computer program, Equation 4 was derived using multiple regression:

$$\text{SBADJ} = [(0.72 \text{ SBD} * \text{THSB}) - 2.5] * [1 - (0.33 (\text{THWR} - 0.5))] \quad (4)$$

where:

- SBD is the strong bed difference—the difference between the strong bed's Unit Rating and the thickness-weighted average of all the Unit Ratings within the bolted interval;
- THSB is the thickness of the strong bed (m); and

- THWR is the thickness of the weak rock suspended from the strong bed (m).

Note that if the strong bed is at the top of the bolted interval, its *full thickness* is used in the calculation of the SBADJ (up to a maximum of 1.2 m).

### Other Adjustments

**Number of Units:** Many workers have indicated that mine roof that contains numerous lithologic contacts is less competent than roof that consists of a single rock type [Karmis and Kane 1984; Kester and Chugh 1980]. When depositional processes change and deposit distinctly different material, there is generally, but not always, a sharp contact between units. Since gradational contacts do not weaken the roof, the characteristics of major bedding contact surfaces (cohesion and roughness) should be noted. The maximum deduction from the CMRR is 5 points when more than four weak contacts are present.

**Groundwater Adjustment:** Groundwater is most prevalent in shallow mines, particularly beneath stream valleys, but it can also be introduced by leakage from pooled water in abandoned mines or fracturing of overlying aquifers during high-extraction mining. The CMRR maintains the RMR system's rating scale, with a maximum deduction for flowing groundwater of 10 points.

**Surcharge:** The strength of rocks overlying the bolted interval is considered only when they are significantly weaker than the rocks within it. An example is a western mine where 1.2 m of relatively strong top coal was overlain by 6 m of weak, rooted claystone. Because the roof beam needed to carry some of the surcharge (extra weight) of the incompetent claystone, stability was reduced. The CMRR accounts for the surcharge with a 3-point deduction.

### THE CMRR COMPUTER PROGRAM

The CMRR program is designed to facilitate the entry, storage, and processing of field data. Either core or underground data can be entered, and calculations are updated instantly when a change is made. This allows the user to vary parameters, such as the bolt length, to see their effect on the final CMRR.

The underground data entry screen contains drop-down menus that are used to enter the data for each of the parameters. In the core data screen, the user has the option of entering PLT test data and having the program automatically determine the mean UCS and diametral  $I_{50}$ . Otherwise, the user can enter the mean strength values directly.

An important feature of the new program is a built-in interface with AutoCAD. Data from up to 200 locations can be entered and saved in a single file, along with their geographic location coordinates. The program can create a

file for export that includes both the calculated CMRR values and the locations. A CMRR layer can then be created in AutoCAD for use in mine planning.

### APPLICATIONS OF THE CMRR

During the past 10 years, the CMRR has been used extensively in the United States. Figure 12 shows the current database, containing 264 observations from more than 200 mines. The figure reveals some very important regional trends. Weak roof predominates in the northern Appalachian and Illinois Basin coalfields, which are also areas where roof falls tend to occur more frequently [Pappas and Mark 2003]. Central Appalachian mines have a wide range of CMRR values, but the typical roof is of moderate strength. Utah mines tend to have the most competent roof in the United States.

A number of mine planning design tools based on the CMRR are discussed below.

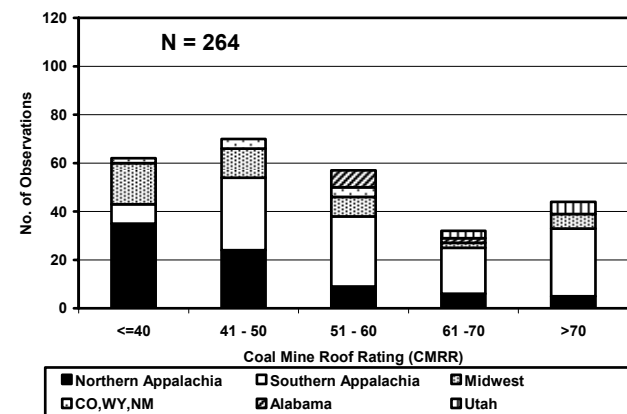


Figure 12.—Current CMRR database.

### Analysis of Longwall Pillar Stability (ALPS)

The first, and perhaps the best known, application of the CMRR is the ALPS pillar design method [Mark et al. 1994]. A large database of longwall case histories was collected from throughout the United States and subjected to statistical analysis. The results showed that when the roof was strong ( $CMRR>65$ ), longwall chain pillars with an ALPS stability factor (SF) as low as 0.7 could provide satisfactory tailgate conditions (Figure 13). On the other hand, when the roof was weak ( $CMRR<45$ ), the ALPS SF might need to be as high as 1.3. ALPS has been the standard technique employed to size pillars for most U.S. longwalls for many years.

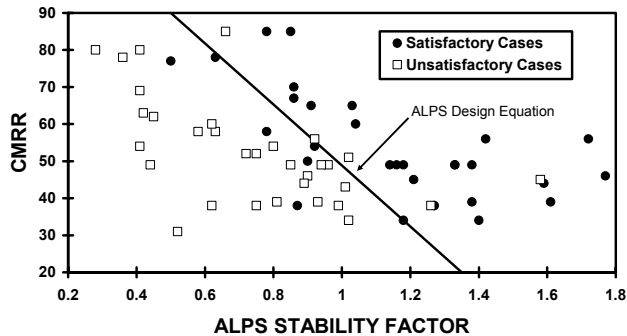


Figure 13.—Relationship between the CMRR and the ALPS SF.

### Longwall Tailgate Design (Australia)

ALPS was the starting point for a project under the Australian Coal Association Research Program (ACARP) to develop an Australian chain pillar design methodology [Colwell et al. 1999]. The project aimed to calibrate ALPS for the different geotechnical and mine layouts used in Australia. Ultimately, case history data were collected from 60% of Australian longwall mines.

The study found strong relationships between the CMRR, the tailgate SF, and the installed level of primary support. Design equations were developed that reflected these trends. The final product, called the Analysis of Longwall Tailgate Serviceability (ALTS), was implemented in a computer program and has become widely used in Australia. Most recently, an expanded study resulted in an updated version called ALTS II [Colwell et al. 2003].

### Stability of Extended Cuts

Place change mining, in which mining equipment moves from entry to entry as the section is advanced, is the standard development method in the United States. The traditional 6-m cut length was determined by the distance from the cutting head to the operator's compartment. With the advent of remote-control continuous miners, extended cuts up to 12 m long have become common. However, many mines with extended-cut permits only take them when conditions allow. Where the roof is competent, extended cuts are routine. At the other extreme, when the roof is very poor, miners may not be able to complete a traditional 6-m cut before the roof collapses.

To help predict when conditions might be suitable for extended cuts, a study was conducted at 36 mines throughout the United States. The study found that when the CMRR was greater than 55, extended cuts were nearly always routine, but when the CMRR was less than 37, they were almost never taken [Mark 1999a]. The data also

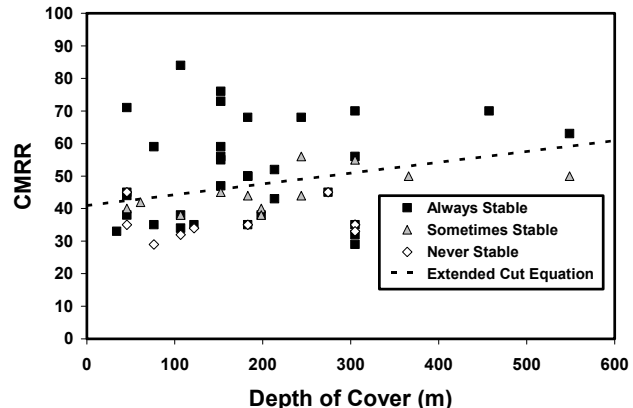


Figure 14.—Relationship between the CMRR and the feasibility of extended cuts.

showed that extended cuts were less likely to be feasible as the roof span or the depth of cover increased (Figure 14).

### Roof Bolt Selection

To help develop scientific guidelines for selecting roof bolt systems, the National Institute for Occupational Safety and Health conducted a study of roof fall rates at 37 U.S. mines [Mark et al. 2001; Molinda et al. 2000]. The study evaluated five different roof bolt variables, including length, tension, grout length, capacity, and pattern. Roof spans and the CMRR were also measured. Performance was measured in terms of the number of roof falls that occurred per 3 km of drivage.

The study found that the depth of cover (which correlates with stress) and the roof quality (measured by the CMRR) were the most important parameters in determining roof bolting requirements. Intersection span was also critical. The study's findings led to guidelines that can be used to select the proper span, bolt lengths, and bolt capacity based on the CMRR. The results have been implemented into a computer program called Analysis of Roof Bolt Systems (ARBS).

### Multiple-seam Mining

Interactions with previous mining in underlying or overlying seams are a major cause of ground instability in the United States. A statistical analysis of a database of more than 360 case histories found that the CMRR was highly significant in predicting the outcome of a multiseam interaction. Other significant variables include the pillar SF, the total pillar stress, whether the previous seam was above or below, and what type of pillar structure is present in the previous seam.

The statistical analysis became the foundation for the Analysis of Multiple-seam Stability (AMSS) software package. The output from AMSS is the critical interburden thickness that is necessary to avoid interactions. AMSS

indicates that, all else being equal, a CMRR=45 roof requires approximately 15 m more interburden than a CMRR=65 roof.

### Longwall Mining Through Open Entries and Recovery Rooms

Unusual circumstances may require that a longwall retreat into or through a previously driven room. The operation is usually completed successfully, but there have been a number of spectacular failures. To help determine which factors contribute to such failures, an international database of 131 case histories was compiled [Oyler et al. 1998]. The study found that the CMRR and the density of standing support were the two most important parameters in predicting severe weighting-type failures. These failures occurred only when the CMRR was less than 55 and when the support density was less than 0.5 MPa. When the CMRR was 40 or less, all of the successful cases employed a standing support density of at least 1.0 MPa.

### Roof Fall Evaluations (South Africa)

The CMRR featured prominently in an important research project sponsored by the Safety in Mines Research Advisory Committee (SIMRAC) and other leading industry, labor, and government organizations in South Africa. The goal of the project was to investigate the causes of fatal roof failures in South African coal mines. A team of recognized experts visited a broad spectrum of mines and collected data at 182 roof fall sites. The study found that roof falls were more likely where the roof was less competent in terms of the CMRR. Another finding was that the CMRR correlated well with roadway widths. Based on data presented by Mark [1999b] (see Figure 15), the study also concluded that “in South African coal mines, less support is used for comparable roof conditions than either the USA or Australia. This supports previous conclusions that in South African coal mines, the density of supports needs to be increased.” [van der Merwe 2001].

Another SIMRAC study found the CMRR easy to use and robust enough to adequately describe the roof conditions at most South African collieries [Butcher 2001]. It took less than 4 hr for a trained geologist to become competent with the method. The results seemed more reasonable than those obtained from the RMR, which tended to overrate ground conditions by at least one class (20 points) due to its lack of sensitivity to the characteristics of bedded strata. Some improvements were suggested for the CMRR, including adjustments for joint orientation, blasting, and horizontal stress.

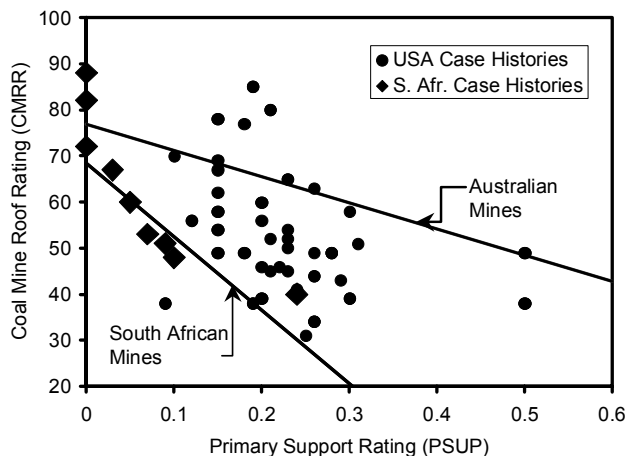


Figure 15.—Relationship between the CMRR and roof bolt density in the United States, Australia, and South Africa.

### Baseline Comparison of Ground Conditions (Canada)

The Canadian underground coal industry is small and geographically dispersed. To assist the mines in maintaining world-class safety standards, the Canada Centre for Mineral and Energy Technology (CANMET) established the Underground Coal Mine Safety Research Consortium. One of the consortium's first projects was aimed at establishing a “best practice” baseline for conducting geological and geomechanical assessments and applying the findings to geotechnical design.

The CMRR was found to be particularly valuable in the assessment [Forgeron et al. 2001]. It allowed the Canadian underground mines to be compared with each other and with international benchmarks. Based on the CMRR, many ground control safety technologies developed in the United States were found to have direct application to Canadian mines.

### Other Applications

- *Highwall mining* can become uneconomic if the roof is so weak that it collapses before the miner has been withdrawn from the hole. The CMRR has been used to evaluate potential highwall mining reserves and to identify potentially unsuitable areas [Hoelle 2003].
- *Tailgate support guidelines* incorporating the CMRR have been included in the Support Technology Optimization Program (STOP) [Barczak 2000].
- *Input for numerical models* have been derived from the CMRR [Karabin and Evanto 1999].

## CONCLUSIONS

Roof geology is central to almost every aspect of ground control. The CMRR makes it possible to quantify roof geology so that it can be included in mine planning decisions. Worldwide experience has shown that the CMRR is a reliable, meaningful, and repeatable measure of roof quality.

A wide variety of design tools based on the CMRR have now been developed. They address a broad range of ground control issues and rely upon large databases of actual mining case histories. Without the CMRR, it would not have been possible to capture this invaluable experience base.

The new core procedures and computer program further expand the potential of the CMRR. It is now possible to routinely collect CMRR data during geologic exploration or from underground mapping, complete the calculations, and integrate the results into mine mapping software. Foreknowledge of conditions means better mine planning and fewer unexpected hazards underground.

## REFERENCES

- Barczak TM [2000]. Optimizing secondary roof support with the NIOSH support technology optimization program (STOP). In: Mark C, Dolinar DR, Tuchman RJ, Barczak TM, Signer SP, Wopat PF, eds. Proceedings: New technology for coal mine roof support. Pittsburgh, PA: U.S. Department of Health and Human Services, Public Health Service, Centers for Disease Control and Prevention, National Institute for Occupational Safety and Health, DHHS (NIOSH) Publication No. 2000-151, IC 9453, pp. 151–163.
- Barton N, Lien R, Lunde J [1974]. Engineering classification of rock masses for the design of tunnel support. *Rock Mech* 6(4):189–236.
- Bieniawski ZT [1973]. Engineering classification of jointed rock masses. *Trans S Afr Inst Civ Eng* 15:335–344.
- Bieniawski ZT [1988]. Rock mass classification as a design aid in tunnelling. *Tunnels and Tunnelling* 29:19–23.
- Buddery PS, Oldroyd DC [1992]. Development of a roof and floor classification applicable to collieries. In: *Proceedings of the Eurock '92 Conference*. London: Thomas Telford, pp. 197–202.
- Butcher RJ [2001]. Application of the coal mine roof rating system in South African collieries. In: Peng SS, Mark C, Khair AW, eds. *Proceedings of the 20th International Conference on Ground Control in Mining*. Morgantown, WV: West Virginia University, pp. 317–321.
- Colwell M, Frith R, Hill D [2003]. ALTS II: a long-wall gateroad design methodology for Australian collieries. In: *Proceedings of the First Australasian Ground Control in Mining Conference* (Sydney, New South Wales, Australia), pp. 123–135.
- Colwell M, Frith RC, Mark C [1999]. Calibration of the Analysis of Longwall Pillar Stability (ALPS) chain pillar design methodology for Australian conditions. In: Peng SS, Mark C, eds. *Proceedings of the 18th International Conference on Ground Control in Mining*. Morgantown, WV: West Virginia University, pp. 282–290.
- Damberger HH, Nelson WJ, Krausse HF [1980]. Effect of geology on roof stability in room-and-pillar mines in the Herrin (No. 6) coal of Illinois. In: *Proceedings of the First Conference Ground Control Problems in the Illinois Coal Basin*. Carbondale, IL: University of Southern Illinois, pp. 14–32.
- Deere DU, Miller RP [1966]. Engineering classification and index properties for intact rock. Technical report No. AFWL-TR-65-116, Air Force Weapons Laboratory, Kirtland Air Force Base, New Mexico.
- Ealy DL, Mazurak RD, Langrand EL [1979]. A geological approach for predicting unstable roof and floor conditions in advance of mining. *Min Congr J Mar*:7-23.
- Ferm JC, Melton RA, Cummins GD, Mathew D, McKenna L, Muir C, et al. [1978]. A study of roof falls in underground mines on the Pocahontas #3 seam, southern West Virginia and southwestern Virginia. University of South Carolina. U.S. Bureau of Mines contract No. H0230028. NTIS No. PB 80-158983.
- Forgeron S, Mark C, Forrester DJ [2001]. Standardisation of geological and geomechanical assessment at underground coal mines in Canada. *CIM Bull July*:83–90.
- Hoek E [1977]. Rock mechanics laboratory testing in the context of a consulting engineering organization. *Intl J Rock Mech Min Sci* 22:93–101.
- Hoelle J [2003]. Analysis of unsupported roof spans for highwall mining at Moura coal mine. In: Aziz N, Kininmonth B, eds. *Proceedings of the Fourth Underground Coal Operators' Conference*. Carlton, Victoria, Australia: Australian Institute of Mining and Metallurgy, pp. 50–62.
- Hylbert DK [1978]. The classification, evaluation, and projection of coal mine roof rocks. *Min Eng* 30:1667–1676.
- ISRM [1982]. *Suggested methods for rock characterization, testing, and monitoring*. London: Pergamon Press.
- ISRM [1985]. *Suggested method for determining the point load strength (revised version)*. *Intl J Rock Mech Min Sci* 22:51–60.
- Karabin GJ, Evanto MA [1999]. Experience with the boundary-element method of numerical modeling to resolve complex ground control problems. In: Mark C, Heasley KA, Iannacchione AT, Tuchman RJ, eds. *Proceedings of the Second International Workshop on Coal Pillar Mechanics and Design*. Pittsburgh, PA: U.S. Department of Health and Human Services, Public Health Service, Centers for Disease Control and Prevention, National Institute for Occupational Safety and Health, DHHS (NIOSH) Publication No. 99-114, IC 9448, pp. 89–113.

- Karmis M, Kane W [1984]. An analysis of the geo-mechanical factors influencing coal mine roof stability in Appalachia. In: Proceedings of the Second International Conference on Stability in Underground Mining (Lexington, KY), pp. 311–328.
- Kester WM, Chugh YP [1980]. Premining investigations and their use in planning ground control in the Illinois coal basin. In: Proceedings of the First Conference Ground Control Problems in the Illinois Coal Basin. Carbondale, IL: University of Southern Illinois, pp. 33–43.
- Lattila JW, van Wijk JJ, Wevill E, Neal D [2002]. Evaluation of the impact splitting technique used for predicting geotechnical conditions in underground coal mines. In: Proceedings of the South African National Institute of Rock Engineering (SANIRE) Symposium.
- Mark C [1999a]. Application of coal mine roof rating (CMRR) to extended cuts. *Min Eng* 51(4):52–56.
- Mark C [1999b]. The state of the art in coal pillar design. SME preprint 99–86. Littleton, CO: Society for Mining, Metallurgy, and Exploration, Inc.
- Mark C, Barczak TM [2000]. Fundamentals of coal mine roof support. In: Mark C, Dolinar DR, Tuchman RJ, Barczak TM, Signer SP, Wopat PF, eds. Proceedings: New technology for coal mine roof support. Pittsburgh, PA: U.S. Department of Health and Human Services, Public Health Service, Centers for Disease Control and Prevention, National Institute for Occupational Safety and Health, DHHS (NIOSH) Publication No. 2000–151, IC 9453, pp. 23–42.
- Mark C, Chase FE, Molinda GM [1994]. Design of longwall gate entry systems using roof classification. In: Mark C, Tuchman RJ, Repsher RC, Simon CL, eds. New Technology for Longwall Ground Control; Proceedings: U.S. Bureau of Mines Technology Transfer Seminar. Pittsburgh, PA: U.S. Department of the Interior, Bureau of Mines, SP 01–94, pp. 5–17.
- Mark C, Molinda GM, Barton TM [2002]. New developments with the coal mine roof rating. In: Peng SS, Mark C, Khair AW, Heasley KA, eds. Proceedings of the 21st International Conference on Ground Control in Mining. Morgantown, WV: West Virginia University, pp. 294–301.
- Mark C, Molinda GM, Dolinar DR [2001]. Analysis of roof bolt systems. In: Peng SS, Mark C, Khair AW, eds. Proceedings of the 20th International Conference on Ground Control in Mining. Morgantown, WV: West Virginia University, pp. 218–225.
- Martin EM, Carr F, Hendon G [1988]. Strata control advances at Jim Walter Resources. In: Peng SS, ed. Proceedings of the Seventh International Conference on Ground Control in Mining. Morgantown, WV: University of West Virginia, pp. 66–75.
- Milici RC, Gathright TM, Miller BW, Gwin MR [1982]. Geologic factors related to coal mine roof falls in Wise County, Virginia. Appalachian Regional Commission, contract No. CO–7232–80–I–302–0206.
- Miller MS [1984]. Composite geologic and linear mapping for defining safe, high productivity mining in the Appalachian coal fields. In: Proceedings of the 15th Annual Institute of Coal Mining, Health, Safety, and Research (Blacksburg, VA), pp. 1–10.
- Moebs NN, Ferm JC [1982]. The relation of geology to mine roof conditions in the Pocahontas No. 3 coalbed. Pittsburgh, PA: U.S. Department of the Interior, Bureau of Mines, IC 8864. NTIS No. PB 83–125294.
- Moebs NN, Stateham RM [1985]. The diagnosis and reduction of mine roof failure. *Coal Min* 22(2):52–55.
- Molinda GM [2003]. Geologic hazards and roof stability in coal mines. Pittsburgh, PA: U.S. Department of Health and Human Services, Public Health Service, Centers for Disease Control and Prevention, National Institute for Occupational Safety and Health, DHHS (NIOSH) Publication No. 2003–152, IC 9466.
- Molinda G, Mark C [1994]. Coal mine roof rating (CMRR): a practical rock mass classification for coal mines. Pittsburgh, PA: U.S. Department of the Interior, Bureau of Mines, IC 9387.
- Molinda GM, Mark C [1996]. Rating the strength of coal mine roof rocks. Pittsburgh, PA: U.S. Department of the Interior, Bureau of Mines, IC 9444. NTIS No. PB96–155072.
- Molinda GM, Mark C, Dolinar DR [2000]. Assessing coal mine roof stability through roof fall analysis. In: Mark C, Dolinar DR, Tuchman RJ, Barczak TM, Signer SP, Wopat PF, eds. Proceedings: New technology for coal mine roof support. Pittsburgh, PA: U.S. Department of Health and Human Services, Public Health Service, Centers for Disease Control and Prevention, National Institute for Occupational Safety and Health, DHHS (NIOSH) Publication No. 2000–151, IC 9453, pp. 53–71.
- Newman DA, Bieniawski ZT [1986]. Modified version of the geomechanics classification for entry design in underground coal mines. Trans SME, Vol. 280. Littleton, CO: Society for Mining, Metallurgy, and Exploration, Inc., pp. 2134–2138.
- Oyler DC, Frith R, Dolinar D, Mark C [1998]. International experience with longwall mining into predriven rooms. In: Peng SS, ed. Proceedings of the 17th International Conference on Ground Control in Mining. Morgantown, WV: University of West Virginia, pp. 44–53.
- Pappas DM, Mark C [2003]. Profile of groundfall incidents in underground coal mines. *Min Eng* 55(9):65–71.
- Priest SD, Hudson JA [1976]. Discontinuity spacings in rock. *Int J Rock Mech Min Sci* 13:135–148.
- Rusnak J, Mark C [2000]. Using the point load test to determine the uniaxial compressive strength of coal measure rock. In: Peng SS, Mark C, eds. Proceedings of the 19th International Conference on Ground Control in Mining. Morgantown, WV: West Virginia University, pp. 362–371.

- Schaffer JF [1985]. Roof fall prediction at an Illinois underground mine. In: Proceedings of the First Conference Ground Control Problems in the Illinois Coal Basin. Carbondale, IL: University of Southern Illinois, pp. 55–63.
- Sickler RA [1986]. Engineering classification of shales. In: Proceedings of the Fifth International Conference on Ground Control in Mining. Morgantown, WV: West Virginia University, pp. 221–233.
- Sinha A, Venkateswarlu V [1986]. Geomechanics classification for support selection in Indian coal mines: case studies. In: Proceedings of the Fifth International Congress of the International Association of Engineering Geology. Vol. 1, pp. 159–164.
- Stingelin RW, Kern JR, Morgan SL [1979]. Premining identification of hazards associated with coal mine roof measures. HRB-Singer, Inc. U.S. Bureau of Mines contract No. J0177038. NTIS No. PB 82–140344.
- van der Merwe JN [2001]. In situ investigation into the causes of falls of roof in South African collieries. In: Peng SS, Mark C, Khair AW, eds. Proceedings of the 20th International Conference on Ground Control in Mining. Morgantown, WV: West Virginia University, pp. 105–118.
- Venkateswarlu V, Ghose AK, Raju NM [1989]. Rock mass classification for design of roof supports: a statistical evaluation of parameters. *Min Sci Technol* 8:97–107.
- Williamson DA [1984]. Unified rock classification system. *Bull Assn Eng Geol* 21:345–354.
- Zhou Y, Haycocks C, Wu W [1988]. Geomechanics classifications for multiple-seam mining. SME preprint 88–11. Littleton, CO: Society for Mining, Metallurgy, and Exploration, Inc.



# PROBLEMS WITH ROCK CLASSIFICATION FOR EMPIRICAL AND NUMERICAL DESIGN

By Douglas Milne, Ph.D.<sup>1</sup>

## ABSTRACT

Most empirical and numerical approaches to design in rock mechanics incorporate rock mass classification. Numerical design methods generally use classification values to calculate input parameters for stress-based failure criteria. Empirical methods use classification to allow comparisons between similar rock mass conditions, generally based on a graphical design technique that differentiates stable and failed opening geometries.

Classification systems are the best tool available for assessing rock mass properties; however, there are problems with classification systems that should be highlighted. Rock mass performance can only be realistically estimated by coupling a unique description of the rock mass with known loading conditions. Current classification systems cannot provide a unique classification value. The weightings applied to quantify rock mass properties for classification can result in significantly different rock masses having the same classification values. These weightings have been proven effective for tunnel design and support, but classification systems are now used for many more applications.

Rock classification systems evolved from a quick and easy field tool for estimating tunnel stability and support requirements. The need for a rapid field tool means that rock mass classification is relatively insensitive to improved methods of measuring rock mass properties.

Problems with classification systems and their application are highlighted in this paper. These problems must be recognized and documented before improvements can be made. An understanding of the evolution of classification systems and their application for both numerical and empirical design approaches is invaluable in highlighting current shortcomings.

## INTRODUCTION

Rock mass classification systems are the basic component of empirical mine design. They have been traditionally used to group areas of similar rock mass properties, to provide guidelines for stability performance, and to estimate support requirements. More recently, rock

mass classification values have been used along with numerical modeling tools. Substantial work has been done linking classification values to various material properties such as Young's modulus, as well as "m" and "s" for Hoek-Brown failure criteria and " $\phi$ " and "c" for Mohr-Coulomb criteria. These values are then used as input for numerical models.

There are many rock mass classification schemes, often developed for site-specific purposes. The most commonly used systems are the Rock Quality Designation (RQD) [Deere et al. 1967], forms of the Rock Mass Rating (RMR) system developed by Bieniawski [1973, 1976, 1979, 1989], and the Norwegian Geotechnical Institute's Q-system [Barton et al. 1974]. The RQD system is a measure of joint spacing and is incorporated as part of both the Q and RMR systems. More recently, the Geological Strength Index (GSI), which has evolved from the RMR system, is being used [Hoek et al. 1995]. The Q, RMR, and GSI systems are discussed in this paper.

There are problems and challenges with rock mass classification systems, primarily due to their numerous and conflicting goals. Initially, classification was done to give a quick and repeatable assessment of the rock mass to provide guidelines for underground opening stability and support requirements. It was made quick and easy to use by limiting the number of rock mass classification categories. A need for greater precision in the estimation of opening stability and support led to an increase in possible classification categories, resulting in increased time needed for classification and increased difficulty in obtaining repeatable results. An additional challenge for rock mass classification is the goal of providing an accurate assessment of rock mass behavior and properties for an increasing array of engineering applications. These include:

- Tunnel and mine opening stability assessments
- Tunnel and mine opening support requirements
- Rock mass properties, including Young's modulus, Poisson's ratio, and strength
- Rock mass failure criteria
- Rock mass slope stability, as well as other varied applications

This paper summarizes some of these issues and suggests approaches for improving the application of field data for rock mechanics.

<sup>1</sup>Associate professor of geological engineering, University of Saskatchewan, Saskatoon, Canada.

## ROCK CLASSIFICATION VERSUS CHARACTERIZATION

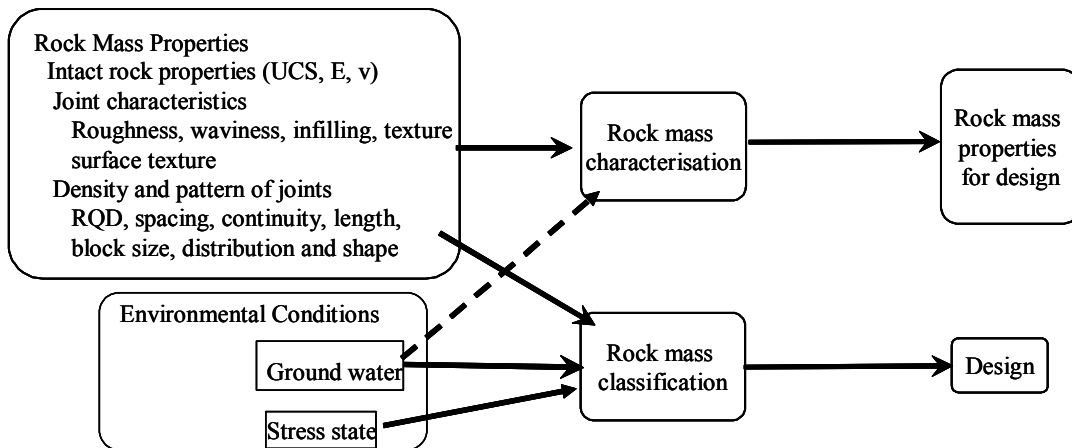
Rock classification is used for many purposes in rock mechanics. Classification systems were originally developed as complete design packages for civil engineering tunnel applications. Given the rock mass classification value and tunnel span, support requirements and estimated tunnel stability could be obtained [Barton et al. 1974; Bieniawski 1976]. These classification systems often included factors to assess stress conditions and the orientation of discontinuities relative to the engineered structure. One of the main differences between tunneling and mining applications of rock classification is the large variation in orientation, depth, and geometry of underground openings in mining. Civil engineering applications are generally applied to tunnels at a fairly constant depth, orientation, and geometry. None of these conditions is constant in most mining applications.

If mining applications included joint orientation and stress conditions in rock classification, the same rock mass could have dozens of classification values throughout the mine depending on the drift orientation, mining level, and the excavation history [Milne et al. 1998]. This would lead to significant confusion and make the classification systems useless. Components of classification systems are often used in empirical mine design applications, with site-specific or stress conditions assessed separately. Numerical design methods also often apply stress conditions with the design process, so the addition of stress factors within the classification system is redundant. Both the RMR and Q classification systems are frequently adjusted for mining applications. The Q' system is used in numerous empirical design techniques and differs from the Q-system in that the stress reduction factor (SRF) is set to 1.0 [Potvin 1988; Clark 1998]. RMR' system is often used for mining span

design. The RMR' system does not include the RMR correction for joint orientation.

Palmström et al. [2001] discuss the difference between rock classification and characterization. Rock mass characterization should consist of the intrinsic properties of the rock mass, which include intact rock properties, discontinuity spacing and pattern, as well as discontinuity properties. If rock characterization is used, loading or environmental factors such as stress or discontinuity orientation should be considered later in the design process. Rock classification systems, however, should be treated as complete design packages and are to be used with the appropriate empirical design charts (Figure 1).

There has been some discussion concerning the assessment of groundwater factors in rock mass classification and characterization. Palmström et al. [2001] suggested that groundwater be excluded from rock mass characterization and added later in the design process since water conditions can vary significantly in the same rock mass. Laubscher and Taylor [1976] incorporated water as a factor, reducing the strength properties on the discontinuity surfaces in their modified RMR system (MRMR). There is also some confusion as to the application of water conditions with the stability graph design method for underground openings [Potvin 1988]. Hoek et al. [1995] state the following concerning the application of Q' for the stability graph method: "The system has not been applied in conditions with significant groundwater, so the joint water reduction factor  $J_w$  is commonly 1.0." The groundwater term in the Q' classification is often ignored when using the stability graph design method. This is not a safe approach because there is nowhere else to assess groundwater conditions in this design method. Similar confusion exists with determining "m" and "s" failure criteria for design [Hoek and Brown 1980]. The original "m" and "s" factors were based on  $RMR_{76}$  classification values, with



<sup>1</sup>Discrete features such as faults and shears are not generally assessed in rock classification schemes.

<sup>2</sup>Ground water has been considered either a rock mass property or an environmental or loading condition.

Figure 1.—Components of rock classification and rock characterization (after Milne and Hadjigeorgiou [2000] and Cai et al. [2004]).

the groundwater factor set to dry conditions [Hoek et al. 1995]. This was done to avoid counting groundwater conditions twice. It assumes that effective stress conditions will be used with numerical modeling “m” and “s” design approaches.

Groundwater conditions are not intrinsic properties of the rock mass and, ideally, groundwater would be assessed later in the design process. Unfortunately, there are few empirical or numerical design techniques that allow groundwater conditions to be added to the design process. It is not safe to remove groundwater from rock mass characterization unless it is known that the groundwater conditions will be assessed later in the design process. As a general rule, any factors known to influence stability should be included in either the rock characterization or the design process.

### QUALITATIVE VERSUS QUANTITATIVE ROCK MASS CHARACTERIZATION

One of the goals of classification systems is that they be a quick assessment of rock mass conditions for support design and stability assessment. A second goal of rock classification is to obtain repeatable results. The repeatability of rock classification can be achieved by assessing the rock mass in very broad, general categories at the cost of precision or by assessing the parameters that make up rock classification systems with quantitative measurements at the cost of speed and ease of use.

One of the earliest rock mass classification systems is attributed to Terzaghi [1946], who states: “From an engineering point of view, knowledge of the type and intensity of the rock defects may be much more important than the type of rock which will be encountered.” Terzaghi’s classification uses terms such as “moderately blocky and seamy” to describe the rock mass and is difficult to assess accurately due to its subjective description of the rock mass. This system was probably easy to use. There were, however, only seven categories of rock masses ranging from intact rock to swelling rock containing clays such as montmorillonite, so it could not be an overly precise assessment of ground conditions.

Modern classification systems, such as the Q and variations of the RMR systems, consist of assessments of the size and perhaps shape of intact blocks of rock bounded by discontinuities, the discontinuity surface condition or frictional properties, intact rock strength, and groundwater conditions.

The method of assessment of these categories has evolved from the mainly subjective assessment of factors in Terzaghi’s classification to more qualitative assessments. The RMR system is based on a numerical assessment of five parameters:

- Intact rock unconfined compressive strength (UCS)
- Rock Quality Designation (RQD)
- Discontinuity spacing
- Discontinuity surface condition and
- Groundwater

Intact rock strength, RQD, and groundwater are assessed in fairly quantitative terms. The discontinuity assessment term is more subjective and contains descriptions such as “very rough surfaces” and “slightly rough surfaces,” which require experience to differentiate between and do not provide a very precise assessment.

The Q classification system is probably the least subjective classification currently in common use. The more analytical and quantitative descriptions used in the Q-system are coupled with an assessment of more rock mass parameters, and these assessments are divided into many more categories. For instance, the RMR<sub>76</sub> system describes the condition of discontinuities with five broad categories. The Q-system, with its assessment of small- and large-scale roughness, alteration, and infilling can differentiate between more than 60 conditions of joint surfaces. The Q-system can give very precise rock classification values; however, this results in making repeatability more difficult to achieve and also increases the time required to obtain an estimate of rock classification.

The RMR system has evolved to give the user the option of estimating rock classification values with more precision. The RMR<sub>89</sub> system is the best example. It allows the user to use the same five categories assessing discontinuity surface conditions, but adds the option of describing joint surface conditions with five properties for assessment, which are:

- Discontinuity length;
- Discontinuity aperture or separation;
- Discontinuity roughness;
- Discontinuity infilling; and
- Discontinuity weathering

Each of these 5 properties is broken down into 5 categories, giving a total of 25 possible joint surface assessments, compared to 60 categories in the Q-system and 5 with RMR<sub>76</sub>.

The GSI system is the newest commonly used rock mass classification system. It makes a conscious attempt to move away from classification systems that quantify or rate individual properties of the rock mass. The RMR classification system has evolved to be more quantifiable [Bieniawski 1989], and others have attempted to improve rock mass characterization by improving our ability to measure rock mass properties such as discontinuity surface properties [Milne et al. 1991; Hadjigeorgiou et al. 1994] and intact block size distributions [Hadjigeorgiou et al. 1998]. In his discussion of the development of the GSI

classification system, Hoek [2004] states: "It was also felt that a system based more heavily on fundamental geological observations and less on 'numbers' was needed." The GSI classification system consists of six categories describing the size and shape of intact rock blocks and five categories describing the surface condition of discontinuities. This system is based on geological observations and avoids the engineering approach of dividing the properties of a rock mass into components and measuring these components as accurately as possible.

The GSI system has been developed to provide rock mass properties for numerical modeling, which may account for the different approach taken for assessing the rock mass. Practitioners are encouraged to avoid precise estimates of classification, but rather to give a range representative of the highly variable properties found in natural materials such as rock masses. This approach is also well suited to numerical modeling, where more precise estimates of rock mass properties may rely on back analysis of observed rock mass behavior.

The following section discusses input for classification systems.

## **INPUT PROPERTIES FOR ROCK MASS CHARACTERIZATION**

Goals of conventional classification systems include quickly obtaining as precise and repeatable an estimate of rock characterization values as possible. These goals are, to a certain extent, contradictory. Increased precision is difficult to duplicate, especially by different practitioners. An approach taken with some systems has been to break the properties of a rock mass into more easily quantified components, which improves the precision and repeatability, but may significantly increase time required to conduct rock characterization. A discussion of the more common components of rock mass characterization follows.

### **Intact Rock Strength**

Intact rock strength is included in all versions of the RMR system. It is an intrinsic part of rock mass characterization; however, in many systems like Q' and GSI, the rock strength assessment is left for the design process.

### **Groundwater Conditions**

Groundwater conditions are part of most classification systems, such as Q, Q', and RMR. If groundwater is not implicitly included in the design, it must be included in the rock mass classification/characterization. The conventional characterization systems assign a weighting to groundwater conditions based on categories such as—

- Dry conditions;
- Damp conditions;
- Water inflow in liters per minute along 10 m of drift; or
- A description or measurement of water pressure.

These descriptions of groundwater conditions seem sufficiently precise and easily quantified for rock characterization purposes. The GSI system does not include water in its basic classification, so it should be treated later as a correction or assessed in the design procedure used.

### **Discontinuity Spacing and Intact Geometry**

The rock mass RQD is used in both the RMR and Q classification systems to assess discontinuity spacing. The actual spacing of discontinuities is included with RMR, and Q looks at the number of joint sets present. The RQD assessment of spacing has significant drawbacks [Milne et al. 1998]. It is sensitive to the measuring direction; however, this can be corrected by using the equation by Palmström [1985] that relates the number of joints found in a cubic meter of rock ( $J_v$ ) to an average RQD:

$$RQD = 115 - 3.3 J_v \quad (1)$$

Other problems with the RQD term include the fact that it is relatively insensitive to discontinuity spacings greater than 30 cm. The RMR system corrects for this by adding a measurement of discontinuity spacing. The Q-system couples RQD with an assessment of the number of joint sets present ( $J_n$ ). It can easily be shown, however, that if three joint sets with equal spacing are present in a rock mass, the ratio of  $RQD/J_n$  becomes a constant at a joint spacing of greater than 0.7 m.

The assessment of joint spacing in classification systems is an attempt to indirectly define block size. Line mapping provides much of the data required for rock mass characterization and can provide realistic estimates of intact block size geometry. There is little justification for discarding much of the data collected by mapping programs simply because the data cannot be applied to currently used rock classification systems. Mapping data can generate realistic three-dimensional discontinuity systems, which can be used to develop more complete information, such as block size distribution, that better represent the discontinuous nature of a rock mass. Based on field work in several underground mines, Hadjigeorgiou et al. [1998] have shown that three-dimensional joint systems can provide a better estimate of block size than that provided by traditional rock classification systems. Figure 2 shows a correlation between RQD, block size, and the  $J_v$  term.

The actual geometry of intact blocks is not included in these systems; however, it is discussed in the GSI system, and other rock mass characterization systems, such as RMi

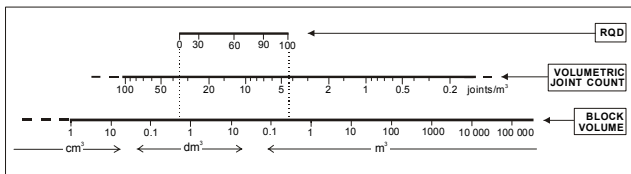


**Figure 2.—Correlation between RQD, block size, and the joint volume term,  $J_v$ .**

[rockmass.net 2007], include an assessment of intact block geometry.

## DISCONTINUITY SURFACE CONDITION

The surface condition of discontinuities is a measure of how easily blocks can move relative to each other and is an important component of rock characterization. The Q-system has one of the most precise approaches for assessing this property and looks at it in terms of the following:

- Large-scale roughness
- Small-scale roughness
- Alteration
- Infilling thickness

The  $RMR_{89}$  system adds terms describing infilling aperture and length. There is some difficulty assessing the Q terms for roughness and alteration, and guidelines have been developed to assist with this.

The following discussion is taken from Milne and Hadjigeorgiou [2000] and Milne et al. [1992]. In the  $RMR$  system, joint roughness is part of the discontinuity description, with no distinction between small- and large-scale roughness. The Q-system identifies two scales of joint roughness as distinct input into  $J_r$ . No qualitative methods of assessing roughness are included with the original classification methods; however, less subjective approaches have been applied to classification.

A study was conducted to improve the precision and repeatability possible for estimating values of joint roughness for the Q classification system. An extensive field data-gathering program was conducted to obtain discontinuity profiles using a 1-m-long “profile comb” (Figure 3) [Milne et al. 1991]. Based on the collection of more than 200 1-m-long discontinuity profiles from 10 mines across Canada, a simple repeatable field-measuring technique has been developed. The joint roughness coefficient (JRC) [Barton and Choubey 1977], coupled with these field data, has been applied to assess small-scale roughness for 10-cm profile lengths. Based on these field data, a JRC value of less than 10, or a joint profile amplitude of less than 2.5 mm over a 10-cm length, is defined as “smooth.” For JRC estimates greater than 10 and amplitudes greater than 2.5 mm, surfaces are defined as “rough.” A small-scale roughness term,  $J_r/r$ , is used to

represent small-scale roughness and is set to 1.0 and 1.5 for smooth and rough joints, respectively. For large-scale waviness,  $J_r/w$ , three categories of waviness have been defined based on field data on profile amplitudes over a 1-m length. Wavy joints have 1-m profile amplitudes of 20 mm or more, and the  $J_r/w$  value is set to 2.0. Planar to wavy joints have amplitudes between 10 and 20 mm and a  $J_r/w$  value is set to 1.5. To obtain a  $J_r$  value for the Q classification, the  $J_r/r$  and  $J_r/w$  values are multiplied together (Equation 2).

$$J_r = J_r/r \times J_r/w \quad (2)$$

Developing more quantitative assessments of rock mass classification systems is more complicated than simply developing improved methods of measuring rock mass properties and superimposing them on existing subjective descriptions. Improved measuring methods must be based on extensive field data collections and should ideally be coupled with a database of case histories.

## Summary of Input Parameters for Existing Rock Classification Systems

More detailed data on rock classification can be applied to some aspects of existing classification systems. In many cases, however, it would be difficult to know how to incorporate detailed information with existing classification. As an example, it is difficult to know how a measure



**Figure 3.—One-meter-long profile comb used to measure discontinuity roughness at 10 mines across Canada.**

of the rock mass block size can be incorporated with current systems that assess the rock mass in terms of joint spacing, RQD, and the number of discontinuity sets present. Work has been done to augment the GSI classification system with more quantifiable terms [Cai et al. 2004]; however, it could be argued that the GSI system was specifically developed to avoid this approach.

The challenges with developing a more precise method of quantifying properties of a rock mass are overshadowed by problems with how classification systems use these data. Classification systems attempt to assess factors influencing rock mass performance and properties and represent that assessment as a single number. To do this, individual rock mass properties are given a weighting, which represents the relative importance of that rock mass property. The next section discusses the importance of these weightings.

### WEIGHTING ASSESSMENTS OF ROCK MASS PROPERTIES

Classification systems attempt to provide a basis for estimating deformation and strength properties for a rock mass, as well as provide data for estimating support requirements [Cai et al. 2004]. They are also used to assist in estimating the overall stability of excavations. To obtain a single classification/characterization value to represent a rock mass, weightings are given to the various rock mass properties. The weightings assigned to the individual properties of a rock mass are, in most cases, the same under all loading conditions. Table 1 summarizes some of these weightings expressed as the influence of each property on the total range in classification values. The assignment of a weighting, or degree of influence, is required to allow an engineer to represent rock mass properties as a single number. This is a significant weakness in rock mechanics. Apart from a fairly major change between the RMR<sub>76</sub> and RMR<sub>89</sub> systems, these weightings have not changed significantly since the early 1970s. The GSI system seems to differ; however, the main difference is that rock strength and groundwater conditions are left for later consideration. The remaining properties of block size and discontinuity condition are given weightings similar to those in the Q-system.

The application of weighting systems within classification schemes means that a rock mass with a relatively large intact block size and smooth slippery joint surfaces can have the same classification value as a rock mass with much smaller intact blocks and rough joints. Table 2 gives an example of two different rock masses (A and B) with different properties, but similar rock mass classification values.

**Table 1.—Influence of rock mass properties on rock classification (after Milne and Hadjigeorgiou [2000])**

	Classification system				
	Q'	Q	RMR <sub>76</sub>	RMR <sub>89</sub>	GSI
Unconfined compressive strength (UCS)					
% of total range.....	0	0	16	16	0
Block size					
% of total range.....	41	33	46	35	50
Discontinuity surface friction					
% of total range.....	38	30	27	33	50
Groundwater					
% of total range.....	21	17	11	16	0
Stress or UCS/stress ratio					
% of total range.....	0	20	0	0	0

**Table 2.—Classification assessment of two different rock masses**

	Rock mass A	Rock mass B
UCS.....	75 MPa	75 MPa
Groundwater .....	Dry	Dry
RQD .....	100%	20%
No. of joint sets .....	2 joint sets	3 joint sets
Average joint spacing.....	2-m spacing	10-cm spacing
10-cm scale JRC.....	<10	>10
Amplitude over 1 m .....	<1 cm	>3 cm
Alteration .....	Chlorite coating, can be dented with a fingernail	Clean joint surfaces
Q'.....	≈ 6	≈ 6
GSI.....	≈ 60–65	≈ 60–65
RMR <sub>76</sub> .....	≈ 74	≈ 55
RMR <sub>89</sub> .....	≈ 77–82	≈ 63

Rock mass A and rock mass B would require significantly different support measures, and it is unlikely that maximum stable tunnel spans or the overall strength or deformation modulus of these two rock masses would be the same. Neither the Q' nor GSI systems reflect this difference. Different variations in discontinuity spacings and conditions could have been chosen to give the same RMR classification values for similar differences in rock mass properties.

The influence of loading conditions and scale effect are two other factors that can have significantly different effects on the performance and properties of the two rock masses described. In a narrow tunnel situation with a span in the order of 3 m, rock mass A would, in most cases, perform much better than rock mass B. Very few intact rock blocks would be exposed in rock mass A, so the intact rock properties would have a greater influence on the overall rock mass compared to rock mass B.

It seems unrealistic to assume that the weightings applied to rock mass parameters will give accurate assessments of stability and rock mass properties at all scales of engineering applications and at all loading conditions. The Q-system reflects the importance of loading conditions with the assessment of intact rock strength. Intact rock strength is included in the SRF factor, and when the UCS

of the intact rock divided by the induced stress exceeds 10, rock strength is not a factor in rock classification. Underground engineering structures range in size from drill holes to small tunnels to open stopes hundreds of meters in extent. It may be necessary to apply some scaling factor to rock classification assessments of intact block geometry to account for the scale of engineering applications.

The inherent weakness in the weighting factors applied in rock classification schemes can be illustrated with some typical design applications using some empirical design methods.

### Tunnel Roof Design

Both the Q classification system and the RMR<sub>76</sub> system were originally developed to assess the stability, standup time, and support requirements of tunnels. Most of the rock mass properties, environmental conditions, and project-related features shown in Figure 1 are combined in some fashion to determine an empirical tunnel design. The success of these empirical design methods implies that all of the features used in the design process do actually influence tunnel stability.

### Pillar Design

There are many empirical pillar design approaches. Commonly used empirical design methods include those developed by Hedley and Grant [1972], Hudyma [1988], and Lunder [1994]. It is interesting to note that none of these empirical design approaches, based on more than 17 mines and a wide range of rock mass properties, use any rock mass classification assessment as a factor influencing stability. These design methods rely only on the UCS of the rock, pillar geometry, and stress induced in the pillars.

### Stope Hanging Wall Design

Stope hanging wall stability involves large rock surfaces, often several thousands of square meters in extent. There are several empirical techniques used for estimating the stability and dilution of large stope hanging walls. The most commonly used empirical design methods are versions of the stability graph and dilution graph [Potvin 1988; Nickson 1992; Clark 1998; Capes et al. 2005]. These design techniques have gained widespread application and rely upon a modified version of Barton's rock quality Q classification system coupled with assessments of induced stresses, joint orientation and surface orientation, and hanging wall geometry. With this design method, neither the rock strength nor the induced stress influence the assessment of the relaxed, low-stress hanging wall condition. This indicates that the data collected for developing the design method were not sensitive to the induced stresses or rock strength [Wang et al. 2007].

## CONCLUSIONS

Rock mass classification and characterization systems are the best tools available for assessing rock mass properties. They were designed to be easily used assessments of the properties believed to be most important for estimating the performance of excavations in rock. Most classification systems were originally developed for civil engineering tunnel design. The application of these systems has greatly increased to areas such as slope stability design and for providing rock mass property input for numerical modeling. Major problems in rock classification and characterization stem from their ease of use and their increasingly wide application.

The easy use of classification systems allows field engineers to quickly make support recommendations while a tunnel is being driven. This original goal for rock classification systems makes them insensitive to improved rock mechanics data. As an example, consider a clean, rough, and wavy joint surface. It would have a Q assessment of  $J_r/J_a$  equal to 3.0 and an RMR<sub>76</sub> assessment of 20. Based on the original classification guidelines, field data estimating JRC, joint amplitude, and joint surface strength would have little or no influence on the classification values. Also, lab tests on discontinuities or even in situ shear tests would also have no effect on the classification values. Some attempts have been made to improve the sensitivity of classification systems to improved data, but this work has not become the industry standard, or even a widely recognized goal.

The process of determining a single number to represent a rock mass classification value necessitates that a weighting system be applied to assess the relative importance of rock strength, block size and geometry, and discontinuity strength. These weighting systems have proven to be effective for assessing support requirements and tunnel back stability. These classification systems now enjoy a wide range of applications and are assumed to be effective at almost any engineering scale and under a wide range of loading conditions. The lack of change in these weighting values over the last 30 years is a reflection of both the accuracy in their initial development as well as the difficulty in making changes to well-used classification schemes. A review of the weighting systems used in rock mass classification is needed.

## RECOMMENDATIONS

The individual properties of a rock mass should be assessed as accurately as possible. The relative importance of these individual properties should be determined empirically for a wide range of loading conditions, with a consideration of scale. Empirical data on pillar design suggest that intact rock strength is the only rock mass property that affects pillar stability for a wide range of rock classification values. It may be possible to make significant improvements to design if the individual properties of a

rock mass are considered separately. We cannot expect to obtain good-quality rock mechanics lab and field data on rock mechanics properties unless the commonly used design tools can make use of these data.

## REFERENCES

- Barton N, Choubey V [1977]. The shear strength of rock joints in theory and practice. *Rock Mech* 10:1–54.
- Barton N, Lien R, Lunde J [1974]. Engineering classification of rock masses for the design of tunnel support. *Rock Mech* 6(4):189–236.
- Bieniawski ZT [1973]. Engineering classification of jointed rock masses. In: *Trans S Afr Inst Civ Eng* 15:335–344.
- Bieniawski ZT, ed. [1976]. Rock mass classification of jointed rock masses. In: *Exploration for Rock Engineering*. Johannesburg, South Africa: Balkema, pp. 97–106.
- Bieniawski ZT [1979]. The geomechanics classification in rock engineering applications. In: *Proceedings of the 4th International Congress on Rock Mechanics (ISRM)* (Montreux, Switzerland). Vol. 2, pp. 41–48.
- Bieniawski ZT [1989]. Engineering rock mass classifications. John Wiley & Sons.
- Cai M, Kaiser P, Uno H, Tasaka Y, Minami M [2004]. Estimation of rock mass deformation modulus and strength of jointed hard rock masses using the GSI system. *Int J Rock Mech Min Sci* 41:3–19.
- Capes G, Milne D, Grant D [2005]. Interpreting core data and rock quality information for stope design. Canadian Institute of Mining, AGM Proceedings (Toronto, Ontario, Canada, May 6, 2005). CD-ROM.
- Clark L [1998]. Minimizing dilution in open stope mining with a focus on stope design and narrow vein long-hole blasting [Thesis]. Vancouver, British Columbia, Canada: University of British Columbia.
- Deere DU, Hendron AJ Jr., Patton FD, Cording EJ [1967]. Design of surface and near surface construction in rock. In: Fairhurst C, ed. *Failure and breakage of rock*. New York: Society of Mining Engineers of AIME, pp. 237–302.
- Hadjigeorgiou J, Germain P, Potvin Y [1994]. In situ estimation of rock joint alteration. *Can Tunnelling*, pp. 155–162.
- Hadjigeorgiou J, Grenon M, Lessard JF [1998]. Defining in-situ block size. *CIM Bull* 91(1020):72–75.
- Hedley DGF, Grant F [1972]. Stope and pillar design for the Elliot Lake uranium mines. *CIM Bull* 65:37–44.
- Hoek E [2004]. A brief history of the development of the Hoek-Brown failure criterion. Discussion paper #7. [<http://www.rocscience.com/hoek/pdf/history%20of%20the%20hoek%20brown%20criterion.pdf>]. Date accessed: April 2007.
- Hoek E, Brown ET [1980]. *Underground excavations in rock*. London: Inst Min Metal, p. 527.
- Hoek E, Kaiser PK, Bawden WF [1995]. *Support of underground excavations in hard rock*. Rotterdam, Netherlands: Balkema.
- Hudyma MR [1988]. Rib pillar design in open stope mining [Thesis]. Vancouver, British Columbia, Canada: University of British Columbia.
- Laubscher DH, Taylor HW [1976]. The importance of geomechanics of jointed rock masses in mining operations. In: *Proceedings of the Symposium on Exploration for Rock Engineering* (Johannesburg, South Africa), pp. 119–128.
- Lunder PJ [1994]. Hard rock pillar strength estimation an applied empirical approach [B.S. Thesis]. Vancouver, British Columbia, Canada: University of British Columbia.
- Milne D, Hadjigeorgiou J [2000]. Practical considerations in the use of rock mass classification in mining. In: *Proceedings of GeoEng 2000 Conference on Geological and Geotechnical Engineering* (Melbourne, Victoria, Australia, November 19–24, 2000).
- Milne D, Germain P, Grant D, Noble P [1991]. Field observation for the standardization of the NGI classification system for underground mine design. In: *Proceedings of the Seventh Congress of the International Society for Rock Mechanics* (Aachen, Germany). Rotterdam, Netherlands: Balkema.
- Milne D, Germain P, Potvin Y [1992]. Measurement of rock mass properties for mine design. In: *Proceedings of the ISRM-Eurock Symposium on Rock Characterization* (Chester, U.K., September 14–17, 1992). A. A. Balkema.
- Milne D, Hadjigeorgiou J, Pakalnis R [1998]. Rock mass characterization for underground hard rock mines. *Tunnelling Undergr Space Technol* 13(4):383–391.
- Nickson S [1992]. Cable support guidelines for underground hard rock mine operations [Thesis]. Vancouver, British Columbia, Canada: University of British Columbia.
- Palmström A [1985]. Application of the volumetric joint count as a measure of rock mass jointing. In: *Proceedings of the International Symposium on Fundamentals of Rock Joints* (Björkliden, Sweden), pp. 103–110.
- Palmström A, Milne D, Peck W [2001]. The reliability of rock mass classification used in underground excavation and support design. *ISRM News J* 6(3):40–41.
- Potvin Y [1988]. Empirical open stope design in Canada [Dissertation]. Vancouver, British Columbia, Canada: University of British Columbia.
- rockmass.net [2007]. Ground characterization and classification in rock engineering. [<http://www.rockmass.net>]. Date accessed: March 2007.
- Terzaghi K [1946]. Rock defects and loads on tunnel supports. In: Proctor RV, White T, eds. *Rock tunnelling with steel supports*. Youngstown, OH: Commercial Shearing and Stamping Co., pp. 15–99.
- Wang J, Milne D, Wegner L, Reeves M [2007]. Numerical evaluation of the effects of stress and excavation surface geometry on the zone of relaxation around open stope hanging walls. *Int J Rock Mech Min Sci* 44(2):289–298.

# WEAK ROCK MASS DESIGN FOR UNDERGROUND MINING OPERATIONS

By Rimas Pakalnis, P.Eng.,<sup>1</sup> Thomas M. Brady,<sup>2</sup> Paul Hughes,<sup>3</sup> Cristian Caceres,<sup>3</sup>  
Andrea M. Ouchi,<sup>3</sup> and Mary M. MacLaughlin, Ph.D.<sup>4</sup>

## ABSTRACT

A major focus of ground control research presently being conducted by the Geomechanics Group at the University of British Columbia, Canada, in conjunction with the National Institute for Occupational Safety and Health's (NIOSH) Spokane Research Laboratory, is the development of design guidelines for underground mining within weak rock masses. The study expands upon the span design curve for man-entry operations and the stability graph for nonentry operations developed at UBC by extending the application to weak rock masses. The original database has been augmented by weak rock mass information from mines throughout the United States, Canada, Australia, Indonesia, and Europe. The common factor in all of these mines is the presence of a weak back and/or walls. This paper expands on the North American database and how the design curves have been employed at mining operations throughout the world. The definition of a weak rock mass for this study has been defined as having an  $RMR_{76}$  under 45% and/or a Q-value under 1.0.

## INTRODUCTION

A comparative analysis by the Mine Safety and Health Administration for Nevada gold mine operations for 1990–2004 (Figure 1) shows that the number of injuries from roof falls in 13 Nevada underground gold mines ranged from a low of 8 in 1990 to a high of 28 in both 1995 and 1997 [Hoch 2001]. This high injury rate was the prime motive for the initial study by NIOSH. The goal was to address the extremely difficult ground conditions associated with mining in a weak rock mass and provide mine operators with a database that could lead to a better understanding of the failure mechanism associated with mining within a weak rock mass. The database summa-

rized in this paper is composed of seven [Potvin 1988] mines in Nevada and several others, which are summarized in Table 1.

A weak rock mass upon review of site conditions observed was identified as having an  $RMR_{76}$  less than 45% and/or a rock mass quality (Q) under 1.0. These values are largely described by Barton [2002] and Bieniawski [1976] as being “very poor” and “fair,” respectively, and are shown schematically in Figure 2.

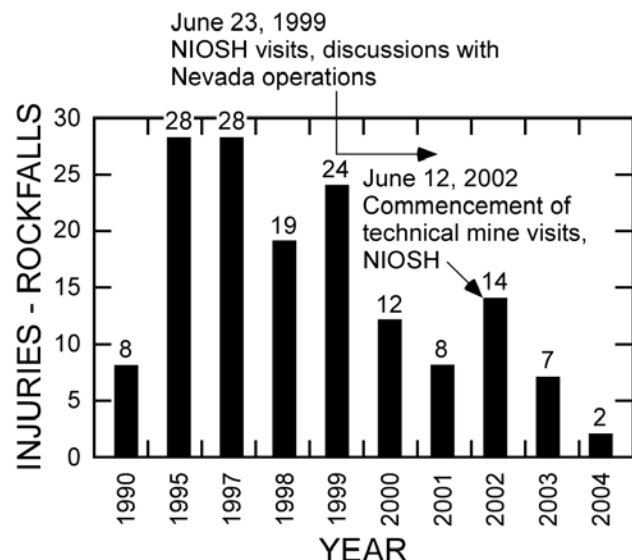


Figure 1.—Injuries from rock falls in Nevada underground mining operations [Hoch 2001].

Table 1.—Weak rock mass database  
( $RMR_{76} < 45\%$ ,  $Q < 1.0$ )

East Carlin Mine (Newmont) .....	Nevada.
Deep Post Mine (Newmont).....	Nevada.
Midas Mine (Newmont) .....	Nevada.
Rodeo Mine (Barrick) .....	Nevada.
Turquoise Ridge Mine (Barrick) ..	Nevada.
Getchell Mine (Barrick).....	Nevada.
Murray Mine (Queenstake) .....	Nevada.
SSX Mine (Queenstake) .....	Nevada.
Nye Operation (Stillwater).....	Montana.
Eskay Creek Mine (Barrick) .....	British Columbia, Canada.
Eagle Point Mine (Cameco) .....	Saskatchewan, Canada.
Quinsam Mine (Hillsborough).....	British Columbia, Canada.
Kencana Mine (Newcrest).....	Halmahera, Indonesia.

<sup>1</sup>Associate professor of mining engineering, University of British Columbia, Vancouver, British Columbia, Canada.

<sup>2</sup>Deputy branch chief, Catastrophic Failure Detection and Prevention Branch, Spokane Research Laboratory, National Institute for Occupational Safety and Health, Spokane, WA.

<sup>3</sup>Graduate student, Department of Mining Engineering, University of British Columbia, Vancouver, Canada.

<sup>4</sup>Professor of geological engineering, Montana Tech of the University of Montana, Butte, MT.

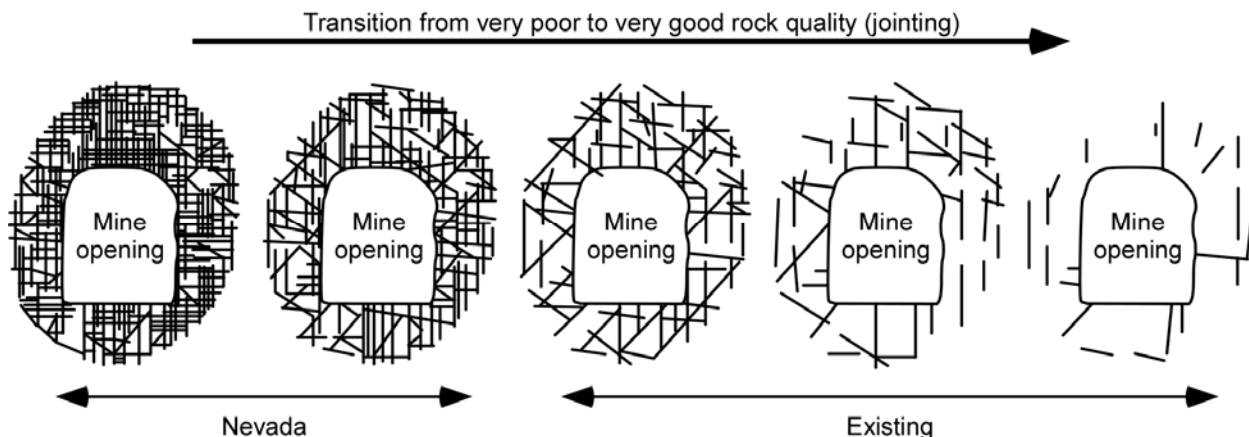


Figure 2.—Schematic showing transition of weak rock mass to stronger and existing databases.

The mining methods practiced in Nevada are largely longhole mining, underhand cut-and-fill, and cut-and-fill. The underhand mining method relies upon an engineered back composed of rock/paste fill and is not addressed within this study, as mining under/adjacent to weak rock masses is largely negated. Underground mining methods as practiced in Nevada dictated which specific databases and stope design curves NIOSH would focus upon. Rock mass values were calculated during mine visits and varied from an RMR<sub>76</sub> high of 70% to a low of 16% in gold-bearing fault gouge. Several rock mass design curves developed by the Geomechanics Group at the University of British Columbia (UBC) [Pakalnis 2002] are available, but they were not thought to be relevant to the mining methods employed within the weak ground of Nevada gold mines and therefore not augmented.

Research began with visits to Nevada operators in June 1999 to address concerns and determine where NIOSH would be able to assist. The first technical site visit was on June 12, 2002, and initial data were collected (Figure 1). The major objectives were to obtain information on weak rock masses and incorporate this information into existing design curves [Lang 1994] for back spans of manned entries and a stability graph [Clark and Pakalnis 1997] for longhole wall design for nonentry operations. The distribution of the original databases was based on Canadian mining data, as summarized in Figure 3, and shows the lack of data for weak rock masses.

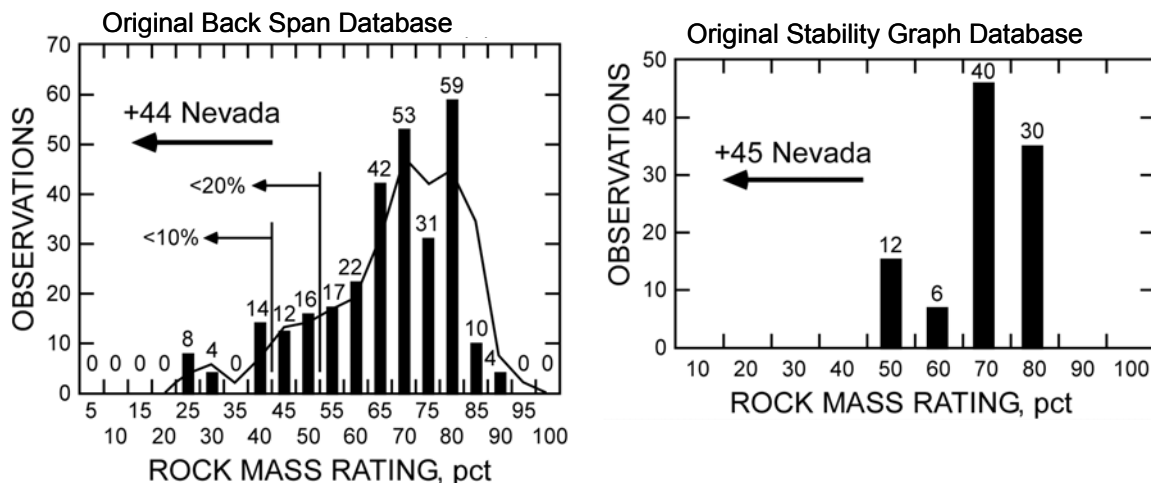


Figure 3.—Distribution of the original database for back span (left) and stability graph (right).

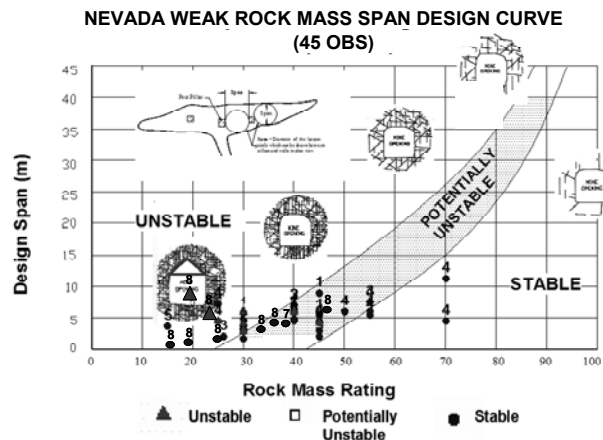


Figure 4.—Critical span curve augmented with Nevada operations (Table 1) (45 observations).

### SPAN DESIGN, MAN ENTRY

The initial span curve was developed by the UBC Geomechanics Group to evaluate back stability in cut-and-fill mines. It consists of two straight lines that divide a graph into three zones: stable, potentially unstable, and unstable. The database for this graph initially consisted of 172 data points from the Detour Lake Mine of Placer Dome, Inc., Ontario, Canada, with most of the points having RMR values in excess of 60% [Lang 1994]. The database was expanded to 292 observations in the year 2000 with case histories from an additional six mines [Wang et al. 2000]. The successful use of empirical design techniques is based upon interpolation rather than extrapolation. Thus, a decision was made to develop a database for a critical span curve in weak rock masses. The term “critical span” refers to the largest circle that can be drawn within the boundaries of the excavation when seen in plan view (Figure 4).

The term “design span” refers to spans that have no support and/or spans incorporating a limited amount of local support (e.g., pattern bolting in which 1.8-m-long mechanical bolts are installed on a 1.2- by 1.2-m pattern). Local support is deemed as support used to confine blocks that may be loose or that might open or fall because of subsequent mining in surrounding areas. The Nevada study added an additional 44 observations to the span design curve as shown in Figure 4 and summarized by Brady et al. [2005], of which 35 had an RMR<sub>76</sub> less than 45%.

The span design curve is used throughout North America. Three operations and their database are summarized in this paper: Stillwater Mining Co.’s Nye Operation in Montana, Barrick Gold, Inc.’s Eskay Creek in British Columbia, Canada, and Cameco, Ltd.’s Eagle Point Mine operation in Saskatchewan, Canada, with the design span curves shown in Figures 5–7, respectively. Of note in Figure 6, where Eskay Creek has established guidelines for

support based on RMR as well as if conventional overhand mining versus underhand will be practiced as a function of rock mass and span. Figure 7 shows two data points within the unstable zone. In this area of the operations, these zones were observed to previously cave and required either increased support (dead weight) and/or mining employing “short rounds” in order to ensure stable conditions for subsequent mining.

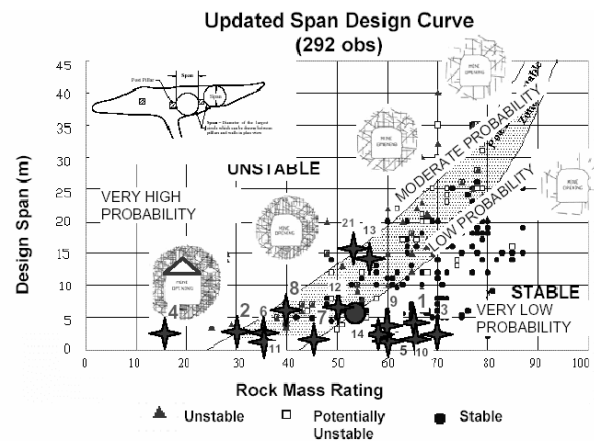


Figure 5.—Critical span curve at Stillwater Mining’s Nye Operation in Montana (292 observations).

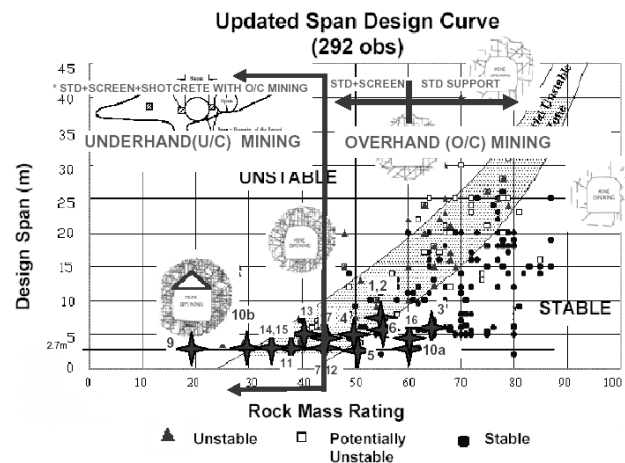


Figure 6.—Critical span curve at Barrick Gold, Inc.’s Eskay Creek Mine in British Columbia, Canada (292 observations).

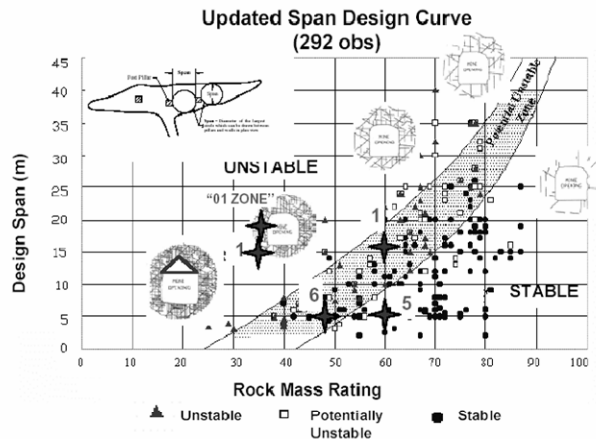


Figure 7.—Critical span curve at Cameco, Ltd.’s Eagle Point Mine, Saskatchewan, Canada (292 observations).

A brief description of the use of the critical span curve is presented; more detail is outlined by Pakalnis [2002].

Excavation stability is classified into three categories; each category is further divided into three subcategories.

1. Stable excavation (S)
  - a) No uncontrolled falls of ground have occurred.
  - b) No movement of the back has been observed.
  - c) No extraordinary support measures have been employed.
2. Potentially unstable excavation
  - a) Extra ground support has been installed to prevent falls of ground.
  - b) Movement has occurred in the back.
  - c) Increased frequency of ground movement has been observed.
3. Unstable excavation (U)
  - a) Area has collapsed.
  - b) Depth of failure of the back is 0.5 times the span (in the absence of major structures). Within a weak rock mass, the depth of failure has been noted as 1 times the span and sometimes even greater.
  - c) Limited local support was not effective in maintaining stability.

A minus-10 correction factor is applied to the final RMR when evaluating rock with shallow dipping or flat joints. However, the applicability of this factor in weak ground is being reassessed because of its amorphous nature. Where discrete ground wedges have been identified, they must be supported before employing the critical span curve. Stability is generally defined in terms of short-term stability because the database is based largely on stoping methods that, by their nature, are of short duration. Movement of the back greater than 1 mm within a 24-hr period has also been defined as a critical amount of

movement for safe access [Pakalnis 2002]. This value is also being addressed for weak rock masses as it applies to the initial database identified in Figure 4. This critical value may be much greater than 1 mm.

## STABILITY GRAPH METHOD: NONENTRY

The original stability method for open-stope design was based largely on Canadian operations and was proposed by Matthews et al. [1981], modified by Potvin [1988], and updated by Nickson [1992]. In all instances, stability was qualitatively assessed as being either stable, potentially unstable, or caved. Recent research at UBC has augmented the stability graph by using stope surveys in which cavity monitoring systems were employed [Clark and Pakalnis 1997]. This research has enabled the amount of dilution to be quantified. A parameter termed the “equivalent linear overbreak/slough” (ELOS) was introduced by Clark and Pakalnis [1997] and was used to express volumetric measurements of overbreak as an average depth over an entire stope surface. This has resulted in a design curve as shown in Figure 8.

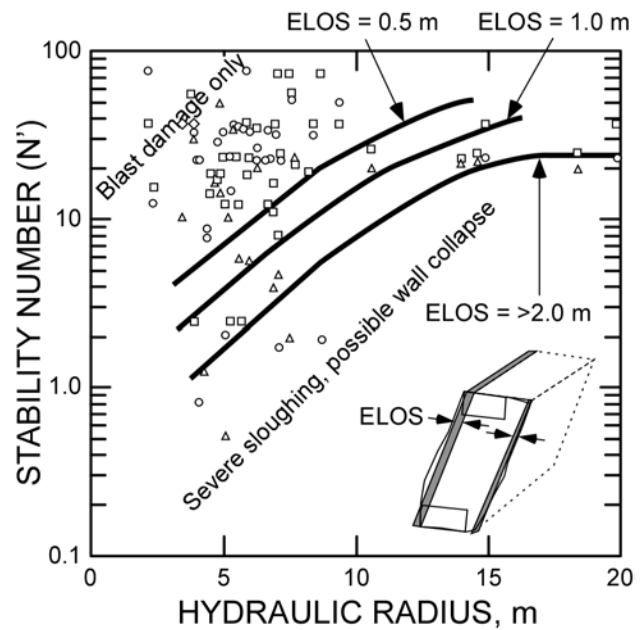


Figure 8.—Stability graph, after Clark and Pakalnis [1997].

A limited number of observations existed for RMR values under 45% (Figure 3). An additional 45 data points were added on the stability graph—nonentry from Nevada operations having an RMR under 45%. In addition, Mine 4 (Table 1) reflects more than 338 observations that have been averaged to reflect the design points as discussed by Brady et al. [2005]. The stability graph relates hydraulic radius of the stope wall to empirical estimates of overbreak

slough. Hydraulic radius is defined as the surface area of an opening divided by perimeter of the exposed wall being analyzed.

Equation 1 was used for calculating parameters for the database shown in Figure 8:

$$N' = Q' * A * B * C \quad (1)$$

where  $N'$  = modified stability number;

$Q'$  = modified Norwegian Geotechnical Institute (NGI) rock quality index [Unal 1983] where the stress reduction factor and joint water reduction factor are equal to 1, as they are accounted for separately within the analysis;

$A$  = stress factor equal to 1.0 due to relaxed hanging wall;

$B$  = rock defect factor. This value results from parallel jointing and the amorphous state of the weak rock mass being set to 0.2 and 0.3, respectively [Brady et al. 2005];

and  $C$  = stope orientation factor as defined in Figures 5–7, i.e.,  $C = 8 - 6 \times \cos \varphi$  (dip of hanging wall).

An initial observation from Figure 9 is that the classical design curves (ELOS) as shown in Figure 6 are inaccurate at low  $N'$  and hydraulic radius values. If hydraulic radius is kept below 3.5 m in a weak rock mass, the ELOS value should remain under 1 m. It seems that a hydraulic radius under 3 m would not result in ELOS values much greater than 1 m. This result is being further evaluated.

## SUPPORT CAPACITY GUIDELINES

The development of support capacity guidelines is critical to the overall success of the mining method selected in terms of ensuring a safe workplace. Ground support in weak rock presents special challenges. Underdesign can lead to costly failures, whereas overdesign can lead to high costs for unneeded ground support. Figure 10 depicts a classic wedge failure controlled by structure. It is critical to design for the dead weight of the wedge in terms of the breaking load of the support, as well as the bond strength associated with embedment length [Brady et al. 2005].

## NEVADA WEAK ROCK MASS - WALL STABILITY GRAPH (45 obs)

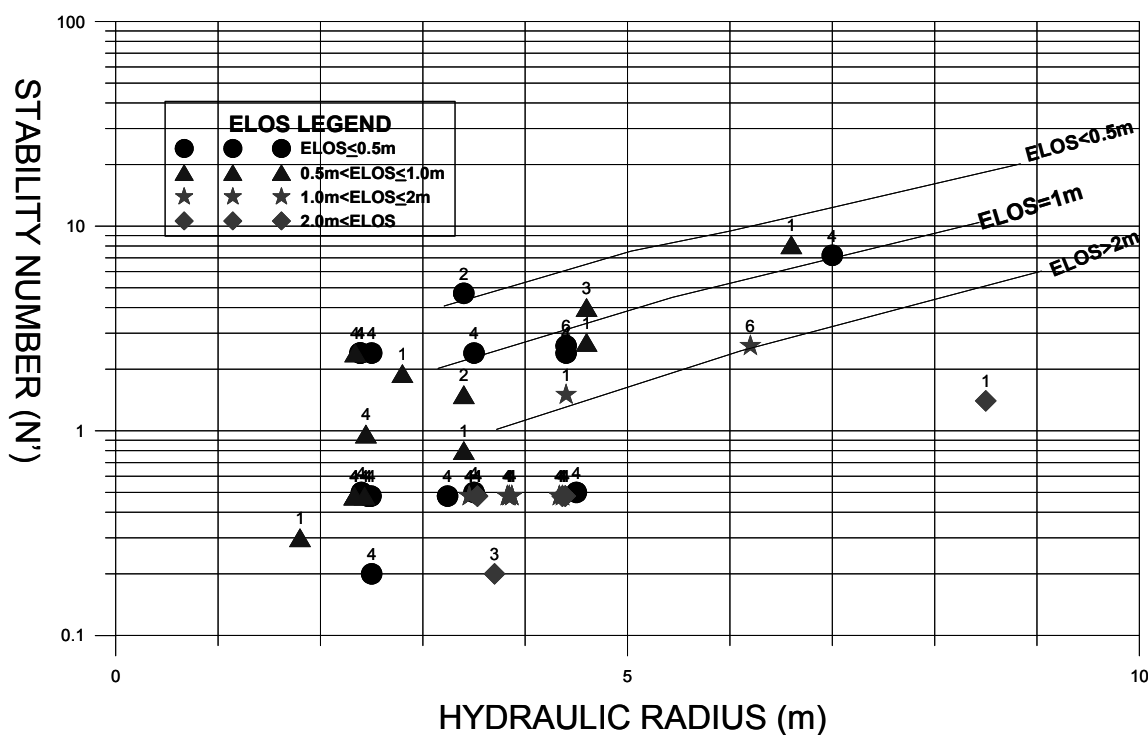


Figure 9.—Wall stability graph as developed for Nevada operations (45 observations).

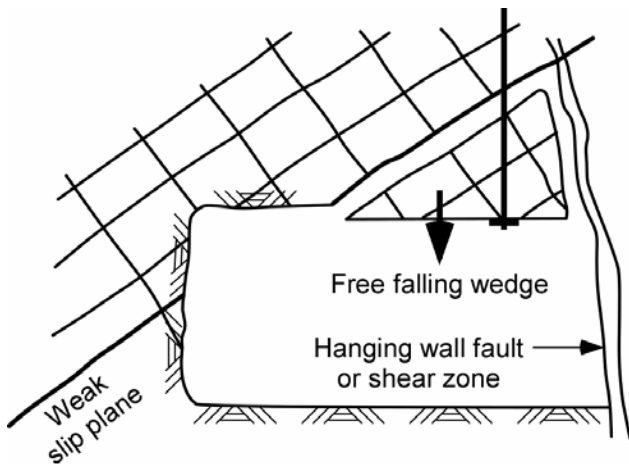


Figure 10.—Structurally controlled wedge.

More than 400,000 Split Set [Brady et al. 2005] friction bolts are used in Nevada mines as primary support. Friction bolts are particularly useful in fissile, buckling, or sheared ground where it is difficult to secure a point anchor. Caution must be used with this method of primary support because of the low bond strength between broken rock and the bolt and because of the susceptibility of the bolt to corrosion. In Mine 4, Split Set bolts had a life of 6 months because of corrosion resulting from acidic ground conditions. An analysis of the performance of friction bolts in mines with weak rock (as determined by RMR) needed to be conducted. With one exception, Nevada mines use 39-mm Split Set bolts (the exception uses 46-mm Split Set bolts). Mines in Canada, however, use 33-mm Split Set bolts. Canadian mines generally use these bolts only in the walls and not in the back. The 46-mm bolts are common in Indonesian operations (Newcrest's Kencana Mine) and Australian underground mines.

Data points gathered from several pull tests in weak rock were plotted as shown in Figure 11, with bond strengths (SS39) shown for Mine 4 in Figure 12. The graph shows a strong trend between RMR and bond strength.

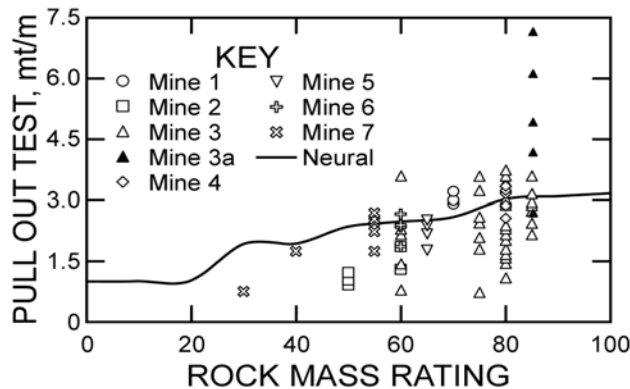


Figure 11.—Pullout load versus RMR for SS39.

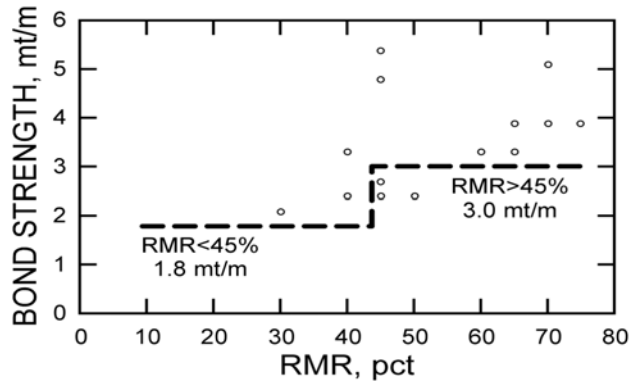


Figure 12.—Pullout load versus RMR for SS39 (Mine 4).

Variability in test results shows the difficulty in assessing overall support for a given heading. Thus, it is important that mines develop a database with respect to the support used so they can design for variable ground conditions. Factors critical to design, such as bond strength, hole size, support type, bond length, and RMR, should be recorded in order to determine where they lie on the design curve. Table 2 shows the design bond strengths determined through field testing at Newcrest's Kencana Mine in Indonesia. Design values differed for grouted versus ungrouted split sets [Villaescusa and Wright 1997] and enabled one to assess the benefit with respect to alternative support, such as Swellex bolts. The Pm12 Swellex bolt provided 8.6 t/m of bond for RMR<sub>76</sub> values ranging from 25% to 55%. These values compare similarly to design field strengths observed at Barrick's Eskay Creek Mine in British Columbia, Canada.

Table 2.—Bond strength SS46/Pm12:  
Kencana Mine, Indonesia

Type	RMR <sub>76</sub>	Bond strength (SS46 mm)	
		Ungrouted (tonnes/m)	Grouted (tonnes/m)
I.....	RMR > 55%	4.1	7.2
II.....	35% < RMR ≤ 55%	2.6	5.8
III.....	25% ≤ RMR ≤ 35%	1.5	4.4

Swellex Pm12 bond strength = 8.6 t/m (RMR 25%–55%).

Table 3 summarizes the updated support table incorporating the weak mass pull-test results conducted at operations throughout this database (Table 1).

**Table 3.—Updated support capacity**

Rock properties, tonnes			Screen	Bag strength, tonnes
Bolt strength	Yield strength	Breaking strength		
5/8-in mechanical	6.1	10.2	4- by 4-in welded mesh, 4 gauge	3.6
Split-Set (SS 33)	8.5	10.6	4- by 4-in welded mesh, 6 gauge	3.3
Split Set (SS 39)	12.7	14.0	4- by 4-in welded mesh, 9 gauge	1.9
Standard Swellex	NA	11.0	4- by 2-in welded mesh, 12 gauge	1.4
Yielding Swellex	NA	9.5	2-in chain link, 11 gauge, bare metal	2.9
Super Swellex	NA	22.0	2-in chain link, 11 gauge, galvanized	1.7
*20-mm rebar, No. 6	12.4	18.5	2-in chain link, 9 gauge, bare metal	3.7
*22-mm rebar, No. 7	16.0	23	2-in chain link, 9 gauge, galvanized	3.2
*25-mm rebar, No. 8	20.5	30.8		
No. 6 Dywidag	11.9	18.0		
No. 7 Dywidag	16.3	24.5		
No. 8 Dywidag	21.5	32.3		
No. 9 Dywidag	27.2	40.9		
No. 10 Dywidag	34.6	52.0		
1/2-in cable bolt	15.9	18.8		
5/8-in cable bolt	21.6	25.5		
1/4 by 4-in strap	25.0	39.0		
Note: No. 6 gauge = 6/8-in diameter; No. 7 gauge = 7/8-in diameter; No. 8 gauge = 1-in diameter.			Shotcrete shear strength = 2 MPa (200 t/m <sup>2</sup> )	
NA = Not applicable.			Bond strength	
			Split-Set, hard rock	0.75-1.5 mt per 0.3 m
			Split-Set, weak ground	0.25-1.2 mt per 0.3 m
			Swellex, hard rock	2.70-4.6 mt per 0.3 m
			Swellex, weak rock	3-3.5 mt per 0.3 m
			Super Swellex, weak rock	>4 mt per 0.3 m
			5/8-in cable bolt, hard rock	26 mt per 1 m
			No. 6 rebar, hard rock	18 mt per 0.3 m, ~12-in granite

## MINING OPERATIONS GUIDELINES

With weak rock masses, blast control is critical to ensure that the weak rock mass is not further disturbed from overblasting. Guidelines for blasting based on RMR values for Queenstake's SSX Mine and Barrick's Goldstrike operation are summarized in Figures 13–14, respectively. In addition, the length of round pulled is related to the rock mass rating for a 5-m supported back span (Figure 13). For example, when the RMR is 15%–20%, only a 1.2-m (4-ft) advance is possible; otherwise,

failure of the unsupported back will result. Spiling is recommended at these RMR thresholds. Figure 14 shows the degree of loading of a development round at Barrick's Goldstrike Mine for a 5-m by 5-m heading with respect to the RMR.

## DEPTH OF FAILURE

Recent parametric analysis employing discrete-element methods of numerical modeling of discontinuous materials were employed by MacLaughlin et al. [2005], whereby

### SSX MINE – QUEENSTAKE/NEVADA (ELKO)

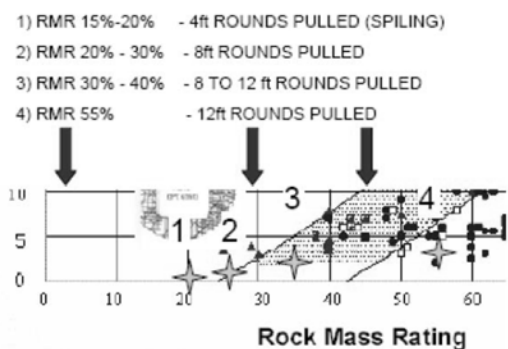


**Figure 13.—RMR versus round advance at Queenstake's SSX Mine.**

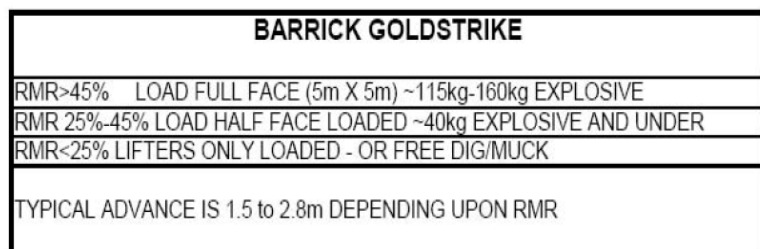


**Figure 14.—Loading of 5-m by 5-m face at Barrick's Goldstrike Mine.**

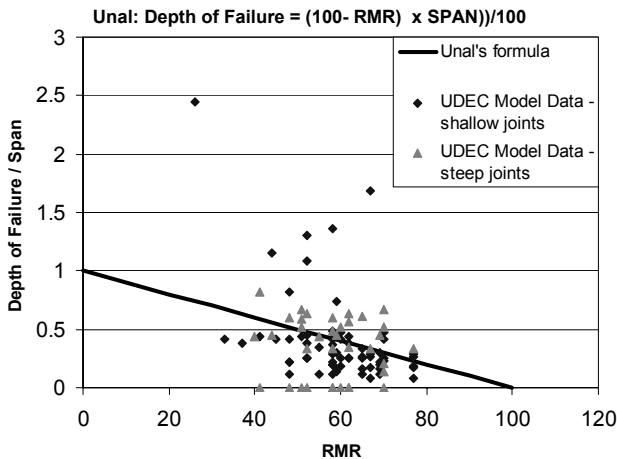


Figure 15.—Modeled depth of failure as a function of RMR [Villaescusa and Wright 1997].

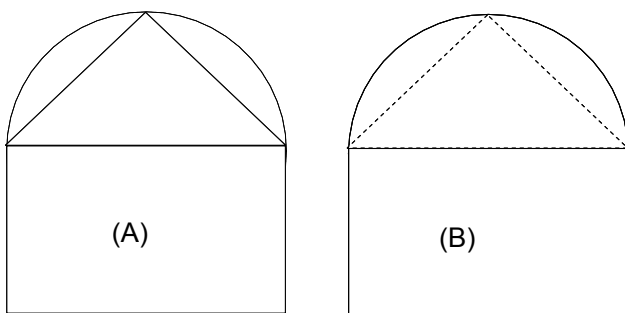


Figure 16.—Illustration of reduction of wedge volume due to arching of back. Depth of failure has been approximated by 0.5 times the span. Note arch has removed the potential for dead-weight failure.

UDEC<sup>5</sup> was employed to determine the depth of failure for a characterized rock mass ranging in RMR<sub>76</sub> from 26% to 77% with variable joint orientations. The results of the modeling showed that the failure mode was highly correlated with both the RMR value and joint condition. The depth of failure was largely found to be a function of drift geometry, with depth largely explained by the Unal [1983] relationship, as shown in Figure 15. This study also showed that the depth of failure was largely confined to 0.5 times the span for RMR values modeled.

In practice [Unal 1983] it was found that for weak rock masses, arching the back dramatically increased the overall stability for a given span. This is schematically shown in Figure 16, whereby the potential wedge volume is significantly decreased by employing an arched back and the effectiveness of the applied support increased as a greater length of bolt passes beyond the failure plane. This has been shown to be a major contributing factor to the overall stability of mines operating within weak rock masses.

## CONCLUSIONS

The NIOSH Spokane Research Laboratory and the UBC Geomechanics Group are focusing on developing safe and cost-effective underground design guidelines for weak rock masses having an RMR in the range of 15%–45%. Weak ground conditions, ground support, and mining methods used in several North American underground mines were observed. The RMR<sub>76</sub> values were calculated to update the span design graph and the stability graph to weak rock mass conditions. The greatest benefit is the implementation of these design relationships and methodologies at the participating mines, as their relevance and ability to predict design requirements have been shown to be workable, safe, and cost-effective.

Variability in field conditions showed the difficulty in assessing overall support for a given heading. It is imperative that mines develop their own databases based on the type of support used in their mines so that unexpected ground conditions can be analyzed and mine stability predicted. The results from augmented design curves and pullout tests are presented in the hope that they will aid mine professionals in their task of designing a safe workplace. A systematic approach allows an operator to understand overall failure mechanisms and resultant loads that could affect the system. This approach would allow an engineer to develop an optimal support strategy for the mining method employed.

This work would not have been possible without the partnership between NIOSH, the UBC Geomechanics Group, and North American mining company personnel. This continued partnership is critical to the development of safe and cost-effective mine design strategies. Figure 1 shows that since the inception of the team approach and resultant collaboration, injury statistics have declined dramatically in Nevada. This decline may be a result of many factors; however, it is clear that this approach is important and relevant to mine operations.

## ACKNOWLEDGMENTS

Specific thanks go to Patrick Carroll, chief engineer, Newmont's Midas Mine; J. J. Hunter, chief rock mechanics engineer, Newmont's East Carlin and Deep Post Mines; Monica Dodd, chief engineer, Newmont's Deep Post Mine; Simon Jackson, chief engineer, Placer Dome, Turquoise Ridge Joint Venture; Shawn Stickler, chief ground control engineer, Queenstake's Murray Mine; and Rad Langston, senior rock mechanics engineer, Stillwater Mining Co., Drew Marr at Barrick's Eskay Creek Mine, Indra Febrian at Newcrest's Kencana Mine, Kresho Galovich at Hillsborough's Quinsam Mine, and Ken Dunne and Jan Romanowski at Cameco's Eagle Point Mine.

<sup>5</sup>Universal Distinct Element Code.

## REFERENCES

- Barton N [2002]. Some new Q-value correlations to assist in site characterization and tunnel design. *Int J Rock Mech Min Sci* 39(2):185–216.
- Bieniawski ZT [1976]. Rock mass classifications in rock engineering. In: *Proceedings of the Symposium on Exploration for Rock Engineering* (Johannesburg, South Africa), pp. 97–106.
- Brady TM, Pakalnis R, Clark L [2005]. Design in weak rock masses: Nevada underground mining operations. SME preprint 05–43. Littleton, CO: Society for Mining, Metallurgy, and Exploration, Inc.
- Clark L, Pakalnis R [1997]. An empirical design approach for estimating unplanned dilution from open stope hangingwalls and footwalls. Presented at the 99th Canadian Institute of Mining Annual Conference (Vancouver, British Columbia, Canada).
- Hoch MT [2001]. Ground control seminar for underground gold mines (Elko, NV, Sept. 20, 2001). Sponsored by the Mine Safety and Health Administration, Roof Control Division, Pittsburgh, PA.
- Lang B [1994]. Span design for entry type excavations. [Thesis]. Vancouver, British Columbia, Canada: University of British Columbia.
- MacLaughlin MM, Pakalnis R, Brady TM [2005]. A distinct element parametric study of failure modes around an underground opening in rock masses of varying quality. In: *Proceedings of the 40th Symposium on Engineering Geology and Geotechnical Engineering* (Logan, UT).
- Matthews KE, Hoek E, Wylie D, Stewart M [1981]. Prediction of stable excavation spans for mining at depths below 1,000 m in hard rock. Ottawa, Ontario, Canada: Canada Centre for Mineral and Energy Technology (CANMET), DSS Serial No. 0sQ80–00081.
- Nickson SD [1992]. Cable support guidelines for underground hard-rock mine operations [Thesis]. Vancouver, British Columbia, Canada: University of British Columbia.
- Pakalnis R [2002]. Empirical design methods: UBC geomechanics update. In: Hammah R, Bawden W, Curran J, Telesnicki M, eds. *Proceedings of NARMS-TAC 2002: Mining and Tunneling Innovation and Opportunity* (Toronto, Ontario, Canada, July 7–10, 2002), Vol. 1.
- Potvin Y [1988]. Empirical open-stope design in Canada [Dissertation]. Vancouver, British Columbia, Canada: University of British Columbia.
- Unal E [1983]. Design guidelines and roof control standards for coal mine roofs [Dissertation]. University Park, PA: The Pennsylvania State University.
- Villaescusa E, Wright J [1997]. Permanent excavation reinforcement using cemented grouted Split Set bolts. In: AusIMM Proceedings (Carlton, Victoria, Australia), Vol. 1, pp. 65–69.
- Wang J, Pakalnis R, Milne D, Lang B [2000]. Empirical underground entry type excavation span design modification. In: *Proceedings of the 53rd Annual Conference, Canadian Geotechnical Society*.



# APPLICATION OF THE Q-SYSTEM TO AUSTRALIAN UNDERGROUND METAL MINES

By Warren A. Peck<sup>1</sup> and Max F. Lee<sup>1</sup>

## ABSTRACT

The applicability of the Q-system [Barton et al. 1974] to Australian underground metal mines is discussed with reference to two common design issues: ground support for horizontal mine development, and assessing the stability of bored raises.

Installed ground support in mine development is compared to empirical estimates using the Q-system and associated support capacity calculations. Data are graphically presented from 59 specially selected sites at 15 contributing mines.

The actual performance of large-diameter raise-bored shafts is also compared to empirical stability assessments using a modified version of Q ( $Q_r$ , after McCracken and Stacey [1989]). Lower-bound  $Q_r$  values are plotted against raise diameter for 47 selected sites at 23 mines in Australia and Papua New Guinea.

The influence on Q and  $Q_r$  of some geotechnical aspects of the Australian landscape, the dynamic nature of mines (compared to civil construction), and occupational health and safety regulations are discussed.

Stability and support assessments that are based just on Q or  $Q_r$  are not always conclusive. It is often necessary to consider other rock mass parameters, the regulatory environment, and risk issues.

These results are interim; further data collection and analysis are required with regard to comparing actual performance versus empirical assessments.

## INTRODUCTION

This study examines the applicability of two aspects of the Q-system [Barton et al. 1974] to Australian underground metal mines:

- For horizontal development, actual installed ground support versus empirical predictions using the Q-system and associated support pressure calculations;
- For raise-bored shafts, actual performance versus empirical predictions of stability using the modified version of Q published by McCracken and Stacey [1989].

The data presented in this paper, with one exception, have been supplied by mine management with the understanding that individual mines would not be identified in any report or published paper. Individual cases are discussed in a way that would not permit their locations to be identified.

## AUSTRALIAN GEOTECHNICAL ENVIRONMENT

Several geotechnical aspects of mines and the Australian occupational health and safety (OH&S) environment have a significant influence on the stability of openings and ground support requirements.

### Deep Weathering

Australia is an old, stable, continental mass. It has undergone numerous climate changes without appreciable erosion or glacial removal of weathered rocks. Weak weathered rocks often extend to depths of up to 90 m below the surface.

Extremely weathered near-surface rocks can be stronger due to the deposition of silica, carbonates, and iron oxides to form "caps" of stronger materials. Below the harder caps, weathered rocks often form a variety of rock-like saprolites through to weak clays. Soil mechanics rather than rock mechanics principles are more applicable to some of these weaker materials.

While the present groundwater level is often near the base of complete oxidation, this may not be the same as the base of weathering.

With regard to shafts, weak near-surface rocks are often the biggest challenge for site investigations, design, and construction. Failures have been relatively common due to a generally poor understanding of their behavior, their highly variable nature, and risk-taking during construction. In some cases, high rock quality designation (RQD) ratings have been erroneously assigned to extremely weathered rocks that were neither hard nor sound and therefore should have been assigned a nominal RQD rating of 10%. Groundwater or wet materials are also often implicated in these failures.

### Alteration and Weak Sheared Contacts

Altered rocks and thick weak sheared contacts are a common feature of some ore body styles, e.g., volcanicogenic lead-zinc deposits and hydrothermal copper or gold deposits. It is often necessary to mine access development

<sup>1</sup>Principal geotechnical engineer, AMC Consultants Pty. Ltd., Melbourne, Victoria, Australia.

and stopes along these weak contacts. Some of the common joint infill minerals include quartz, carbonates, chlorites, sericite, talc, zeolites, clays (both swelling and nonswelling), and gypsum.

In the case of porphyry copper deposits, the associated alteration is typically more pervasive and associated with intense fracturing. The entire rock mass is often either silicified, carbonated, or sericitized, and weak joint infill materials are common. Normally, strong igneous rock can be decomposed to clay at depths of hundreds of meters below the ground surface, while the surrounding jointed rock may be recemented by the gypsum released in the hydrothermal alteration process. Graphite is a common (low-friction) joint infill material in carbonate-hosted base metal deposits.

### Weak Ultramafic Host Rocks

Soft, weak ultramafic rocks are a feature of Australia's (Achaean) nickel mines. Their geologic history is varied and complex, as is their behavior, which is often significantly time-dependent.

A wide variety of soft, weak talc-rich ultramafic lavas are present due to serpentization very soon after eruption, variable grades of metamorphism, possible carbonation or potassium metasomatism, and finally deep weathering. Some rocks contain the very water-sensitive mineral brucite (magnesium hydroxide).

Ground conditions are very challenging, especially as soft, weak ultramafics can abut much stiffer and stronger rocks. Ground conditions and ground support are often extreme. Significant squeezing has occurred in ultramafics as shallow as 250 m, but as the ores can have very high values, mining has, thus far, reached 1,400 m below surface in one mine.

### Groundwater

Although high groundwater pressures are not common in mines, groundwater is often acidic or saline. Both influence the longevity of installed support, which typically must have an effective life of 10+ years. Point corrosion or rusting of bolts, possibly leading to premature failure, is also assisted by the tendency of mine rock masses to crack and loosen with time, especially when they are adjacent to stoping areas.

The effective life of support can be extended by using galvanized elements, fully grouted bolts (resin or cement), or plastic sheaves or (very expensive) low-grade stainless steel support elements. However, experience has shown that none of these measures guarantees the long-term integrity and effectiveness of support. There is also, presently, no foolproof method of testing or monitoring the adequacy of acid- or salt-challenged bolts with time.

### High Horizontal Stresses

In contrast to stresses in other tectonic plates, in situ measurements of premining rock stresses in Australian mines have demonstrated large variations in principal stress magnitudes with depth (Figure 1). While the major principal stress is often horizontal, its orientation can also vary widely between local regions [Lee et al. 2006].

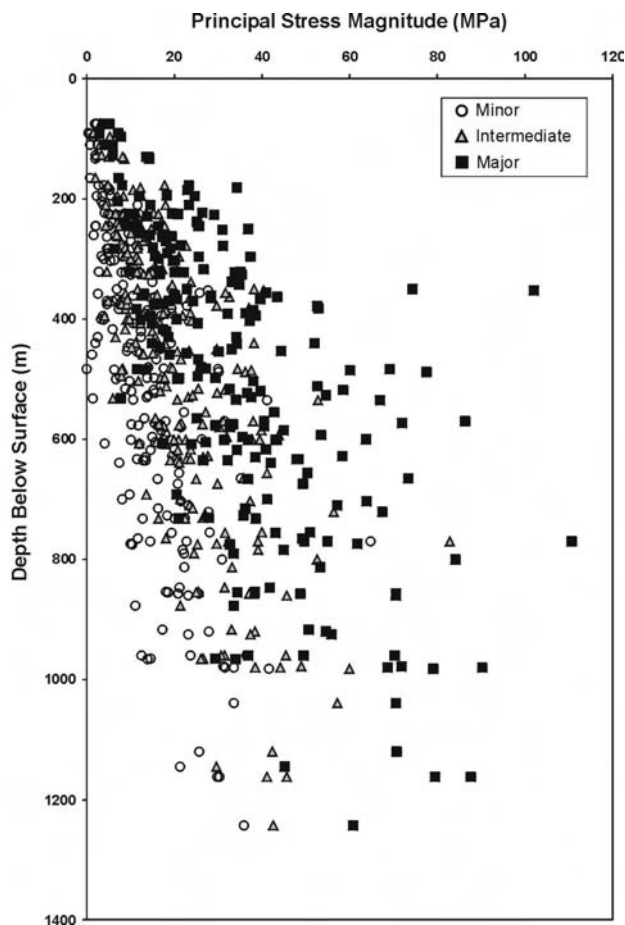


**Figure 1.—Australian principal stress magnitudes versus depth.**

Compared to similar mining provinces in eastern Australia and in other tectonic plates, anomalously high and deviatoric horizontal stresses are a feature of the Achaean Yilgarn Craton in the southwestern corner of Western Australia. This area hosts numerous gold, nickel, and copper-zinc mines, which currently stope to depths of up to 1,500 m. Mine openings typically have very high tangential stresses in development backs and shaft walls, often close to the strength of the rock mass [Lee et al. 2001].

Mining-induced seismicity is common in some of the deeper mines in strong, often jointed, stiff rocks due to both violent fracture through intact rock and shearing on

structures. In stark contrast, some of the softer and weaker talc-rich rocks and schist tend to squeeze, even at shallow depths.

### Mining-induced Stress Changes

Stress changes around openings are not usually an issue in civil engineering projects, but they are an important feature of mining. Due to nearby stoping, an opening might first be subjected to high or excessive abutment stresses, then low confining stresses as the opening is shielded by stoping. Both can encourage local shearing on structures, with associated cracking of the intact rock, and dilation plus loosening of the rock mass.

The installed support must be able to accommodate all of the associated movements and loosening, yet still adequately support the rock mass. Areas affected by stoping can therefore often seem to be oversupported.

### Mining-induced Seismicity and Blast Damage

For deep mines or those considered to be prone to seismic damage, significantly more support is often installed. It usually comprises the following:

- Fibercrete (minimum 50 mm) + rebars (backs) and friction anchors (walls); then:
- Mesh + friction anchors (backs + walls); and then maybe:
- An extra 50 mm of fibercrete.

The Q-system does not presently have a facility to assess ground behavior in potentially seismically active areas. Ground support design in such areas usually considers the toughness or energy absorption (kilojoules per square meter) capacity of the support system, rather than the support capacity of bolts in tonnes per square meter.

Vibration damage from large-stope production blasts is sometimes addressed in the same manner as seismicity. In addition to the support of credible or worst-case wedges defined by structures, it is usually sufficient to install mesh with friction anchor bolts in backs and walls that might be exposed to blast damage.

### OH&S Regulations

OH&S regulations and company policy often dictate the minimum support that must be installed, irrespective of ground conditions.

Under the “general duty of care” provisions of the Western Australian Mines Safety and Inspection Act 1994:

- “An employer must, as far as practicable, provide a work environment in which employees are not exposed to hazards and provide information, instruction, training and supervision;

- Employees must take reasonable care for their own safety and health, and that of others, at work; and
- Self-employed persons must, as far as practicable, ensure their work does not adversely affect the safety and health of others.”

In terms of human exposure to possible falls of ground, guidelines relating to the above provisions imply that “nobody is allowed to work beneath unsupported ground,” no matter how competent the ground may seem. Mining companies and the governments of the other Australian states have generally adopted this policy.

In terms of ground support requirements, guidelines relating to the above provisions imply that “all development backs must be scaled or adequately supported down to a height of 3.5 m, unless a report by a competent person justifies otherwise.” After firing, development backs in Australian mines are now either routinely meshed or sprayed with a minimum 50-mm thickness of fibercrete, then bolted.

The above regulations and policies also influence the choice of excavation support ratio (ESR) when determining ground support using the Q-system chart. There is a growing awareness in Australian mines that the appropriate minimum ESR value is 1.3 for all human-access development, whether it is permanent or just a temporary stope access, because miners must travel and work in both. The only difference to the installed support in permanent, versus temporary, openings might be the use of galvanized support elements and fully grouted bolts to improve their longevity. Recognition of the limited life of ground support is not embodied into the existing Q-system chart.

## HORIZONTAL DEVELOPMENT

Prior to the early 1980s, development openings in most Australian mines were typically small, up to 4.5 by 4.5 m, and often manually mined and supported. Backs were also often flat, and only a few bolt types were available and used, mostly 2.4-m mechanical point-anchored bolts. Openings were routinely check-scaled, and mesh was only used in exceptional circumstances.

When decline access and large trackless equipment became popular, development was mined and supported using multiboom jumbos and their size increased to be nominally 5.5 by 5.5 m. But this small increase in development width implied a large increase in the required support capacity (approximately 50%), which was partly offset by arching the development backs. Friction anchor bolts (often referred to as Split Sets) also became popular because they are cheaper (per unit), easily installed using the jumbo, and they are an excellent bolt to pin mesh tightly to irregular development backs and walls. However, they have a much lower end-anchorage capacity than point-anchored solid bar bolts.

Unless short friction anchors are used to just pin mesh, by inserting them in previously installed longer friction anchors, the minimum standard bolt length is typically 2.4 m. Ground support typically comprises a mix of friction anchors, solid rebar bolts, and cable dowels.

Falls of ground became more common. OH&S regulations were reviewed. Mines also began to focus on the design and adequacy of ground support.

Barton's Q database is dominated by civil engineering examples, not mining ones, where ground conditions can be more dynamic. It contains few, if any, cases from mining in Australia under the current legislative environment.

It is a significant challenge to provide adequate ground support for all of the diverse areas and situations in (underground metalliferous) mines all the time. Unlike most civil projects, ground conditions can change with time because of weathering and oxidation of minerals and the rock mass, variations in moisture content due to seasonal or ventilation changes, stress history, and/or damage to exposures due to nearby stope blasting, seismicity, etc.

### Previous Australian Studies

Mikula and Lee [2003] considered that "applying Q to a mine is like importing a knowledge database to a mine. Because the knowledge was compiled elsewhere, it should be confirmed to ensure relevance and correct use in the new environment." They reported that Q is a suitable design tool for assisting ground support selection at the Mt. Charlotte gold mine, provided appropriate stress reduction factor (SRF) values are used and allowance is made for stress field anisotropy.

An unpublished 1999–2002 survey of 183 km of development headings with spans of 4.0–5.5 m in 20 Australian mine sites concluded that significantly more support was being used than is recommended by the Q-system tunnel reinforcement design chart (after Grimstad and Barton [1993]). Support usage was obtained from warehouse documentation, and Q values were averaged over several months of mining development headings. Q values ranged from 34 to 0.01.

The following examples indicate that significant amounts of support are being used at some Australian mines:

- Development in ultramafic rock at depths in excess of 1 km, with average  $Q = 1.0$  and a minimum  $Q = 0.54$ . Support averaged 32 friction anchors (commonly called Split Sets) per meter advance plus 75 mm of fibercrete. This is about twice the number of friction anchors suggested by the Q chart for  $Q = 0.5$ , when the predicted number of solid bar bolts is converted to an equivalent number of friction anchors having the same support capacity.

- Development in folded and faulted Paleozoic volcanics at depths in excess of 900 m, with  $Q$  ranging between 6.0 and 16.2. Support averaged nine friction anchors per meter plus 50 mm of fibercrete. The Q chart suggests that minimal support is required, and to satisfy OH&S regulations the minimum back support is only about seven anchors plus mesh per meter advance.

A major shortcoming of the 1999–2002 survey was that actual support patterns were not correlated with specific ground conditions and actual Q values.

### Applicability of Q in Horizontal Development

A significant concern with the way the Australian mining industry has used the Q versus the equivalent dimension design chart [Grimstad and Barton 1993] has been the assumption that "bolts" referred to in the design chart has included friction anchors. However, the bolts in the Q chart were nominal 20-mm-diam solid mild steel bolts, fully grouted using either cement or resin.

Fortunately, there is a growing awareness in the Australian mining industry that pattern bolting using only friction anchors often provides insufficient support for many situations, and supplementary solid steel bars are required.

### Data Collection

The 1999–2002 survey mentioned above used averaged Q values. As this approach can skew the data, it has not been used below.

General mine-wide databases of ground condition versus minimum support standards have also been ignored. It is was considered that company policy and government OH&S requirements dictate the quantity of ground support installed. This is especially a concern in good-quality rock, which might not technically require support to ensure the stability of some openings.

This survey uses specific Q values determined by mapping at the same location where the actual installed support was also recorded. To maximize the impact of the local ground conditions for support selection, numerous sites in the poorer rock classes were included, especially where the following was true:

- The installed support was considered to be just sufficient for the ground conditions; or
- There had been a fall of ground and the support had been upgraded.

The database contains 59 data sets from 15 mine sites drawn from all six Australian states and the Northern Territory. Nearly all of the data apply to 5.5-m-wide and variably arched development.

## Installed Support Capacity Versus Q

The end-anchored capacity (at yield) of installed support was calculated in tonnes per meter squared. The following assumptions were used for the three commonly installed support types:

- Friction anchors = 3 tonnes
- Solid bar bolts = 15 tonnes
- Cable dowels = 21 tonnes

No capacity allowance was made for mesh or fibercrete, as they rarely extend down the walls to invert level, often stopping about 3 m above floor level. Their main function is to retain loosened pieces of rock and transfer the weight of loosened blocks to the rock bolts. Except in areas prone to seismicity, both are often capable of supporting the deadweight of any loose material or small wedges that might develop between reasonably spaced bolt collars.

*Q* values are plotted against the installed support capacities in Figure 2. In four cases, two data points plot on top of each other.

While one might expect the installed support capacity to vary inversely with the *Q* values, there is significant scatter in Figure 2, particularly in the 30 data points at bolt capacities less than 3 t/m<sup>2</sup>. Friction anchors were used at 27 of these 30 sites.

The almost Australia-wide requirement (government OH&S regulations and/or company policy) for backs to be screened and supported (with either mesh plus bolts or fibercrete plus bolts) implies a minimum bolting pattern of either 1.1 m by 1.1 m or 1.1 m by 1.4 m for either 2.4-m

by 2.4-m or 2.4-m by 3.0-m mesh, allowing for overlap. Thus, if only friction anchors are used, the minimum end-anchored bolt capacity is in the range of 2–2.5 t/m<sup>2</sup>.

The data in Figure 2 show that a bolt capacity of less than 3 t/m<sup>2</sup> was used in some Australian mines for *Q* values ranging from 90 to 0.3, and the *Q*-system predicted support capacity is up to several times the actual installed capacity. The extent to which this is the result of substituting friction anchors for the solid bar bolts intended by Grimstad and Barton's 1993 chart is unknown.

As only 3 sites in this group of 30 sites required rehabilitation, it is possible that local site experience has shown that some sites are sufficiently stable for mining purposes with less support than predicted by the *Q*-system. Alternatively, the *Q* values may have been optimistically estimated.

There is a large zone in Figure 2 where the installed support capacity is less than half the empirical predicted requirements. There is also a diagonal band where the ratio of actual to predicted support capacity ranges from 0.5 to <3.0. Finally, there is a zone where the ratio of the installed to predicted support capacity exceeds 3.0.

If *Q* values have been accurately assessed and if it can be assumed that the installed support is just adequate, the data in Figure 2 suggest that there is a tendency in the Australian mining environment for the *Q*-system to underestimate the support required for the "good" and "very good" rock classes, probably due to the OH&S considerations discussed above, and to overestimate support requirements for "poor" to "extremely poor" rock classes.

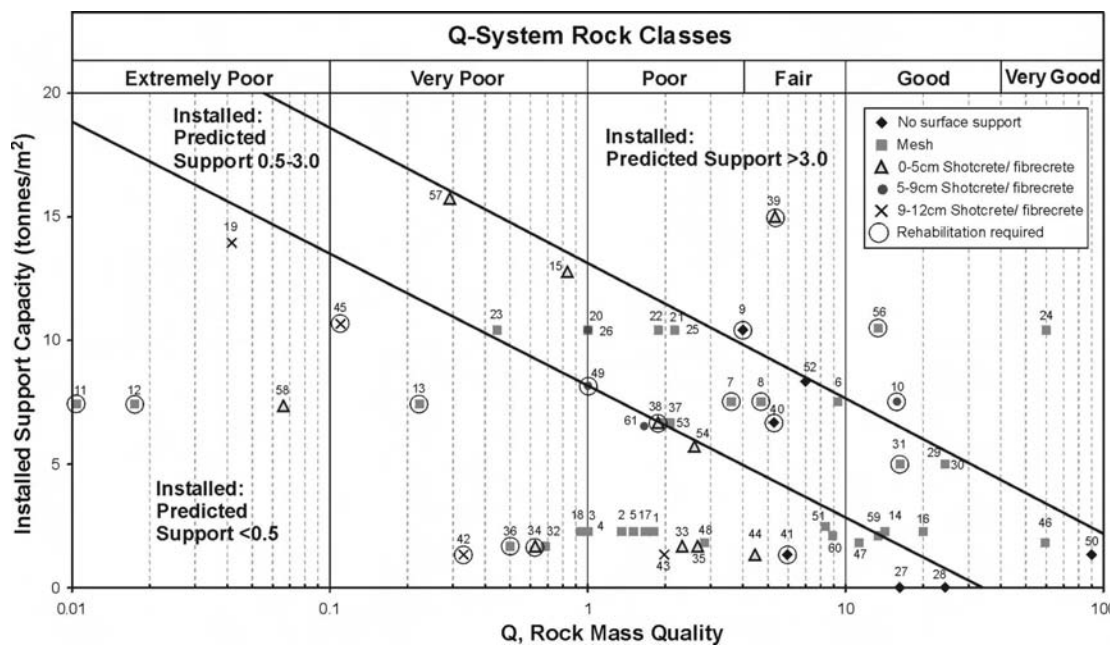


Figure 2.—Installed support capacity versus *Q*.

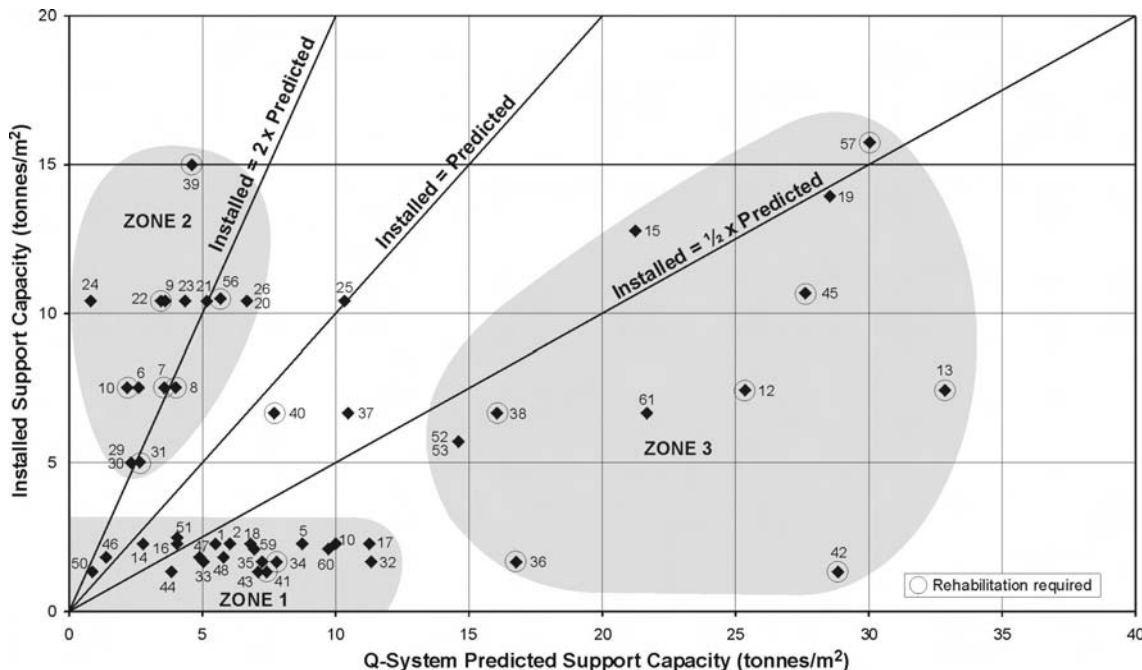


Figure 3.—Installed versus Q-predicted support capacities.

### Installed Versus Predicted Support Capacity

Predicted support capacity, P, has been calculated in tonnes of required bolt capacity per square meter prior to bolt yield, using the following relationships involving Q,  $J_n$ , and  $J_r$  published by Barton et al. [1974]:

$$P = (20 J_n^{1/2} Q^{-1/3}) / 3 J_r \text{ (for fewer than three joint sets, } J_n < 9) \quad (1)$$

$$P = (20 Q^{-1/3}) / J_r \text{ (for three or more joint sets, } J_n \geq 9) \quad (2)$$

Installed versus predicted support capacities are shown in 3 of the 15 surveyed mines (Figure 3). The cases where resupport was needed as part of a rehabilitation program have been highlighted.

It can be immediately recognized that only a few of the data points plot close to the line representing the condition where the predicted support requirements were matched by what the mine actually used. For ease of discussion, three general areas, or zones, have been delineated.

- Zone 1 contains those data points where the actual installed support capacity is less than 3 t/m<sup>2</sup> and the Q-system predicted support capacity was less than 12 t/m<sup>2</sup>.
- Zone 2 contains data where the installed support is greater than predicted.
- Zone 3 contains data points where the installed support is less than predicted.

### Zone 1

There are 23 data points within Zone 1, all of which have used friction anchors and 21 of which are sites shallower than 500 m depth. Only three sites plot close to the line, indicating that the predicted support capacity equals that actually used. Although the remaining 20 sites have predicted support capacity requirements up to five times the installed support capacity, only two of them required rehabilitation. This suggests that at depths of less than 500 m, local site experience should be used in conjunction with the Q-system to dimension ground support requirements for mines.

### Zone 2

There are 16 points in Zone 2, 12 of which are located at depths >900 m; 3 of the 12 have required rehabilitation. SRF values used by the site technical staff are regarded as being low, but SRF values suggested by strength versus stress relationships do not move these data points much closer to the line where the installed support capacity equals that predicted by the Q-system. All 12 sites experienced high stresses, and some experienced seismic events.

The remaining four data points in Zone 2 occur at depths of 200–550 m, and all required rehabilitation. The SRF values at three of them have been underestimated, but only in one case is the revision sufficient to get the predicted support capacity within 50% of that actually used.

## Zone 3

There are 12 data points in Zone 3 at depths ranging between 145 and 1,600 m, 7 of which required rehabilitation. This is not surprising at three sites where the installed support capacity was less than 25% of the predicted support capacity required.

### Suggested Modifications to Q-system Investigations

In a number of the cases already discussed, both the predicted support requirement and the SRF seem to have been underestimated. While underestimation of the SRF does not seem to be the sole reason for underestimating support requirements, it is significant. Peck [2000] discusses the problem of determining the SRF of highly stressed, jointed rock. The authors strongly recommend that practitioners calculate the support requirement using Barton's 1974 equations (see Equations 1–2 above), particularly as friction anchors are not considered in the Grimstad and Barton 1993 chart.

## RAISE-BORED SHAFTS

Working in vertical openings is recognized as being more hazardous than horizontal development. Thus, there has been a concerted effort in Australia to reduce miners' exposure to vertical openings [Minahan 1974].

If a raise-bored shaft can be successfully completed without damage to, or loss of, the in-hole equipment, the potential savings over conventional shaft sinking can be up to about 30%. Unfortunately, raise boring in Australia has not been universally successful, and failures can be very expensive in terms of lost equipment and delays to production. Not only have some raises collapsed during reaming, some of the 310-mm-diam pilot holes have also been lost. Methods of reliably assessing the unaided stability of raise-bored shafts are therefore required.

The McCracken and Stacey [1989] method of assessing geotechnical risk for large-diameter raise-bored shafts has been widely used in Australia. It was successfully applied in 1989 to the planned Airshaft No. 5 at Broken Hill. The method predicted severe instability if raise boring was attempted at the planned 6-m diameter. Some overbreak was even predicted at a raise-bore diameter of 1.8 m. The method gained significant credibility when the predicted overbreak occurred during reaming at 1.8 m diameter prior to enlargement to 6.7 m by V-moling [Bennet and de Bruin 1993].

## McCracken and Stacey Method

McCracken and Stacey [1989] applied the principles of the Q-system [Barton et al. 1974] to the problem of assessing raise-bore stability following the collapse of a number of large-diameter shafts during raise boring. The Q-system had developed a relationship between Q and the Maximum Stable Unsupported Span (MSUS). Additionally, the Q-system had established the ESR to account for different degrees of allowable instability based on excavation service life and usage. McCracken and Stacey used these concepts to develop the relationship between Raise Rock Quality ( $Q_r$ ) and the maximum stable raise diameter (Figure 4).  $Q_r$  is based on the Q value obtained using Kirsten's [1983] approach to determine the SRF, with further corrections to accommodate adversely oriented sets of discontinuities, weathering, and alteration.

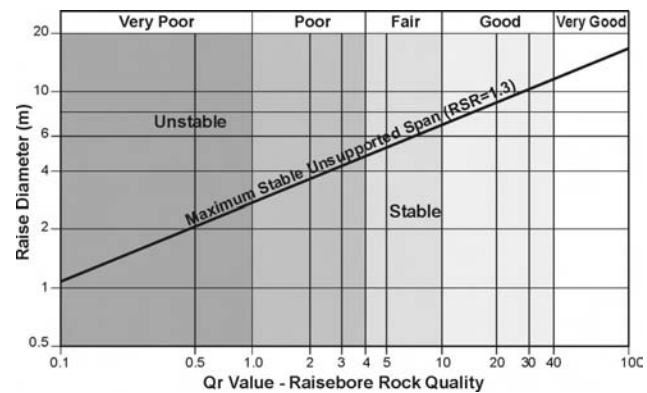


Figure 4.— $Q_r$ , raise diameter and stability (after McCracken and Stacey [1989]).

Kirsten [1983] developed a relationship between the SRF and the extent to which the rock is overstressed. His approach calculates an SRF value for the ground stress condition and another value for rock mass loosening and uses whichever SRF value is greater. Peck [2000] published similar SRF equations for Australian conditions.

Figure 4 demonstrates that the required  $Q_r$  value for stability significantly increases with increasing raise diameter. While a 2-m raise is likely to be stable in poor-quality rock ( $Q_r = 1$  to 4), a 5-m raise requires fair-quality rock and a 6-m raise requires fair- to good-quality rock ( $Q_r > 8$ ). McCracken and Stacey also defined raise-bore rock quality in terms of block size ( $RQD/J_n$ ) and low inter-block shear strength ( $J_r/J_a$ ). Their paper drew attention to the fact that problems may be expected in large-diameter raises if the critical parameter values for  $RQD/J_n$  and  $J_r/J_a$  are poor or worse, using the guidelines they published.

## Stability and Standup Time

Ideally, raises should be located in rock and sized so that they are permanently stable. Unfortunately, this is not always possible, and progressively larger raises are being bored as equipment is being improved.

While the Q database contains no shafts or raises, it does include data for walls of caverns. Bored shafts and raises with their circular cross-sections are inherently more stable than planar cavern walls. Different ESRs might also be more applicable to shaft walls (often progressively exposed, manually supported, and then permanently lined) than bored raises, which must often be permanently stable immediately after exposure.

Standup time is also important. Where a raise has intersected a marginally stable horizon, several weeks may elapse before it can be supported, e.g., by either installing a lining, manually bolting the raise walls, or remotely spraying fibercrete. In some cases, prereinforcement of marginally stable sections is also possible.

Unstable rock excavations without support will collapse in time, ranging from less than an hour to more than a year. The time-dependent behavior of unstable rock masses is complex and as yet poorly understood. The Q-system does not include any correlation between Q values and standup times.

Bieniawski [1993] published a correlation between the span of an opening, maximum standup time, and RMR value based on a study of a large number of mine openings and tunnels. Unfortunately, RMR values are not easily related to Q values, as not all of the same parameters are used to assess rock quality. For example, only Q gives a rating for the ground stress condition, while only RMR rates the persistence or continuity of the individual rock defects such as joints.

Bieniawski's chart suggests that to stand unsupported for 6 months, a 3-m span needs an RMR of at least 58 and a 6-m span requires an RMR of at least 64. As the RMR system rates good rock as having values between 61 and 80, fair to good rock is needed for 3- to 6-m spans to stand unsupported for 6 months.

## Lower-bound Geotechnical Conditions

The lower-bound  $Q_r$  value is a key geotechnical parameter in the McCracken and Stacey method of determining the maximum diameter at which a raise can be reamed without exceeding the acceptable probability of failure. Unfortunately, they did not define the logging intervals, which is perhaps relative to the intended raise diameter, over which the lower-bound  $Q_r$  value should apply. For example, a 1-m-thick sheared or blocky zone might give a very low  $Q_r$  value, but when it is included with 4 m of good-quality rock, the average may be greater than the lower-bound  $Q_r$ . The orientation and thickness of the sheared or broken zone are also important. A 1-m-thick

sheared zone may be of no consequence if it is shallow-dipping and confined between good-quality rock. Conversely, a thin, weak, and continuous steeply dipping structure within a poor zone may control significant unraveling.

Figure 5 shows two images from closed-circuit television monitoring of the walls of a recently completed and unlined raise. Figure 5A shows the relatively smooth raise walls in a section of the raise where no overbreak has occurred. Figure 5B shows the result of overbreak along joints.

Comparisons of preexcavation borehole logs with video camera inspections of completed raises has enabled estimates to be made of the minimum thickness of poor-quality rock in otherwise good-quality rock, which is needed to destabilize the walls of a raise.

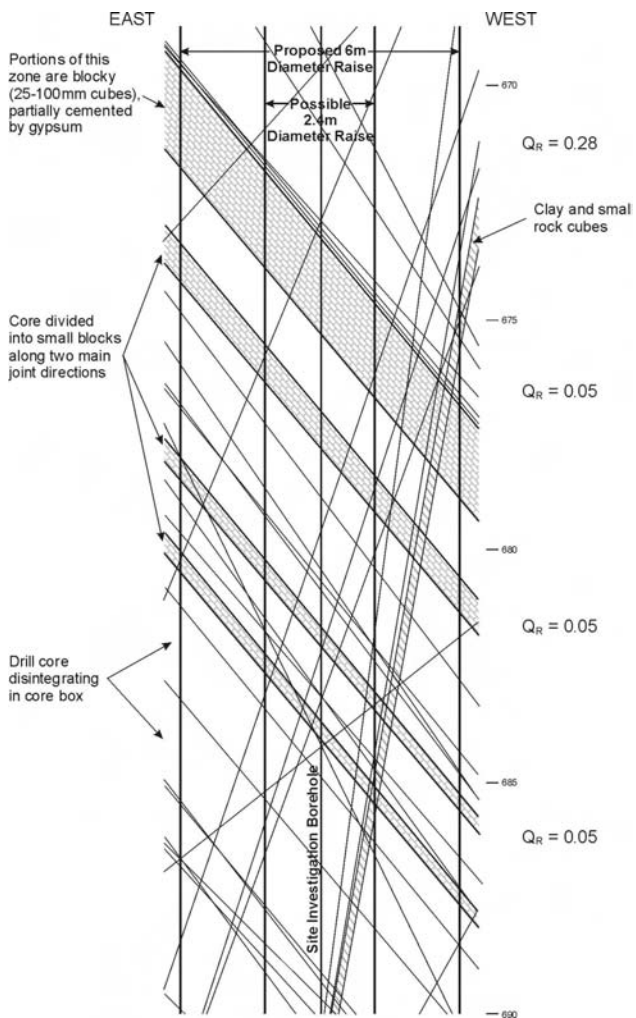


Figure 5.—No overbreak (A) versus overbreak (B) in a raise-bored shaft.

While thin shears and zones of blocky rock might produce some localized overbreak, zones of poor-quality rock need to be greater than 3 m to significantly impact the stability of raise walls. It is therefore recommended that core logging and analysis be done over lengths of about 1–1.5 m. Raise stability assessments should then use “rolling average” techniques to average rock quality over 3-m increments, i.e., to calculate lower-bound  $Q_r$  values.

### Stability Assessment

McCracken and Stacey stated that the preliminary geotechnical assessment should be aimed at determining the average and lower-bound geotechnical conditions: “The range and distribution of the raise-bore rock quality  $Q_r$ , and the most important  $RQD/J_n$  and  $J_r/J_a$  parameters must be compared to the required minima for stability at the proposed shaft diameter.” It is not sufficient to simply look at the variation of MSUS with depth.



**Figure 6.—Detailed stability analysis for a proposed raise.**

“At the preliminary evaluation stage the risk should only be deemed ‘acceptable’ if the tunnelling quality is consistently indicated to significantly exceed (i.e., be in the next class up from), the required quality throughout its length.” Their paper goes on to state that marginal cases occur where the indicated quality  $Q_r$  either straddles the required value for stability or is not confidently known.

McCracken and Stacey also state: “In addition to simply assessing the range of predicted  $Q_r$  values against those required, the rock mass properties and discontinuity orientations would be used as input to detailed stability analysis.”

Figure 6 presents a detailed analysis for a proposed large-diameter raise where the apparent dip is shown for every discontinuity that had not been rehealed. The core was obtained from a diamond drill hole bored down the proposed alignment of the raise and was oriented using the metamorphic foliation, which was known to have a consistent orientation in that part of the mine.

This example is from the 1989 analysis for Airshaft No. 5 at Broken Hill. The small joint-block sizes within some structures, the numerous steeply dipping joints with low-friction coatings, such as talc, and the rapid deterioration of some of the core in the core boxes clearly indicated the potential to collapse if bored at 6 m diameter. Overbreak occurred in the interval shown in Figure 6 when it was raise-bored at a diameter of 1.8 m. However, this overbreak was not sufficient to cause general collapse prior to enlargement of the raise by V-moling and lining.

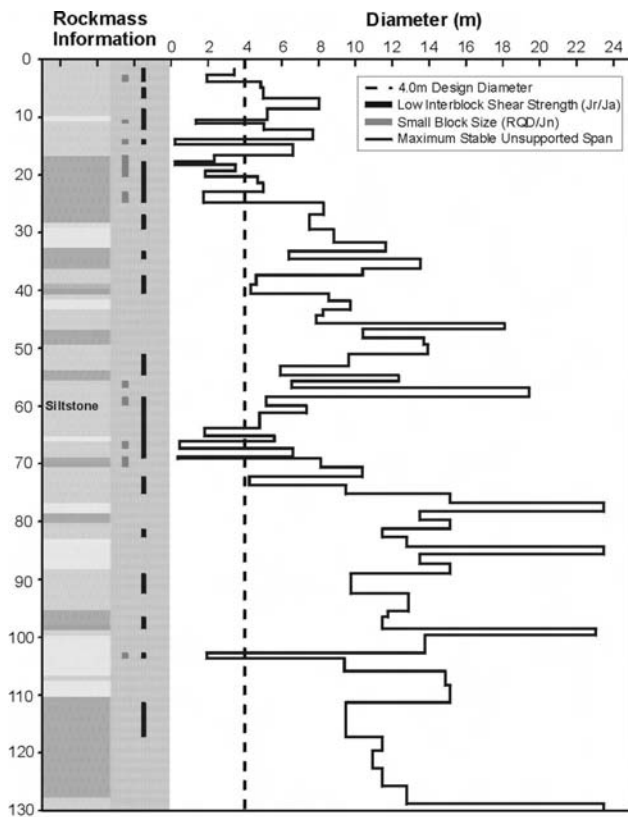
### Presenting McCracken and Stacey Results

Figure 7 presents a typical plot of MSUS (expressed as a diameter) versus depth. Zones having small block size and low interblock shear strength have been identified. Two potentially unstable zones are identified, the first at the shaft collar (0–25 m) and the second between 60 and 70 m. Both were reinforced prior to raise boring. A 1-m-thick zone with an MSUS of only 2 m occurs at a depth of about 103 m. The  $Q_r$  value in this zone is only 0.5, but the  $Q_r$  values above and below it are of the order of 25. It was concluded that these zones would provide adequate stability for the thin weak layer. The raise was successfully bored at the planned 4-m diameter.

### Highly Stressed Rock

In highly stressed rock, induced rock fracturing can occur in advance of the reaming head and in opposite walls of the completed raise. The generation of loose slabs at the cutting face can mean overbreak of large blocks into the cutters. Then high and irregular torque on the drilling string is possible during reaming.

Stacey and Harte [1989] described this failure mechanism for raises at depths in excess of 2 km in southern Africa. They analyzed spontaneous fracturing ahead of the



**Figure 7.—Typical plot of MSUS (diameter) and critical rock quality.**

face and derived a means of predicting its extent. O'Toole and Sidea [2005] demonstrated that significant fracturing was possible ahead of the raise-bore face at depths of 880 m in Australia.

High or deviatoric horizontal stresses can mean very high and low stresses around the raise wall. Both can assist loosening of rock masses by local shearing and dilation on joints. Deep high-stress fracturing and overbreak are possible where wall stresses exceed the strength of the rock mass. Rock mass strength can vary with rock type and blockiness, but it is typically half the strength of intact rock [Lee et al. 2001].

O'Toole and Sidea [2005] concluded: “[D]ue to the high risk of in-hole equipment damage and increased maintenance, the full costs associated with raise boring in highly stressed rock are likely to be significantly higher than reaming the equivalent strength rock in a low-stress environment.”

The use of stress/strength-based SRF values in the McCracken and Stacey method and the consequential reduction in  $Q_r$  values should alert geotechnical engineers to the existence of potential high-stress issues. It is now common for raise-boring contractors to torque-limit their machines. It may occasionally be necessary to lower the

cutting head and remove large slabs of rock from the cutting head whenever high torque demand is reported.

Postconstruction videos of raise walls are also becoming increasing common in Australia to compare predicted and actual performance. Selected wall support may be necessary and can be provided by remotely spraying fibercrete.

### Contrasting Face Conditions

When the raise-bore reaming head encounters a steeply dipping interface between rocks of contrasting strength, such as weak siltstone overlain by a steeply dipping strong sandstone, the head attempts to remain in the weaker material. This generates unbalanced forces that cause the head to tilt and the raise-bore drill rods to bend. Mechanical failure of the head or drill rods is possible, sometimes with the head plus rods falling to the bottom of the raise.

The McCracken and Stacey method does not provide any warning of this possibility. Other geotechnical investigations are required to complement Q-based analyses.

### Australian Raise Performance Versus Predicted $Q_r$

A database of Australia raise-boring experience has been compiled and is plotted in Figure 8. It comprises 47 data points of raise diameter, actual performance and component  $Q$  values for lower-bound  $Q_r$  situations from 23 mine sites in Australia and Papua New Guinea. All of the raises plotted are known to at least one of the authors who also had access to the site investigation reports and borehole logs. For consistency, the lower-bound  $Q_r$  values data presented in Figure 8 were determined by the authors using a “rolling average” of 3-m increments, as described above.

The following trends are illustrated in Figure 8:

- For lower-bound  $Q_r$  values of less than 0.10, there is a high chance (9 in 10) of raise collapse or significant overbreak, irrespective of the proposed raise diameter.
- For raise diameters between 3 and 6 m and if the lower-bound  $Q_r$  value is between 0.1 and 1.0, raise-bore performance ranges from stable to collapsed. A detailed stability analysis is recommended using the McCracken and Stacey method.
- For a raise diameter of less than 5 m and a lower-bound  $Q_r$  value greater than 1.0, there is an excellent chance of constructing a stable raise (10 stable and 3 stable with support, out of 13). A detailed stability analysis should still be carried out if the rock structure rating (RSR) is greater than 1.3 for the desired raise diameter.

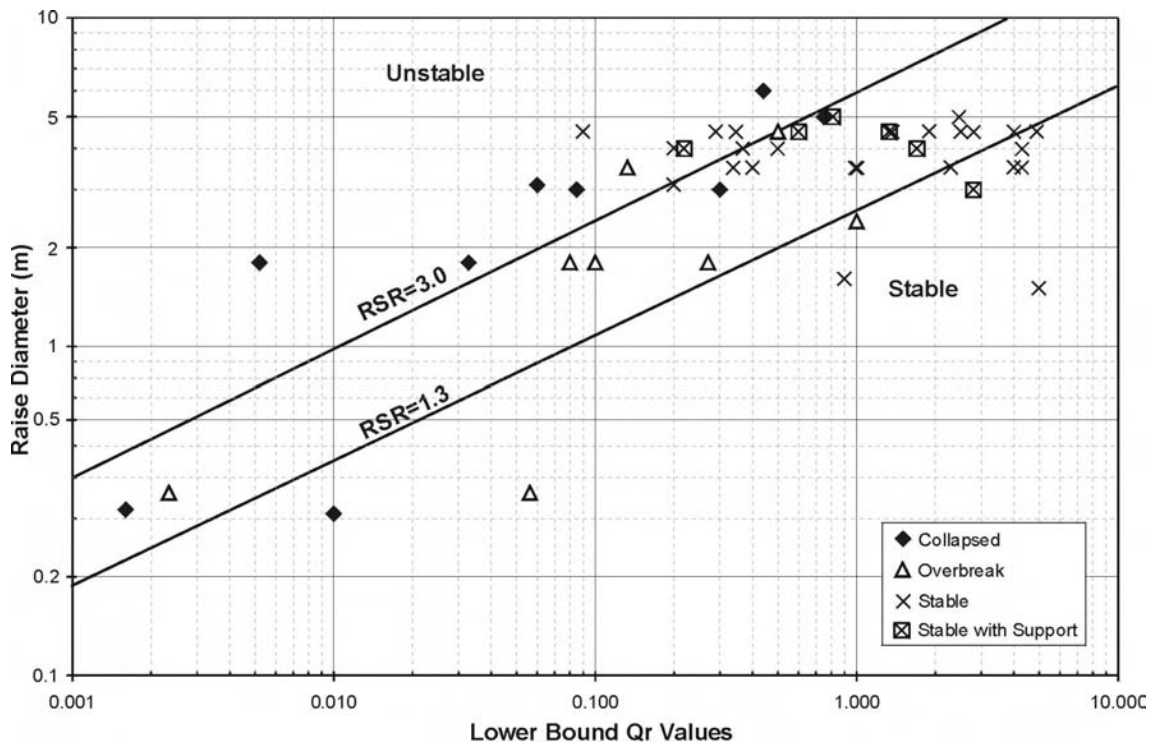


**Figure 8.—Raise-bore diameter versus lower-bound  $Q_r$  values.**

- There are 11 data points on the unstable side of  $RSR = 3.0$ , including 5 collapsed raises. McCracken and Stacey considered there was a probability of failure of 1 in 4 for an  $RSR = 3.0$ .

The intermingling of collapsed and stable raises for  $Q_r$  values between 0.05 and 1.0 and  $RSR \geq 2.0$  demonstrates the need to acquire and closely consider additional geotechnical data for these cases. This was recommended by McCracken and Stacey where the proposed raise plotted on the unstable side of  $RSR = 1.3$ .

## CONCLUSIONS

Despite the harsh geotechnical environment in many Australian underground metal mines, there is a reasonable correlation between actual ground performance and  $Q$  and  $Q_r$  values. However,  $Q$  and  $Q_r$  are not always conclusive if considered in isolation from other rock mass parameters. While significantly less support is being used in some areas than is indicated by the  $Q$ -system, there are other areas where much more support is required than the  $Q$ -system would indicate, e.g., deeper than 900 m below surface.

The calculated MSUS does not always indicate actual raise stability and additional investigation is required, particularly in cases of marginal stability. For these

situations, greater emphasis should be given to the ratios  $RQD/J_n$ ,  $J_r/J_a$ , and  $\sigma_c/\sigma_1$  and the possibility of time-dependent behavior of some joint infillings, such as gypsum, chlorite, sericite, and talc.

Although there are several deficiencies for special cases, it is concluded that the  $Q$ -system is a suitable method of assessing rock mass conditions. It can be used to assess the likely stability of openings and the selection of ground support requirements, provided appropriate SRF values are used and other geotechnical parameters are considered in conjunction with  $Q$  and  $Q_r$ . Local site experience is a valuable component of the process.

## ACKNOWLEDGMENTS

The authors wish to acknowledge the many and varied helpful inputs from our colleagues at AMC Consultants Pty. Ltd. We also wish to acknowledge the support of the management of the 23 mines that kindly supplied valuable data to this research and the contributions from our professional colleagues who are members of the Eastern Australia Ground Control Group (Marnie Pascoe, Chair; Andrew Campbell, Secretary).

## REFERENCES

- Barton N, Lien R, Lunde J [1974]. Engineering classification of rock masses for the design of tunnel support. *Rock Mech* 6(4):189–236.
- Bennet AG, de Bruin NJH [1993]. Investigation and development of Pasminco No. 5 ventilation shaft, Broken Hill. In: Proceedings of the Eighth Australian Tunnelling Conference (Sydney, New South Wales, Australia). Australasian Institute of Mining and Metallurgy (AusIMM), pp. 55–63.
- Bieniawski ZT [1993]. Classification of rock masses for engineering: the RMR system and future trends. In: Hudson J, ed. *Comprehensive rock engineering*. Vol. 3. Pergamon Press, pp. 553–573.
- Grimstad E, Barton N [1993]. Updating the Q-system for NMT. In: Kompen, Opsahl, Berg, eds. *Proceedings of the International Symposium on Sprayed Concrete*. Oslo, Norway: Norwegian Concrete Association.
- Kirsten HAD [1983]. The combined Q-NATM system: the design and specification of primary tunnel support. *S Afr Tunnelling* 6(1).
- Lee MF, Mollison LJ, Mikula PM, Pascoe MJ [2006]. In situ rock stress measurements in western Australia's Yilgarn Craton. In: *Proceedings of the International Symposium on In Situ Rock Stress* (Trondheim, Norway, June 18–24, 2006). International Society for Rock Mechanics.
- Lee MF, Pascoe MJ, Mikula PA [2001]. Virgin rock stresses versus rock mass strength in western Australia's Yilgarn Greenstones. In: *Proceedings of the Western Australia Ground Control Workshop* (Perth, Western Australia, June 22, 2001).
- McCracken A, Stacey TR [1989]. Geotechnical risk assessment of large diameter raise-bored shafts. *Shaft Engineering*, Inst Min Met, pp. 309–316.
- Mikula PA, Lee MF [2003]. Confirmation of Q classification for use at Mt. Charlotte mine. In: *Proceedings of the First Australasian Ground Control in Mining Conference* (Sydney, New South Wales, Australia, November 11–12, 2003), pp. 179–183.
- Minahan PJ [1974]. The impact of raiseboring on a major mining operation. AusIMM Regional Meeting on Recent Technical and Social Advances in the North Australian Minerals Industry, Mount Isa.
- O'Toole D, Sidea D [2005]. Recent developments in Australian shaft excavation practice: raise bored shafts in highly stressed rock. In: *Proceedings of the Ninth Underground Operators' Conference* (Perth, Western Australia, March 7–9, 2005). Australasian Institute of Mining and Metallurgy (AusIMM), pp. 29–32.
- Peck WA [2000]. Determining the stress reduction factor in highly stressed jointed rock. *Aust Geomech* 35(2).
- Stacey TR, Harte ND [1989]. Deep level raise boring: prediction of rock problems. In: Maury V, Fourmaintraux D, eds. *Rock at great depth*. Rotterdam, Netherlands: Balkema, pp. 583–588.

# ROCK MASS CLASSIFICATION IN GERMAN HARD-COAL MINING: STANDARDS AND APPLICATION

By Holger Witthaus, Dr.-Ing.,<sup>1</sup> and Nikolaos Polysos, Dr. rer. nat.<sup>1</sup>

## INTRODUCTION

The classification system for German coal mining is the result of approximately 100 years of experience in roadway development and longwall mining. It is also based on different research projects covered by national and European research programs.

Over the past 30 years, more than 600,000 m of roadways have been driven and employed for mining activities. To properly describe the German rock mass classification system, therefore, it is useful to take a look at the main geomechanical preferences and common support systems.

The decision about the most effective development technique and support system is based on a synthesis of rock mass classification and geomechanical analysis. The properties of surrounding rock, the in situ stress, and the influence of mining activities in several seams at each German mine must be considered for the evaluation of the expected deformation of the roadway.

The mine layout, the requirements of ventilation and fire prevention, as well as the need to maintain emergency escape routes for the miners, require that the gate roads remain usable after the passage of the longwall face in most cases. Moreover, the gate roads must be maintained despite the high stresses that are applied during longwall retreat mining. Therefore, gate road design must address a broad spectrum of potential deformation environments.

In the past, when gate roads were supported solely with yielding steel arches, lithologic descriptions of the surrounding strata conditions were adequate for the dimensioning of support and the prediction of the roadway deformation. The current conditions of multiple-seam mining at depths of up to 1,700 m require combined support systems, including pattern bolting and backfilled steel arches.

Rock bolt support is used for development, after which (typically 50–100 m outby the face) the steel arches are installed and backfilled with building material (concrete) in order to achieve an optimized development rate.

The rock mass classification system described below was developed especially for the conditions of German hard-coal mining. It includes the stress distribution caused by multiseam workings (including crossing goaf edges of former longwalls), as well as in situ stresses due to great

depth and the presence of tectonic faults. It is based on the evaluation of four parameters:

- Geotechnical analysis of drill cores
- Geotechnical observation of the development face
- Geotechnical classification of tectonic structures (faults)
- Standard classification derived from geotechnical assessment and evaluation of stress conditions (using numerical modeling for stress calculation)

## ROCK STRENGTH

One of the most important input parameters for describing strata conditions is the strength of the rock. The German classification system is based on a description of lithotypes. This method has been used successfully since the 1950s and is based mainly on the uniaxial compressive strength (UCS) of the material.

An evaluation of the rock strength observed in a survey of approximately 82,500 samples of rock core yielded the results shown in Figure 1. The three most common coal measure rock types are mudstone, siltstone, and sandstone. Each shows a specific mean UCS level and a different spread between the minimum and maximum values. Sandstones, in particular, have a wide spectrum of compressive strength, ranging from approximately 40 MPa to greater than 130 MPa, with an average of 85 MPa. The causes of this wide range include different sedimentological preconditions, facies, and diagenetic processes.

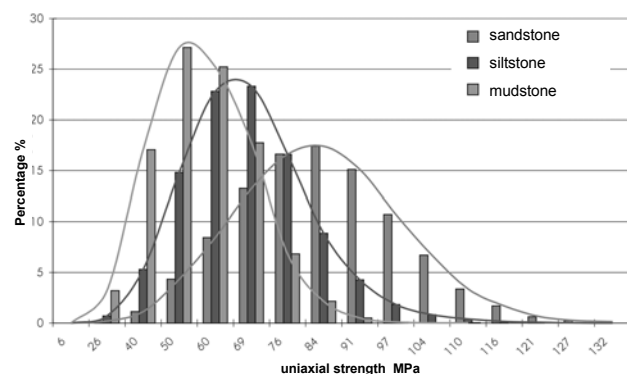


Figure 1.—Frequency distribution of uniaxial strength for typical lithotypes from German coal mines.

<sup>1</sup>Certified expert in geomechanics and support systems, Deutsche Steinkohle AG (DSK), Herne, Germany.

## GEOTECHNICAL ROCK EVALUATION

The assessment of strata conditions, which can be conducted either by analyzing drill cores or by evaluating the development face, requires data on 14 parameters. Figure 2 gives an overview of this system of rock evaluation. Each parameter is rated as “poor,” “mean,” or “good,” depending on the characteristic that is being analyzed. For example, the intensity of stratification is rated according to the structure of bedding, as follows:

- *Good conditions:* No significant stratification or no regular stratification;
- *Mean conditions:* Some typical regular bedding areas; or

- *Poor conditions:* Regular stratification of thin beds in a banded bedding structure.

While parameters 1–8 and 13 can be determined either from drill core or from observations made in the headings, parameters 9–12 and 14 can only be obtained from underground observations.

The evaluation focuses on the rock properties to provide some idea of the rock strength, the character of the stratification, and the description of separation. These elements are used for description of the expected deformation of a roadway under the influence of high stress.

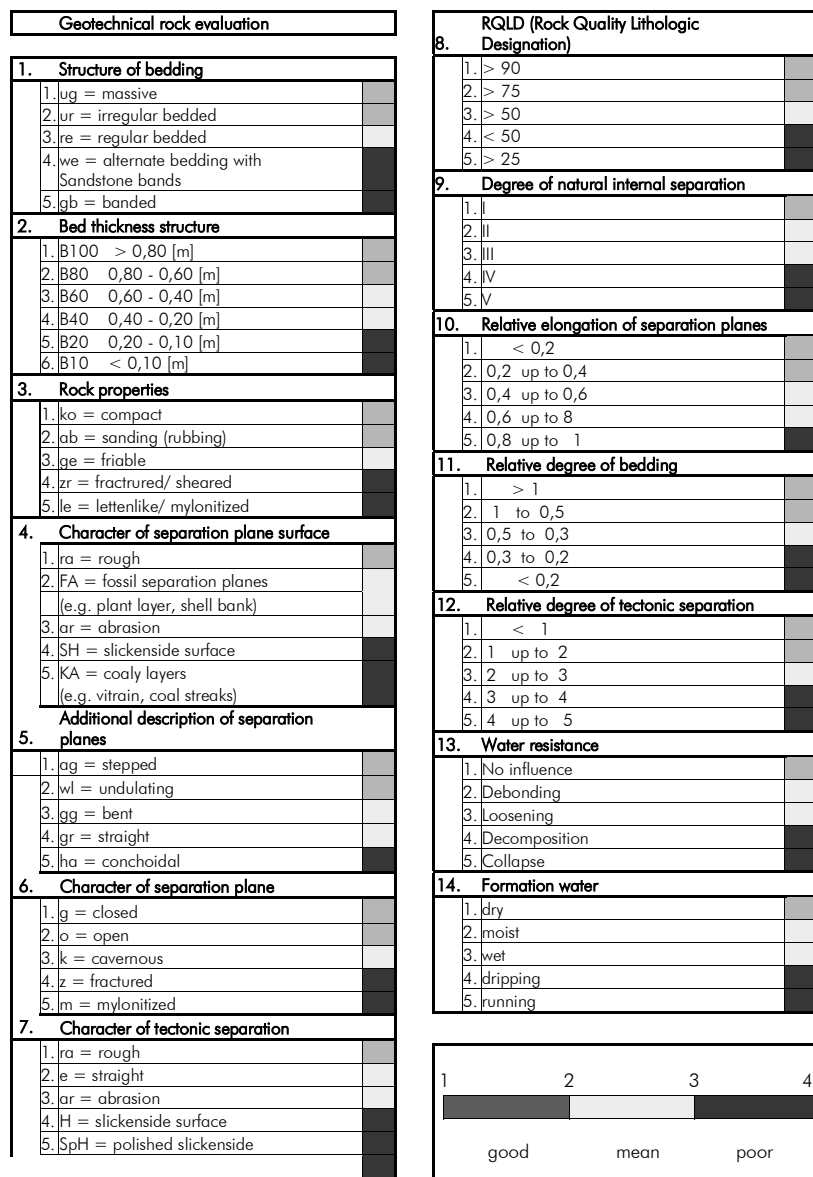


Figure 2.—Matrix for geotechnical rock evaluation.

The strata evaluation is conducted in three areas around a roadway:

- The floor area (0–6 m below the roadway);
- The mined strata (between floor and roof of the roadway); and
- The roof area (0–6 m above the roof of the roadway).

For larger roadways, with widths of more than 6 m, the area evaluated is increased to a distance equal to the roadway width above and below the roadway.

### RATING STRUCTURAL FAULTS

The typical German hard-coal deposit includes a lot of tectonic faults. The panel layout has to consider these features, but, in some cases, it is not possible to avoid having a longwall cross a fault. Experience has shown that faults can cause a wide range of effects on the mining process and the supports. The rating matrix shown in Figure 3 was developed to evaluate faults. The fault classification is based on a geometrical description of the fault itself, together with underground observations of the separation and strength of surrounding strata.

The objective of the fault classification is to provide an idea of the consequences for the roadway, in terms of the expected deformation and support requirements for the

face and the face entry T-junction, in the area of the tectonically disturbed strata.

### ROCK MASS CLASSIFICATION USING BOREHOLE GEOPHYSICS

Data collection for classification includes applied geophysical methods. Borehole geophysics provides information about the lithologic and physical parameters of the strata.

The most important geophysical logs include natural gamma, density, electrical resistance, seismic velocity and reflection, acoustic imaging, and caliper. By combining these logs and processing them together with information about the lithology, it is possible to obtain data on the structure of the rock mass, the elastic parameters of rock, and the location and properties of weak areas. Table 1 gives an overview of the criteria used in the geophysical classification of coal measure strata in German coal mines.

### EVALUATION AND REPORTING OF GEOTECHNICAL PARAMETERS

The strata assessment method described above allows a comparison between geotechnical data derived from drill core and underground observations made in the headings. The results can be used to optimize the support system. In addition, the universal character of the classification method allows for a broad range of applications, including:

Mine:			
Exploration:			
Drilling depth/roadway section:			
Fault type/displacement:	Good	Medium	Poor
Strike relative to direction of drivage	perpendicular	diagonal	parallel
Dip relative to direction of drivage	in	against	transverse
Width of fault relative to roadway width (W)	< 1 W	1 W	> 1 W
Fault characteristic	Slickenside surface	Fractured zone	Gouge zone
Tectonic stress of rock strata	low	medium	strong
Fault associated structure	parallel	diagonal	perpendicular
Structure characteristics	Slickenside surface	Fractured zone	Gouge zone
Water delivery	dry	moist	trickling
Seam distance	W heading face	W floor	W roof
Potential caving	$\leq \frac{1}{4} W$	Up to $\frac{1}{2} W$	$\geq 1 W$
Degree of rock separation (ahead of fault)	II	III	IV
Degree of rock separation (beyond fault)	II	III	IV
Rock strength ( $N/mm^2$ )	$\geq 67$	66–41	$\leq 40$
Roof			
Heading face			
Floor			

Figure 3.—Geotechnical fault rating matrix.

**Table 1.—Criteria for geophysical classification of coal measure rock in German mines**

	Classification		
	Good	Mean	Poor
Caliper (mm).....	127–128	127–135	130–135
Stiffness modulus M (GPa) .....	90–95	40–50	<40
FEL (Ωm).....	1.5–1.9	1.3–1.5	<1.4
DipLog Spur 1.....	<9,000 (FEL > 1.6 and reflectivity >2,000)	9,000–11,000	>11,000 (FEL <1.3 and reflectivity <1,700)
BHTV reflectivity .....	1,700–2,500	1,300–1,700	<1,300
dtvp (μsec/m).....	260–230	260–230	>250
dtvs (μsec/m).....	350–410	450–410	>430
Density (g/cm <sup>3</sup> ) .....	2.6–2.7	2.5–2.6	2–2.5

- Estimation of critical support loads;
  - Analysis of strata movement after development and during retreat mining activities; and
  - Roof control in the face and in the area of face end T-junction.

The goal of geological and geotechnical description is to quantify the relevant rock properties. The description has to be coordinated with the mining activities and roadway development, and it has to include the survey by drill core analysis. A special method based on COREDAT software was developed for German coal mining, taking into consideration the parameters shown in Figure 4. The form provides a matrix of description that includes the orientation of separation planes, a geotechnical description of

lithological elements and stratification, and different classification elements for the bedding separations.

In addition to the core description, the geotechnical parameters can be derived from an evaluation of a development face using the form shown in Figure 5. The evaluation includes the amount of caving in the roof and sides, the lithotypes observed, the presence of separation planes, and relevant geometrical data. The degree of separation can be classified very simply by measuring the spacing between the lithologic and tectonic separation planes. Another important piece of information is the inclination and orientation of jointing. This information is used to estimate the maximum support loads from potential wedges within the sides and roof of the roadway, and it can be compared to the output from the drill core analysis.

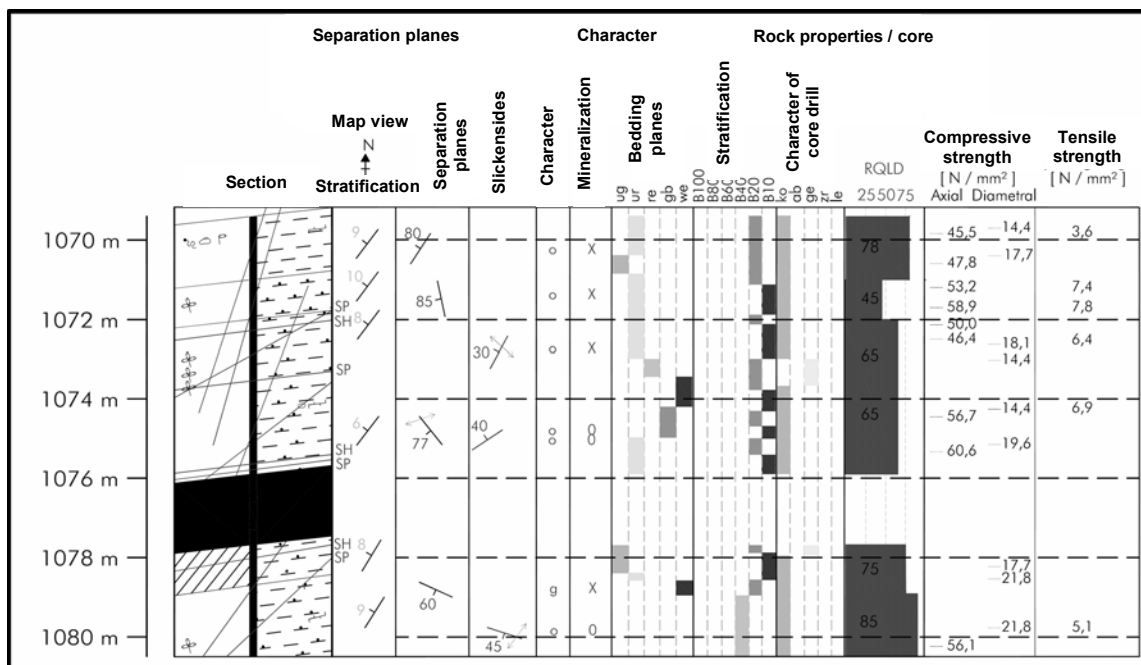


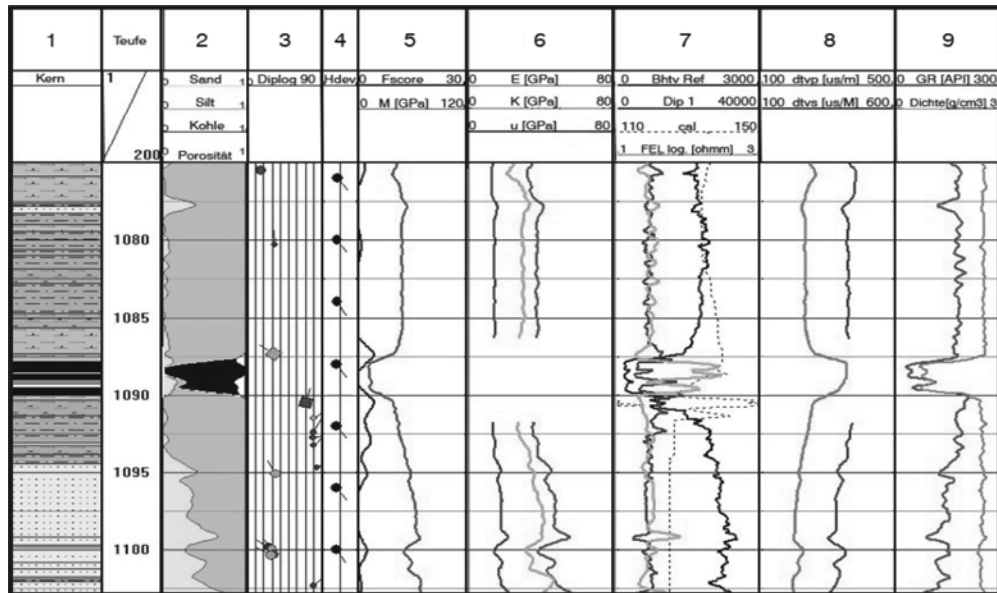
Figure 4.—Form of geotechnical analysis from drill cores by COREDAT software (DMT).

BTT-B		Geotechnische Ortsbrustaufnahme				DSK																																																																						
BW:		Bearbeiter:		Datum:		Zeit:																																																																						
Strecke: Richtung: gon		Betriebspunkt Nr. :		Flöz:		BH:																																																																						
Station:		Bemerkungen:																																																																										
 Firsthöhe : 4,45 m		<table border="1"> <thead> <tr> <th>M [m]</th> <th>BA [m]</th> <th>GE</th> <th>AS</th> <th>OS</th> <th>TB</th> <th>GW</th> </tr> </thead> <tbody> <tr> <td>&lt;0,1</td> <td>ko</td> <td>unregelm.</td> <td>ur</td> <td>KA</td> <td>g</td> <td>hoher</td> </tr> <tr> <td>0,1-0,2</td> <td>ob</td> <td>unregelm./ wellig/abgesetzt</td> <td>re</td> <td>SP</td> <td>u</td> <td>Feuchtigkeit</td> </tr> <tr> <td>0,2-0,4</td> <td>ge</td> <td>gebrüchig</td> <td>ur</td> <td>SP</td> <td>u</td> <td>moist</td> </tr> <tr> <td>0,4-0,6</td> <td>tr</td> <td>zerrissen/ zerkleinert</td> <td>gb</td> <td>ob</td> <td>u</td> <td>steif</td> </tr> <tr> <td>0,6-0,8</td> <td>re</td> <td>regel- mäßig</td> <td></td> <td></td> <td>t</td> <td>trocken</td> </tr> <tr> <td>&gt;0,8</td> <td>we</td> <td>wechselseitig/ m. Sandstr.-bind.</td> <td></td> <td></td> <td></td> <td>fest</td> </tr> </tbody> </table> <table border="1"> <thead> <tr> <th>d [cm]</th> <th>AK</th> <th>DG</th> <th>Fl. Struktur</th> </tr> </thead> <tbody> <tr> <td>K1</td> <td>80</td> <td>ra</td> <td>K</td> </tr> <tr> <td>K2</td> <td>150</td> <td>H</td> <td>B</td> </tr> <tr> <td>K3</td> <td>100</td> <td>e</td> <td></td> </tr> <tr> <td>K4</td> <td></td> <td></td> <td></td> </tr> </tbody> </table> 300 Schieferton 301 Schieferton sandfrei 302 Schieferton schwach sandig 303 Schieferton sandig 304 Schieferton stark sandig 305 Schieferton sandstreifig 306 Schieferton bituminös 350 Sandstein 351 Sandstein feinkörnig 352 Sandstein mittelkörnig 353 Sandstein grobkörnig 732 Wurzelböden 730 Wurzelreste						M [m]	BA [m]	GE	AS	OS	TB	GW	<0,1	ko	unregelm.	ur	KA	g	hoher	0,1-0,2	ob	unregelm./ wellig/abgesetzt	re	SP	u	Feuchtigkeit	0,2-0,4	ge	gebrüchig	ur	SP	u	moist	0,4-0,6	tr	zerrissen/ zerkleinert	gb	ob	u	steif	0,6-0,8	re	regel- mäßig			t	trocken	>0,8	we	wechselseitig/ m. Sandstr.-bind.				fest	d [cm]	AK	DG	Fl. Struktur	K1	80	ra	K	K2	150	H	B	K3	100	e		K4			
M [m]	BA [m]	GE	AS	OS	TB	GW																																																																						
<0,1	ko	unregelm.	ur	KA	g	hoher																																																																						
0,1-0,2	ob	unregelm./ wellig/abgesetzt	re	SP	u	Feuchtigkeit																																																																						
0,2-0,4	ge	gebrüchig	ur	SP	u	moist																																																																						
0,4-0,6	tr	zerrissen/ zerkleinert	gb	ob	u	steif																																																																						
0,6-0,8	re	regel- mäßig			t	trocken																																																																						
>0,8	we	wechselseitig/ m. Sandstr.-bind.				fest																																																																						
d [cm]	AK	DG	Fl. Struktur																																																																									
K1	80	ra	K																																																																									
K2	150	H	B																																																																									
K3	100	e																																																																										
K4																																																																												
 Sohlebreite : 6,20 m		 Kluftabstand d1 (cm)																																																																										

Figure 5.—Form for geotechnical observation of a heading front.

The form shown in Figure 5 was developed to complement basic geotechnical engineering and allows a comparison to the information obtained from the survey. The combined data set gives a detailed overview of the rock properties in, above, and below the roadway section.

The synoptic imaging of an analyzed geophysical drill core is shown in Figure 6. The meaning of each curve is described in the figure. Taken together, these data provide the basic information needed for geological engineering, design of panel layouts, dimensioning of roadway support, and support of the face T-junction.



Column No.	Heading note	Description
1	Core	Core description
2	(composite log)	Porosity - sand, clay, coal
3	Diplog	Dipping
4	Hdev	Horizontal orthographic deviation
5	Fscore	Fissures / m
	M	Stiffness modulus
6	E	Elastic modulus
	K	Compression modulus
	U	Poisson - rate
7	BHTV ref	Reflectivity from BHTV measurement
	Dip 1	resistance Diplog Pad 1
	Cal	borehole caliper
	FEL	Focused Electric Log
8	dtvp	Run duration P – wave
	dtvs	Run duration S – wave
9	GR	Gamma ray
	Density	Density

**Figure 6.—Geophysical drill core analysis.**

## RELIABILITY OF GEOMECHANICAL PARAMETERS

In geomechanical planning work, it is important to know how reliable the data are for the specific strata being evaluated. The probability of occurrence is mainly influenced by the lithofacies, the tectonic conditions, and the density of survey. When the degree of reliability is known, a risk analysis can be conducted by analyzing each measured input parameter.

Table 2 shows a reliability ranking based on the density and quality of the survey. The five classes reflect the different levels of reliability and give a simple scheme for assessing geologic and geotechnical information. Combining the information from boreholes and roadway observations normally leads to a reliability rating of "confident" or "probably."

**Table 2.—Influence of exposure-density on probability of occurrence**

	Probability of occurrence	Distance of exposures
1 .....	<i>Confident</i> Margin of error 10% Probability of occurrence 90%	Up to 200 m.
2 .....	<i>Probably</i> Margin of error 20% Probability of occurrence 75%–90%	Up to 300 m.
3 .....	<i>Potential</i> Margin of error 30% Probability of occurrence 50%–75%	Up to 400 m.
4 .....	<i>Indicated</i> Margin of error >30% Probability of occurrence 30%–50%	Up to 500 m.
5 .....	<i>Supposed</i> Margin of error >50% Probability of occurrence <30%	More than 200 m.

For any specific pattern of boreholes, the need for additional boreholes can be determined by evaluating the characteristics of the deposit and the longwall panel layout with respect to the sedimentologic analysis and lithofacies. This is particularly important when dealing with layers of sandstone whose thickness can change over short distances.

The result of the geomechanical classification is only as good as the quality of the information on which it is based. An important part of the process is to identify the remaining risk and manage it. Therefore, the current geomechanical planning standard is designed not only with the aim of defining the operational required parameters, but also to point out the risks that could arise during the development and use of the roadways. The procedure

provides a basis for the design of support and the engineering of reinforcement measures.

## ROCK MASS CLASSIFICATION

The German rock mass classification system includes both geotechnical rock analysis and geomechanical prediction of stress and roadway convergence. The prediction of the stress level is based on numerical modeling of the stress field under the influence of multiple-seam mining. A system of equations for predicting convergence and roadway deformation during development and longwall mining is based on empirical analysis of measurements that have been collected since the 1960s.

The most important issue for classification is that it must be flexible enough to adapt to a broad range of mining scenarios (e.g., panel design and dimensioning of support). It must also be able to adapt to the different types of input data that are available from drill cores and underground observations. Since the rock rating system can use data from either drill cores or underground observations, it provides maximum flexibility in advance of mining for optimization of support or panel layout.

Drawing upon mining experience gained in the past 5 decades, the German rock mass classification system represents a compromise between practicality and the best possible characterization. The parameters that are included are sufficient to represent the actual geological and rock mechanics conditions, and they can be determined from the currently available technical survey methods.

The rock rating clearly identifies the critical combination of geotechnical parameters within a large quantity of data. However, using it requires experience and a multidisciplinary knowledge. In doing so, one has to recognize that each parameter has different influence on the different mining tasks. The rating system developed by Deutsche Steinkohle AG (DSK) contains 21 parameters, each of which is evaluated individually.

Figure 7 shows how the process works. Each parameter is given one of five rating levels (A through E). Associated with each individual rating is a numerical evaluation index. The 21 individual evaluation indices are then summed to obtain an overall rating for the rock. Depending on the overall rating, the rock is classified into one of five types, ranging from "stable" to "squeezing," as shown on the bottom line of Figure 7. The rating for the example in Figure 7 is 535.5, which is considered "squeezing" rock quality.

Rock Classification											
No	Parameters	A	Index	B	Index	C	Index	D	Index	E	Index
1	Bonding strength Roof [N/mm <sup>2</sup> ]	80	4.6	60	9.3	45	18.5	30	37	≤25	74
2	Bonding strength Face [N/mm <sup>2</sup> ]	80	4.1	60	8.3	45	16.5	30	33	≤25	66
3	Bonding strength Floor [N/mm <sup>2</sup> ]	80	3.7	60	7.3	45	14.5	30	29	≤25	58
4	Driving-pressure [MPa]	0.4 Bs R	4.5	0.6 Bs R	9.0	0.8 Bs R	18.0	1 Bs R	36	>1 Bs R	72
5		0.4 Bs F	3.9	0.6 Bs F	7.8	0.8 Bs F	15.5	1 Bs F	31	>1 Bs F	62
6		0.4 Bs Fl	3.3	0.6 Bs Fl	6.5	0.8 Bs Fl	13.0	1 Bs Fl	26	>1 Bs Fl	52
7	Course and no. of working boundaries	0	4.1	FAB	8.3	PAB	16.5	SAN	33	PAN	66
8	Distance to bound. of overlying workings [m]	≥350	4.4	>200	8.8	>100	17.5	>50	35	≤50	70
9	Distance to bound. of underlying workings [m]	≥350	4.5	>200	9.0	>100	18.0	>50	36	≤50	72
10	Age of working boundaries	≥10 years	4.5	≥5 years	9.0	≥2 years	18.0	≥1 years	36	during driving	72
11	Distance between fault and roadway	≤4B	3.0	≤3B	6.0	≤2B	12.0	≤B	24	≤0.5B	48
12	Distance between fold and roadway	≤4B	2.5	≤3B	5.0	≤2B	10.0	≤B	20	≤0.5B	40
13	Seam distance roof	≤3B	4.1	≤2B	8.3	=B	16.5	≤0.5B	33	≤0.25B	66
14	Seam distance floor	≤3B	2.5	≤2B	5.0	=B	10.0	≤0.5B	20	≤0.25B	40
15	Bed thickn. structure	thick-bedded	2.7	bedded	5.3	laminated	10.5	thin-lamin.	21	flaky	42
16	Character of separat. plane surface	irregular	2.2	undulating	4.3	even	8.5	slickensided	17	polished	34
17	Degree of natural internal separation	I	3.2	II	6.3	III	12.5	IV	25	V	50
18	Slickensided/“Lösen”-surfaces	≤2B	3.0	≤B	6.0	≤0.5B	12.0	≤0.25B	24	In roadway cross-section	48
19	Room to move of jointed rock body relative to roadway	joints and bedding visible	3.2	along bedding	6.3	along bed. and 1 joint direction	12.5	along bed. and 2 joint directions	25	Along bed. And several joint directions	50
20	Formation water	dry	4.4	moist	8.8	wet	17.5	dripping	35	running	70
21	Resistance to water	not soluble	2.7	sanding	5.3	loose	10.5	deconsolid.	21	Disintegrated	42
Remarks										$\sum \text{Indices} : 535.5$	

Figure 7.—German mining standard rock mass rating matrix.

The evaluation is done continuously, and the results are merged into a single rock quality class for the analyzed section of roadway during drivage. The aim of the rock rating, besides determining the rock quality class, is to define the support class. Both the rock quality and support classes are dependent on mining technology and excavation

technique. Increasing rock quality means lower support requirements. Depending on the required support, it may be possible to optimize the support installation timing, for example, by installing temporary bolting at the time of initial installation and completing the bolting pattern later with the setting of long tendons. The rock quality

can also indicate the maximum allowable distance between the face and where the arches must be backfilled, which can help optimize the mining method to achieve the best development rate.

## APPLICATION OF GEOTECHNICAL ANALYSIS AND ROCK MASS RATING

Today, the German rock mass rating system is used in geomechanical planning work for design of development headings, selection of support classes, and risk management. Rock mass rating is an important element of a closed loop of planning work for strata control. This closed loop was defined in the 1970s for German coal mining when it was recognized that optimized planning is based on performance review by monitoring. Another aspect is the successful development of planning tools and support systems. Both require a performance review because they are based on empirical processing.

Operational experience with the application of the rock mass rating system gives the results summarized in Table 3. A rating of up to 131 points indicates stable rock quality. Only minimal roadway deformation is expected, and just a few local displacements are likely. The separation planes, either joints or bedding planes, are closed and maintain high frictional strength. These conditions require the lowest level of support system with, in principle, only a need for lagging to prevent small pieces of rock from falling out of the roof. Unfortunately, these conditions are seldom encountered in German hard-coal mining.

The next class of rating, between 132 and 264 points, indicates caving rock quality. Poor rock quality is designated as “friable” (264–521) or “squeezing” (>521). Increasing roadway deformation that starts within the heading process must be taken into account. In most cases, combined support systems with both rock bolt systems and additional backfilled steel arches are used for roadway support.

**Table 3.—Rock classification and rock types**

Rating index	Class	Rock type
Up to 80 .....	Ia	<i>Stable rock:</i> Local displacement, closed joints and bedding elements (separation planes)
Up to 131 .....	Ib	<i>Caving rock:</i> Local displacement and sporadic caving areas up to decimeter size in the roof and the upper sides, particular separation planes
Up to 196 .....	IIa	
Up to 264 .....	IIb	
Up to 304 .....	IIIa	<i>Friable rock:</i> Increased separation results in displacements and caving up to meter size, separation planes pronounced and partially opened
Up to 347 .....	IIIb	
Up to 434 .....	IVa	<i>Very friable rock:</i> High density of jointing and intensive transaction results in regular displacement caving up to 1 m sliding gravity wedges
Up to 521 .....	IVb	
>621 .....	Va	<i>Squeezing rock:</i> Local gouge zones and squeezing areas, opened separation plane, high density of separation and intensive transaction, loosening of strata, and high mobility of gravity wedges
	Vb	

The rock mass rating has to be interpreted for different assignments of tasks. Looking at the roadway support for gate roads, for example, a rating of 434 is the limit of the applicability of backfilled steel arches as exclusive support. Below this rating, for rectangular starting rooms, it is typical to employ combined support with rock bolts and additional steel canopies and hydraulic props. For detailed design of support patterns in this range, it is necessary to take a close look at the geomechanical parameters.

As the rock mass rating increases, the quality of the rock decreases. This results in an increasing effort for roadway support. Table 4 gives some examples of the rock bolting densities required in different rock qualities. The example shown is for an arched-shaped roadway with a width of 6.4 m and a height of 4.5 m.

**Table 4.—Required bolting density for support depending on rock mass quality**

Rock mass quality	Bolting density in bolts/m <sup>2</sup> of bolted roof and side	Number of bolts per meter of roadway length	Support resistance of bolting pattern (kN/m <sup>2</sup> )
Stable .....	0.8	6.5	231
Caving .....	1.3	10.5	370
Friable .....	1.6	13	463
Very friable .....	2.0	15.6	552
Squeezing .....	2.4	19	678

In this case, for stable rock (i.e., competent strata condition), a bolt density of approximately 0.8 bolts/m<sup>2</sup> of arch peripheral area is specified. This bolt density is only one-third of that needed for the squeezing rock quality, which requires approximately 2.4 bolts/m<sup>2</sup>.

In Figure 8, the range of common support classes for German coal mines is assigned according to the rock mass rating and rock quality. The increasing effort required for support is clear in this figure. An optimized roadway development rate can be achieved with a multiphased support installation. The sequential installation of different support measures behind the face requires quite good rock conditions. In contrast, poor conditions require immediate support during development.

## CONCLUSIONS

The German rock mass rating system for hard-coal mining has been developed particularly for application in multiple-seam mining at great depth and for use with a variety of support systems. It takes into account the service function of the roadways, including not only retreat longwall mining, but also reuse of the roadways after the passage of one longwall face.

The system is a compromise between the best possible rock mass description and the practical limitations of available measurement methods. Because the aim of

classification is to provide the basic information needed for dimensioning of support, it takes into account both the in situ stress and the stresses caused by multiple-seam mining activities. Basic experiences from German hard-coal mining are included in the system through lithologic descriptions.

The system has been routinely applied in all DSK mines for the past 3 years. The class number determined by the rock classification provides the essential information needed for a detailed support design. It also provides an opportunity for comparing different seam conditions across borderlines between mines and panel layouts. The classification is an important addition to the descriptive geologic parameters.

The class number also gives a sense of rock quality and, therefore, it helps in assessment support requirements. However, it is not possible to predict roadway convergence with a single number, particularly for the later phases of roadway use. This means that it is still necessary to analyze the classification parameters and measure deformation to determine the maximum amount of convergence during roadway use. It is important to consider that the German method of mining employs single roadway systems and requires reuse of the roadway after passage of the face.

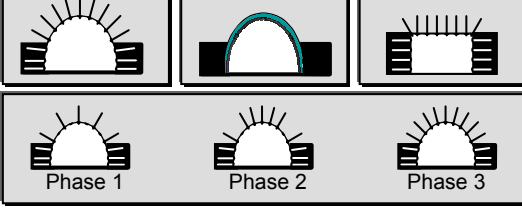
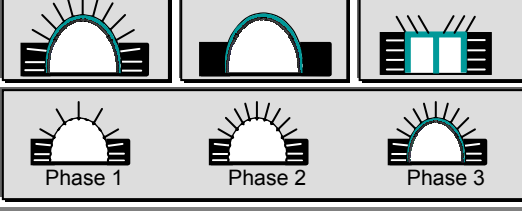
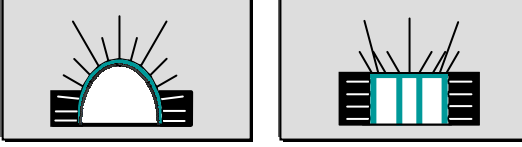
Rock mass rating	Rock mass quality	Support class/support system
$\leq 196$	stable – caving	 Phase 1      Phase 2      Phase 3
$\leq 434$	friable – very friable	 Phase 1      Phase 2      Phase 3
$> 434$	very friable – squeezing	

Figure 8.—Rock mass quality and support measures.

Every time the standard is used, the classifying parameters from drill cores and roadway observations allow a retrospective evaluation of the main factors influencing support performance. This information is documented and maintained in a central data pool for knowledge management within DSK and, therefore, serves as an important tool for future support designs.

## BIBLIOGRAPHY

- Everling G, Meyer A-G [1972]. Ein Gebirgsdruckrechenmodell als Planungshilfe (in German). Glückauf-Forschungshefte 33:81–88.
- Jacobi O [1981]. Praxis der Gebirgsbeherrschung (in German). 2. Aufl. Essen, Germany: Verlag Glückauf.
- Junker M, et al. [2006]. Gebirgsbeherrschung von Flözstrecken (in German). Glückauf-Verlag.
- Müller W [1989]. Messung der absoluten Gebirgsspannungen im Steinkohlenbergbau (in German). Glückauf-Forschungshefte 50:105–112.
- Opolony K, Witthaus H [2003]. Comparison of multiple- and single-entry roadway systems for highly stressed longwalls. In: Peng SS, Mark C, Khair AW, Heasley KA, eds. Proceedings of the 22nd International Conference on Ground Control in Mining. Morgantown, WV: West Virginia University, pp. 33–36.
- Opolony K, Polysos N, Bartel R, Lüttig F [2000]. Ankertechnik bei der DSK Theorie und Praxis (in German). Glückauf 136.
- Polysos N, Peters S [2002]. Application of geotechnical and geophysical parameters to improve planning certainty in roadway driving. In: Peng SS, Mark C, Khair AW, eds. Proceedings of the 21st International Conference on Ground Control in Mining. Morgantown, WV: West Virginia University, pp. 302–309.
- Polysos N, Brandt K-H, Peters S [2003]. Geotechnische Gebirgsbewertung im Hinblick auf die Hangendbegherrschung im Strebraum (in German). 2. Intern. Colloquium on High-performance Mining Production (Aachen, Germany).
- Witthaus H [2001]. Die Planung von Ankerausbau in Flözstrecken (in German). 4. Intern. Colloquium: Ankerausbau im Bergbau (Aachen, Germany).
- Witthaus H [2006]. Entwicklung einer Planungsmethode für Ankerausbau im deutschen Steinkohlenbergbau unter Berücksichtigung der Gebirgsstruktur und der Gebirgsbeanspruchung [Dissertation] (in German). Aachen, Germany: Verlag Mainz.
- Witthaus H, Adams M, Junker M [2000]. Die ausbau-technische Planung für vorbauartig und doppelt genutzte Ankerstrecken (in German). Glückauf 136.
- Witthaus H, Polysos N, Peters S [2006]. Applied geomechanics for support design in German deep coal mines. In: Peng SS, Mark C, Finfinger GL, Tadolini SC, Khair AW, Heasley KA, Luo Y, eds. Proceedings of the 25th International Conference on Ground Control in Mining. Morgantown, WV: West Virginia University, pp. 208–212.



# NUMERICAL MODELING PROCEDURES FOR PRACTICAL COAL MINE DESIGN

By R. Karl Zipf, Jr., Ph.D., P.E.<sup>1</sup>

## ABSTRACT

A method is presented for creating realistic numerical models for practical coal mine ground control. The method includes procedures to collect the necessary mechanical input parameters from a geologic core log, procedures to set up a model, and procedures to interpret calculation results. The input parameters come from a detailed geologic core log and extensive point load tests of estimate rock layer strength. A suite of material property input parameters is proposed that allows the user to go from core log to numerical model inputs. Rock bolt anchorage properties are also linked to the material properties of each geologic layer in the model. Following this procedure leads to very realistic calculations of the rock failure process and rock support system behavior. These calculations in turn enable realistic comparison of the effectiveness of alternative rock support systems.

## INTRODUCTION

Reducing ground failure fatalities and injuries is a priority of the National Institute for Occupational Safety and Health's (NIOSH) mine safety and health research program. Ground failures have historically accounted for up to 50% of the fatalities in U.S. underground mines, and nonfatal injuries due to ground failure are almost always severe. Ground failures helped trigger recent mine disasters in Alabama (2001) and Utah (2000) by disrupting ventilation that led to gas explosions. Together, these incidents claimed the lives of 15 coal miners. In 2006, 10 underground coal miners lost their lives in 7 roof falls, 2 rib rolls, and 1 coal mine bump.

To reduce fatalities and injuries due to ground failure, NIOSH researchers are working toward improved understanding of rock mass failure mechanics using numerical analysis models. Promoting more widespread use of numerical models for ground control engineering may lead to the desired safety improvements; however, several barriers exist toward that end. Considerable guidance is needed for collecting necessary input data, setting up a model, and finally interpreting the analysis results. Such guidance should have the agreement of all parties involved in practical ground control, including mining companies, consultants, suppliers, and regulatory authorities. To

enable better communication among mining engineers working in coal mine ground control, NIOSH researchers have made progress toward a set of input parameters for use in FLAC<sup>2</sup> [Itasca Consulting Group 1994] that result in very realistic models of coal mine rock behavior and rock bolts. Finally, the suggested guidance is not intended as a substitute for sound engineering judgment.

Obtaining the input parameters requires collection of certain information from rock core. The input parameters include material properties for a strain-softening, ubiquitous-joint constitutive model, rock bolt properties, and model initialization and loading. Use of these input parameters seems to lead automatically to (1) realistic modeling of the failure mechanics, (2) calculation of displacement and stress that are consistent with field measurements, and (3) a reasonable forecast of the effectiveness of rock support alternatives. This paper discusses a core logging procedure to obtain numerical model input parameters, presents a suite of input parameters for practical coal mine models, and demonstrates their use with a practical example.

## CORE LOGGING FOR INPUT PARAMETERS

Obtaining meaningful results from a numerical model begins with the collection of adequate geologic information. The method described for translating a geologic core log into input parameters for a numerical model follows a philosophy developed by Gale and Tarrant [1997] of "letting the rocks tell us their behavior." For numerical modeling of coal mines, the logger must record two essential details, namely, individual geologic layers of homogeneous character and the strength of those geologic layers. Figure 1 shows a typical section of core with several distinct layers and other essential features to record.

The logging detail necessary depends on the scale of the numerical model. Small-scale models of coal mine entry behavior may require logging geologic layers as small as 50 mm. Larger-scale coal mine models for subsidence prediction may require less logging detail. Of particular importance to note are the soft clay layers or major bedding planes with weak infilling as indicated in Figure 1.

Having defined the geologic layering in sufficient detail, the logger must next estimate the strength of those layers, including the strength of the rock material and the strength of bedding plane discontinuities. Uniaxial compressive strength (UCS) tests, triaxial tests, or multistage

<sup>1</sup>Senior research mining engineer, Pittsburgh Research Laboratory, National Institute for Occupational Safety and Health, Pittsburgh, PA.

<sup>2</sup>Fast Lagrangian Analysis of Continua.



**Figure 1.—Photograph of core showing different rock layers and a prominent clay layer from 1.4 to 1.5 ft.**

triaxial tests on core specimens oriented both perpendicular to bedding and at a 30° angle to bedding are the best way to measure cohesion and friction angle for the rock material and bedding plane discontinuities. However, conducting extensive tests is rarely a feasible option. Index tests are the preferred option and have the distinct advantage of providing multiple strength estimates for each geologic layer. Basic soil and rock descriptions of the International Society for Rock Mechanics [ISRM 1981] can provide a crude estimate of strength. Other options include simple hammer blow tests [ISRM 1981; Molinda and Mark 1996] or the Schmidt Hammer test for stronger materials [ISRM 1993]. The Point Load Index [ISRM 1985] seems to be the simplest and most reliable method at present to estimate rock material and bedding plane strength through an axial or diametral point load test, respectively. Based upon thousands of tests, reliable correlations between Point Load Index and UCS have been developed for a variety of coal mine rocks throughout the United States [Rusnak and Mark 2000]. Techniques to estimate rock layer strength based on downhole geophysical measurements are also well developed [Medhurst and Hatherly 2005]; however, the methods have never been adopted widely by the U.S. coal industry. Figure 2 shows estimates of the rock material and bedding plane strength for each geologic layer based on point load tests.

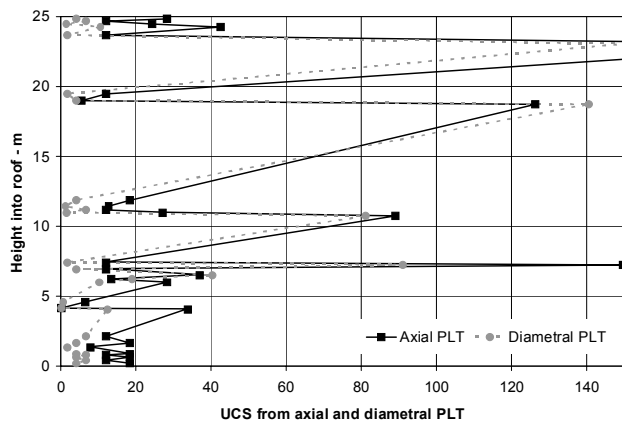


**Figure 2.—Typical strength data along rock core from axial and diametral point load tests (PLT).**

Detailed geologic logging for numerical modeling purposes has a relation to the Coal Mine Roof Rating (CMRR) used to describe coal mine roof rock in practical ground control [Mark et al. 2002b]. The CMRR Unit Rating for each rock layer is composed of two parts. The UCS rating for the rock material strength ranges from 5 to 30 for a range of strengths between 0 and 138 MPa as determined from axial point load tests. The discontinuity rating for the bedding plane strength ranges from 25 to 60 corresponding to strength of about 6–52 MPa based on diametral point load tests.

## MATERIAL PROPERTIES

For general modeling of rock behavior in coal mine ground control, the FLAC program [Itasca Consulting Group 1994] contains many useful features, in particular, the SU constitutive model. “SU” stands for the strain-softening, ubiquitous-joint model and is ideal for simulating laminated coal measure rocks. In essence, this constitutive model allows for strain-softening behavior of the rock matrix and/or failure along a predefined weakness plane such as bedding planes. Failure through the rock matrix or along a bedding plane can occur via shear or tension, and the dominant failure mode can change at any time. The “state” variable within FLAC tracks the failure mode in each model element as either shear or tensile failure through the rock matrix or along a bedding plane.

The SU constitutive model requires four major input parameters, namely, cohesion, friction angle, dilation angle, and tensile strength for both the rock matrix and the bedding planes. Based on a Mohr-Coulomb strength model, the UCS of a rock depends on cohesion and friction angle as

$$UCS = \frac{2c \cos \phi}{1 - \sin \phi} \quad (1)$$

where  $c$  is the cohesion and  $\phi$  is the friction angle. Careful geologic core logging along with point load testing to estimate the UCS of each rock layer provides a rational basis to estimate the most important input parameters to the SU constitutive model.

Tables 1 and 2 summarize the name, UCS, and the initial value for input parameters of a proposed suite of “numerical rocks,” along with a corresponding geologic description of the rock. The UCS values indicated in Tables 1 and 2 are field-scale or model-scale values that are reduced from the laboratory-scale values determined from point load tests during geologic logging. Following the lead of Gale and Tarrant [1997] again, these laboratory values of UCS for rock and coal, but not soil, are reduced by a factor of 0.56 to produce the field-scale UCS and hence the input parameters to the numerical model. This scaling factor works well for rock masses associated with coal mining; however, it does not apply outside this narrow scope.

**Table 1.—Initial values for rock material input parameters**

Material name	Description	Lab UCS (MPa)	Field UCS (MPa)	Young's modulus (GPa)	Cohesion (MPa)	Friction angle, °	Dilation angle, °	Tensile strength (MPa)
Soil 1.....	Paste	0.04	0.02	1	0.007	21	10	0.002
Soil 2.....	Very soft soil	0.07	0.04	1	0.014	21	10	0.004
Soil 3.....	Soft soil	0.14	0.08	1	0.028	21	10	0.008
Soil 4.....	Firm soil	0.29	0.16	1.5	0.055	21	10	0.016
Soil 5.....	Stiff soil	0.63	0.35	2	0.120	21	10	0.035
Soil 6.....	Very stiff soil	3.6	2.0	2.5	0.69	21	10	0.20
Rock 1.....	Claystone, fireclay	6.4	3.6	3	1.2	22	10	0.3
Rock 2.....	Black shale	11	6	4	2.0	23	10	0.6
Rock 3.....	Black shale, gray shale	18	10	5	3.3	24	10	1.0
Rock 4.....	Gray shale	25	14	6	4.5	25	10	1.4
Rock 5.....	Siltstone, gray shale	34	19	7	6	26	10	1.9
Rock 6.....	Siltstone	48	27	8	8	28	10	2.7
Rock 7.....	Siltstone, sandstone	63	35	10	10	30	10	3.5
Rock 8.....	Sandstone, limestone	77	43	12	12	32	10	4.2
Rock 9.....	Sandstone	95	53	15	14	34	10	5.2
Rock 10.....	Limestone	139	78	20	20	36	10	7.7
Coal 1.....	Banded, bright coal	3.6	2.0	2.5	0.6	29	10	0.17
Coal 2.....	Banded coal	6.3	3.5	2.5	1.0	30	10	0.29
Coal 3.....	Banded, dull coal	12	6.7	2.5	1.9	31	10	0.60
Coal 4.....	Dull coal	17	9.7	2.5	2.7	32	10	0.85

**Table 2.—Initial values for bedding plane input parameters**

Material Name	Description	Lab strength (MPa)	Field strength (MPa)	Young's modulus (GPa)	Cohesion (MPa)	Friction angle, °	Dilation angle, °	Tensile strength (MPa)
Soil 1.....	Paste	0.04	0.02	1	0.007	21	10	0.002
Soil 2.....	Very soft soil	0.07	0.04	1	0.014	21	10	0.004
Soil 3.....	Soft soil	0.14	0.08	1	0.028	21	10	0.008
Soil 4.....	Firm soil	0.29	0.16	1.5	0.055	21	10	0.016
Soil 5.....	Stiff soil	0.63	0.35	2	0.120	21	10	0.035
Soil 6.....	Very stiff soil	1.4	0.80	2.5	0.27	21	10	0.080
Rock 1.....	Claystone, fireclay	2.7	1.5	3	0.5	21	10	0.15
Rock 2.....	Black shale	5.4	3.0	4	1.0	22	10	0.30
Rock 3.....	Black shale, gray shale	10	5.7	5	1.9	23	10	0.60
Rock 4.....	Gray shale	18	10	6	3.3	24	10	1.0
Rock 5.....	Siltstone, gray shale	25	14	7	4.5	25	10	1.4
Rock 6.....	Siltstone	32	18	8	5.5	26	10	1.7
Rock 7.....	Siltstone, sandstone	41	23	10	7	27	10	2.3
Rock 8.....	Sandstone, limestone	59	33	12	10	28	10	3.3
Rock 9.....	Sandstone	86	48	15	14	29	10	4.8
Rock 10.....	Limestone	123	69	20	20	30	10	6.8
Coal 1.....	Banded, bright coal	1.6	0.9	2.5	0.3	25	10	0.08
Coal 2.....	Banded coal	2.9	1.6	2.5	0.5	26	10	0.15
Coal 3.....	Banded, dull coal	6.4	3.6	2.5	1.1	27	10	0.30
Coal 4.....	Dull coal	12	6.7	2.5	2.0	28	10	0.60

The material suite shown in Tables 1 and 2 includes very weak soils and claylike materials with a UCS of 0.02 MPa and weak, medium, and strong rocks with a UCS of about 150 MPa. Also included is coal, which ranges from the most friable with a UCS of 2 MPa to a strong coal with a UCS of 12 MPa. The soil material models are isotropic, i.e., the soil matrix properties are the same as those for the horizontal weakness plane. However, the rock models exhibit anisotropy since the strength along bedding planes is less than the UCS of the rock matrix. Following results of point load tests by Molinda and Mark [1996], weak rocks are the most anisotropic, with the strength

along bedding planes about 50% of the rock matrix UCS, while stronger rocks have less anisotropy, with the strength along bedding planes about 90% of the rock matrix. The coal models have a similar trend in strength anisotropy, with the stronger coal less anisotropic than the weaker coal. For the stronger coal, the ratio of axial strength to strength parallel to bedding is about 1.5 to 1, whereas for the weaker coal the ratio is about 2.2 to 1. The weaker coal models would apply to more cleated coal, i.e., containing more closely spaced joints. The extensive material property suite for coal mine rocks proposed in Tables 1 and 2 is

generally consistent with a smaller set of properties proposed by Reddish et al. [2000].

Note that in proposing this suite of numerical rock properties, the UCS of the rock matrix is independent from the strength of the bedding planes. In the absence of specific data, the user will usually specify the rock matrix and bedding plane strength as a pair with strength ratio similar to that noted by Molinda and Mark [1996] for an extensive database of axial and diametral point load tests. However, the strength values for the rock matrix and bedding planes are independent in the material property suite, and the user can specify any value for the bedding plane strength up to that of the rock matrix UCS.

In creating the material model suites, friction angle for the matrix and bedding planes are assumed to vary as shown in Tables 1 and 2, respectively. These assumptions for friction angle along with Equation 1 then imply the values for peak cohesion shown in Tables 1 and 2. Thus, the UCS of the rock matrix and the bedding plane strength provide two of the four major input parameters to the SU constitutive model in FLAC.

Assumed friction angle values for the rock matrix ranges are 21° for soil- and claylike materials up to 36° for the strongest rocks. These values may be somewhat low compared to published values of Jaeger and Cook [1979] and Farmer [1968]. Later revisions of this material property suite may include a one friction angle range for application at low confinement and another for application at high confinement. Assumed friction angle values for the bedding plane are 21° for soil- and claylike materials up to 30° for the strongest rocks. These values are consistent with data developed by Barton and summarized by Hoek et al. [1995].

Other major assumptions within this material model suite are as follows:

1. Moduli for the materials range from 1 to 20 GPa. Weaker materials have a lower modulus, while stronger materials have a higher modulus. The ratio of modulus to UCS of the rock matrix varies from about 1,000 for the weakest to about 100 for the strongest materials. The moduli for the material and the modulus-to-UCS ratio are consistent with data shown in Jaeger and Cook [1979] and Gale and Fabjanczyk [1993].
2. Cohesion decreases from its peak value given in Tables 1 and 2 to a residual value of 10% of peak over 5 millistrain of postfailure strain. It is this decrease in cohesion with postfailure strain that gives rise to strain-softening behavior of both the rock matrix and the bedding planes.
3. Friction angle remains constant at the values shown in Tables 1 and 2, even in the postfailure regime.
4. Tensile strength is equal to cohesion for the soil materials and decreases to 0 over 1 millistrain of postfailure strain.

5. Tensile strength values are generally about 10% of UCS. It also decreases to 0 over 1 millistrain of postfailure strain. This strength ratio is again consistent with rock strength data shown in Jaeger and Cook [1979] and Farmer [1968].
6. Dilation angle is initially 10° and decreases to 0° over 5 millistrain of postfailure strain.

## ROCK BOLT PROPERTIES

In addition to its robust constitutive models, FLAC includes various structural support elements. The structural element called “cable” represents rock support as an axial force along a line, and this approach suffices for most rock or cable bolts in practical coal mining applications. If the shear or moment resistance of a rock bolt is significant, the “pile” structural element may be a more appropriate choice.

Properties required by the “cable” element are the structural characteristics of the steel, namely, elastic modulus, cross-sectional area, and yield strength, along with the structural characteristics of the anchor. Resin along with some cement grout now dominates most anchors used with rock and cable bolts in U.S. mines [Dolinar and Bhatt 2000]. Two properties represent the anchor characteristics in FLAC: “Kbond,” which is the stiffness of the grout, and “Sbond,” which is its cohesive strength.

Kbond, or anchorage stiffness, depends on grout properties and the annulus thickness, i.e., hole radius minus bolt radius. Based on numerical studies by St. John and Van Dillen [1983] of the grout-rock interface, the FLAC manuals [Itasca Consulting Group 1994] suggest the following expression for a practical estimate of Kbond for use in FLAC:

$$K_{\text{bond}} \equiv \frac{2\pi G}{10 \ln(1 + 2t/D)} \quad (2)$$

where G is the grout shear modulus, D is the bolt diameter, and t is the annulus thickness.

Farmer [1975] reports a value of 2.25 GPa (455,000 psi) for the Young’s modulus of resin grout. For a typical 19-mm (0.75-in) rock bolt in a 28.6-mm (1.125-in) hole, Kbond is approximately  $1.4 \times 10^9$  N/m/m. Over the practical range of rock bolt and hole diameters and the likely range for grout modulus, Kbond varies at most from about 1 to  $2 \times 10^9$  N/m/m.

Numerical modeling of laboratory measurements of rock bolt behavior confirms this estimate of Kbond. Numerous researchers [Kwitowski and Wade 1980; Serbousek and Signer 1987; Signer 1990; Tadolini 1986] used strain gauges to measure the load distribution along fully grouted, 1-m-long rock bolts embedded in large blocks of limestone, shale, or concrete. Figure 3 shows

various measured load profiles where the bolt load at zero distance along the bolt is the actual applied load. Note the exponential decay of bolt load with distance, which is consistent with analytical models proposed by Farmer [1975] and Serbousek and Signer [1987]. A simple FLAC model of these laboratory pull tests was used to calculate the bolt load distribution for Kbond values of 0.5, 1, and  $2 \times 10^9$  N/m/m and an applied load of 60 kN. As seen in Figure 4, Kbond equal to  $1 \times 10^9$  N/m/m matches the laboratory measurements well.

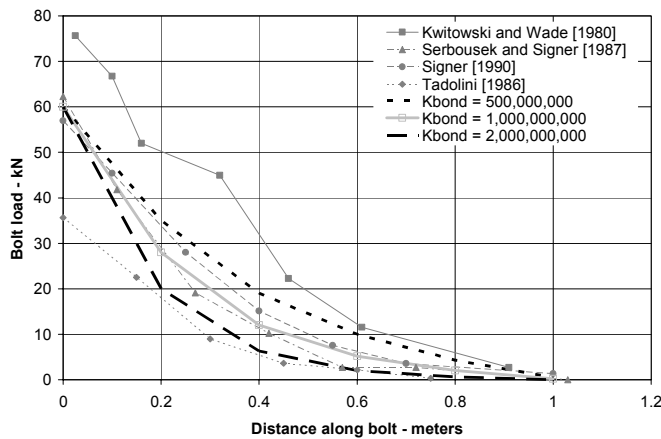


**Figure 3.—Measured and calculated load profiles along rock bolts.**

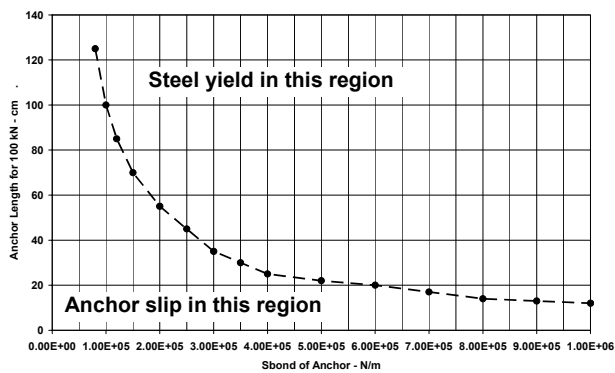


**Figure 4.—Anchor length required for 100-kN capacity for various Sbond.**

Sbond is also known as bond factor, anchor factor, or grip factor and has a typical value of about 350 kN/m (1 ton/in) in coal mine rocks. Its value depends on the likely failure mode of the bolt anchor. If the grout is weak, shear failure occurs along the bolt-grout interface, and Sbond depends on the grout cohesion and the perimeter of the bolt. Farmer [1975] reports a value of 160 MPa for the compressive strength of resin grout. Assuming that the

cohesion is one-third of this value, Sbond at the bolt-grout interface for a typical 19-mm (0.75-in) bolt is about 3.2 MN/m.

However, in coal mine rocks, shear failure typically occurs along the grout-rock interface, where Sbond depends on the lesser of the rock or grout cohesion and the perimeter of the hole. Table 1 indicates that rock cohesion varies from 1.2 to 20 MPa and is even less for the occasional thin clay layers. Thus, for a hole diameter in the 25- to 35-mm range, Sbond varies from 80 kN/m to 2.2 MN/m (0.2 to 4.5 tons/in) depending on the rock material strength. Table 3 shows the range of Sbond values for various rock materials. For practical coal mine modeling with FLAC, the user should specify bolt sections that correspond to the top and bottom of a geologic layer and then assign an Sbond value for that section consistent with the rock material properties for that layer. Table 4 shows Sbond values for various rocks either measured directly or inferred from select pull test data. Values range from 77 to 1,225 kN/m and are consistent with the Sbond input parameters shown in Table 3. Note that the values for Kbond and Sbond discussed here assume a unit bolt spacing of 1 m between rows of bolts. These rock bolt properties and others require scaling according to the actual rock bolt spacing.

**Table 3.—Sbond values for various rock materials**

Material name	Description	Cohesion (MPa)	Sbond for 25-mm hole (N/m)	Sbond for 35-mm hole (N/m)
Soil 1	Paste	0.007	559	770
Soil 2	Very soft soil	0.014	1,120	1,540
Soil 3	Soft soil	0.028	2,230	3,080
Soil 4	Firm soil	0.055	4,390	6,050
Soil 5	Stiff soil	0.120	9,580	13,200
Soil 6	Very stiff soil	0.69	55,100	75,900
Rock 1	Claystone, fireclay	1.2	95,800	132,000
Rock 2	Black shale	2.0	160,000	220,000
Rock 3	Black shale, gray shale	3.3	263,000	363,000
Rock 4	Gray shale	4.5	359,000	495,000
Rock 5	Siltstone, gray shale	6	479,000	660,000
Rock 6	Siltstone	8	638,000	880,000
Rock 7	Siltstone, sandstone	10	798,000	1,100,000
Rock 8	Sandstone, limestone	12	958,000	1,320,000
Rock 9	Sandstone	14	1,120,000	1,540,000
Rock 10	Limestone	20	1,600,000	2,200,000
Coal 1	Banded, bright coal	0.6	47,900	66,000
Coal 2	Banded coal	1.0	79,800	110,000
Coal 3	Banded, dull coal	1.9	152,000	209,000
Coal 4	Dull coal	2.7	215,000	297,000

**Table 4.—Measured Sbond in various rocks.**

Rock	Sbond (N/m)	Reference
Shale-concrete ....	77,000	Bartels and Pappas [1985].
Plaster .....	126,000	Bartels and Pappas [1985].
Chalk .....	193,000	Franklin and Woodfield [1971].
Dark gray fireclay .....	220,500	Mark et al. [2002a].
Layered dark gray shale.....	252,000	Mark et al. [2002a].
Sandstone .....	289,000	Franklin and Woodfield [1971].
Concrete blocks...	290,000	Pettibone [1987].
Thinly banded gray shale.....	290,500	Mark et al. [2002a].
Clay, claystone ....	304,500	Mark et al. [2002a].
Dark gray shale ...	364,000	Mark et al. [2002a].
Coal .....	385,000	Franklin and Woodfield [1971].
Gypsum .....	385,000	Dunham [1974].
Limestone.....	400,000	Dunham [1974].
Anhydrite .....	526,000	Dunham [1974].
Limestone.....	1,225,000	Franklin and Woodfield [1971].
Coal/shale .....	300,000–900,000	Yearby [1991].
Sandstone/limestone .....	1,000,000–2,500,000	Yearby [1991].

Additional simple FLAC models calculated the minimum anchor length to hold 100 kN (about 10 tons) without slipping. Again, these models consider a 19-mm bolt of varying length and assumed yield strength for the steel of 200 kN to ensure anchorage slip and not steel failure. Consistent with expectations, the critical anchor length ranged from 1 m at a low Sbond value of 100 kN/m down to 10 cm with a high Sbond value of 1,000 kN/m, as shown in Figure 4. For a given Sbond, a bolt with anchor length more than this critical value will fail by yield of the bolt steel, and with anchor length less than this critical value, anchor slip will occur. Figure 4 suggests that for stronger rocks with Sbond more than 350 kN/m (1 ton/in), short encapsulation pull tests with anchor length of much less than 30 cm (1 ft) are necessary to measure Sbond directly.

## INITIALIZATION AND LOADING CONDITIONS

A recent summary of horizontal stress measurements in U.S. coal mines by Dolinar [2003] demonstrated that the horizontal stress magnitude depends on the elastic modulus of the rock layers. Horizontal stress varies according to the relative stiffness of each geologic layer, such that stiff limestone or sandstone layers attract higher horizontal stress than less stiff black shale or claystone layers.

To initialize horizontal stress in a model, the analyst must first calculate the average horizontal strain as

$$\epsilon_{H \text{ average}} = \frac{\sigma_{H \text{ average}}}{E_{\text{average}}} \quad (3)$$

where  $\sigma_{H \text{ average}}$  is the average horizontal tectonic stress and  $E_{\text{average}}$  is the average modulus. Using Dolinar's approach,

a tectonic strain could also be used directly for the initial far-field boundary condition. Alternatively, if the horizontal stress and modulus are known for a particular layer within a model, the horizontal strain can be calculated on that basis.

Horizontal stress for each layer in the model has a tectonic component and a Poisson component and is calculated as

$$\sigma_{H i} = (\epsilon_{H \text{ average}})(E_i) + \left( \frac{v}{1-v} \right) (\sigma_{v i}) \quad (4)$$

where  $E_i$  is the Young's modulus for a layer,  $v$  is Poisson's ratio, and  $\sigma_{v i}$  is the vertical stress in a layer. Vertical stress in each layer depends on depth in the usual way. Figure 5 shows a layered model of coal mine rocks initialized with this procedure. Average initial vertical and horizontal stress is 5 and 8 MPa.

## PUTTING IT ALL TOGETHER: AN EXAMPLE

This example demonstrates the complete modeling procedure for a coal mine gate road entry in the Pittsburgh Coalbed that is first subject to initial development loading, then additional loading from mining the first longwall panel, and finally more loading as a second longwall panel approaches. Again, Figure 2 shows estimates of axial and diametral point load strength as measured along a core. The point load tests used to estimate the UCS of the rock matrix and the bedding plane strength lead directly to material property assignments based on Tables 1 and 2. Table 5 summarizes a section of the geologic column, strength values from point load tests, and the resulting material property inputs for the model. Figure 5 reflects the layering detail in the overall model. Initial horizontal stress magnitude applied to the model generally correlates to high- or low-strength rock layers. The rock bolts in the model are composed of many sections, where each section corresponds to the top and bottom of a geologic layer. Each bolt section is then assigned an Sbond value consistent with the rock material properties for that layer.

Table 6 indicates the average horizontal and vertical stress applied to the model at different stages. The stresses shown in Table 6 are a two-dimensional approximation to a complex three-dimensional problem. In the gate road development phase, applied stresses are the same as in situ stresses. Mining the first longwall panel effectively induces higher horizontal and vertical stresses far field from the model coal mine entry. The approaching second longwall panel and passage of that second panel induces additional horizontal and vertical stresses. Again, the stress path indicated in Table 6 is only a simple two-dimensional approximation of the actual complex three-dimensional stress field applied to the coal mine entry.



**Figure 5.—Initial horizontal stresses. Warm colors indicate high horizontal stress in stiffer layers; cool colors indicate low horizontal stress in less stiff layers. The future entry is shown at center.**

**Table 5.—Going from core log to numerical model input parameters**

Height into roof (m)	Rock type	UCS axial PLT (MPa)	Bedding strength diam. PLT (MPa)	Rock matrix code (Table 1)	Bedding plane code (Table 2)
3.00.....	Sandy bl sh	33.70	12.40	RM5	RBP3
2.90.....	Sandy bl sh	33.70	12.40	RM5	RBP3
2.80.....	Sandy bl sh	33.70	12.40	RM5	RBP3
2.70.....	Sandy bl sh	33.70	12.40	RM5	RBP3
2.55.....	Sandy bl sh	33.70	12.40	RM5	RBP3
2.40.....	Coal	12.00	6.70	CM3	CBP3
2.30.....	Coal	12.00	6.70	CM3	CBP3
2.20.....	Coal	12.00	6.70	CM3	CBP3
2.10.....	Coal	12.00	6.70	CM3	CBP3
2.03.....	Coal	12.00	6.70	CM3	CBP3
1.90.....	Bl sh + coal	18.00	4.00	RM3	RBP2
1.80.....	Bl sh + coal	18.00	4.00	RM3	RBP2
1.69.....	Bl sh + coal	18.00	4.00	RM3	RBP2
1.60.....	Claystone	8.00	2.00	RM2	RBP1
1.50.....	Claystone	8.00	2.00	RM2	RBP1
1.40.....	Claystone	8.00	2.00	RM2	RBP1
1.30.....	Claystone	8.00	2.00	RM2	RBP1
1.18.....	Claystone	8.00	2.00	RM2	RBP1
1.08.....	Black shale	18.00	4.00	RM3	RBP2
0.98.....	Coal	12.00	6.70	CM3	CBP3
0.88.....	Coal	12.00	6.70	CM3	CBP3
0.76.....	Black shale	18.00	4.00	RM3	RBP2
0.64.....	Black shale	18.00	4.00	RM3	RBP2
0.52.....	Coal	12.00	6.70	CM3	CBP3
0.40.....	Coal	12.00	6.70	CM3	CBP3
0.28.....	Black shale	18.00	4.00	RM3	RBP2
0.16.....	Black shale	18.00	4.00	RM3	RBP2
0.00.....	Coal	12.00	6.70	CM3	CBP3

Bl sh = Black shale. PLT = point load test.

**Table 6.—Applied stress path at model boundary**

Loading condition	Average horizontal stress (MPa)	Average vertical stress (MPa)
Development .....	8	5
1st panel mining .....	14	9
2nd panel mining .....	17.6	11.4
Postmining.....	20	13

To apply these additional horizontal and vertical stresses to the model, equivalent average strains are calculated based on a weighted average modulus for the model. Based on the overall model dimensions, equivalent displacements at the model boundary are calculated. These displacements are then achieved in the model by slowly applying a velocity at the boundary for a prescribed number of computational steps. Velocity at the model boundary is then set to zero for additional computational steps to achieve equilibrium.

The modeling analyzes two alternative support systems, namely, 2.4-m fully grouted rock bolts alone and with 4-m-long cable bolts. Figure 6 compares these alternatives by showing rock bolt loads, rock bolt anchor slip, rock bolt breakage, and rock mass shear failure superimposed on the UCS of the rock matrix. Different shades represent rock layers of different rock matrix strength. Generally in the Pittsburgh Coalbed, the immediate roof rock is low-strength black shale, thin coal layers, and claystone. Above the immediate roof rock is somewhat higher-strength gray shale and siltstone beds. Rock mass failure has occurred throughout the immediate roof. Zones

of intense bedding plane slip exist above the upper corners of the entry, and these zones propagate 2 to 3 m into the roof. Bedding plane separation has also developed 1.5, 2.5, and 4.5 m into the roof rock, as shown in Figure 7.

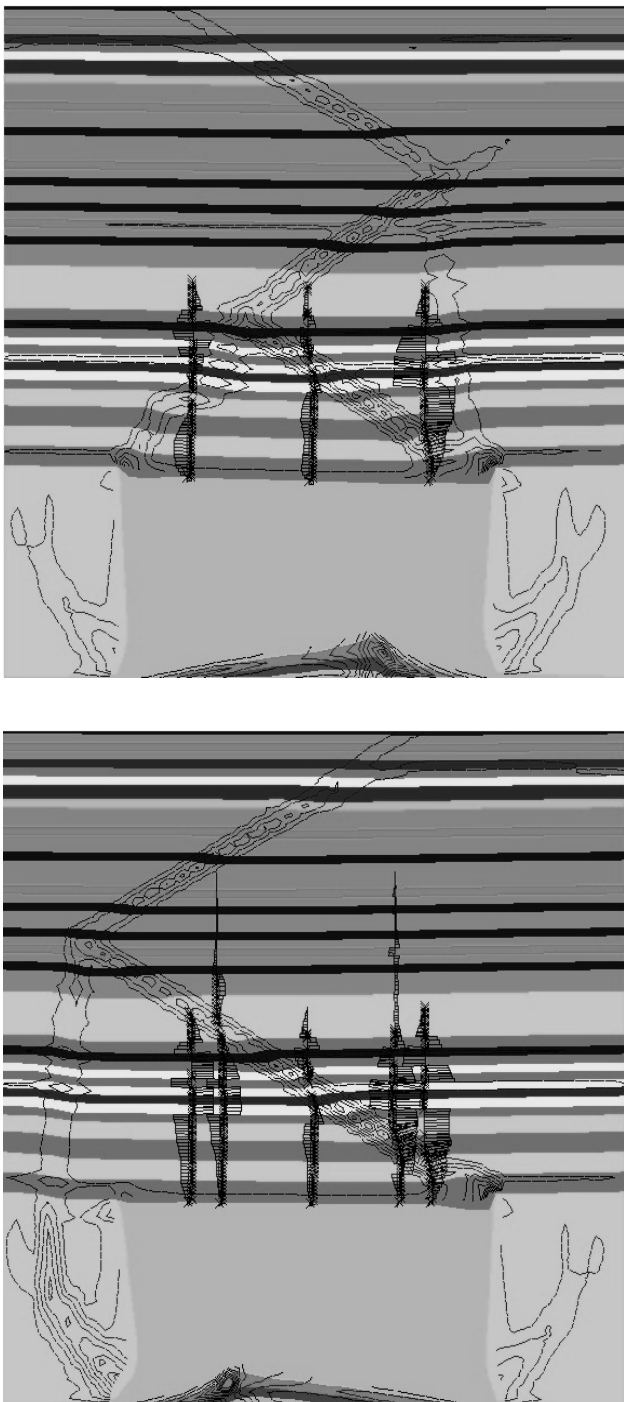


**Figure 6.—Support system performance with 2.4-m bolts alone (top) and with 2.4-m bolts with 4-m cables (bottom).**  
Rock layers of different strength are shaded. Shear zones are contoured. Maximum shear strain contour is 0.5. Rock bolt load is indicated.

Compressive failure of the immediate roof rock has localized into several “shear bands,” as indicated in Figure 6 with the shear strain index parameter in FLAC. These shear bands are more developed with the lighter support system consisting of bolts alone. The failure has also tended to favor one side of the roof more than the other. Downward roof movement is much greater on the left than on the right. The magnitude of rock bolt load is plotted as a percentage of yield strength of the steel. For the untensioned, fully grouted rock bolts used in this model, the load increases from zero at the bolt head, rises to a maximum somewhere in the middle, and decreases back to zero at the anchorage end. The shape of the load profile follows the measured laboratory experiments, as shown in Figure 3. All bolt loads are tensile, no matter whether the load is plotted left or right of the bolt. Anchorage slip is indicated by crosses along the bolt. At the highest load applied to the model, anchor slip has occurred almost everywhere along the rock bolts and the lower portion of the cable bolts. Rock bolt or cable bolt breakage can occur if load on the bolt equals the yield load and if strain in the bolt exceeds 2%. Bolt breakage occurs in the left and center bolts for the bolts-alone case and only in the center bolt if cable bolts are also installed. Although the broken section of bolt is not visible in Figure 6, the low axial loads on either side of the shear zone mark the location of the broken bolt section.

Figure 7 shows the effectiveness of the two alternative rock support systems for controlling immediate roof movement under progressively higher load conditions. Under development conditions with horizontal and vertical stresses of 8 and 5 MPa, respectively, roof displacement is less than 10 mm and both bolt alternatives behave identically. Mining the first longwall panel increases horizontal and vertical stresses to 14 and 9 MPa; however, calculated roof displacements remain under 30 mm, and there is still negligible difference between the two alternatives. When the second longwall panel approaches, the necessity of the cable bolts becomes evident. In the alternative without cables, downward roof displacement at

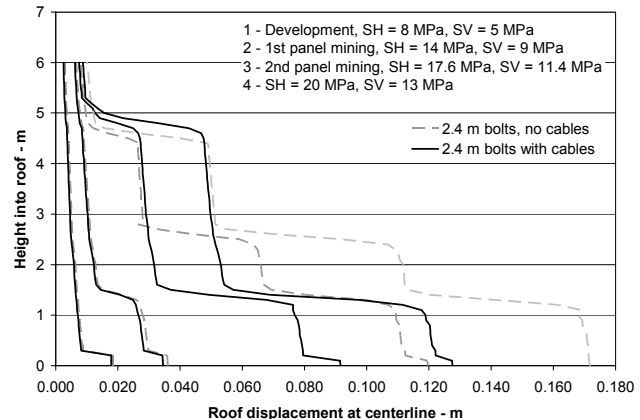


**Figure 7.—Immediate roof displacement response for two rock support alternatives.**

2-m horizon approaches 70 mm, whereas with cables movement at this horizon is about 30 mm. Total downward roof movement in excess of 50 mm and sudden jumps in that movement with small increases in the applied load on the model are indicative of roof instability and ineffective roof support.

## CONCLUSIONS

This paper presents progress toward a standard method for the use of numerical models in practical ground control planning. The method includes procedures for collecting the needed input data, setting up a model, and interpreting the results of calculations.

Collecting the input data needed for a numerical model begins with development of a detailed geologic core log. This core log must capture geologic layers of similar mechanical properties and also note particular features such as exceptionally weak clay layers. Point load testing is a convenient method to estimate the UCS of the rock matrix and the bedding plane strength for each geologic layer.

This paper proposes a suite of material property input parameters aimed at the SU constitutive model in FLAC. This suite of “numerical rocks” includes very weak soils and weak rocks to the strongest rocks found in coal mining. Having estimates of UCS and bedding plane strength for each geologic layer, the user can readily create a numerical model that correctly reflects the geologic situation. The suggested procedure has the distinct advantage of being organized and reproducible. In principle, two different individuals could examine a geologic section, describe it, test it, and develop the same numerical model inputs for the field conditions.

This paper also presents select properties needed to represent rock supports in a numerical model. The significant feature of the rock bolt properties is the linkage between rock bolt anchorage and the specific geologic layer containing that section of the rock bolt. Sections of a rock bolt in weak rocks have low anchor strength and vice versa in stronger rocks.

A practical example of a numerical model that follows the proposed procedure leads to very realistic results. The calculations capture the rock failure process correctly and agree with failure observations in the field. Calculated stresses and displacements in the model are consistent with field measurements of the same.

## REFERENCES

Bartels JR, Pappas DM [1985]. Comparative laboratory evaluation of resin-grouted roof bolt elements. Pittsburgh, PA: U.S. Department of the Interior, Bureau of Mines, RI 8924. NTIS No. PB 85-193449.

Dolinar DR [2003]. Variation of horizontal stresses and strains in mines in bedded deposits in the eastern and

midwestern United States. In: Peng SS, Mark C, Khair AW, Heasley KA, eds. Proceedings of the 22nd International Conference on Ground Control in Mining. Morgantown, WV: West Virginia University, pp. 178–185.

Dolinar DR, Bhatt SK [2000]. Trends in roof bolt application. In: Mark C, Dolinar DR, Tuchman RJ, Barczak TM, Signer SP, Wopat PF, eds. Proceedings: New technology for coal mine roof support. Pittsburgh, PA: U.S. Department of Health and Human Services, Public Health Service, Centers for Disease Control and Prevention, National Institute for Occupational Safety and Health, DHHS (NIOSH) Publication No. 2000-151, IC 9453, pp. 43–51.

Dunham RK [1974]. Field testing of resin anchored rock bolts. *Colliery Guardian* 222:147–151.

Farmer IW [1968]. Engineering properties of rocks. London: E. & F. N. Spon, Ltd.

Farmer IW [1975]. Stress distribution along a resin grouted rock anchor. *Int J Rock Mech Min Sci Geomech Abstr* 12:347–351.

Franklin JA, Woodfield PF [1971]. Comparison of a polyester resin and a mechanical rockbolt anchor. *Trans Inst Min Metal (Section A: Mining Industry)*, A91–A100.

Gale WJ, Fabjanczyk MW [1993]. Design approach to assess coal mine roadway stability and support requirements. In: Proceedings of the Eighth Australian Tunneling Conference (Sydney, New South Wales, Australia), pp. 1–7.

Gale WJ, Tarrant GC [1997]. Let the rocks tell us. In: Proceedings of the Symposium on Safety in Mines: The Role of Geology, pp. 153–160.

Hoek E, Kaiser PK, Bawden WF [1995]. Support of underground excavations in hard rock. Rotterdam, Netherlands: Balkema.

ISRM [1981]. Basic geotechnical description of rock masses. International Society for Rock Mechanics.

ISRM [1985]. Suggested methods for determining point load strength. International Society for Rock Mechanics.

ISRM [1993]. Supporting paper on a suggested improvement to the Schmidt rebound hardness ISRM suggested method with particular reference to rock machineability. International Society for Rock Mechanics.

Itasca Consulting Group [1994]. Fast Lagrangian analysis of continua. Minneapolis, MN: Itasca Consulting Group, Inc.

Jaeger JC, Cook NGW [1979]. Fundamentals of rock mechanics. 3rd ed. New York: Chapman and Hall.

Kwitowski AJ, Wade LV [1980]. Reinforcement mechanisms of untensioned full-column resin bolts. Pittsburgh, PA: U.S. Department of the Interior, Bureau of Mines, RI 8439. NTIS No. PB 81-147266.

Mark C, Compton CS, Oyler DC, Dolinar DR [2002]. Anchorage pull testing for fully grouted roof bolts. In: Peng SS, Mark C, Khair AW, Heasley KA, eds. Proceedings of the 21st International Conference on Ground

Control in Mining. Morgantown, WV: West Virginia University, pp. 105–113.

Mark C, Molinda GM, Barton TM [2002]. New developments with the coal mine roof rating. In: Peng SS, Mark C, Khair AW, Heasley KA, eds. Proceedings of the 21st International Conference on Ground Control in Mining. Morgantown, WV: West Virginia University, pp. 294–301.

Medhurst T, Hatherly P [2005]. Geotechnical strata characterization using geophysical borehole logs. In: Peng SS, Mark C, Tadolini SC, Finfinger GL, Khair AW, Heasley KA, eds. Proceedings of the 24th International Conference on Ground Control in Mining. Morgantown, WV: West Virginia University, pp. 179–186.

Molinda GM, Mark C [1996]. Rating the strength of coal mine roof rocks. Pittsburgh, PA: U.S. Department of the Interior, Bureau of Mines, IC 9444. NTIS No. PB96-155072.

Pettibone HC [1987]. Avoiding anchorage problems with resin-grouted roof bolts. Spokane, WA: U.S. Department of the Interior, Bureau of Mines, RI 9129. NTIS No. PB 88-230172.

Reddish DJ, Whittles DN, Stace LR [2000]. The application of rock classification principles to coal mine design in U.K. conditions. In: Peng SS, Mark C, eds. Proceedings of the 19th International Conference on Ground Control in Mining. Morgantown, WV: West Virginia University, pp. 348–357.

Rusnak J, Mark C [2000]. Using the point load test to determine the uniaxial compressive strength of coal measure rock. In: Peng SS, Mark C, eds. Proceedings of the 19th International Conference on Ground Control in Mining. Morgantown, WV: West Virginia University, pp. 362–371.

St. John CM, Van Dillen DE [1983]. Rockbolts: a new numerical representation and its application in tunnel design. In: Proceedings of the 24th U.S. Symposium on Rock Mechanics. New York: Association of Engineering Geologists, pp. 13–26.

Serbosek MO, Signer SP [1987]. Linear load-transfer mechanics of fully grouted roof bolts. Spokane, WA: U.S. Department of the Interior, Bureau of Mines, RI 9135. NTIS No. PB 88-230230.

Signer SP [1990]. Field verification of load-transfer mechanics of fully grouted roof bolts. Spokane, WA: U.S. Department of the Interior, Bureau of Mines, RI 9301. NTIS No. PB 90-225871.

Tadolini SC [1986]. Anchorage capacities in thick coal roofs. Denver, CO: U.S. Department of the Interior, Bureau of Mines, IC 9058. NTIS No. PB 86-169174.

Yearby M [1991]. Practical guide to rock bolting. Newcastle, New South Wales, Australia: ANI Arnall, Ltd.



***Delivering on the Nation's promise:  
Safety and health at work for all people  
through research and prevention***

To receive documents or more information about occupational safety and health topics,  
contact NIOSH at

1-800-35-NIOSH (1-800-356-4674)  
Fax: 513-533-8573  
E-mail: [pubstaft@cdc.gov](mailto:pubstaft@cdc.gov)

or visit the NIOSH Web site at [www.cdc.gov/niosh](http://www.cdc.gov/niosh)

**DHHS (NIOSH) Publication No. 2007-128**

**SAFER • HEALTHIER • PEOPLE™**